ISSN 2542-1565

Vol. 16 2023 No. 02

GEOGRAPHY
ENVIRONMENT
SUSTAINABILITY

«The journal GEOGRAPHY, ENVIRONMENT, SUSTAINABILITY was founded in 2008 by Russian Geographical Society, the Lomonosov Moscow State University Geography Department, and the Russian Academy of Sciences Institute of Geography. Since that time the journal publishes **4 issues per year**, containing original research papers and reviews. The journal issues are open source and distributed through subscriptions, library exchanges of leading universities, and via the website through the world»

FOUNDERS OF THE JOURNAL: Russian Geographical Society, Faculty of Geography, Lomonosov Moscow State University and Institute of Geography of the Russian Academy of Sciences

The journal is published with financial support of the Russian Geographical Society.

The journal is registered in Federal service on supervision of observance of the legislation in sphere of mass communications and protection of a cultural heritage. The certificate of registration: ПИ № ФС77-67752, 2016, December 21.

PUBLISHER
Russian Geographical Society
Moscow, 109012 Russia
Novaya ploshchad, 10, korp. 2
Phone 8-800-700-18-45
E-mail: press@rgo.ru
www.rgo.ru/en

EDITORIAL OFFICE
Lomonosov Moscow State University
Moscow 119991 Russia
Leninskie Gory, 1,
Faculty of Geography, 1806a
Phone 7-495-9391552
Fax 7-495-9391552
E-mail: ges-journal@geogr.msu.ru
www.ges.rgo.ru

DESIGN
Layout designer: Tereshkin Anton
Moscow, 115088,
26 Simonovsky Val str., bldg. One
Phone: +7 (903) 108-04-44
E-mail: smile.tai@gmail.com

DOI prefix: 10.24057

Format A4 (210x297mm)

"GEOGRAPHY, ENVIRONMENT, SUSTAINABILITY" is the only original English-language journal in the field of geography and environmental sciences published in Russia. It is supposed to be an outlet from the Russian-speaking countries to Europe and an inlet from Europe to the Russian-speaking countries regarding environmental and Earth sciences, geography and sustainability. The main sections of the journal are the theory of geography and ecology, the theory of sustainable development, use of natural resources, natural resources assessment, global and regional changes of environment and climate, social-economical geography, ecological regional planning, sustainable regional development, applied aspects of geography and ecology, geoinformatics and ecological cartography, ecological problems of oil and gas sector, nature conservations, health and environment, and education for sustainable development.

Date of publication: July 1st, 2023.

EDITORIAL BOARD

EDITORIAL OFFICE

CONTENTS

Disclaimer:

The information and opinions presented in the Journal reflect the views of the authors and not of the Journal or its Editorial Board or the Publisher. The GES Journal has used its best endeavors to ensure that the information is correct and current at the time of publication.

RESEARCH PAPER

WATER FLOW CHANGES IN THE DON RIVER (EUROPEAN RUSSIA) DURING 1891–2019

Alexander G. Georgiadi[1*], Irina P. Milyukova[1], Oleg O. Borodin[2], Artyom V. Gusarov[3]

[1]Institute of Geography, Russian Academy of Sciences, Staromonetny Alley, Moscow, 119017, Russia

[2]Water Problems Institute, Russian Academy of Sciences, Gubkin Street, Moscow, 117971, Russia

[3]Institute of Geology and Petroleum Technologies, Kazan Federal University, Kremlyovskaya Street, Kazan, 420008, Russia

***Corresponding author:** georgiadi@igras.ru

Received: May 1st, 2022 / Accepted: May 4th, 2023 / Published: July 1st, 2023

https://DOI-10.24057/2071-9388-2022-083

ABSTRACT. The Don River Long near Razdorskaya Village had long phases (lasting 33–86 years) of increased/decreased naturalized annual and seasonal water flow, and their properties for 1891–2019 were identified. Long-term changes in the annual and snow-melt flood flow occurred in the opposite phase relative to changes in the winter and summer-autumn flow. Annual hydrographs in the phase of decreased flow were characterized by an increase in water discharge during the low-water seasons of the year, but a noticeable decrease in daily flood water discharge and maximum water discharge. The share of high-water years (years with a flow exceedance probability equal to or less than 25%) in the phase of increased flow is significantly higher than the share of low-water years (years with a flow exceedance probability equal to or more than 75%). And on the contrary. At the same time the cumulative share of low- and high-water years remains relatively stable. The total changes in the annual and seasonal flow, caused by both anthropogenic and climatic factors, throughout the entire period of modern global warming (since 1989) consisted in a decrease of the annual and snow-melt flood flow and an increase of flow values during low-water seasons.

KEYWORDS: hydrological change, long-term phase, high- and low-water year, global warming, anthropogenic factor, hydrograph transformation, cumulative deviation curve

CITATION: Georgiadi A. G., Milyukova I. P., Borodin O. O., Gusarov A. V. (2023). Water Flow Changes In The Don River (European Russia) During 1891–2019. Geography, Environment, Sustainability, 2(16), 6-17
https://DOI-10.24057/2071-9388-2022-083

ACKNOWLEDGEMENTS: This research was funded by the Russian Science Foundation, project no. 20-17-00209; the methodological framework for contrasting phases analysis was developed under Governmental Order to the RAS Institute of Geography, AAAA-A19-119021990093-8 (FMGE-2019-0007). The work is also carried out in accordance with the Strategic Academic Leadership Program "Priority 2030" of the Kazan Federal University of the Government of the Russian Federation.

Conflict of interests: The authors reported no potential conflict of interest.

INTRODUCTION

Studies relating to long-term changes in river water flow and other components of environmental flow which are regarded to be particularly susceptible to ongoing climate change, are given a great deal of attention due to current global warming began in the 1970s and 1980s (Hinzmann et al. 2005; Water Resources … 2008; Shiklomanov et al. 2013; Georgiadi et al. 2014; Magritsky 2015; Georgiadi et al. 2018; Shiklomanov et al. 2020; Scientific and applied reference … 2021; Georgiadi and Groisman 2022; Frolova et al. 2022; Zhuravlev et al. 2022). A large number of scientific publications is devoted to the evaluation of changes that happened in various hydrological characteristics during the global warming period compared to the relatively cooler baseline period (Shiklomanov and Georgievskii 2007; Water Resources … 2008; Georgiadi et al. 2019). As a rule, such estimates are made based on a comparison of the studied flow characteristic values for both periods of global warming and preceding baseline period. In addition, the problem of long-term periods (phases according to the terminology adopted in the former USSR (Andreyanov 1959; Kuzin 1979) and Russia (Georgiadi et al. 2014) of increased/decreased values of the river water flow characteristics and other geo-runoff (a term proposed by (Muraveysky 1960)) components (sediment, chemical, biological and heat fluxes from a catchment area) during XIX-XXI centuries is of considerable interest. The successive change of contrasting long-term phases is an important feature of the long-term dynamics of hydrological characteristics due to climate change. It should be noted that the deviation of values between such phases is considered statistically significant. The duration of these contrasting periods ranges from 10–15 years up to several decades (Georgiadi et al. 2014; Georgiadi et al. 2018; Georgiadi et al. 2019). In this regard, annual and seasonal changes in water flow in various regions of the world have recently been studied (Sharma and Singh 2017; Bolgov et al. 2018; Georgiadi et al. 2018; Shi 2019; Georgiadi et al. 2020). However, despite a rather wide range of studies on long-term phases of increased/decreased river water flow for various regions of the world, specifically for Russia's river basins, the spatial range of such studies still awaits significant enhancement.

One of the main problems in the development of this research topic is to determine the time boundaries between contrasting multi-year phases of water flow, as well as between the background (baseline) period and the period of global warming. In addition to various natural factors affecting the change in river flow (including factors associated with climate change), human activity in the channels and watersheds of rivers has a significant impact on the values under consideration (Water Resources … 2008; Georgiadi et al. 2014). At the same time, the set of acting anthropogenic factors, as well as their intensity, change over a long period. This raises the problem of identifying factors of change.

To determine the current changes in river water flow as a result of human impact, the authors developed two separate approaches (Georgiadi et al. 2014). The first of them concerns an integral assessment of the anthropogenic and climatic impact on the change in water flow by naturalizing the river water flow and its further comparison with the measured values. The naturalization procedure includes an analysis of the relationship between the hydrological characteristics of the studied river and its tributaries, which are in zones of slightly noticeable human impact and, thus, are indicators of climate change features. The other approach mainly includes various water balance methods and analysis of water management statistics. It allows assessing the influence of individual anthropogenic factors or their entire complex. Two approaches are used for naturalize river runoff. The regression model of the main river water flow based on river indicators of climate change features was used to naturalize long-term annual and seasonal water flow series (Georgiadi et al. 2014). In addition, daily water discharge values could be naturalized based on hydrograph transformation (Sokolovskii and Shiklomanov 1965; Georgievskii and Moiseenkov 1984; Shiklomanov et al. 2011; Stuefer et al. 2011) using travel time function (methods of unit hydrograph, isochrone lines, Kalinin-Milyukov, Muskingum, etc.). The concept and reliability of the second approach are similar to the method of river indicators of climate change features.

This research is devoted to studying long phases of increased and decreased naturalized annual and seasonal water flow as well the frequency structure of water flow time series for one of the largest rivers of Eastern Europe, namely the Don River, for the observation period of 1891–2019. In addition, the objective of this study was to assess the impact of current global warming and anthropogenic factors on river water flow characteristics including daily water discharge hydrographs.

MATERIALS AND METHODS

Study Area

One of the largest rivers of European Russia – the Don River – was chosen as the study object (Fig. 1). The total area of the Don River basin is 422,000 km^2, and 378,000 km^2 – at Razdorskaya village. The Don River basin is located mainly in the steppe (63%) and forest-steppe (32%) landscape zones.

Most of the annual water flow (62.4%) of the Don River occurs during the snow-melt flood (March-May), when there is an intensive melting of the snow cover. During the summer-autumn period, 25.4% of the annual water flow is formed. The winter period, which lasts from December to February, brings 12.4% of the annual water flow of this river. The calculation (as well as other estimations of the characteristics of the Don runoff presented in the paper) was made by authors based on the time series of naturalized daily average water discharge values (for naturalization methodology see below).

The natural landscapes of the Don River basin have changed significantly due to primarily agricultural activities in recent centuries (Arc Atlas: Our Earth 1996). Human-altered landscapes occupy more than 80% of the total area of the river's basin and are mainly used for non-irrigated

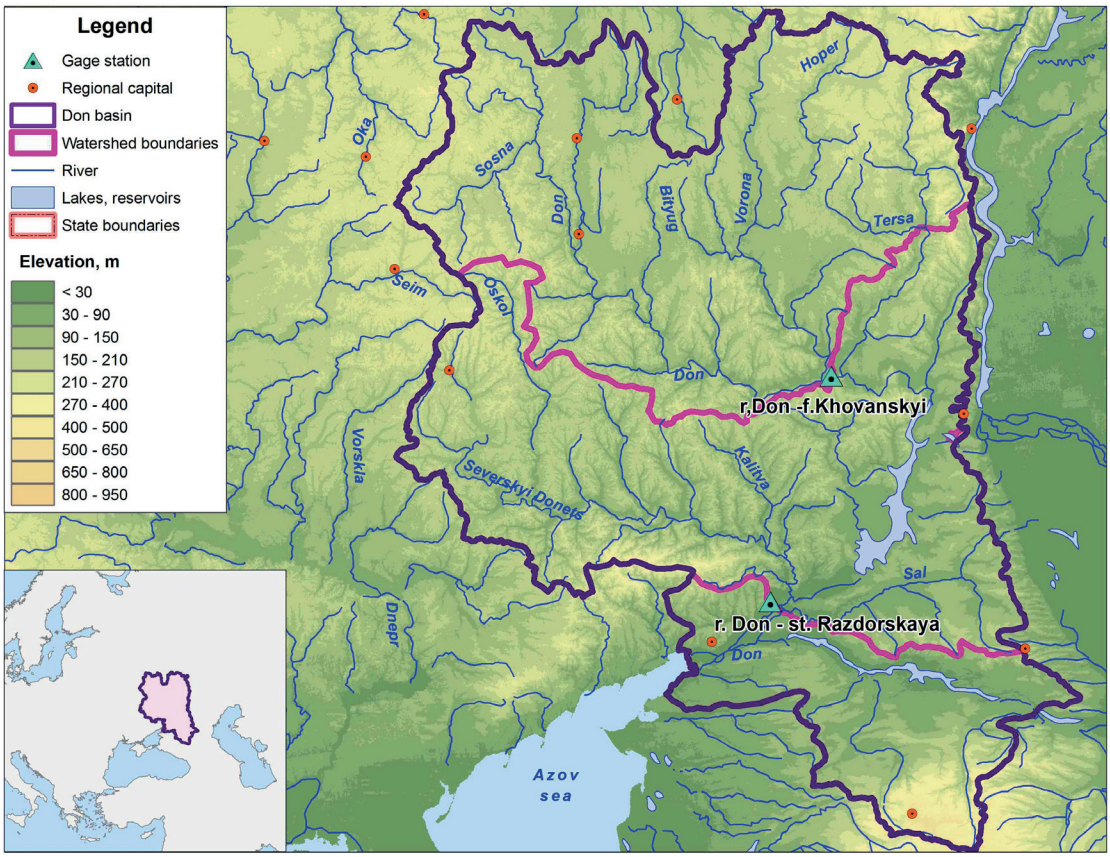

Fig. 1. Location of the Don River basin

agriculture. And since the 1980s no significant changes in the structure of land use within the Don basin have been revealed up to the present times (Kireeva et al. 2018).

Reservoirs, industry, agriculture (including irrigation), urban areas, as well as roads and pipelines, have a significant impact on the water regime of both the Don River and its tributaries, despite the fact that they occupy no more than 4% of the total basin area (Georgiadi et al. 2014; Varentsova et al. 2021). The cumulative anthropogenic impact (acting mainly through reservoir management, water withdrawal and subsequent discharge) is most noticeable when comparing hydrographs of water flow of the Don River, built according to data of periods before and after the construction of large hydraulic structures in its basin (see below). The most noticeable effect on the annual and especially seasonal water flow is exerted by the interannually regulated Tsimlyansk Reservoir which was filled in 1953. Its total volume is 23.9 km^3, including 11.5 km^3 of active storage. The long-term annual average water flow (for 1891–2019) of the Don River near Razdorskaya was found to be equal to 24.33 km^3.

Data

The research was based on a long-term series of daily average water discharge values of the Don River measured at Razdorskaya village and Khovansky farmstead (Fig. 1) between 1936 and 2019, and monthly average water discharge values at Razdorskaya from 1891 to 2019. These series were used to create a set of long-term naturalized water flow data (meaning that anthropogenic influence was excluded), as well as to calculate the observed flow values for main hydrological seasons (snow-melt flood, summer-autumn and winter low-flow seasons) and for the whole period within the designated time frame. The time limits of hydrological seasons were defined on the basis of information on the long-term average dates of the beginning and end of snowmelt floods and river freezing. Two separate periods stand out from the entire period of observation of the Don River's hydrological characteristics at Razdorskaya. The first is characterized by a rather low anthropogenic impact, while the second is characterized by significant changes in the flow of the Don River due to intense anthropogenic impact. The year 1951 was adopted as the dividing line between these two periods. At that point, the Tsimlyansk Reservoir started to fill.

Time series of air temperature and precipitation for the years 1936 to 2019 were obtained from measurements at a network of meteorological stations using the data array of the World Data Center of the Russian Institute of Hydrometeorological Information (RIHMI-WDC) dataset (http://meteo.ru).

Methodology

Method of naturalization of the hydrograph of daily average water discharge. To naturalize the values of the daily average water discharge of the Don River at Razdorskaya, a series of measured daily average discharge of the Don River at Khovansky (the basin area is 169,000 km^2) was used. The hydrological regime at Khovansky gauging station is characterized by considerably small changes due to anthropogenic factors mainly related to non-irrigated agriculture, urbanization, and water consumption by house-holds or industry. Furthermore, the anthropogenic impact is partly compensated by itself coming from different sources (Georgiadi et al. 2014).

The Kalinin–Milyukov method (Kalinin and Milyukov 1958) was used to naturalize a hydrograph with a small external impact on the hydrological regime. The Kalinin-Milyukov flow routing method conceptualizes a relation between the inflow and outflow of a river section as a linear function of water stored within the reach. According to this scheme, the water discharge at the lower boundary of the river section is calculated by the formula:

$$Q(t) = \int_0^t q(t) P(t-\tau)\, d\tau \quad (1)$$

where $Q(t)$ is an outflow of a river section at time t, $q(t)$ is an inflow of a river section at time t; $P(t)$ is the water travel time curve function:

$$P(t) = \frac{1}{\tau (n-1)!}\left(\frac{t}{\tau}\right)^{n-1} e^{-\left(\frac{t}{\tau}\right)} \quad (2)$$

where n is the number of characteristic sites with an identical travel time value equal to τ.

J. Nash (Nash 1959), independently of G. Kalinin and P. Milyukov (1958), derived the same equation for the lag-curve. The parameters used in the travel time function were determined based on the daily average water discharge series for the Don River at Razdorskaya and Khovansky for the years 1938 to 1950. This time frame was chosen due to the lack of a significant anthropogenic impact on the flow values of the Don River. In order to maintain a water balance between the above-mentioned stations, the flow hydrograph at Razdorskaya was calculated as the sum of the transformed discharge at Khovansky and the lateral inflow. The overall volume of the lateral inflow was calculated based on the difference in the flow volume of the Don between the Razdorskaya and Khovansky stations. Then it was distributed among the period of interest daily in accordance with empirical coefficients selected for the low water period, rising, and recession of the flood wave. The estimated travel time (n^*t) between the Khovansky and Razdorskaya stations was found to be equal to 21.6 days, and for the lateral inflow – 16.8 days. The quality of the performed analysis was recognized as sufficient according to the Nash-Sutcliffe performance criteria–NSE (Nash and Sutcliff 1970; Moriasi, et al. 2007). The NSE value for daily water discharge for annual and snowmelt flood periods was found equal to 0.91, for the summer-autumn period–0.97, and for winter–0.89.

Hydrological regime shift (change) point detection for annual and seasonal water flow. The time boundaries between individual long phases of increased and decreased values of annual and seasonal water flow were determined using normalized cumulative deviation curves (Andreyanov 1959; Georgiadi et al. 2018) in combination with the statistical homogeneity of the average values of the series using the Student t-test (Stepanek 2008; Lemeshko et al. 2018) and Mann-Whitney-Pettitt (MWP) test (Pettitt 1979) in the AnClim software for analysis time series. The estimates of the shift points of the contrasting phases, determined by different methods, mostly coincided with the conclusions made earlier for Russian rivers (Georgiadi et al. 2018).

Normalized CDCs represent the cumulative sum of deviations of a certain characteristic (variable) from its long-term annual average value, calculated for the entire observation period (Andreyanov 1959; Georgiadi et al. 2018). Often deviations are normalized to the coefficient of variation so that the temporal variability of dissimilar characteristics can be compared. Normalized CDCs were calculated using the following formulas:

$$CDC_\tau = \frac{1}{C_v}\sum_{i-1}^{\tau}(K_i - 1) \quad (3)$$

$$K_i = E_i / E_m \quad (4)$$

$$C_v = \frac{\sigma}{E_m} \quad (5)$$

$$\sigma = \sqrt{\frac{1}{n-1}\sum_{i=1}^{n}(E_i - E_m)^2} \quad (6)$$

where CDC_τ is the coordinate value of the cumulative deviation curve at time moment τ; E_i is the value of the i-th term of the series (i = 1, 2 … n); n is the number of terms in the time series; E_m is the long-term annual mean of the time series; K_i is the modular coefficient of the i-th term of the time series; C_v is the coefficient of variation of the time series; σ is the standard deviation of the time series.

Normalized CDCs are used to identify long-term phases (10–15 years or more) of values that have steadily increased or decreased compared to the time series averages over the entire observation period. In most of the cases considered, the necessary change points between long-term phases could be determined from the extreme (minimum or maximum) CDC values. They provide a graphical representation of the transition between different long-term phases of long-term averages for each of the hydrological characteristics.

The Student t-test and Mann-Whitney-Pettitt (MWP) test were used to identify the statistical heterogeneity of time series data, to assess the statistical significance of these deviations from the average values of the series for contrasting long-term phases of hydrological characteristics (variables), and also to determine the years in which changes occurred (change points). The MWP test and Student's t-test examined whether the average values in two different phases were the same or different.

The MWP test is a nonparametric rank-based test for identifying changes in a of a series' average. It uses cumulative sums to test the null hypothesis of no change. It divides data into two groups and investigates whether they come from the same distribution (Xie et al. 2014). It is a commonly used test primarily because it is distribution-free and insensitive to outliers and skewness in the data (Hedberg 2015; Yeh et al. 2015; Sharma and Singh 2017). The well-known Student's t-test is a parametric test based on a comparison of the mean values of two samples with unknown but equal variances (Lemeshko et al. 2018). This equality is confirmed by the results of Fisher criterion calculations for most characteristics considered in this paper for the rivers under study.

Estimation of the frequency of occurrence of low-, medium- and high-water years. A year was classified as high-water one if its annual and seasonal water flow values were not less than the flow of 25% exceedance probability and as low-water if both the annual and seasonal flow were not greater than its value with 75% exceedance probability. Accordingly, the medium-flow years were the ones with flow between 25% and 75% exceedance probability.

The assessment of the frequency of the specific water flow value was carried out based on the empirical curves of the frequency of the naturalized annual and seasonal water flow, constructed from their series for the years 1891 to 2019. The empirical value of the exceedance probability of water flow in year i (Qi), PQ_i, was calculated using the following formula:

$$PQ_i = \left(\frac{m_i}{(n+1)}\right) * 100\% \quad (7)$$

where mi is the rank position of the year in the list of discharge values in descending order, and n is the total number of water discharge values in the series.

Assessment of annual and seasonal changes in water flow in the Don River basin upstream of Razdorskaya due to climate change and anthropogenic impact. The assessment of the climate change and anthropogenic impact effects on the overall change in water flow value during the ongoing global warming period is based on a comparison of naturalized long-term annual and seasonal average water flow values for the baseline period with observed and naturalized water flow values for the modern global warming period. The time limit between the baseline period and the current period of global warming was determined using the cumulative deviation curves of the long-term air temperature values averaged over the territory of the Don River basin (Georgiadi et al. 2014). The assessment of the contribution of anthropogenic impact and global warming towards the total runoff changes is based on comparing the runoff for the base period (which was either relatively poorly affected by economic activity or, as in our case, anthropogenic changes were excluded from it) with the actual (anthropogenic-modified) and restored (conditionally natural) runoff for the period of active global warming and significant anthropogenic impact within the catchment area and the river channel itself. Furthermore, the difference between the restored (virtually natural) runoff of the second period and the quasi-natural runoff of the baseline period characterizes the effect of global warming (and related climatic changes), while the difference between the restored (conditionally natural) and actual (observed) runoff of the second period defines the contribution of anthropogenic influence on the total changes in runoff.

RESULTS

Long-term phases of annual and seasonal water flow

The annual and seasonal water flow series of the Don River at Razdorskaya are characterized by two long-term phases (Fig. 2). Moreover, a phase of increased water flow was observed at the start of the studied period (since 1891) for snowmelt flood season and annual flow values while for the summer-autumn and winter low-water seasons started with a phase of decreased flow (since 1891 and 1898, respectively).

These phases were changed in 1965 for the values of annual and melted flood flow, and in 1977 and 1979 – for values of winter and summer-autumn water flow. Apparently, they will persist for some time in the future. The duration of the identified contrasting long-term phases ranges from 30 years for the phase of increased summer-autumn flow to 86 years for the phase of reduced winter flow (Table 1).

At the same time, the duration of increased flow periods for annual and snowmelt flood flow was found to substantially exceed the duration of the opposite phases. As was previously mentioned, the opposite was true for long contrasting phases of winter water flow. The situation for the summer-autumn low-water period flow values, however, was somewhat more complex. Within the long-term reduced phase of summer-autumn flow (1898–1978), two shorter incorporated phases could be distinguished. The first one was characterized by enlarged flow values

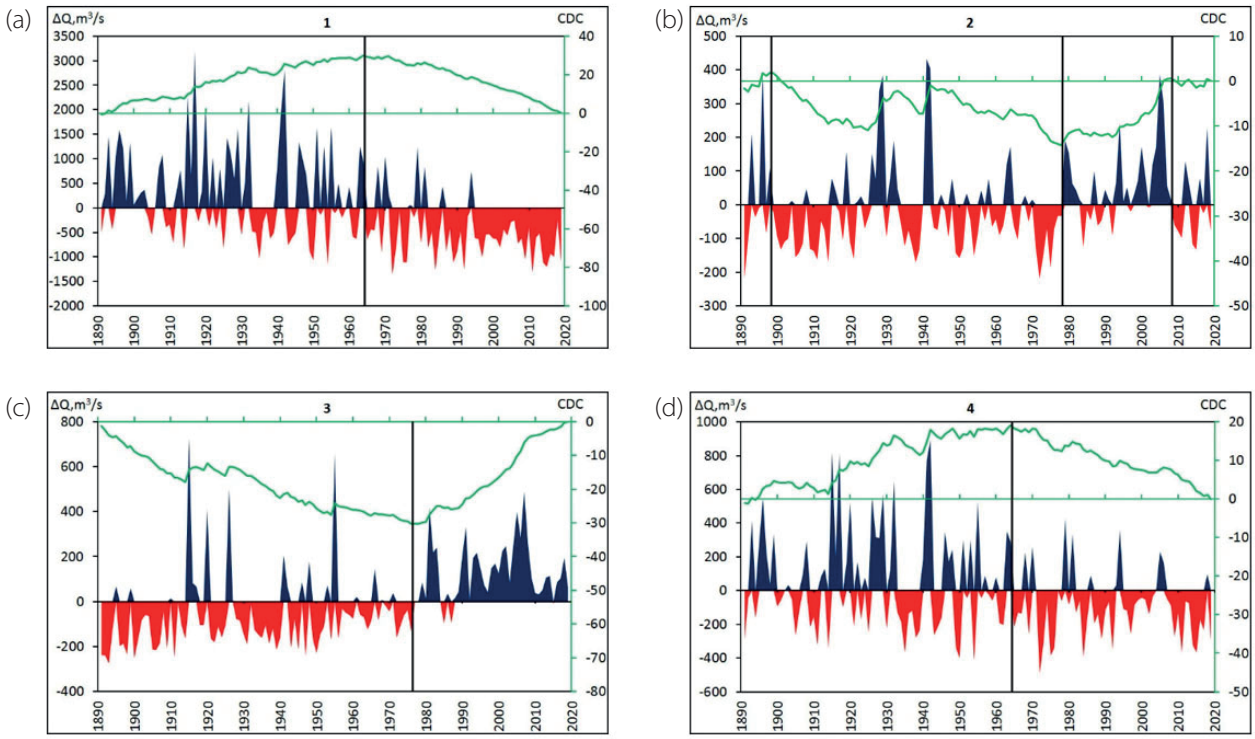

Fig. 2. Long-term changes in naturalized (a) snowmelt flood flow, (b) summer-autumn water flow, (c) winter water flow, and (d) annual average water flow of the Don River at Razdorskaya. Blue and red fields are positive and negative deviations relative to long-term averages, respectively; the green line is normalized cumulative deviation curves (CDC)

Table 1. Characteristics of contrasting phases of naturalized water flow of the Don River at Razdorskaya

Long-term phase	Water flow, km³			
	Annual (January-December)	Snow-melt flood (March-May)	Summer-Autumn (June-November)	Winter (December-February)
	Phase boundaries/phase duration (years)/average value of characteristics			
DV[a]	1965–2019/55/21.22	1965–2019/55/11.11	1899–1978/80/5.76	1891–1976/86/4.03
IV[a]	1891–1964/74/26.65	1891–1964/74/18.24	1979–2008/30/7.23	1977–2019/33/2.5
IVav[a]	26.65	18.24	7.23	4.03
DVav[a]	21.22	11.11	5.76	2.5
(IVav – DVav)	5.43	7.13	1.55	1.53
(IVav – DVav), % relative to DVav	25.6	64.2	26.9	61.2

[a] DV, IV – decreased and increased values, respectively; DVav, IVav – hydrological characteristics averaged over long-term phases of their decreased and increased values.

and observed in 1926–1933. The consequent short phase of decreased water flow was identified between 1934 and 1940.

The most noticeable difference between the flow values of different contrasting phases is observed for the winter and flood periods, where it reaches more than 60% (Table 1). The least significant deviation between phases is observed for annual flow (~25%) and the summer-autumn low-water period (27%). However, considering the shorter phase of increased summer-autumn flow, the deviation value for this season reaches 37%.

Shift point analyses of multi-year changes of annual and seasonal water flow.

Comparison of the determined shift points obtained using normalized CDCs (Fig. 2) and using criteria of statistical homogeneity (Table 2) confirmed the previously drawn conclusion (Georgiadi et al. 2018) about the similarity of the results of these methods.

Long-term changes in daily water discharge annual hydrograph.

Annual hydrographs produced based on the naturalized water discharge values and averaged over long-term phases of increased (1951–1964) and decreased (1965–2019) water flow found for annual and snow-melt flood flow data vary drastically between each other (Fig. 3). Moreover, the total volume of water coming with snow-melt as well as peak discharge values are reducing significantly during the long phase of decreased runoff. However, the time limits of snow-melt floods remain almost the same. The values of water discharge for low-water seasons (winter and summer-autumn) increase in the phase of decreased annual and flood water flow especially during the winter low-water season.

Table 2. Shift points for contrasting phases of naturalized water flow of the Don River at Razdorskaya

The direction of the change of contrasting phases	Methods				
	Cumulative deviations curve anomalies	Student - *t* test		MWP Test	
	Shift point	Shift point	*p*-Value	Shift point	*p*-Value
Snow-melt flood water flow					
Increased→Decreased	1965	1972	0.05	1972	0.01
Summer-Autumn water flow					
Decreased→Increased	1979	1979	0.05	1978	0.01
Winter water flow					
Decreased→Increased	1977	1979	0.05	1977	0.01
Annual water flow					
Decreased→Increased	1965	1965	0.05	1965	0.05

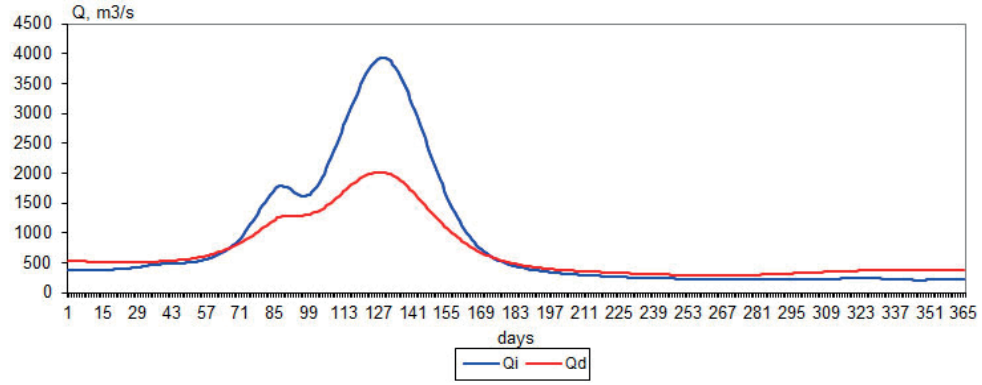

Fig. 3. Annual hydrographs of naturalized daily average water discharge (Q) of the Don River at Razdorskaya for contrasting phases of annual and snowmelt flood flow. Q_d and Q_i are water discharge values for decreased and increased water flow phases, respectively

A comparison of annual hydrographs averaged over the long-term phases of increased (for the period from 1979 to 2019) and decreased (for the period from 1945 to 1976) flow for the long-term phases of lower-water hydrological seasons shows that the hydrographs characteristic of them are close to the hydrographs of the contrasting phases of annual and flood flow considered above. The differences between them are largely explained by the mismatch of the boundaries of their contrasting phases.

River water flow frequency structure in the phases of increased and decreased annual and seasonal water flow. It was found that the number of high-water years (years with a probability of flow exceeding equal to or less than 25%) and low-water years (years with a probability of exceeding 75% or more) vary drastically during contrasting long-term phases of increased or decreased flow (Fig. 4). In this regard, the relative number of high-water years observed during the long-term increased flow phase according to the annual flow values, as well as depending on the flow rate of snow-melt flood, winter, and summer-autumn low-water seasons, has reached 35, 36, 55, and 42%, respectively.

At the same time, the proportion of low-water years during this phase was found to be significantly smaller reaching 22%, 11%, 0%, and 11%, respectively. The reverse pattern was observed for the long-term decreased flow phase (Fig. 4). Meanwhile, the total proportion of both low- and high-water years remains relatively stable changing from 40% to 52% for decreased flow phase and even less, between 47% and 56%, for increased flow phase. Thus, the proportion of years with a probability of flow exceeding from 25% to 75% (mid-water years) is also considered fairly stable and fluctuates within similar limits. It varies from 44% to 54% for the increased flow phase and between 45% and 60% for the decreased flow phase.

Changes in annual and seasonal flow values during the modern global warming period The starting point of the modern period of global warming in the Don River basin. An analysis of the curves of cumulative deviations showed that the onset of increased warming (according to air temperature values) in the study area can be attributed to 1988 (Fig. 5). Thus, the period from 1939 to 1988, characterized by relatively lower air temperatures, was taken as the base period in this study. In the Don River basin, there are significant discrepancies between the average long-term climate variables for the initial and subsequent (warmer) periods: the annual average air temperature was 6.0°C and 7.4°C, and the annual precipitation was 423 mm and 476 mm, respectively.

Annual and seasonal river water flow changes. The variability in annual and seasonal flow values due to both climate change and anthropogenic influence effect has shown ambiguous patterns (Table 3). It can be seen that during the period of modern global warming, snow-melt flood flow has noticeably decreased, while the values of winter and summer-autumn low-water flow have increased significantly. Thus, although the annual water flow for the study period decreased, but to a lesser extent than in the snowmelt flood period.

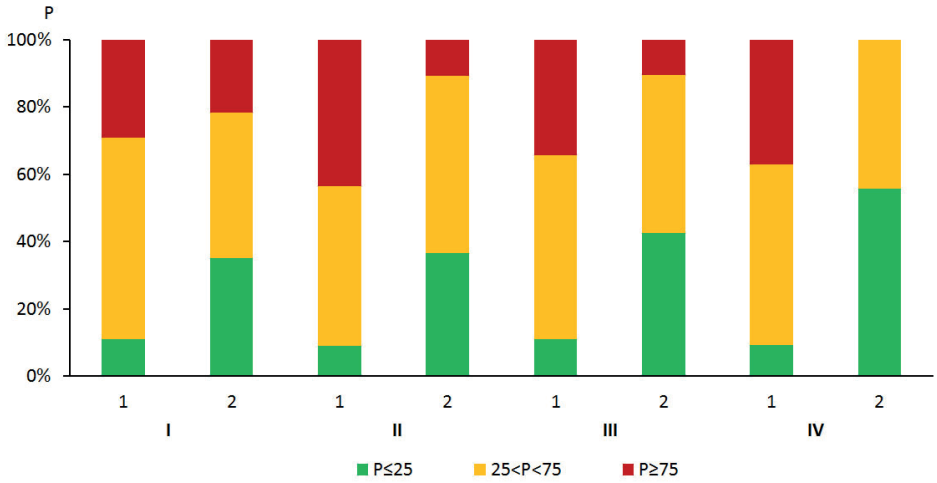

Fig. 4. Frequency structure of (I) annual, (II) snow-melt flood, (III) summer-autumn, and (IV) winter water flow in the Don River at Razdorskaya during the long-term phases of (1) increased and (2) decreased water flow. The proportion of years with water flow: red – equal to or less than that corresponding to 75% exceedance probability; yellow – greater than that corresponding to 75% and less than that corresponding to 25% exceedance probability; green – equal to or greater than that corresponding to 25% exceedance probability

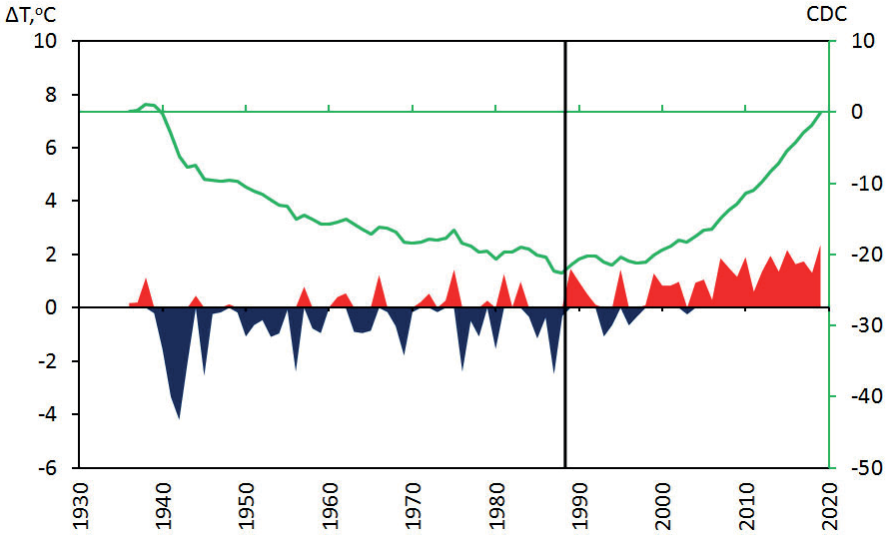

Fig. 5. Long-term changes of the annual average air temperatures in the Don River basin, expressed in the coordinates of the normalized cumulative deviation curves (CDC) and deviations from their long-term average values (red and blue fields)

Table 3. Total annual and seasonal water flow changes during the modern global warming period (1989–2019) due to cumulative climate change and anthropogenic influence effect compared to values naturalized from the baseline period (1939–1988)

Period	Naturalized long-term average flow for baseline period, km³/year	Modern global warming period		
		Actual long-term average flow, km³/year	Long-term average flow changes	
			km³/year	%
Year	24.17	19.58	–4.59	–19.0
Snow-melt flood	15.43	6.21	–9.22	–59.7
Summer-autumn low-water period	5.94	8.91	2.97	50.0
Winter low-water period	2.87	4.48	1.61	56.1

However, anthropogenic and climatic factors that caused changes in annual and seasonal water flow were unidirectional (Table 4). They resulted in a significant flow decrease during the snow-melt flood period (up to 24% and 36%, respectively). The flow during summer-autumn and winter low-water periods, in their turn, have increased due to the influence of anthropogenic and climate change-related factors. It is important to note that the respective contribution of both factors varied for winter and summer-autumn periods. If the summer-autumn flow was mainly influenced by anthropogenic causes, then the winter flow was largely influenced by factors associated with climate change.

Changes in daily water discharge annual hydrograph. The sudden transformation of annual hydrographs for observed daily water discharge values (with anthropogenic changes included) in the Don River at Razdorskaya has happened as a result of global warming influence compared to the cooler baseline period (Fig. 6).

Table 4. Anthropogenic and climate-related changes in long-term annual and seasonal average water flow over the modern global warming period (1989–2019) compared to their naturalized values for the baseline period (1939–1988)

Period	Anthropogenic changes		Climate-induced changes	
	km³/year	%	km³/year	%
Year	–1.45	–6.0	–3.14	–13.0
Snow-melt flood	–3.64	–23.6	–5.58	–36.2
Summer-autumn low-water period	1.92	32.3	1.05	17.7
Winter low-water period	0.25	8.7	1.36	47.4

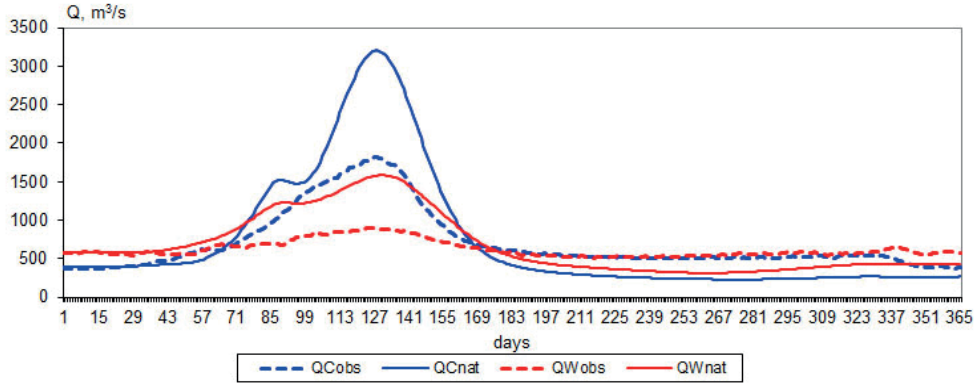

Fig. 6. Annual hydrographs of naturalized and measured (with anthropogenic influence included) daily water discharge values in the Don River at Razdorskaya for the baseline period and the period of modern global warming. QW_{nat} and QW_{obs} are naturalized and measured (with anthropogenic influence included) water discharge values, respectively, for the global warming period (1989–2019); QC_{nat}, QC_{obs} are naturalized and measured (with anthropogenic influence included) water discharge values, respectively, for the baseline period (1939–1988)

A significant reduction in both naturalized and measured snow-melt flood daily water discharges is observed during the period of intensified global warming influence. At the same time, the water discharge was found to noticeably rise in low-water seasons within the same period. On the other hand, the measured water discharges for the summer-autumn low-water season were found to almost coincide with the baseline period water discharge values while the winter flow discharges have shown a substantial increase. This irregularity was mainly caused by the Tsimlyansk Reservoir management procedure.

Changes in frequency structure of annual and seasonal river water flow. A character of deviations in the number of high-water (with the flow equal to or less than 25% exceedance probability) and low-water (with the flow equal to or more than 75% exceedance probability) years between the baseline period and the period of modern global warming considering seasonal low-water periods does not differ significantly from the ones observed for respective contrasting long-term phases of increased/decreased flow values (Fig. 7). This is due to the relatively small-time gap between these contrasting phases and the manifestation of global warming processes in the region. Consequently, the features of long-term variability between the compared periods for both cases do not vary significantly. The period of global warming almost coincided with the phase of increase in the flow of low-water seasons (winter and summer-autumn) relative to their time limits.

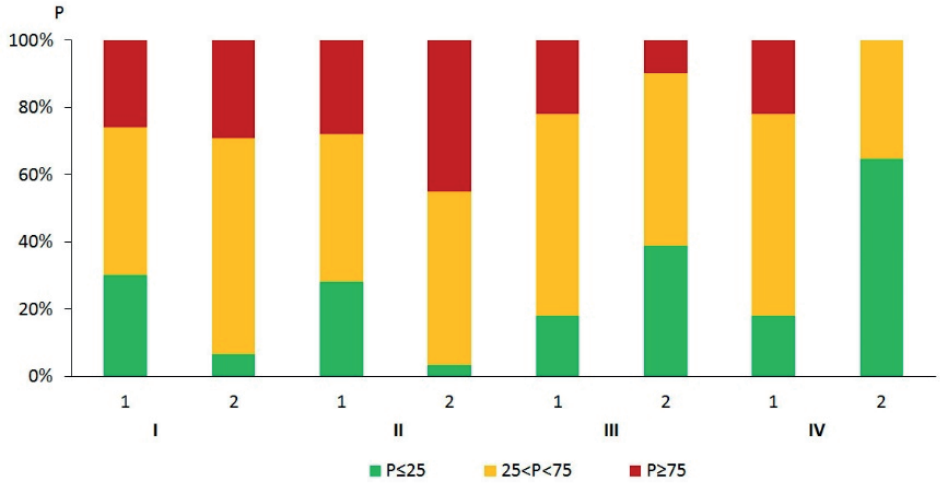

Fig. 7. Frequency structure of (I) annual, (II) snow-melt flood, (III) summer-autumn, and (IV) winter water flow of the Don River at Razdorskaya during (1) the baseline period (1939–1988) and (2) the global warming period (1989–2019). The proportion of years with water flow: red – equal to or less than that corresponding to 75% exceedance probability; yellow – greater than that corresponding to 75% and less than that corresponding to 25% exceedance probability; green – equal to or greater than that corresponding to 25% exceedance probability

The mismatch of the global warming period, starting from the shift point between the contrasting phases of annual and snow-melt flood flows, is considered to be much more significant and reaches a range of 25 years. The global warming period overlaps the part of the long-term phase of reduced annual and snow-melt flood flow values. The period before the beginning of the global warming effect on the Don River basin has incorporated phases of both increased and decreased annual and snow-melt flood flow values to an equal extent. This is the main reason for the noticeable discrepancy in the number of low-, medium- and high-water years between the contrasting phases, as well as between the background (baseline) period and the period of global warming intensification.

DISCUSSION

The time series of daily water discharge annual hydrograph in the Don River at Razdorskaya for the period of intensified anthropogenic influence (1951–2019) was naturalized using the annual hydrograph transformation method. As a result, a unique long-term series of natural annual and seasonal water flow values for 1891–2019 was obtained. This also made it possible to identify and analyze the features of the hydrological regime of the Don River, including long-term phases of increased/decreased annual and seasonal flow, the annual hydrograph of daily water discharge, as well as differences in the number of low-, medium- and high-water years. Finally, it has enabled an estimation of modern global warming on these characteristics. Thus, a sufficient contribution was made to the development of a modern methodology for studying changes in river water flow.

It is important to note that the characteristics of contrasting phases of both annual and seasonal water runoff values for the Don near Razdorskaya, as well as the contribution of climatic and anthropogenic factors to their interannual changes observed during global warming, were estimated close to the results obtained by the authors while using another method of runoff naturalization (Georgiadi et al. 2014; Georgiadi et al. 2019). That method was based on a regression model built between annual and seasonal runoff of the Don near Razdorskaya and corresponding values for the Don River at Kazanskaya and the Khoper River at Besplemyanovsky.

In contrast to estimates based on regression analysis of annual and seasonal runoff, the approach, which uses the transformation of the annual hydrograph of daily water discharges, also creates the basis for a detailed analysis of long-term changes in genetic components of seasonal and annual river runoff taking into account long-term changes in the seasonal boundaries. However, this approach also has limitations, the most serious of which is related to the limited extent of simultaneous observations during the period of the conditionally natural water regime.

Evidently, the naturalization procedure for water flow should include a set of methods, including hydrological models that describe hydrological processes with various level of detail (Motovilov et al. 1999; Kalugin 2022).

One of the main problems in studying long-term flow changes is related to the determination of shift points between contrasting multi-year phases or between the period of global warming and the base period. Generally, specialized statistical criteria for long-term series homogeneity are used (Frolova et al. 2022). Our experience of previous studies shows that the optimal set of methods for identifying the time boundary between heterogeneous periods includes the mentioned criteria (parametric and non-parametric), as well as the analysis of the cumulative deviation curve (Georgiadi et al. 2018; Georgiadi and Groisman 2022). This makes it possible to determine the shift points with a high degree of certainty.

Although there is some progress in studies of long-term phases of hydrological characteristics, including those made for the territory of Russia, many issues still require further investigation. This covers specifically the spatial distribution patterns of characteristics of long-term contrasting flow phases. At the same time, promising results have been presented already concerning the synchronism of long-term contrasting phases of seasonal runoff on the rivers of the Russian Plain (Georgiadi et al. 2014) and the regionalization of the territory of Russia with respect to the boundaries of the change of long-term periods of increased/decreased annual and maximum runoff (Frolova et al. 2022) and changes in the pattern of the intra-annual distribution of runoff on the rivers of the Russian Plain during the period of global warming (Ivanov et al. 2022).

One of the important methodological problems while assessing the impact of global warming on river runoff is to determine both its spatial boundaries, as well as temporal boundaries of the baseline period with which the characteristics of river runoff are compared. The shift points between the long-term phases of decreased and increased values of annual air temperature averaged for the Don basin over the 1939–2019 period was used as the starting point of global warming effects in the Don basin in this study (1989). It should be noted that, in order to assess the scale of modern changes in river flow associated with global warming, the characteristics of two periods with different climate conditions were compared. The choice of a time boundary between them was not always justified. Therefore, it was often suggested to use different years (1978, 1980, etc.). The study area's spatial coverage, meanwhile, covered extremely large areas. Occasionally, the main reason for choosing certain years as the time limits of the compared periods was lying in the need to have a sufficient duration of each of the compared periods so that statistically reliable estimates could be obtained (Georgiadi and Kashutina 2016). Often, the transition between long periods (phases) of decreased and increased flow, which are evidently related to global warming, has served as justification for choosing a specific year as the boundary. However, it turned out that the boundaries between contrasting flow phases differ significantly not only for rivers of different regions but also for annual and seasonal flow volumes of the same river (Georgiadi 2014; Georgiadi et al. 2019; Milyukova et al. 2020; Georgiadi et al. 2020; Georgiadi and Groisman 2022; Frolova et al. 2022, etc.).

The points of contrasting phases shifting, in general, do not coincide for river flow and air temperature and may differ very significantly. Due to differences in estimates of both the global warming and baseline period boundaries, the results of runoff variation assessment differ as well. However, in most cases, those differences are not so significant. For instance, the estimates for the Don given in this article compared to our previous publications (Georgiadi et al. 2014; Georgiadi et al. 2019) differed considerably only for winter runoff although other boundaries for the compared periods and different methods of naturalizing annual and seasonal runoff were used there.

CONCLUSIONS

The long-term series of naturalized natural monthly water flow values of the Don River at Razdorskaya from 1891 to 2019 was obtained by the exclusion of human-induced flow changes (mainly those explained by interannual and seasonal water flow regulation of the Tsimlyansk Reservoir in 1951–2019). This was done based on the transformation of the annual hydrograph of daily water discharge of the river. The described procedure allowed determining and analyzing features of the Don River's hydrological regime such as annual hydrograph of daily water discharge, long-term phases of increased/decreased annual and seasonal flow, and differences in the number of low-, medium-, and high-water years between these phases. In addition, an analysis of modern global warming was carried out on the basis of this.

Two long-term phases of annual and seasonal flow were identified. The shift points obtained using the normalized cumulative deviation curve analysis and statistical homogeneity tests were almost identical, which means a high level of reliability of these methods. The comparison between the distinguished contrasting phases has shown significant differences in values between both periods. Annual and snowmelt flood flow values have entered a phase of increased flow since the 1890s, while the phase of decreased flow was observed for the winter and summer-autumn low-water seasons. In the 1960s and 1970s these phases changed. The duration of contrasting phases for different seasons varied from 30 to 86 years. The most recognizable deviation between flow values in different phases were observed during the winter low-water season and snow-melt flood when it has reached over 60%. Significantly smaller variation was typical for the annual (~25%) and summer-autumn period (27%).

The annual hydrographs of daily average naturalized water discharge averaged over long-term phases of increased and decreased water flow found based on annual and snow-melt flood flow values series have shown noticeable dissimilarity. Peak and volume of snow-melt water runoff were noticeably reduced in the long phase of decreased water flow. However, the time limits of the snow-melt flood in contrast long phases does not differ significantly. On the contrary, during low-water seasons, especially in winter, the water flow increases.

The share of high-water years in the phase of increased flow is significantly higher than the share of low-water years, although the cumulative share of low- and high-water years remains relatively stable. Thus, the proportion of medium-water years (25–75% exceedance probability) is also considered sufficiently stable during any contrasting phase.

During the modern global warming period (which was observed in the region through increased air temperatures since 1989) the changes in annual and seasonal flow was caused by both anthropogenic and climate change-related factors, and thus, has shown an ambiguous nature. It could be seen that snow-melt flood flow has been reduced noticeably during the modern global warming period while the flow in winter and summer-autumn low-water periods have risen substantially. Thus, even though the annual water flow has decreased over the studied period, the reduction was to a lesser extent than that of the snow-melt flood period.

Anthropogenic and climate change-related changes in annual and seasonal flow during the global warming period was unidirectional. They resulted in a significant decrease in the snow-melt flood flow. At the same time, the flow increased in the summer-autumn and winter low-water seasons under their influence. It should be noted that the corresponding contribution of both factors were different for the winter and summer-autumn seasons. If the summer-autumn water flow was mainly influenced by anthropogenic causes, then the winter flow was largely influenced by factors associated with climate change.

The sudden transformation of annual hydrographs for observed (with anthropogenic changes included) and naturalized daily average water discharge values has happened under the influence of global warming compared to the cooler baseline period. A significant decrease in values of both measured and naturalized snow-melt flood water discharge was observed, while the low-water seasons were characterized by a noticeable rise in river water flow. Despite a significant increase in winter flow, water discharge in the summer-autumn season did not significantly exceed baseline values. This unevenness is mainly caused by the peculiarities of the management of the Tsimlyansk Reservoir.

Since the shift points for the global warming period and long-term phase of increased naturalized flow for low-water seasons almost coincide, the deviation in frequency of low-, medium-, and high-water years occurrence does not differ significantly. However, the substantial discrepancy between the time boundaries of phases of both reduced annual and snow-melt flood flow and of the global warming period results in noticeable differences in the number of low-, medium-, and high-water years.

REFERENCES

Andreyanov V.N. (1959). Cyclic fluctuations of annual water flow and their accounting for hydrological calculations. Proc. SHI. Flow calculations. Gidrometeoizdat: Leningrad, USSR, 686 3-50 (in Russian).

Arc Atlas: Our Earth (1996). MacOdrum Library – Carleton University [online]. Available at: https://library.carleton.ca/find/gis/geospatial-data/arc-atlas-our-earth [Accessed 29 Oct. 2021].

Bolgov M.V., Filippova I.A., Osipova N.V., Korobkina E.A. and Trubetskova M.D. (2018). Current features of the hydrological regime of rivers in the Volga Basin. Hydrological Changes. Problems of Geography, 145, 206-221 (in Russian).

Frolova N.L., Magritskii D.V., Kireeva M.B., Grigor'ev V.Y., Gelfan A.N., Sazonov A.A. and Shevchenko A.I. (2022). Streamflow of the Russian rivers under current and forecasted climate chfnges. A review of publications. 1. Assessment of changes in the water regime of Russian rivers by observation data. Water Resources, 49(3), 333-350, DOI: 10.1134/S0097807822030046.

Georgiadi A.G. and Groisman P.Ya. (2022). Long-term changes of water flow, water temperature and heat flux of two largest arctic rivers of European Russia, Northern Dvina and Pechora. Environmental Research Letters, 17(8), DOI: 10.1088/1748-9326/ac82c1.

Georgiadi A.G. and Kashutina E.A. (2016). Long-Term Runoff Changes of the Largest Siberian Rivers. Izvestiya Rossiiskoi Akademii Nauk, Seriya Geograficheskaya, 5, 70-81 (in Russian).

Georgiadi A.G., Kashutina E.A. and Milyukova I.P. (2019) Long periods of increased/decreased runoffs of large Russian rivers. IOP Conf. Ser.: Earth Environ. Sci., 386, 012-048, DOI: 10.1088/1755-1315/386/1/012048.

Georgiadi A.G., Koronkevich N.I., Milyukova I.P., Kashutina E.A. and Barabanova E.A. (2014). Contemporary and Scenario Changes in River Runoff in the Basins of the Largest Russian Rivers. Part 2. Basins of the Volga and Don. Maks Press: Moscow, Russia (in Russian).

Georgiadi A.G., Kashutina E.A. and Milyukova I.P. (2018). Long-term changes of water flow, water temperature and heat flux of the largest Siberian rivers. Polarforschung, 87(2), 167-176, DOI: 10.2312/polarforschung.87.2.167.

Georgiadi A.G., Milyukova I.P. and Kashutina E.A. (2020). Contemporary and scenario changes in river runoff in the Don Basin. Water Resources, 47, 913-923, DOI: 10.1134/S0097807820060068.

Georgievskii V.Yu. and Moiseenkov A.I. (1984). Restoration of natural hydrographs of the flow of large rivers, regulated by a cascade of reservoirs (the example of the Volga River). Proc. SHI, 291, 54-61 (in Russian).

Hedberg S. (2015). Regional Quantification of Climatic and Anthropogenic Impacts on Streamflows in Sweden. Institutionen för geovetenskaper: Uppsala, Sweden.

Hinzmann L.D., Bettez N.D., Bolton W.R., Cyapini F.S., Dyurgerov M.B., Fasti C.F., Griffith B., Hollisters R.D., Hope A., Hantington H.R., et al. (2005). Evidence and implications of recent climate change in Northern Alaska and other Arctic regions. Climatic Change, 72, 251–298, DOI: 10.1007/s10584-005-5352-2.

Ivanov A.M., Gorbarenko A.V., Kireeva M.B. and Povalishnikova E.S. (2022). Identifying climate change impacts on hydrological behavior on large-scale with machine learning algorithms. Geography, Environment, Sustainability, 3(15), 80-87, DOI: 10.24057/2071-9388-2022-087.

Kalinin G.P. and Milyukov P.I. (1958). Approximate Calculation of Unsteady Motion of Water Masses. Proceedings of the Central Institute of Forecasts. Gidrometeoizdat: Leningrad, USSR, 66, 72 p. (in Russian).

Kalugin A. (2022). Hydrological and meteorological variability in the Volga River basin under global warming by 1.5 and 2 degrees. Climate, 10, 107, DOI: 10.3390/cli10070107.

Kireeva M.V., Ilich V.P., Sazonov A.A. and Mikhaylyukova P.G. (2018). An assessment of changes in land use and their impact on Don River basin runoff using satellite imagery. Sovremennye problemy distantsionnogo zondirovaniya Zemli iz kosmosa (Current problems in remote sensing of the Earth from space), 15(2), 191-200 (in Russian).

Kuzin P.S. (1979). Cyclic fluctuations in the water flow of rivers of the Northern hemisphere. Gidrometeoizdat: Leningrad, USSR (in Russian).

Lemeshko B., Lemeshko S., Veretelnikova I. and Novikova A. (2018). On the application of checking criteria for homogeneity of means. Bulletin of Siberian State University of Telecommunications and Informatics, 1, 41-55 (in Russian).

Magritsky D.V. (2015). Factors and trends of the long-term fluctuations of water, sediment and heat flux in the lower reaches of the Lena River and the Vilyui River. Moscow University Bulletin. Series 5, Geography, 6, 17-30 (in Russian).

Milyukova I.P., Georgiadi A.G. and Borodin O.O. (2020). Long-term changes in water flow of the Volga basin rivers. E3S Web of Conferences, 163(2), 05008, DOI: 10.1051/e3sconf/202016305008.

Motovilov Y.G., Gottschalk L., Engeland K., and Rodhe A. (1999). Validation of a distributed hydrological model against spatial observations. Agricultural and Forest Meteorology, 98, 257-277.

Moriasi D.N., Arnold J.G., Van Liew M.W., Bingner R.L., Harmel R.D. and Veith T.L. (2007). Model evaluation guidelines for systematic quantification of accuracy in watershed simulations. Transactions of the ASABE, 50(3), 885-900, DOI: 10.13031/2013.23153.

Muraveisky S.D. (1960). Rivers and lakes, Hydrobiology. Runoff. Geografgiz: Moscow, USSR, 388 p. (in Russian).

Nash J.E. (1959). Systematic determination of unit hydrograph parameters. Journal of Geophysical Research, 64, 111-115.

Nash J.E. and Sutcliff J.V. (1970). River flow forecasting through conceptual models. Part I—A Discussion of Principles. Journal of Hydrology, 10, 282-290.

Pettitt A.N. (1979). A non-parametric approach to the change-point problem. Journal of the Royal Statistical Society. Series C (Applied Statistics), 28, 126-135.

Sharma S. and Singh P.K. (2017). Long term spatiotemporal variability in rainfall trends over the state of Jharkhand. India Climate, 5, 2-18.

Shi X., Qin T., Nie H., Weng B. and He Sh. (2019). Changes in major global river discharges directed into the ocean. Int. J. of Environ. Res. And Public Health, 16(8), 1-19, DOI: 10.3390/ijerph16081469.

Shiklomanov I.A. and Georgievskii V.Yu. (2007). Effect of climate changes on the hydrological regime and water resources of Russian rivers. Proc. British–Russian Conf. "Hydrological Effects of Climate Changes", Novosibirsk, Russia, 143–151 (in Russian).

Shiklomanov A.I., Golovanov O., Lammers R.B., Tretjyakov M. and Yang D. (2011). Dam/Reservoir-Induced Hydrological Changes in Large Siberian Rivers. Amer. Geophys. Union, Fall Meeting 2011, Abstract C31B-06.

Shiklomanov A.I., Lammers R.B., Lettenmaier D.R., Polischuk Yu., et al. (2013). Hydrological changes: historical analysis, contemporary status, and future projections in Regional Environ. In: Changes in Siberia and Their Global Consequences, Ch. 4, Editor 1, Groisman, P.Ya., Editor 2, Gutman, G. Springer Sci.+Business Media: Dordrecht, Netherlands, 111–154.

Shiklomanov A., Déry S., Tretiakov M., Yang D., Magritsky D., Georgiadi A. and Tang W. (2020). River Freshwater Flux to the Arctic Ocean. In: Arctic Hydrology, Permafrost and Ecosystems. Editor 1, Yang, D., Editor 2, Kane, D.L. Springer: Cham, Switzerland, 703-738, DOI: 10.1007/978-3-030-50930-9_24.

Scientific and applied reference: Long-term fluctuations and variability of water resources and the main characteristics of the flow of rivers of the Russian Federation (2021). REAL: St. Petersburg, Russia, 190 p. (in Russian).

Sokolovskii D.L and Shiklomanov I.A. (1965). Calculations of flood hydrographs using electronic modeling devices. Proc. LGMI, 23, 65-79 (in Russian).

Stepanek P. (2008). AnClim–software for time series analysis [online]. Department of Geography, Faculty of Sciences, Masaric University, Brno, Czech Republic. Available at: http://www.climehom.eu [Accessed 29 Oct. 2021]

Stuefer S., Yang D. and Shiklomanov A. (2011). Effect of stream flow regulation on mean annual discharge variability of the Yenisey River. IAHS Publ., 346, 27-32.

Varentsova N.A., Grechushnikova M.G., Povalishnikova E.S., Kireeva M.B., Kharlamov M.A. and Frolova N.L. (2021). Influence of climatic and anthropogenic factors on spring runoff in the Don basin. Bulletin of the Moscow University. Series 5. Geography, 5, 91-108.

Water Resources of Russia and their Use (2008). State Hydrological Institute: St. Petersburg, Russia (in Russian).

Xie H., Li D. and Xiong L. (2014). Exploring the ability of the Pettitt method for detecting change point by Monte Carlo simulation. Stochastic Environmental Research and Risk Assessment, 28, 1643-1655, DOI: 10.1007/s00477-013-0814-y.

Zhuravlev S.A., Georgievsky V.Yu., Balonishnikova Zh.A. and Shamin S.I. (2022). Water management / Third assessment report on climate change and its consequences on the territory of the Russian Federation / Edited by V. M. Kattsov; Rosgidromet: St. Petersburg, Russia, 344-356 (in Russian).

Yeh C.-F., Wang J., Yeh H.-F., Lee C.-H. (2015). Spatial and temporal streamflow trends in Northern Taiwan. Water, 7(2), 634-651, DOI: 10.3390/w7020634.

RESEARCH PAPER

PERCEPTIONS OF VILLAGERS ON ENVIRONMENTAL DEVELOPMENT OF RURAL CHINA IN THE CONTEXT OF RAPID URBANIZATION

Xiaolei Zhao[1, 2], Shuo Shen[1], Haiying Teng[1], Shuping Zhang[1*], Renqing Wang[1]

[1]School of Life Sciences, Shandong University, No. 72 Binhai Road, Jimo District, 266237, Qingdao, Shandong Province, P.R. China

[2]Changle No.2 Middle School, No.7 Xinzheng West Street, Changle County, Weifang, Shandong Province, P.R. China

***Corresponding author:** spzhang@sdu.edu.cn

Received: April 15th, 2022 / Accepted: May 4th, 2023 / Published: July 1st, 2023

https://DOI-10.24057/2071-9388-2022-063

ABSTRACT. In the context of rapid urbanization, pollution and ecological degradation problems have frequently shown up and influenced environmental sustainability of rural China in the past decades. The rural residents have begun to pay attention to local environment protection, and researchers have been taking public perceptions into regional planning. However, comprehensive studies on the perceptions of villagers on rural environment development still remain less.

This research carried out a face-to-face questionnaire investigation of 187 villages and ten residents from each village at a nationwide scale of China. The investigated village committee managers and residents were interviewed by asking the questions including the existing environmental problems, the targets of rural environment development, the ways to achieve these targets and the willingness to pay for pollution control. The results showed that household waste pollution, air pollution and pesticides pollution etc. are top concerned problems. A big proportion (65%) of the interviewed residents chose "environment with good quality for health" as their preferred living environment. While, more than half of the interviewed village managers took "green villages with sustainable agriculture" as their village development targets. And more than 50% of the interviewed residents advocated to increase the forest coverage rate to mitigate the degeneration of rural ecosystem services. As well, most residents strongly support rural green development and are willing to pay for pollution control. Our findings may provide new insights into rural environment development and rural revitalization in the context of rapid urbanization.

KEYWORDS: green development, environment sustainability, public participation, rural revitalization, urbanization

CITATION: Zhao X., Sheng S., Teng H., Zhang S., Wang R. (2023). Perceptions Of Villagers On Environmental Development Of Rural China In The Context Of Rapid Urbanization. Geography, Environment, Sustainability, 2(16), 18-30
https://DOI-10.24057/2071-9388-2022-063

ACKNOWLEDGEMENTS: This work is supported by the National Key Technology R&D Program (2013BAJ10B0403) and Shandong Provincial Science and Technology Development Program (2010GSF10618). Thanks to Edward Mignot, Shandong University, for linguistic advice.

Conflict of interests: The authors reported no potential conflict of interests.

INTRODUCTION

China is a traditional agricultural country confronting rapid urbanization. The seventh national census in 2020 showed that the rural population covered 36.11% of the total population in China. Compared with the sixth national census in 2010, the proportion of urban population has increased by 14.21 percentage points. Rural development of China matters for the prosperity of the whole country. Urban-rural integration strategy provided a potential way to narrow the development gap between urban and rural areas, therefore to change the dual structure between urban and rural areas (Jing and Zhang 2003; Shi 2013). However, at the present stage, the rural natural environment is confronting rapid changes, some of which lead to the imbalance of the existing rural natural ecosystems and serious destruction of some rural settlements locally (Zhang 2022).

Both environmental pollution and ecological degradation of rural areas in China have accumulated in the past decades. The first national pollution census report published in 2010 showed that the emissions of rural pollutants has accounted for half of the total of the whole country, in which COD (chemical oxygen demand) accounted for 43%, total nitrogen accounted for 57% and total phosphorus covered 67% (The Environmental Protection Agency 2010). The National Environmental Bulletin summary between 2010 and 2013 showed that the rural ecological and environmental problems of China mainly concentrated in water pollution, soil pollution and cultivated land degradation.

These problems are caused by livestock and poultry pollution, rural industrial pollution, rural household waste pollution, agricultural non-point source pollution and transfer of urban-rural pollution etc. (The Environmental

Protection Agency 2011; The Environmental Protection Agency 2012; The Environmental Protection Agency 2013; The Environmental Protection Agency 2014). The rural ecological and environmental deterioration has already affected the agricultural production and daily life of the rural residents seriously, even resulting in occurrence of cancer village phenomenon (Liu 2013).

The perceptions of the local residents on the environment and their behaviors might produce dramatic effects on rural environment protection (Zhang et al. 2016). Environmental behaviors of rural residents mediated by their perceptions on environmental development therefore influence the environmental protection practices (Tian et al. 2011). Scholars generally believe that the multi-governance model is the inevitable choice of rural environment pollution control, and the public should be involved in rural environment management (Xiao and Zhu 2016). Thus, to understand and mitigate degradation of the rural ecological environment in the context of urban-rural integrative development and rapid urbanization, it is crucial to make sense of the perceptions of villagers on the future of the rural environment.

Integrating public perceptions in decision making can improve the management efficiency (Donaldson-Selby et al. 2007; Kobori and Primack 2003) and provide more people with opportunities of realizing their demands (Lestrelin et al. 2011). As early as in the "Rio Declaration on Development", integrating public perceptions via public participation mechanism has been taken into account as an important prerequisite for sustainable development (The United Nations, 1992). Later, the role of integrating public perception in decision-making has been highlighted frequently (Macnaghten and Jacobs 1997; Meadowcroft 1997). Public perceptions have significant positive impacts on villagers' cooperative management of household waste, and the local governments should enhance and internalize villagers' perception (Lin et al. 2021). As well, the emerging successful models of new villages and beautiful villages guided by central and local governments and driven by communities demonstrated the importance of involving local residents during rural environment protection (Gao et al. 2020).

Recently, researchers and local officers of China have been taking public perceptions into regional planning in various ways. However, the perceptions of residents on rural development and environment planning sometimes are less considered (Gu et al. 2013). It has resulted in occurrence of some serious conflicts among rural residents, decision makers and other stakeholders (Wu and Wang 2013). Actually, the perception of villagers may provide very different perspectives on rural development and environmental protection. As well, their experiences with the living surroundings may confer them valuable wisdom to solve the conflicts between development and environment protection. Thus, it is critical to understand the perceptions of rural residents on the existing and potential environment problems under the context of rapid urbanization.

To understand the perceptions of rural residents and local managers on the existing and potential problems as well as possible solutions, we investigated 1867 residents and 187 managing committees from 187 villages by face-to-face questionnaire interviews. By analyzing the perceptions of the villagers and managers on rural development and environment protection, we try to answer the following three questions. (1) What are the existing perceptible serious environmental problems in rural areas of China? (2) From the perspectives of local villagers, what are the preferred alternative targets of rural environment development and the practical ways to achieve these targets? (3) What is the willingness of villagers to participate in the future rural environment improvement?

MATERIALS AND METHODS

Design of the interview questionnaire

In order to obtain reliable data, we used an on-site face-to-face interview questionnaire. The questionnaire included two parts and 25 questions: 15 questions for residents and 10 questions for village managers (director or vice director of the village administrative committee) (See Appendices Questionnaire).

The questionnaire consists of questions of four aspects including local existing ecological environment problems, alternative targets of rural environment development, possible ways to achieve the targets of rural environment development and the willingness of villagers to involve into rural environment improvement.

Sampling strategy of villages and residents

We chose 187 villages of 24 provinces, cities and autonomous regions from the Northeast, North, East, Central, South, Southwest and Northwest part of China for investigation during January to October of 2014 (Fig. 1). On average, six to nine villages from each province were randomly sampled for the investigation. The sampled villages included large settlements close to the near cities, large villages close to the towns and small hamlets far from the towns. One manager and five to ten randomly selected residents of each village have been interviewed and questioned. Totally 187 village managers and 1867 residents were sampled. In order to guarantee that the questionnaires can reflect the real condition of each region, the interviewees with different gender, age, career were involved (Table 1).

To control the consistency of the questionnaire process and to avoid the influences of personal differences among interviewers, a training workshop and a pilot survey has been organized in January of 2014. And an instant communication mechanism has been established and worked until the end of all surveys. The trained interviewers completed questionnaires for managers and residents by face-to-face interview and each interview lasted about ten minutes. Considering some respondents are poorly educated, part of the questions was answered by the respondents and recorded by the interviewers. At the same time, the relationships with respect and trust between interviewers and interviewees were established, to ensure the data are true and correct.

Data analysis

All the collected data were compiled using Microsoft Excel (ME). The descriptive statistics, bar plot and pie plot on categorical variables were done using Origin2016. And the distribution map of sampled villages was drawn using Geographic Information System (GIS).

RESULTS

The existing problems of rural ecological environment perceived by villagers

The results showed that household waste pollution, air pollution, water pollution, soil pollution, vegetation degradation and farmland occupation etc. are common concerns of the managers and residents in rural areas.

Table 1. The proportional composition of the interviewed residents by gender, age, education and profession

Characteristics	Categories	Proportion (%)
Gender	Female	42
	Male	58
Age	Under 18	0.3
	18-64	94
	65 and more	6
Degree of education	Under middle school	61
	High school	27
	Junior college	6
	Bachelor degree	12
	Master and Ph.D degree	0.4
Profession	Farmer	45
	Worker	27
	Village manager	9
	Teacher	5
	Doctor	2
	Priviate business owner	10
	Civil servant	2
	Others	0.7

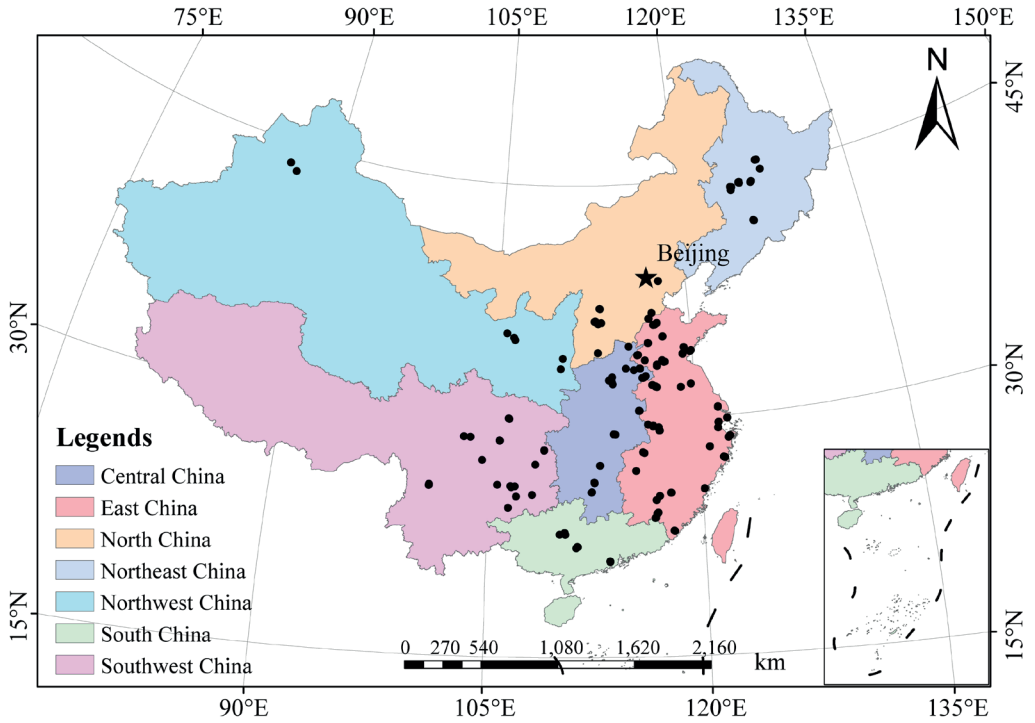

Fig. 1. The map of the locations of 187 sampled villages using solid black dots

Amongst the household waste pollution, air pollution, pesticides pollution, water pollution, straw burning and livestock and poultry manure etc. ranked in turn (Fig. 2).

The percentage values indicated the proportion of interviewed residents, who choose the option as the most serious existing environmental problem (Fig. 2).

Household waste pollution took the top problem the villagers claimed, particularly the kitchen organic waste. The average annual production of kitchen organic waste reaches to 27 kg per household (Fig. 3). Most kinds of household waste could be recycled and reused such as glasses, paper, metal waste, hard plastic and cans etc. However, the interviewees seriously claimed the kitchen

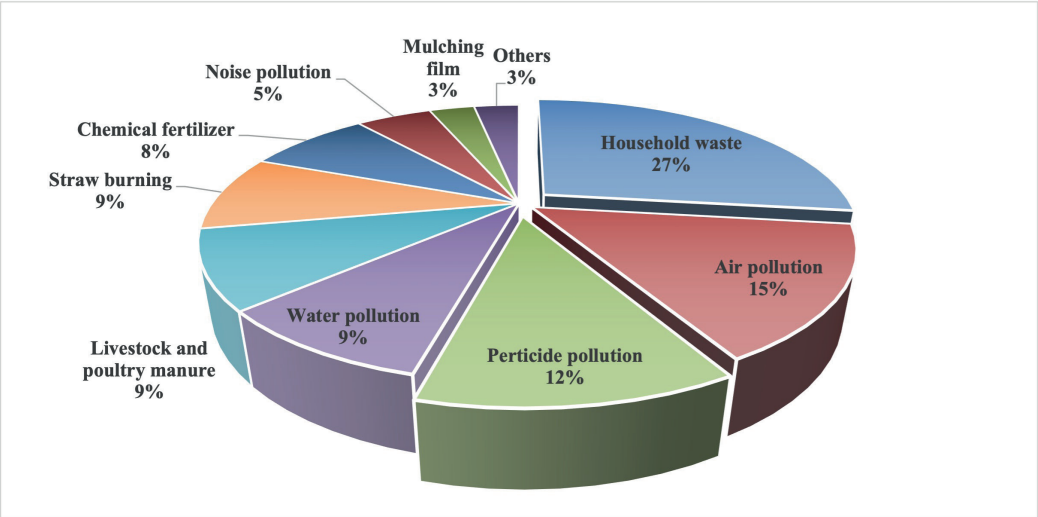

Fig. 2. The pie chart of top ten existing environmental problems from perceptions of residents

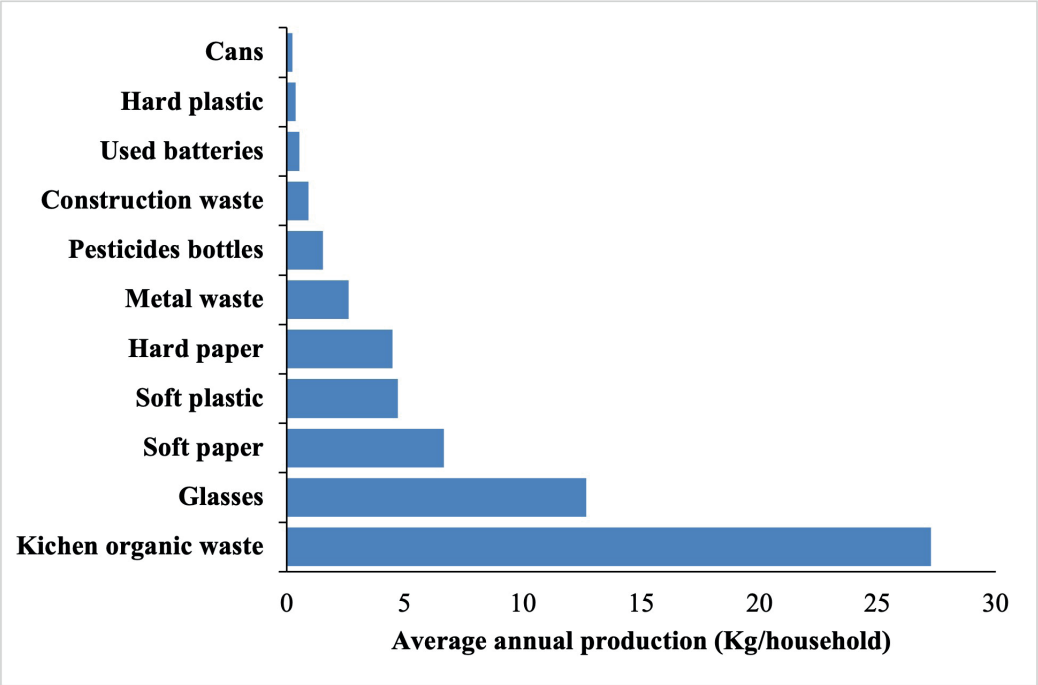

Fig. 3. The bar chart of average annual production (Kg/household) of different kinds of household wastes of the sampled villages

organic waste mixing with soft plastic bags and packages, because the organic waste is easy to get stink and the soft plastics is difficult to degrade.

Amongst the household wastes, the average annual production of kitchen organic waste took first place (Fig. 3). As the second concerned environment problems, air pollution was frequently claimed by interviewees (Fig. 2). And 97% of the interviewees thought that the straw burning during harvesting seasons, coal burning for heating in winter and industrial pollution contribute much to the air pollution in the rural areas. Otherwise, water pollution took the top fourth existing environmental problems (Fig. 2). 96% of interviewees said that surface water pollution is "common". The lack of basic sewage infrastructure is one of the main reasons. 73% of the investigated villages have no sewage treatment facilities, all their sewage discharge into rivers or ponds directly without any treatments. The household sewage discharge and agricultural non-point source pollution (ANPSP) were considered to contribute much more to the surface water pollution.

From the perceptions of the interviewed village managers, the existing environmental problems are interacted with each other and the pollution sources are various. The surface water and soil share many pollution sources such as household waste, sewage and ANPSP. Amongst the interviewee, 99% of them think that pesticides, chemical fertilizer and herbicides are the main pollution sources of soil. Most of the pollutants in soils could be washed into the surface water and ground water by rain runoff.

Besides the physical environment, the degradation of ecosystem structure, function and their services are a common concern of the interviewees. The interviewees, who thought these phenomena are visible and perceptible deterioration of rural ecological environment, commonly claimed that farmland occupied by industries and urban, deforestation and species reduction.

The perceptions of villagers on the alternative targets of rural environment development

From the perceptions of the interviewed residents, their preferences on the living neighborhood environment were concentrated. A big proportion (65%) of the interviewees chose "environment with good quality for health" as their preferred living environment. The option "environment with good quality for health" means that

the environmental quality meets basic requirements of "Guidelines for the construction of beautiful village (GB/T 32000-2015)". Whereas, only 17% of the interviewees chose "convenience for employment" and 9% of them chose "big houses" or "go to school with convenience". It indicates that the value and recognition of villagers on environmental quality are increasing.

Concerning the alternative development targets of the villages, more than half of the interviewed village managers took "green villages with sustainable agriculture". As well, "ecological villages with tourism" and "rich villages with industries" also were favorite targets of more than ten percent of the village managers. A few interviewees chose villages with labor output or move to the cities nearby as their development targets (Fig. 4).

The pie chart showed that most village managers choose "Green villages with sustainable agriculture", but few village managers choose "Villages with Labor output" or "Keep the status quo" (Fig. 4).

To achieve the green targets of rural environment development, the interviewed residents and village managers have different perspectives. Overall, 51% of the interviewed residents prefer to "move to the combined new neighborhoods with apartments". The combined new neighborhoods with apartments usually are equipped similarly to urban neighborhoods but located in places near the villages. However, there was only 37% of the village managers took this option. 39% of the village managers chose to "live in the original neighborhoods with environmental improvement".

Otherwise, the preferred possible ways of residents to achieve the environmental development targets were various among sampled regions. To the option "combine villages into new neighborhoods", a regional strategy aiming at radically improving the rural living environment and enhancing rural environment infrastructure, the residents of the North and Northwest of China more like to "move to the combined new neighborhoods with apartments" than the residents do from other regions. Comparatively the residents from East and Southeast China prefer to "live in the original neighborhoods with environmental improvement" (Fig. 5).

The seven regional parts of China were referred to as the Northwest, Southwest, South, Central, East, North, and Southeast respectively. The four alternative options to achieve the rural environment targets include (A) Move to the cities nearby; (B) Move to the new combined neighborhoods with apartments; (C) Live in the original neighborhoods with environment improvement; and (D) Others (Fig. 5).

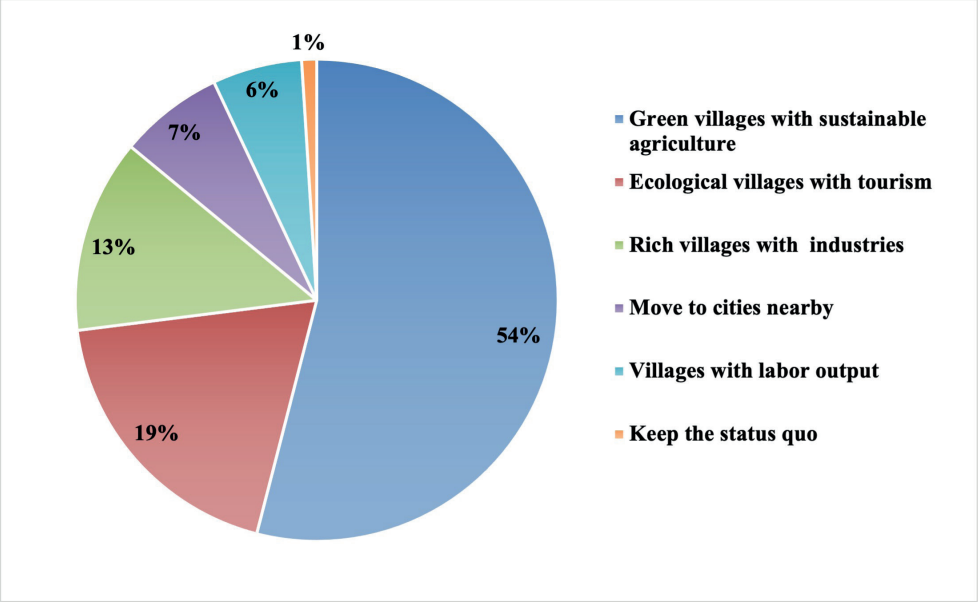

Fig. 4. The pie chart of proportions of village managers took alternative targets of rural environment development

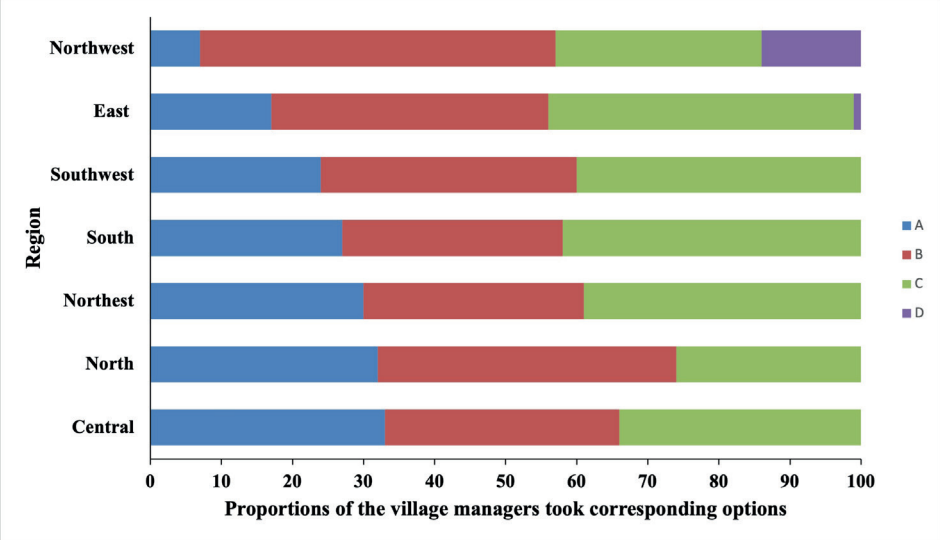

Fig. 4. The stack bar chart of the proportions of the interviewees choose respective possible ways to achieve the rural environment targets

To cope with the ecological environment degradation problems, more than 50% of the residents from all regions advocated to increase the forest coverage rate, which is expected to mitigate the degeneration of ecosystem services. However, the perceptions of the residents on other prior approaches differed among regions. The residents from Southwest China prior to restoring degraded mines, while the residents from South China thought limiting groundwater exploitation is more urgent instead. Otherwise, more than 20% of the interwiewees from Northwest, East and Central part of China highlighted the importance of choosing safe areas for construction of the combined new neighborhoods to avoid possible natural and man-made disasters.

The willingness of villagers to involve into rural environment improvement

A great proportion of villagers are willing to be involved in the related activities of rural environment improvement in various ways. Fifty percent of the residents are willing to "participate in the related activities as volunteers", 37% of them tend to "share environmental investment appropriately", and 8% of them choose to give "oral support", only 5% of them choose "no concern". Most of the residents prefer to pay for treatment of household waste and sewage according to production (Table 2). As well, the residents are willing to pay for professional environmental management firms. As well they are willing to transit to use clean energy replacing fossil fuels at a same or lower price. The monthly cost amount the residents are willing to pay for environment management and improvement is various. Most of the residents choose to calculate the payments by the amount of garbage/sewage or by the number of people per household. Some residents are willing to pay 10-30 RMB per household per month, and a small number of them choose to pay more than 30 RMB per household per month (Table 2). Otherwise, a few of the residents are not willing to be charged.

To tackle the ecological environment problems and greening the villages, most of the village managers would initiate some planning and practical projects, combining the technical assistance and money investments from various stakeholders and bodies. To greening the neighborhoods, 70% of the residents hope to select "native ornamental plants with economic value" or "local plants can easily survive" as greening plants, 23% of them choose multifunctional "crops, vegetables and fruit trees" and other 9% of them choose "exotic and rare plants". That indicated the residents have their own understanding of rural greening and hope to participate in the process of design and practice.

DISCUSSIONS

The existing problems of rural ecological environment perceived by villagers

Our results showed that the household wastes, air pollution and pesticide pollution took the top three existing environmental problems. That means these problems are raising its importance compared to water and soil pollution, which were frequently recognized as the most serious environmental problems in previous studies (Chen 2007; He et al. 2008; Wang et al. 2008) as well as the national environmental bulletins. (The Environmental Protection Agency 2011; The Environmental Protection Agency 2012; The Environmental Protection Agency 2013; The Environmental Protection Agency 2014).

There are lots of publications demonstrating the critical impacts of household waste littering on the living environment of rural residents, because the kinds and production of rural household wastes have been increasing rapidly in the past decades (Guan and Qiu 2008; Wang et al. 2012). Disorderly stacking of household wastes, open burning, surrounding villages with garbage can be seen frequently in rural areas, which not only breeds germs and spreads diseases, but also pollutes land, groundwater and surface water (Jia et al. 2019). And our survey showed a high average household waste production per year and amongst the kitchen organic waste and soft plastics are most problematic. The dropped organic wastes mixed with soft plastic packages around curbsides, roadsides and riversides can result in environmental deterioration such as smell, diseases and secondary water pollution etc. (Beylot et al. 2013; Manfredi et al. 2010; Thomsen et al. 2012).

The air pollution was emphasized by 15% of residents in the survey. Currently, air pollution is seriously harmful to the environment and people's health around the world (Chen 2021). Although urban air pollution poses a serious health problem for people, rural air pollution is higher ($PM10 \geq 20 \mu g/m^3$ annual mean, $PM2.5 \geq 10 \mu g/m^3$ annual mean) (Liu et al. 2020). The air pollution by straw burning in summer and by coal burning in winter is very common and frequently claimed (Hong et al. 2016; Jin et al. 2006; Mestl et al. 2007; Zhang et al. 2014). Even the serious smog can occur in rural areas combining with the air pollution events from industries and cities at large scales (Zhou et al. 2015). These air pollution events also lead to more attention of villagers to the problem. (Gilbert-López et al. 2012; Wang et al. 2015; Zhou et al. 2015)

The pesticide pollution was put forward by the interviewees, because they thought it is one of main pollutants remaining in food, drinking water and soil. The impacts of pesticides on food and drinking water safety have been reported by a lot of scientific and governmental reports (Gilbert-López et al. 2012; Yadav et al. 2015;

Table 2. The ways and monthly amount the rural residents are willing to pay for pollution control at neighborhood scale

Counting Approaches and monthly amount of payment for pollution control	Proportion of the residents choosing corresponding counting approach and monthly amount (%)	
	living garbage	Sewage
Calculated by the amount of garbage/sewage	39	40
Calculated by the number of people per household	34	35
10-30 RMB per household per month	25	23
More than 30 RBM per household per month	2	2
Total	100	100

Srivastava et al. 2019; Ridoutt et al. 2022). That means there is already a common view on the pesticide pollution among rural residents, academic communities and governmental agencies.

Otherwise, the interviewed villagers not only pointed out the existing serious environmental problems, but also highlighted the interactions between these problems including contaminants transportation between living environment, water and soil environments. That means the villagers are strengthening their awareness and concerns on the environmental problems (Duan et al. 2014; Li et al. 2012). It is different from a dominant point that the rural residents have poor awareness and concerns on the environmental problems (Hong 2005; Ma 2005; Zhu 2001).

The perceptions of villagers on the alternative targets of rural environment development

Our result showed that neighborhoods with good environmental quality are favorite choices rather than "big houses" and "close to workplace and/or school". That means the rural residents already have a clear recognition of the value of a healthy environment and a strong desire to improve their living environment. The recognition and desire for a healthy living environment have been reported worldwide across urban and rural areas (Lee and Kim 2015). Moreover, the village managers have a similar perspective on the environmental development targets of their villages. The "green village with sustainable agriculture" and the "ecological village with tourism" are their top preferences. The values of interviewed village managers on rural environment development are similar with the targets of some "green villages" and "eco-villages" (Hu and Wang 1998; Takeuchi et al. 1998; Wenxia 2011; Xue 2014), as well as some suburb and urban "green communities" (Zhou et al. 2011). This informs that the rural areas of China are getting ready to transit to a green future. Actually, there already is a great number of "green villages", "ecological villages" and "beautiful villages" emerging (Duan et al. 2011; Hu and Wang 1998; Li and Miao 2011; Wu and Wu 2014).

To enhance the environmental infrastructure and improve living environment, the interviewed residents showed stronger willingness to "move to the combined new neighborhoods with apartments" than the villager managers. There are some potential reasons resulting in the difference. From the residents' side, they are encouraged by more and more emerging successful combined new neighborhoods and financial compensation from local governments (Hu et al. 2015; Qian 2015). Poverty and deprivation, for example, could be tackled through encouraging community development (Dinnie and Fischer 2020). From the managers' side, they might be worried about some problems during and after moving into the new neighborhoods, such as integration of land and administrative authorities, decrease of natural resources and its impacts on long-term sustainable development (Lin 2012; Shi 2008; Zheng and Ding 2013).

Otherwise, our results showed a regional pattern of village managers' perspectives on the strategy "combine villages into the new neighborhoods". Actually, all choices of the village managers were made based on maximizing the benefits and minimizing the costs. Therefore, it is understandable that the village managers from the North and Northwest China are more willing to move to the "the combined new neighborhoods with apartments", because their villages have lower income, worse living environment and stronger motivation to change the situation (Liu and Xu 2006; Xia 2002; Yuan 1985). However, the villages from the East and South China have relatively higher income, better living environment and infrastructures (Fu and Liu 2001; Guo and Wei 2012), thus the village managers there prefer to "live in the original neighborhoods with environment improvement".

The residents from different regions also showed different perceptions on how to cope with environmental degradation problems. It is consistent with the regional differences of the natural environment and its degradation. For example, the restoration of degraded mines in Southwest China was the prior problem of the interviewed residents; as well it has been highlighted frequently by local governments and existing studies (Chen et al. 2007; Hao and Jiang 2015; LEI and DUAN 2008; Wei 2002). Otherwise, many interviewed residents simultaneously took "increase forest coverage rate" as the top prior approach to restore the degraded environment. The residents are aware of the link between forest degradation and other environmental problems such as water resource shortage, air pollution, drought and flooding etc. (Zaimeche and Liu 1994; Fan et al. 2003; Zhao 1986). Definitely, forest protection and restoration should be put forward in the future rural environment improvement of China.

The willingness of villagers to involve into environment improvement

The interviewed residents showed strong motivation to participate in rural environment improvement and willingness to share environmental investment. It is a big encouragement for the local governments and some environmental enterprises. For a long time, the rural residents were considered lacking concern for their living environment and not willing to invest in environmental improvement (Yu 2014). Nowadays, the rural residents have raised their environmental awareness and desire along with advancement of their education and income (Nan et al. 2011).

Most of the interviewed residents prefer to pay for household waste and sewage treatment according to the amount of waste and sewage they produce monthly. In addition, this way is most popular worldwide, particularly in most cities and towns (Dahlén and Lagerkvist 2010). We found that some residents prefer to pay according to household size, because their village administrations charge a fee for water supply that way to avoid the cost for installing water meters. And it is practical for some remote villages' lack of technical and financial support. Whether in urban or rural areas, it is a common approach to charge a fee for household waste according to households with or without considering family size (Li 2009). Overall, the approach to charge fee according to production might be the most effective, fair and acceptable (Park 2018; Miranda and Aldy 1998; Wertz 1976).

Most residents are willing to pay 10-30 RMB per household per month for waste and sewage treatment. 92.36% of farmers are willing to pay the related expenses of household waste treatment (Chen and Qian 2022). 73.38% of farmers are willing to participate in rural household waste treatment, and the average family willingness to pay is 13.14 RMB per household per month (Jia and Zhao 2019). It is slightly higher than the average monthly fee of an urban household (Cao 2010; Li 2009). However, the majority of organic waste sewage could be reused as resources for composting, anaerobic fermentation, irrigation etc. in situ or in a short distance (Alvarenga et al. 2015; Cesaro et al. 2015). Potentially it could cut the collection and treatment cost (Ratanatamskul et al. 2015).

Both the interviewed village managers and residents are motivated to cope with environment degradation problems and greening their villages. Moreover, they showed unique

views on selection of landscape plants. Their preferences on "native ornamental plants with economic value" and "native local plants" are different from the prevalence of pure ornamental plants and introduced plants in some new urban areas (Acar et al. 2007). Along with the transition of urban green space from artificial to natural styles (Wang et al. 2004), the green spaces of rural neighborhoods should take the perceptions of local residents into account and avoid simply urbanization.

CONCLUSIONS

Overall, household waste pollution, air pollution and pesticide pollution are the most concerned problems by the villagers. A big proportion of the interviewees chose "environment with good quality for health" or "green villages with sustainable agriculture" as their desirable living environment via various ways to achieve these targets. The expected environment quality of most rural residents is consistent with the environmental targets of "Guidelines for the construction of beautiful village (GB/T 32000-2015)". Meanwhile, sustainable agriculture is a practical way to achieve the environment targets for many villages. Most of the residents strongly support rural green development and are willing to pay for rural pollution control. And the village managers and residents have many valuable views on rural environment improvement. Thus, the perceptions of rural residents on green development are accordant with the national strategies of beautiful village construction and rural revitalization of China. The main findings may shed lights on green development of the rural areas in the context of rapid urbanization. The various perceptions of the villagers on rural environment development targets across regions implies that regionally diverse and adaptive strategies should be highlighted in future research.

REFERENCES

Acar C., Acar H., and Eroğlu E. (2007). Evaluation of ornamental plant resources to urban biodiversity and cultural changing: A case study of residential landscapes in Trabzon city (Turkey). Building and Environment, 42, 218–229, DOI: 10.1016/j.buildenv.2005.08.030.

Alvarenga P., Mourinha C., Farto M., Santos T., Palma P., Sengo J., Morais M. C., and Cunha-Queda C. (2015). Sewage sludge, compost and other representative organic wastes as agricultural soil amendments: Benefits versus limiting factors. Waste Management, 40, 44–52, DOI: 10.1016/j.wasman.2015.01.027.

Beylot A., Villeneuve J., and Bellenfant G. (2013). Life Cycle Assessment of landfill biogas management: Sensitivity to diffuse and combustion air emissions. Waste Management, 33, 401–411, DOI: 10.1016/j.wasman.2012.08.017.

Cao N. (2010). Research on the pricing of waste disposal in the city. Master Degree Dissertation, China University of Geosciences (Beijing) (in Chinese).

Cesaro A., Belgiorno V., and Guida M. (2015). Compost from organic solid waste: Quality assessment and European regulations for its sustainable use. Resources, Conservation and Recycling, 94, 72–79, DOI: 10.1016/j.resconrec.2014.11.003.

Chen J. (2007). Rapid urbanization in China: A real challenge to soil protection and food security. Catena, 69(1), 1–15, DOI: 10.1016/j.catena.2006.04.019.

Chen J. F. (2021). Harm of atmospheric environmental pollution and control measures. Leather Manufacture and Environmental Technology, 2, 126-127 (in Chinese).

Chen J., Shen B., and Liu F. (2007). Mine environmental geological problems in southwest China. Multipurpose Utilization of Mineral Resources, 2007(4), 43–46 (in Chinese).

Chen X.X and Qian D.W. (2022). Study on influencing factors of rural residents' willingness to pay for household waste treatment-taking Fujian Province as an example. Journal of Yunnan Agricultural University (Social Sciences), 16(3), 71-77 (in Chinese).

Dahlén L and Lagerkvist A. (2010). Pay as you throw: Strengths and weaknesses of weight-based billing in household waste collection systems in Sweden. Waste Management, 30, 23–31, DOI: 10.1016/j.wasman.2009.09.022.

Dinnie E and Fischer A. (2020). The trouble with community: How "Sense of community" influences participation in formal, community-led organizations and rural governance. Sociologia Ruralis, 60, 243–259, DOI: 10.1111/soru.12273.

Donaldson-Selby G., Hill T., and Korrubel J. (2007). Photorealistic visualization of urban greening in a low-cost high-density housing settlement, Durban, South Africa. Urban Forestry and Urban Greening, 6, 3–14, DOI: 10.1016/j.ufug.2006.11.001.

Duan H.X., Yan-Li L., and Yan L. (2014). Chinese Public's Willingness to Pay for CO2 Emissions Reductions: A Case Study from Four Provinces/Cities. Advances in Climate Change Research, 5, 100–110, DOI: 10.3724/SP.J.1248.2014.100.

Duan N., Lin C., Liu X.D., Wang Y., Zhang X.J., and Hou Y. (2011). Study on the effect of biogas projects on the development of low carbon circular economy -A case study of Beilangzhong eco-village. Procedia Environmental Sciences, 5, 160-166, DOI: 10.1016/j.proenv.2011.03.062.

Fan B.M., Dong Y., Zhang J.C., and Yin J.Y. (2003). Deforestation in the history of China to the influence of flood and drought disaster (FDD) – try to talk about the forest climate and hydrological effect. Scientia Silvae Sinicae, 2003(3), 136–142 (in Chinese).

Fu G and Liu C. (2001). Southeast China food production and water problems. Resources Science, 23(5), 52–57 (in Chinese).

Gao X., Xu W., Hou Y., and Ouyang Z. (2020). Market-based instruments for ecosystem services: framework and case study in Lishui City, China. Ecosystem Health and Sustainability, 6(1), 1835445, DOI: 10.1080/20964129.2020.1835445.

Gilbert-López B., Jaén-Martos L., García-Reyes J.F., Villar-Pulido M., Polgar L., Ramos-Martos N., and Molina-Díaz A. (2012). Study on the occurrence of pesticide residues in fruit-based soft drinks from the EU market and Morocco using liquid chromatography–mass spectrometry. Food Control, 26, 341–346, DOI: 10.1016/j.foodcont.2012.01.025.

Gu L. h., Wu Y.J., Liu D.J., and Yu L. (2013). Thinking in innovation of rural public products and public service supply mechanism: a case study of Jingjiang city. Reality Only, 2013(12), 64-67 (in Chinese).

Guan D and Qiu C. (2008). Current situation and problems of the rural living garbage and its countermeasures. China Resources Comprehensive Utilization, 2008(8), 29–31 (in Chinese).

Guo Y.B and Wei H.K. (2012). Review of the research on regional differences of rural residents' income in China. Economic Perspectives, 2012(6), 68-76 (in Chinese).

Hao Q and Jiang C. (2015). Heavy metal concentrations in soils and plants in Rongxi Manganese Mine of Chongqing, Southwest of China. Acta Ecologica Sinica, 35, 46–51, DOI: 10.1016/j.chnaes.2015.01.002.

He H., Zhou J., Wu Y., Zhang W., and Xie X. (2008). Modeling the response of surface water quality to urbanization in Xi'an, China. Journal of Environmental Management, 86, 731–749, DOI: 10.1016/j.jenvman.2006.12.043.

Hong D. (2005). China's urban residents' environmental awareness. Jiangsu Social Sciences, 2005(01), 127–132 (in Chinese).

Hong J., Ren L., Hong J., and Xu C. (2016). Environmental impact assessment of corn straw utilization in China. Journal of Cleaner Production, 112(2), 1700-1708, DOI: 10.1016/j.jclepro.2015.02.081.

Hu D and Wang R. (1998). Exploring eco-construction for local sustainability: An eco-village case study in China1. Ecological Engineering, 11, 167–176, DOI: 10.1016/S0925-8574(98)00032-9.

Hu Y., Hooimeijer P., Bolt G., and Sun D. (2015). Uneven compensation and relocation for displaced residents: The case of Nanjing. Habitat International, 47, 83–92, DOI: 10.1016/j.habitatint.2015.01.016.

Jia Y.J and Zhao M.J. (2019). The influence of environmental concern and institutional trust on farmers' willingness to participate in rural domestic waste treatment. Resources Science, 41(8), 1500-1512, DOI: 10.18402/resci.2019.08.10 (in Chinese).

Jin Y., Ma X., Chen X., Cheng Y., Baris E., and Ezzati M. (2006). Exposure to indoor air pollution from household energy use in rural China: The interactions of technology, behavior, and knowledge in health risk management. Social Science and Medicine, 62, 3161–3176, DOI: 10.1016/j.socscimed.2005.11.029.

Jing P and Zhang F. (2003). Latest development in studies on urban and rural integration. City Planning Review, 27, 30–35, DOI: 10.3321/j.issn:1002-1329.2003.06.006 (in Chinese).

Kobori H and Primack R.B. (2003). Participatory Conservation Approaches for Satoyama, the Traditional Forest and Agricultural Landscape of Japan. AMBIO: A Journal of the Human Environment, 32(4), 307–311, DOI: 10.1579/0044-7447-32.4.307.

Lee T.K and Kim J.T. (2015). Residents' responses on indoor environment quality and energy use in apartments. Energy and Buildings, 98, 34–38, DOI: 10.1016/j.enbuild.2014.10.084.

LEI D and DUAN C. (2008). Restoration potential of pioneer plants growing on lead-zinc mine tailings in Lanping, southwest China. Journal of Environmental Sciences, 20, 1202–1209, DOI: 10.1016/S1001-0742(08)62210-X.

Lestrelin G., Bourgoin J., Bouahom B., and Castella J.C. (2011). Measuring participation: Case studies on village land use planning in northern Lao PDR. Applied Geography, 31, 950–958, DOI: 10.1016/j.apgeog.2011.01.003.

Li F. (2009). The current situation of urban living garbage disposal fee system and countermeasures research. Inner Mongolia Science Technology and Economy, 2009(10), 57–58 (in Chinese).

Li M and Miao R. (2011). South Korea's low carbon green countryside construction presents the situation and the enlightenment to our country. Environmental Protection and Circular Economy, 31(11), 24–27 (in Chinese).

Li W., Liu J., and Li D. (2012). Getting their voices heard: Three cases of public participation in environmental protection in China. Journal of Environmental Management, 98, 65–72, DOI: 10.1016/j.jenvman.2011.12.019.

Lin J. (2012). Villages merge and develop the rural community. The Journal of Humanities, 2012(01), 160–164, DOI: 10.15895/j.cnki.rwzz.2012.01.029 (in Chinese).

Lin L.M., He X.L., and Han Y.Q. (2021). Influence of ecological cognition and relationship network on cooperative treatment behavior of villagers' household waste: an empirical analysis based on 501 questionnaires of villagers in Fujian Province. Journal of Ecology and Rural Environment, 37(10), 1301-1309, DOI: 10.19741/j.issn.1673-4831.2020.1028 (in Chinese).

Liu C and Xu J. (2006). Benefit compensation and sharing mechanism under the lack of policy failure problem study in northwest-based on the analysis of the environmental reconstruction. Economic Review, 2006(04), 54–58, DOI: 10.19361/j.er.2006.04.009 (in Chinese).

Liu L. (2013). Geographic approaches to resolving environmental problems in search of the path to sustainability: The case of polluting plant relocation in China. Applied Geography, 45, 138–146, DOI: 10.1016/j.apgeog.2013.08.011.

Liu X.S., Jürgen S.K., Zhang X., Bendl J., Khedr M., Jakobi G., Schloter-Hai B., Hovorka J., and Zimmermann R. (2020). Integration of air pollution data collected by mobile measurement to derive a preliminary spatiotemporal air pollution pro file from two neighboring German-Czech border villages. Science of the Total Environment, 722, 1879-1026, DOI: 10.1016/j.scitotenv.2020.137632.

Ma X. (2005). Environmental education system construction to improve rural residents environmental awareness. Journal of Hangzhou Medical College, 2005(5), 45–47 (in Chinese).

Macnaghten P and Jacobs M. (1997). Public identification with sustainable development: Investigating cultural barriers to participation. Global Environmental Change, 7, 5–24, DOI: 10.1016/S0959-3780(96)00023-4.

Manfredi S., Tonini D., and Christensen T.H. (2010). Contribution of individual waste fractions to the environmental impacts from landfilling of municipal solid waste. Waste Management, 30, 433–440, DOI: 10.1016/j.wasman.2009.09.017.

Meadowcroft J. (1997). Planning, Democracy and the Challenge of Sustainable Development. International Political Science Review, 18, 167–189, DOI: 10.1177/019251297018002004.

Mestl H.E.S., Aunan K., Seip H.M., Wang S., Zhao Y., and Zhang D. (2007). Urban and rural exposure to indoor air pollution from domestic biomass and coal burning across China. Science of The Total Environment, 377, 12–26, DOI: 10.1016/j.scitotenv.2007.01.087.

Miranda M.L. and Aldy J.E. (1998). Unit pricing of residential municipal solid waste: lessons from nine case study communities. Journal of Environmental Management, 52, 79–93, DOI: 10.1006/jema.1997.0161.

Nan W., Banghong Z., and Haifen Y. (2011). A Research on Impacting Factor of Rural Environment and Environment Protection Awareness of Famers. Energy Procedia, 5, 2623–2628, DOI: 10.1016/j.egypro.2011.03.341.

Park S. (2018). Factors influencing the recycling rate under the volume-based waste fee system in South Korea. Waste Management, 74, 43-51, DOI: 10.1016/j.wasman.2018.01.008.

Qian Z. (2015). Land acquisition compensation in post-reform China: Evolution, structure and challenges in Hangzhou. Land Use Policy, 46, 250–257, DOI: 10.1016/j.landusepol.2015.02.013.

Ratanatamskul C., Wattanayommanaporn O., and Yamamoto K. (2015). An on-site prototype two-stage anaerobic digester for co-digestion of food waste and sewage sludge for biogas production from high-rise buildings. International Biodeterioration & Biodegradation, 102, 143-148, DOI: 10.1016/j.ibiod.2015.03.019.

Ridoutt B., Baird D., and Navarro J. (2022). Pesticide Toxicity Footprints of Australian Dietary Choices. Nutrients, 13, 12, DOI: 10.3390/nu13124314.

Shi W.L. (2008). The performance and causes of environmental problems in rural urbanization. Market Modernization, 2008(10), 358-359 (in Chinese).

Shi Y. (2013). New-Type Urbanization and Small-Town Development in China. Economic Geography, 33(7), 47–52, DOI: 10.15957/j.cnki.jjdl.2013.07.006 (in Chinese).

Srivastava A., Jangid N.K., Srivastava M., and Rawat V. (2019). Pesticides as Water Pollutants. Advances in Environmental Engineering and Green Technologies, 1-19, DOI: 10.4018/978-1-5225-6111-8.ch001.

Takeuchi K., Namiki Y., and Tanaka H. (1998). Designing eco-villages for revitalizing Japanese rural areas1. Ecological Engineering, 11, 177–197, DOI: 10.1016/S0925-8574(98)00031-7.

The Environmental Protection Agency. (2010). The first national pollution census of 2010 [online]. Available at: http://jcs.mep.gov.cn/hjzl/zkgb/2010zkgb/ [Accessed 15 Mar. 2021] (in Chinese).

The Environmental Protection Agency. (2011). Chinese environmental bulletin of 2011, [online] Available at: http://jcs.mep.gov.cn/hjzl/zkgb/2011zkgb/ [Accessed 15 Mar. 2021] (in Chinese).

The Environmental Protection Agency. (2012). Chinese environmental bulletin of 2012, [online] Available at: http://jcs.mep.gov.cn/hjzl/zkgb/2012zkgb/ [Accessed 15 Mar. 2021] (in Chinese).

The Environmental Protection Agency. (2013). Chinese environmental bulletin of 2013, [online] Available at: http://jcs.mep.gov.cn/hjzl/zkgb/2013zkgb/ [Accessed 15 Mar. 2021] (in Chinese).

The Environmental Protection Agency. (2014). Chinese environmental bulletin of 2014, [online] Available at: http://jcs.mep.gov.cn/hjzl/zkgb/ [Accessed 15 Mar. 2021] (in Chinese).

The United Nations. (1992). Earth Summit Agenda 21. the United Nations programme of action from Rio.

Thomsen N.I., Milosevic N., and Bjerg P.L. (2012). Application of a contaminant mass balance method at an old landfill to assess the impact on water resources. Waste Management, 32, 2406–2417, DOI: 10.1016/j.wasman.2012.06.014.

Tian C.Q., Zhao Z.L., and Zhao N.S. (2011). The influence of the farmers' environmental behavior of the life type to the village environment. Ecological Economy, 2011(2), 179-183 (in Chinese).

Wang B.Z., Wang C.X., He P., and Shen S.Y. (2004). The review of urban green space research. Urban Planning Forum, 2004(4), 62–68+96 (in Chinese).

Wang J., Da L., Song K., and Li B.L. (2008). Temporal variations of surface water quality in urban, suburban and rural areas during rapid urbanization in Shanghai, China. Environmental Pollution, 152, 387–393, DOI: 10.1016/j.envpol.2007.06.050.

Wang M., Zhao Y., and Wang B. (2012). The rural living garbage pollution presents a situation and countermeasures. Private science and technology, 2012(2), 102 (in Chinese).

Wang Y., Sun M., Yang X., and Yuan X. (2015). Public awareness and willingness to pay for tackling smog pollution in China: a case study. Journal of Cleaner Production, 112(2), 1627-1634, DOI: 10.1016/j.jclepro.2015.04.135.

Wei L. (2002). The mine environmental geological problems and countermeasures in southwest China. Journal of Geological Hazards and Environment Preservation, 2002(1), 6–8 (in Chinese).

Wenxia L. (2011). Research on the "Villages Merged" Community Building in the Perspective of "Green" Idea. Energy Procedia, 5, 867–871, DOI: 10.1016/j.egypro.2011.03.153.

Wertz K.L. (1976). Economic factors influencing households' production of refuse. Journal of Environmental Economics and Management, 2(4), 263–272, DOI: 10.1016/S0095-0696(76)80004-6.

Wu H and Wang W. (2013). Research on public participation in new rural planning. Journal of Huaihai Institute of Technology (Humanities and Social Sciences Edition), 11(17), 106–110 (in Chinese).

Wu L.C. and Wu K.F. (2014). Four modes of construction in beautiful countryside and their comparison-based on the investigation in Anji, Yongjia, Gaochun and Jiangning. Journal of Huazhong Agricultural University (Social Science Edition), 33(1), 15-22 (in Chinese).

Xia J. (2002). Water cycle and water security in north China: problems and challenges. Progress in Geography, 2002(6), 517–526 (in Chinese).

Xiao P and Zhu G.H. (2016). Research on the third-party governance contract of rural environmental pollution. Rural economy, 2016(4), 104-108 (in Chinese).

Xue J. (2014). Is eco-village/urban village the future of a degrowth society? An urban planner's perspective. Ecological Economics, 105, 130–138, DOI: 10.1016/j.ecolecon.2014.06.003.

Yadav I.C., Devi N.L., Syed J.H., Cheng Z., Li J., Zhang G., and Jones K.C. (2015). Current status of persistent organic pesticides residues in air, water, and soil, and their possible effect on neighboring countries: A comprehensive review of India. Science of The Total Environment, 511, 123–137, DOI: 10.1016/j.scitotenv.2014.12.041.

Yu X. (2014). Is the environment "a city thing" in China? Rural–urban differences in environmental attitudes. Journal of Environmental Psychology, 38, 39–48, DOI: 10.1016/j.jenvp.2013.12.009.

Yuan H.R. (1985). Environmental, agricultural, immigration, and development. Northwest Population Journal, 1985(1), 6-12, DOI: 10.15884/j.cnki.issn.1007-0672.1985.01.003 (in Chinese).

Zaimeche S.E. and Liu C.J. (1994). The consequences of the rapid destruction of forests: a case of North Africa. AMBIO- Journal of Human Environment, 23(2), 136-140.

Zhang B. (2022). Research on rural ecological environment problems from the perspective of rural revitalization. Shanxi Agricultural Economy, 2022(3), 133-135, DOI: 10.16675/j.cnki.cn14-1065/f.2022.03.044 (in Chinese).

Zhang Y., Zang G.Q., Tang Z.H., Chen X.H., and Yu Y.S. (2014). Burning straw, air pollution, and respiratory infections in China. American Journal of Infection Control, 42, 815, DOI: 10.1016/j.ajic.2014.03.015.

Zhang Y.L., Zhang J., Ye Y., Wu Q.T., Jin L.X., and Zhang H.G. (2016). Residents' Environmental Conservation Behaviors at Tourist Sites: Broadening the Norm Activation Framework by Adopting Environment Attachment. Sustainability, 8(6), 571-582, DOI: 10.3390/su8060571.

Zhao X. H. (1986). The Amazon Forest suffered destruction and its serious consequences. Yunnan Forestry, 1986(5), 28 (in Chinese).

Zheng F and Ding D. (2013). Land Issues in Village Relocation and Combination: Status, Cause and Countermeasures. Modern Urban Research, 28(6), 20–24 (in Chinese).

Zhou C., Dai X., Wang R., and Huang J. (2011). Studies on the evaluation index system of ecological communities. Acta Ecologica Sinica, 31(16), 4749–4759 (in Chinese).

Zhou M., He G., Fan M., Wang Z., Liu Y., Ma J., Ma Z., Liu J., Liu Y., Wang L., and Liu Y. (2015). Smog episodes, fine particulate pollution and mortality in China. Environmental research, 136, 396-404, DOI: 10.1016/j.envres.2014.09.038.

Zhu Q. (2001). A problem has not caused enough attention – survey about farmers' environmental consciousness and thinking. The World of Survey and Research, 2001(1), 28–31, DOI: 10.13778/j.cnki.11-3705/c.2001.01.008 (in Chinese), DOI: 10.3390/w7020634.

APPENDICES
Questionnaire

Part A Questions for the village residents

1. What are the most serious environmental problems influencing your life in rural areas? (Tick one please)

(A) Water pollution. (B) Air pollution. (C) Household waste pollution.
(D) Noise pollution. (E) Livestock and poultry manure. (F) Straw burning.
(G) Chemical fertilizer. (H) Pesticide pollution. (I) Mulching film. (J) Others.

2. Table for classification and output of various wastes of the interviewed resident' family

Type	Annual output (Kg)
Kitchen organic waste (leftovers, ort, etc.)	
Glasses (bottles for wine, cans, medicine, sauce, etc.)	
Hard plastic (packages, bottles, barrels)	
Soft plastic (used thin film, packages)	
Used batteries	
Livestock and poultry manure	
Toilet stool	
Straws, branches, leaves, etc.	
Waste fruits and vegetables in the fields	
Cans	
Soft paper	
Hard paper	
Metal waste	
Pesticide bottles	
Construction waste	

3. What is the trend of the changes of environmental quality status in your living area?

(A) Extreme improvement. (B) Extreme degradation. (C) No changes.

4. What are the serious ecological environment problems in your area? (Multiple-choice)

(A) Timber cutting. (B) Farmland occupation. (C) Disappearance of animals and plants.
(D) Other problems.

5. Where is your wastewater, such as washing and toilet water discharged to?

(A) Directly to the nearby river or ponds.
(B) To the river or ponds after being collected but without treatment.
(C) To the river or ponds after being collected and treated.

6. What are your preferences on the living neighborhood environment?

(A) Environment with good quality for health. (The environment quality meets basic requirements of basic requirements of "Guidelines for the construction of beautiful village (GB/T 32000-2015)")
(B) Big houses.
(C) Convenience for employment.
(D) Go to school with convenience.

7. If possible, what is your most preferred way to achieve the rural environment targets?

(A) Move to the cities nearby.
(B) Move to the new combined neighborhoods with apartments. (The combined new neighborhoods with apartments usually are equipped similarly to urban neighborhoods but located in places near the villages)
(C) Live in the original neighborhoods with environmental improvement.
(D) No changes.

8. What is your first option to cope with the environmental degradation problems and avoid natural disasters?
(A) increasing the forest coverage rate.
(B) Restoring degraded mines.
(C) Limiting groundwater exploitation.
(D) Choosing safe areas for construction of the combined new neighborhoods.
(E) Others.
9. What is your willingness to be involved in rural environment improvement?
(A) Share environmental investment appropriately.
(B) Participate in the related activities as volunteers.
(C) Oral support.
(D) No concern.
10. What is your preferred way to manage household waste in the rural community?
(A) Cost sharing for professional clearing.
(B) Resource utilization under classification direction.
(C) I do not care and will not do anything.
11. How much would you like to pay for treatment of household waste?
(A) Calculated by the amount of garbage.
(B) Calculated by the number of people per household.
(C) 10-30 RMB per household per month.
(D) More than 30 RBM per household per month.
12. What would you rather like for health and clean water sources?
(A) Total treatment, with proper-shared investment.
(B) Quit poison pesticides under professional direction.
(C) Decreasing sewage discharge under technical direction.
(D) Decreasing fertilizers under professional direction.
13. How much would you like to pay for community sewage treatment?
(A) Calculated by the amount of sewage.
(B) Calculated by the number of people per household.
(C) 10-30 RMB per household per month.
(D) More than 30 RBM per household per month.
14. What would you rather like to mitigate air pollution caused by coal burning?
(A) Using clean energy at the same price or a little higher price.
(B) Energy saving under technical direction.
(C) No changes.
15. What is your option on plant species for greening the rural neighborhood?
(A) Exotic and rare plants.
(B) Native ornamental plants with economic value.
(C) Local plants can easily survive.
(D) Crops, vegetables and fruit trees.

Part B Questions for the village managers

16. How serious is the air pollution in your village?
(A) Heavy pollution. (B) Pollution exists. (C) No pollution.
17. What is the main pollution source, if there is air pollution?
(A) Industrial pollution. (B) Straw burning pollution. (C) Coal burning pollution. (D) Other pollution.
18. How serious is the water pollution in your village?
(A) Heavy pollution. (B) Pollution exists. (C) No pollution.
19. What is the main pollution source, if there is pollution?
(A) Industrial pollution. (B) Straw burning. (C) Coal burning. (D) Other pollution.
20. How serious is the soil pollution in your village?
(A) Heavy pollution. (B) Pollution exists. (C) No pollution.
21. What is the main pollution source, if there is pollution?
(A) Industrial pollution.
(B) Household waste.
(C) Pesticide and other chemical pollution.
(D) Other pollution.
22. What is the status of the forest around your village?
(A) Very good. (B) Good. (C) Ordinary. (D) Bad.
(E) Very bad.
23. What is the status of the wild animal species around your village?
(A) Many species. (B) Gradually increasing. (C) Gradually decreasing.
(D) Nearly no wild animals.
24. What is the preferred environmental development target of your village?
(A) Rich village with industries.
(B) Green villages with sustainable agriculture.
(C) Ecological villages with tourism.
(D) Villages with labor output.
(E) Move to cities nearby.
(F) Keep the status quo.
25. What is your preferred way to achieve the environmental development target of your village?
(A) Move to the cities nearby.
(B) Move to the new combined neighborhoods.
(C) Live in the original neighborhoods with environmental improvement.
(D) No changes.
26. What would the village committee rather like to make the air clear?
(A) Limiting the entering of enterprises that may cause air pollution.
(B) Optimize energy structure under technical direction.
(C) Strengthening afforestation.
(D) Training the residents and proposing green living style.
27. What is your preferred way to guarantee safety of drinking water in your village?
(A) Bringing in municipal tap water.
(B) Establishing sewage treatment facilities.
(C) Limiting sewage-discharging enterprises.
(D) Training the residents to decrease the use of pesticides and fertilizers.
28. What is your preferred way to treat household waste in your village?
(A) Collecting and treating by the village committee with an arranged fund.
(B) Resource utilization under classification direction.
(C) It is a tough problem.

RESEARCH PAPER

EARLY MIDDLE PLEISTOCENE FAUNA OF FOSSIL RODENTS AND LOESS-PALEOSOL SERIES OF THE PEKLA KEY SECTION (TAMAN PENINSULA, RUSSIA)

Anastasia K. Markova[1]*, Svetlana A. Sycheva[1], Tatiana M. Gorbacheva[2]
[1]Institute of Geography RAS, Staromonetny per. 29, Moscow, 119017 Russian Federation
[2]High School of Economics, Pokrovsky boulevard 11, Moscow, 109028 Russian Federation
***Corresponding author:** amarkova@list.ru
Received: December 22st, 2022 / Accepted: May 4th, 2023 / Published: July 1st, 2023
https://DOI-10.24057/2071-9388-2022-169

ABSTRACT. The history of the early Middle Pleistocene small mammal faunas of Eastern Europe is very complicated. The early Middle Pleistocene which spanned from the Brunhes-Matuyama transition (772.9 ka BP, within MIS 19) till the beginning of the Likhvin Interglacial (424 ka BP, MIS 11) includes a number of interglacials and glaciations. Rodent species of the Tiraspolian faunal assemblage were found in the Chaudian fluvial deposits of the Cape Pekla section (northern coast of the Taman Peninsula). The evolutional level of the Pekla rodents are similar to those from the stratotype section of the Tiraspolian faunal assemblage in the Kolkotova Balka in Moldova (MIS 17) , which includes *Eolagurus* sp., *Mimomys savini, Microtus (Terricola) arvalidens, Microtus (Alexandromys)* ex gr. *oeconomus* and other species. The Pekla fauna also resembles the rodent fauna from famous English West Runton Freshwater Bed locality formed during the Cromerian Interglacial II and some other East and West European faunas. In the current work the entire loess-paleosol sequence of the Pekla section was described with five paleosols from the Middle to the Late Pleistocene. The sequence reflects the complexity of climatic fluctuations from the early Middle Pleistocene to the Holocene.

KEYWORDS: Pleistocene, rodents, Taman Peninsula, loess, paleosols

CITATION: Markova A. K., Sycheva S. A., Gorbacheva T. M. (2023). Early Middle Pleistocene Fauna Of Fossil Rodents And Loess-Paleosol Series Of The Pekla Key Section (Taman Peninsula, Russia). Geography, Environment, Sustainability, 2(16), 31-39
https://DOI-10.24057/2071-9388-2022-169

ACKNOWLEDGEMENTS: We were very grateful for the useful comments provided by the editors and reviewers of our work. We are appreciative of Dr. Lutz Christian Maul's improvements to the English text and important suggestions (Senckenberg Research Station of Quaternary Palaeontology, Weimar, Germany) as well as Dr. Aleksandr Tsatskin's helpful comments (Zinman Institute of Archaeology, University of Haifa, Israel). The paper was written as part of the themes of the Institute of Geography in Moscow of the Russian Academy of Sciences No.0148-2019-0007 (AAAA-A19-119021990093-8) "Assessment of Physical-Geographical, Hydrological and Biotic Environmental Changes and their Consequences for Establishing the Basis of Sustainable Nature management" and No. AAAA-A19-119022190169-5 (FMGE-2019-0006) "Geography, genesis, evolution and carbon cycle of natural and Anthropogenic-changed soils on the basis of modern concepts and technology for the aims of rational nature management'

Conflict of interests: The authors reported no potential conflict of interest.

INTRODUCTION

Remains of fossil small mammals are often used for palaeogeographic and stratigraphical implications. In addition, the presence of certain small mammal species makes it possible to reconstruct the paleoenvironmental circumstances that existed at the time the fossil assemblage was formed. The evolutionary peculiarities of the mammals in the various phylogenetic lineages also make it possible to determine the age of the enclosing deposits. This is especially important for fossil deposits that cannot be determined using physical dating methods such as the radiocarbon method, OSL and others. When combined with geological and stratigraphic research, the study of fossil small mammal remains gives us a complete picture of the environment during the mammal community's time of existence.

The discovery of the small mammal locality at Cape Pekla (Taman Peninsula) provided additional arguments for reconstructing the environmental conditions and the time of their deposition. The corresponding geological conditions might now be clarified thanks to new studies on this area. In the present current paper we would like to consider the particularities of the small mammal community found in the described fluvial deposits and their position in the Pleistocene stratigraphy. We would also like to present the Pekla section's deposits in detail, playing special attention to the numerous fossil soils that were discovered there.

METHODS AND MATERIALS

Geographical setting of Pekla section

Cape Pekla is located in the northwestern part of the Taman Peninsula, between the Black Sea and the Sea of Azov. The study area is located on the southern coast of the Sea of Azov, in the northwestern part of the Taman Peninsula, which, together with Crimea, separates the waters of the Black and Azov Seas (Fig. 1a).

The studied Pekla section presents one of the variants of the structure of a vast outcrop on the Sea of Azov's southern coast, in the area of the village of Kuchugury in the Temryuk region of the Krasnodar Territory of the Russian Federation (Fig. 1b). Its geographic location is at N 45°25'56.1" and E 36°55'12.0". It is located on a high marine terrace 37 meters high, at the edge of a cirque-like depression into which several hollows are descended. The section is located on the outlier between two hollows. One of them descends into a depression in which the mud volcano Plevok is located. Another hollow leads to the sea.

The geological setting of the Pekla section with the exposure of several fossil soils divided by loess horizons was described by (Dodonov et al. 2006). In this paper, these fossil soils were described as Bryansk (MIS 3), Mikulino (MIS 5e), Inzhava (MIS 11) and Vorona (MIS 15) fossil soils according the terminology of (Velichko et al. 1992).

Later, this section was studied by specialists from the Institute of Geography of the RAS. The geological structure of the section and the peculiarities of the paleosols were described by S. A. Sycheva (Timireva et al. 2022). During the last studies, the geological-paleopedological investigations of the Pekla section were carried out. These studies were based on the macromorphological description of the deposits with special attention to the structure of the Holocene and Pleistocene paleosols, their genetic characteristics and the digenetic transformations. The samples were collected for every 6 cm. Some results of their analysis (granulometric analysis, magnetic susceptibility, OSL dating, and others) have been published (Timireva et al. 2022).

The small mammal remains were obtained from washing and screening (0.5 mm screen) the marine-liman deposits underlying the loess-paleosol series. The material was dried in the sun and then the fossil remains were collected for analysis. In the second phase, the fossils were examined under the binocular microscope (type SMC4, Askania) and were drawned with a help of the drawing apparatus.

The fossil remains are yellow in color and consist mainly of isolated teeth and bone fragments. Mandibles and maxillas are absent.

MATERIALS AND RESULTS OF THE INVESTIGATION

A geological and paleopedological study of the Pekla outcrop located on the steep southern coast of the Sea of Azov (Cape Pekla), was carried out. The study is based on a thorough macromorphological description. Special attention is paid to the analysis of the structure of the Holocene soil and the Pleistocene paleosols, their genetic properties and digenetic transformations.

The samples were taken every 6 cm from a continuous column. They were used to perform a series of analyses, the results of which (granulometric analysis, determination of loss on ignition, determination of magnetic susceptibility, optically stimulated luminescence (OSL)) have already been published (Timireva et al. 2022).

Pekla geological section

The Pekla outcrop section (Fig. 2 and Fig. 3) shows a complex sequence of eolian loess and loess-like deposits interstratified with well-developed paleosols about 11 meters thick (Timireva et al. 2022). The subaerial sequence overlies marine sands and clays.

The main part of the section may be divided into the upper part attributed to Holocene – Late Pleistocene loess-paleosol series (LPS) (layers 1–12 in Fig. 2) and the Lower part attributed to the Middle Pleistocene LPS (layers 14–19

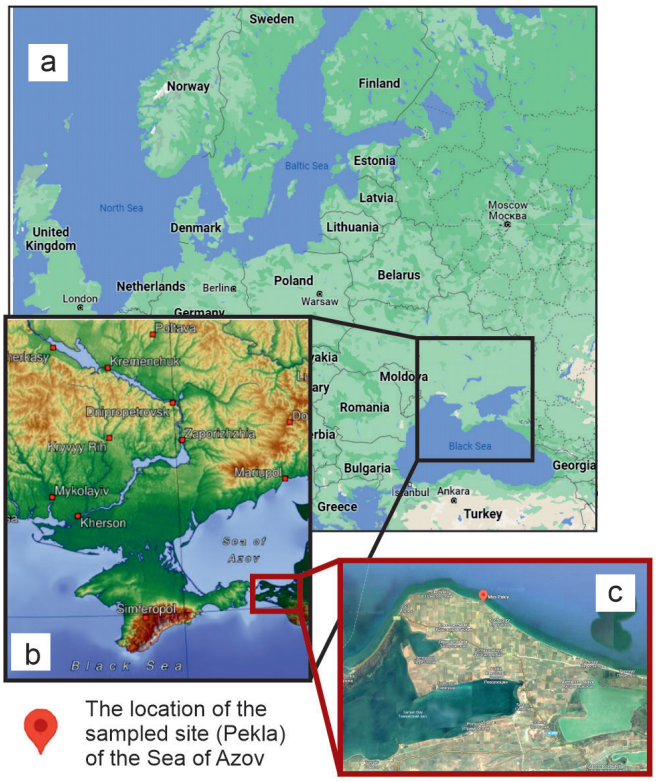

Fig. 1. The location of the Pekla section (Taman Peninsula, the Sea of Azov)
a – map of Europe with countries and capitals, b – location of the Taman Peninsula, c – location of Cape Pekla on the Taman Peninsula

in Fig 2). These loess-paleosol sequences are separated by marine sand of layer 13 (Fig. 2). Marine sediments that are about 20 meters thick are also exposed at the base of the Pekla outcrop (Fig. 2 and Fig. 3). The upper sands in the lowermost marine bed yielded conspicuous remains of small mammals described in the next section.

Detailed morphological descriptions of paleosols are critical for robust paleopedological reconstructions. Hence, we focused in the field on both paleosol profile organization and the nature of disturbances along the contact between the paleosol and the loess cover. The latter allows us to comprehend the evolution of the paleosol before and after burial better. Overall, Late Pleistocene LPS includes three paleosols, while the Middle Pleistocene LPS includes two paleosols. All paleosols are represented by incomplete profiles lacking a surficial humus Ah horizon.

The evidence of the former Ah horizon is furnished either by humus-clay coatings in subsurface B horizons or by fillings of small mammal burrows (moleholes, or krotovina in Russian) by dark colored humified material of the topsoil. Ah horizon was no longer preserved maybe as a result of the truncation of a paleosol by denudation processes. These moleholes are readily distinguishable in the field against the yellowish B horizons of loess-derived paleosols. In this way one may conjecture whether paleosol underwent erosion prior to burial.

The upper LPS includes the PS0 Holocene chernozem on loess-like loam, a layer of typical loess and three closely spaced Late Pleistocene paleosols (PS 1-3) (Fig. 2).

Layers 1-5. Holocene chernozem has a well-developed profile: Ad (0-0.06 m)-Ah (0.06-0.42 m)-AB (0.42-0.78 m)-BkA (0.78 -1.08 m)-Bk (1.08-2.04 m). The Ah and AB horizons are heavily bioturbated by soil mesofauna (e.g.,

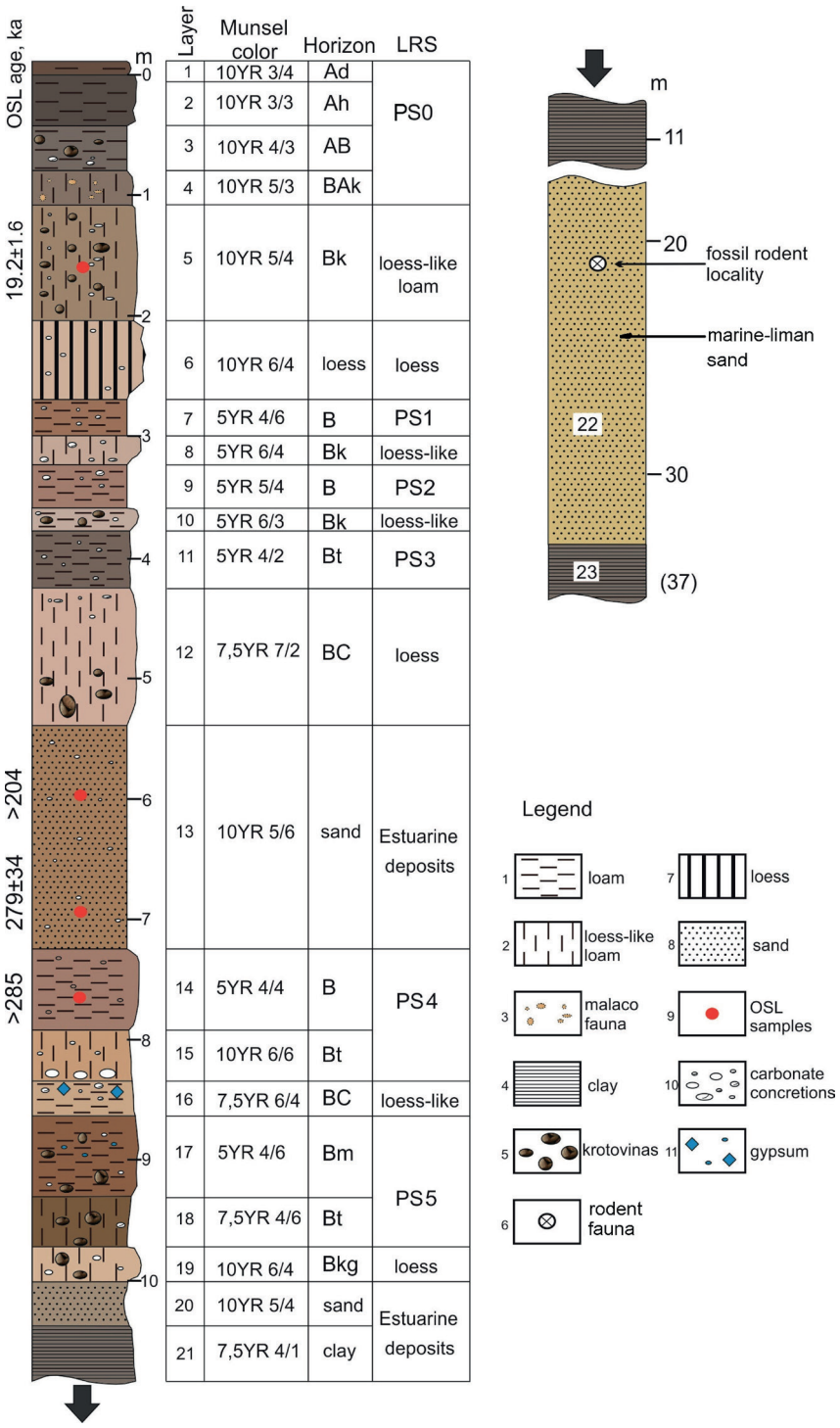

Fig. 2. Loess-paleosol thickness (LPS) and fluvial deposits of the Pekla section

earthworms), strongly humified, dark grey in color, and granular in structure. Carbonate pedofeatures in the form of pseudomycelia appear from the depth of 78 cm. When looking downward, the horizon appears to be loess-like loam (layer 5 on Fig. 2) that has been strongly bioturbated as evidenced by dark-colored moleholes that range in diameter from 5-7 cm to 10-12 cm. The Bk horizon is pale-brown (10YR 5/4 Munsell, Fig. 2). It is abundant with soft calcareous nodules that range in size from 0.5-2 cm to 2-3 cm. As a result, the surface soil is classified as ordinary micellar-carbonate chernozem according to Russian soil classification (Shishov et al. 2004) or Haplic Chernozem Loam according to WRB (2015). Significantly, the layer 5 was dated by OSL luminescence to 19.2 ± 1.6 thousand years (Timireva et al. 2022) and in this way it may corresponds to late Valdai (Weichselian) period.

Layer 6 (2.04-2.70 m) is a typical loess that has ancient moleholes. This layer is yellowish, silty, finely porous, calcareous silty loam. Its lower contact shows two types of disturbances: a) narrow subvertical fissures dissecting the underlying paleosol, and b) occasional dark-colored lenses filled with paleosol material displaced from below into loess. These features testify to intense disturbances at the time of paleosols burial.

Three paleosols from the Late Pleistocene LPS, each with incomplete profiles and showing transitional Bk horizons of varied thickness alone, are included in the LPS.

Layers 7, 8. Upper paleosol – PS1 has a profile: B (2.70 m-3.00 m) - Bk (3.00 m-3.24 m).

The B horizon is brown silty loam with reddish hue, small angular and granular structure, abundant Mn films in pores, some traces of clay illuviation and gleying. The paleosol can be defined as meadow soil (Chernozem Stagnic) apparently partially eroded. A linear, sharp transition from PS1 to lower PS2 paleosol is an indication of a stratigraphic and erosion gap of unknown duration.

Layers 9, 10. Middle paleosol – PS2 is represented by horizons: B (3.24-3.6 m) and the Bk horizon (3.6-3.78 m). The B horizon is dark brown loess-like silty loam, finely porous, while the Bk horizon shows prismatic structure and abundance of calcareous pedofeatures such as impregnation in the groundmass and pseudomycelia. The paleosol may be classified as eroded Chernozem-like soil (Haplic Chernozem).

Layers 11, 12. Lower paleosol (PS3) is represented by horizons: Bt (3.78-4.26 m) - Bk (4.26-5.4 m). The Bt horizon is dark brown loam, with angular aggregates covered by dark humus-clay coatings as indication of the process of clay illuviation. Lower in the profile in the Bk horizon calcareous pedofeatures are superposed on clay coatings. In addition, small dense carbonate concretions from 0.5 to 1 cm in diameter are present. The described features definitely indicate changes in humidity during the apparently long period of soil formation. The paleosol is classified as eroded Dark Gray soil (Phaeozem Calcic).

Upper lying marine deposits

Layer 13, depth 5.4-7.26 m. The sand layer (Fig. 2) is dark yellow (10YR 5/6), contains abundant wormholes throughout, rare gypsum and carbonate nodules. The sand is probably of marine origin (beach facies). OSL dating from the lower part of the sand layer is 279.4 ± 34.6 ka BP (Timireva et al. 2022). It is possible that most of it was formed in MIS 7. However, this date refers to MIS 8 (Lisiecki and Raymo 2005). And therefore, it can be assumed that the Uzunlar transgression began at the end of MIS 8 and continued in MIS 7.

The Middle Pleistocene LPS includes two paleosols.

Layers 14, 15. The PS4 paleosol: Bth horizon (7.26-7.92 m) and Bk (7.92-8.34 m) horizon. The Bth horizon is dark-yellow loam, fine- and medium-porous, with fine-diamond-shaped structure; faces of angular peds are covered by humus-clay and clay coatings, occasionally superposed with gypsum crystals and brown iron-staining mottles. The Bk horizon is brownish-yellow loess-like loam with thin clay and manganese coatings along with large carbonate concretions up to 10 cm in size. The paleosol may be defined as eroded Black Meadow Chernozem (Luvic Chernozem Stagnic).

Layer 16 (8.34-8.64 m; Fig. 2). The brown loess-like loam shows pronounced disturbances in the form of vertical cracks 4-5 cm wide. Notably, the layer contains manganese films in pores along with gypsum druses and dense carbonate concretions.

Layers 17, 18, 19. PS5 paleosol shows the strongest and most complex polygenetic profile consisting of the subsurface Bs horizon (8.64-9.3 m), Bk horizon (9.3-9.72 m) and lowermost Bgk horizon (9.72-10.02 m). The Bs horizon is strong red-brown dense loam, strong angular aggregates, and abundant Mn coatings in pores and upon aggregates. The Bk shows complex multi-layered coatings suggesting several stages of soil development. Strong bioturbation with molehills infilled with red-brown loam is indication of steppic stage in the polygenetic history of the paleosol formation. The lower Bgk horizon is bluish-yellow (10YR 6/4 Munsell) loam, reflecting the initial hydromorphic conditions of paleosol formation. The PS5 paleosol may be defined as Chromic Luvisol Calcic.

Underlying marine-liman deposits

Layer 20. Dark yellow sand (10.02–10.38 m), processed in the upper part by soil formation processes, broken up by veinlets from the overlying soil with cutane inclusions.

Layer 21. Dislocated firth-marine black clays (10.38-10.8 m).

Layer 22. A sequence of alluvial-estuary deposits of the Chaudian age (~20 m thick), represented mainly by sands (Svitoch and Novichkova 2001; Dodonov et al. 2006). The remains of fossil rodents were found in the upper part of this sequence (Fig. 2 and Fig. 3).

Fig. 3. Pekla section (photo of A.E. Dodonov)

Layer 23. The lowermost deposits exposed at the site are represented by dark clay attributed to Neogene (Dodonov et al. 2006).

Fossil rodents

The fossil rodent remains were recovered from the fluvial deposits below the loess-paleosol sequence during the field works of complex geology-paleontological studies headed by A.E. Dodonov (Geological Institute of the Russian Academy of Sciences) (Dodonov et al. 2006). The rodent locality was found in the sand deposits 5 meters below the Vorona paleosol (the lower paleosol of the Pekla section) (Markova 2002). This complicated paleosol was formed during the Muchkap and maybe also the Ikoretsk Interglacials (Shik 2014).

The following rodent species were distinguished (number of specimens in brackets): *Spermophilus* sp. (1), *Eolagurus* sp. (7), *Mimomys savini* Hinton (4), *Microtus (Terricola) arvalidens* Kretzoi (4), *Microtus (Alexandromys)* ex gr. *oeconomus* Pallas (1), Arvicolinae indet. (10) (Fig. 4). This species composition is characteristic of the faunas of the Tiraspolian faunal assemblage. The combination of species such as voles of the genus *Mimomys* with the vole species *Microtus (Terricola) arvalidens* is typical of the developed Tiraspolian faunas and in particular of the stratotype section from the Kolkotova Balka section near the city of Tiraspol (Nikiforova et al. 1971; Alexandrova 1976).

These deposits also include the Chaudian mollusk fauna with *Didacna baericrassa, Monodacna subcolorata, Adacna* aff. *plicata, Dreissena polymorpha, Dr. rostriformis, Paludina dresseli, Bythinia vucotinovici, Didacna rudi, Monodacna subcolorata, Unio* ex gr. *pictorum* (Svitoch and Novichkova 2001).

The rather small Pekla fauna includes the extinct species *Mimomys savini* and M. (T.) *arvalidens*. Their ecology is unclear. The presence of the remains of the yellow steppe lemming, *Eolagurus*, indicates the distribution of open environments near the section. The vole *Microtus oeconomus* is native to the vicinity of water reservoirs of different genesis (rivers, lakes and others). Its range extends from the northern forest-tundra to the southern steppe and semi-desert. It is very likely that the open steppe-like environments existed during the deposition of marine-liman sand deposits.

It is important to note that M. (T.) *arvalidens* is absent from older Tiraspolian faunas, for example it is absent from the Shamin fauna (Don basin) (Markova 1982, 2007; Markova and Puzachenko 2016, 2018). The species composition of small mammals from Shamin includes *Mimomys pusillus, Prolagurus posterius, Eolagurus* cf. *argyropuloi, Allophaiomys pliocaenicus, Lasiopodomys (Stenocranius) hintoni, Microtus* ex gr. oeconomus, *M. arvalinus (= M. nivaloides)* and others.

M. (T.) arvalidens is also absent from the Litvin small mammal fauna found in the deposits from the beginning of the Chauda transgression (Taman Peninsula) (Markova

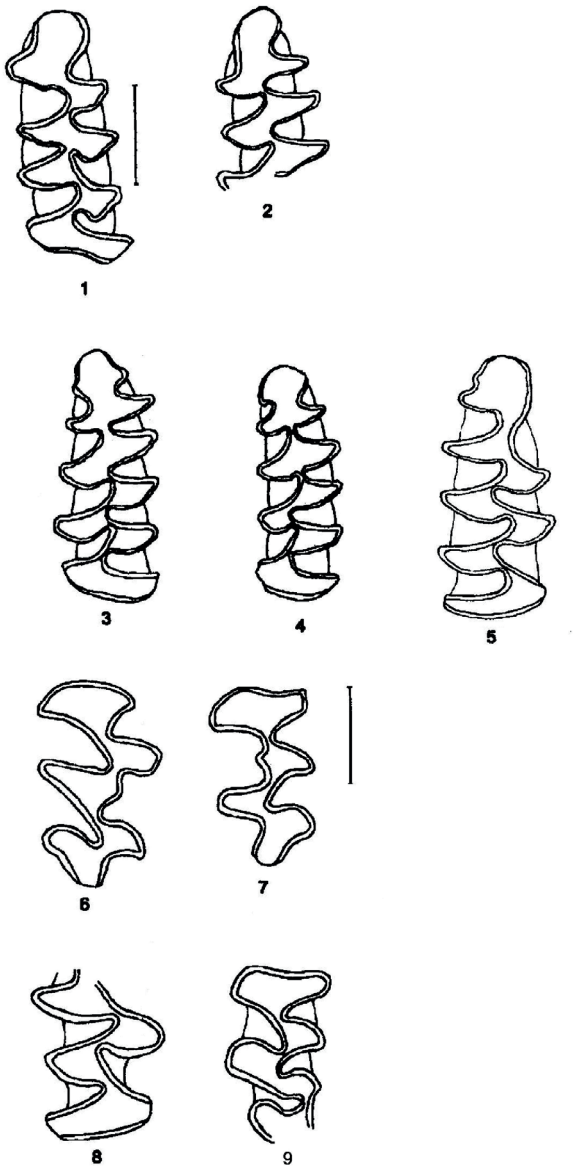

Fig. 4. Rodent species. 1-4 – m1 *Microtus (Terricola) arvalidens*; 5 – m1 *Microtus (Alexandromys) oeconomus*; 6 – M1, 7 – M2 – *Eolagurus* sp.; 8 - m1 (fragment), 9 – M3 - *Mimomys savini*

2014; Markova and Puzachenko 2018). The Litvin locality includes *Ochotona* sp., *Allactaga* sp., *Mimomys savini, Borsodia fejervaryi, Prolagurus pannonicus, Eolagurus simplicidens gromovi, Allophaiomys pliocaenicus, Lasiopodomys (Stenocranius) hintoni-gregaloides, Microtus oeconomus* and others. This fauna is older than that of Pekla.

Palaeomagnetic studies indicated a reverse magnetization of the deposits, which included the Shamin locality (Velichko et al. 1983b). This site is located in deposits correlated with the uppermost interval of the Maruyama palaeomagnetic epoch.

In contrast, the Litvin fauna was found in the Chauda deposits formed at the beginning of the Brunhes palaeomagnetic epoch (Zubakov 2005). The early Tiraspolian faunas thus existed both during the end of Matuyama epoch, and at the beginning of the Bruhnes epoch.

More advanced evolutional features have the small mammals discovered in the fluvial deposits of the VI Dniester terrace in the Kolkotova Balka section. Based on geological and faunistic (mammals, mollusks) arguments the finds from Kolkotova Balka were assigned to the so-called "Tiraspolian faunal assemblage" (Nikiforova et al. 1971). There remains were found of *Mimomys savini, Prolagurus posterius, Lagurus transiens, Microtus (Terricola) arvalidens, M. arvalinus* (Alexandrova 1976). The Levada small mammal locality (Moldova), which was found in the fluvial deposits of VI Dniester terrace, also contained a similar mammal species (Markova et al. 2021).

The faunas of this evolutionary level are correlated with MIS 17 (Markova and Puzachenko 2018). The species composition of the Pekla fauna is similar to these faunas and could also be correlated with MIS 17 (Fig. 5).

Younger Tiraspolian faunas were described from the deposits of the Don Glaciation (MIS 16) and the Muchkap Interglacial (MIS 15).

A fauna with cold-adapted species *Dicrostonyx* ex gr. *simplicior*, and also *Lasiopodomys (Stenocranius) gregaloides, Prolagurus* cf. *pannonicus, Microtus* ex gr. *hyperboreus, M. oeconomus* was discovered in the Bogdanovka locality (Don basin), located directly below the Don till, down to the fluvio-glacial deposits with moraine gravel (Markova 1990, 1992). This fauna is correlated with MIS 16 (Fig. 5)

The first appearance of *Lasiopodomys (Stenocranius) gregalis* is found in the faunas of the Muchkap Interglacial. Besides *L. (S.) gregalis, Mimomys savini, Lagurus transiens, M. (T.) arvalidens* also occurred in this interglacial (Fig. 5). Such faunas were found in several regions of the Russian Plain – in the Danube basin (Suvorovo locality), in the Don basin (Korotoyak 4, Korostylevo 2, Kuznetsovka, Perevoz, Posevkino and many other localities). All of these sites are deposited above the Don till in the Don basin. The first appearance of *L. (S.) gregalis* reflects the more advanced stage in the evolution of the Tiraspolian small mammal faunas correlated with the Muchkap Interglacial (Agadjanian 2009; Mikhailesku and Markova 1992; Markova 1992; Markova and Puzachenko 2018).

DISCUSSION

Many researchers studying the structure of LPS in the Sea of Azov and the Northern Black Sea region for decades have identified paleosols and pedocomplexes of different ages corresponding to interglacials and interstadials (e.g., Dodonov et al. 2006; Pilipenko and Trubikhin 2011; Pilipenko et al. 2010; Timireva et al. 2022; Velichko et al. 1973a; Zubakov 1988).

The paleosols we studied in the Pekla section did not retain their original appearance, as they were largely exposed to wind and water erosion and other diagenetic changes: cracking as a result of desiccation and, possibly, freezing, secondary biogenic overgrowth, and the impact of soil solutions after burial. Therefore, their diagnosis is difficult. Nevertheless, the morphotypic appearance of some of the paleosols has been preserved. Their stratigraphic position and the results of OSL dating allow us to draw the following conclusions:

The Holocene chernozem was formed in MIS 1, initially transforming the upper part of loess-like loams (layers 4 and 5) accumulated in the second half of MIS 2. This is confirmed by the OSL date of 19.2 ± 1.6 ka (Timireva et al. 2022).

A typical loess (layer 6) was deposited during the maximum of the Valdai glaciation, in the first half of MIS 2. The severity of the conditions at that time is evidenced by subvertical cracks of cryogenic origin, breaking up the PS1 paleosol.

This PS1 paleosol (layer 7) formed in the Middle Valdai Megainterstadial (MIS 3) before the last glacial maximum. In the Pekla section, it does not have properties characteristic of typical Bryansk soils of the East European Plain (Velichko and Morozova 2010). It is characterized by a finely ridged structure, clay coats along the edges of the peds, and reddish tones in color. Perhaps these differences are related to the zonality of the soil cover (southern variant of the soil), but, more likely, to the earlier generation. Most likely, it can be compared with the Alexandrovka paleosol, which was formed at the beginning of MIS 3 (Sycheva et al. 2021). Thermoluminescence dating – 40 ± 5 ka, obtained from a sample of the uppermost loess horizon (above the first paleosol) in a nearby outcrop at the southern end of lake Tsokur (Taman Peninsula) (Zubakov 1988) gives grounds to attribute the formation of this paleosol to the first half of MIS 3.

The erosional contact between the upper paleosol PS1 and the underlying loess indicates a break in loess accumulation, as well as a rearrangement of the relief form during the transition from the cold time (MIS 4) to the megainterstadial (MIS 3). The loess, subsequently transformed into the carbonate horizon of the PS1 paleosol (layer 8), thus accumulated in MIS 4.

In the Pekla section, the next two paleosols, an interstadial (PS2, layer 9) and an interglacial (PS3, layer 11), have been separated by loess, and transformed into the carbonate horizon of the second soil (layer 10) formed in MIS 5. Both soils are forest-steppe soils, but the lower one is more developed and originated in more humid conditions. The second soil, the Krutitsa soil according to (Velichko et al. 1997) or the Kukuevka paleosol according to (Sycheva et al. 2020) was formed in one of the two interstadials of the Early Valdai, rather the first one (MIS 5c). The third paleosol has all the diagnostic characteristics of the soil of the Mikulino Interglacial (MIS 5e): the Salyn paleosol according to (Velichko et al. 1997) or its temporary analogue, the Ryshkovo paleosol according to (Sycheva et al. 2020). These characteristics are a bright brown illuvial-clayey horizon with a nutty structure and abundant clay coatings along the edges of soil aggregates, indicating the accumulation of illuvial clay from the overlying but not preserved horizon. Interglacial paleosol PS3 is developed on loesses (layer 12) of the end of the Moscow glaciation (MIS 6) and is a horizon marking the boundary between the Middle and Upper Pleistocene. This soil is represented in many reference sections of the Russian Plain and in other areas, as well as in the Northern and Southern Sea of Azov

(Panin et al. 2018; Sedov et al. 2013; Sycheva and Sedov 2012; Velichko et al. 1977).

Previously, the OSL age of sandy rocks from the Pekla section separating the paleosols was determined to be 156 ± 10 ka without correction for bleaching, and >204 ka, considering the bleaching rate (Pilipenko et al. 2010). Based on this date, the authors reasonably attributed the accumulation of these deposits to the Uzunlar transgression of the Black Sea. The available information on the date of this transgression suggests that a marine basin here between 240 and 280 thousand years ago, that is, in MIS 7 (Svitoch et al. 1998). For the lower part of the layer of coastal-marine sands (layer 13), the new OSL date of 279.4 ± 34.6 ka turned out to be significantly older than the previous one (Timireva et al. 2022).

The deposition of the sands (layer 13) probably started at the end of MIS 8, i.e., in the initial phase of the Uzunlar transgression. The age of the coastal-marine sands (layer 13) underlying the loess (layer 12) is 279.4±34.6 ka and their stratigraphic position in the section makes it possible to compare the time of their accumulation with the Uzunlar transgression (Timireva et al. 2022). The Uzunlar transgression of the Black Sea occurred in the period from 220 to 280 thousand years ago, that is, in MIS 7-8 and probably extended to the Azov region (Svitoch et al. 1998). The new data obtained show that the sand deposition most likely began at the end of MIS 8 and continued in MIS 7.

The underlying Middle Pleistocene loess-soil series contains two interglacial paleosols. The main phase of the late Middle Pleistocene soil is correlated with the Inzhavino paleosol (PS 4, layers 14, 15), which was formed during the Likhvin interglacial (MIS 11). This soil's tendency to divide into separate blocks, as well as the quantity of humus-clay and clay films on the faces of diamond-shaped peds, are defining characteristics of its morphology (Iosifova et al. 2009; Panin et al. 2018, 2019; Velichko and Morozova 2010). It was formed in the warm temperate climate of the steppes.

The four upper soils thus formed under forest-steppe and steppe conditions of temperate and temperate warm climates. Only the lower one, or rather the PS 5 pedocomplex (layers 17-18), developed during its main period in a subtropical climate. The large thickness of the profile and the complex structure of this pedocomplex indicate several stages of development. This suggests that the PS 5 pedocomplex developed during not just one, but two interglacials. There is no doubt that this paleosol can be compared with the Middle Pleistocene Vorona pedocomplex, whose profile contains at least two interglacial soil phases (Panin et al. 2018; Velichko et al. 1973 a, b; Velichko et al. 1992; Velichko and Morozova 1973, 2010). Moreover, the two-phase nature of the pedocomplex is also clearly seen in the studied Pekla section. The lower horizon has distinctive features indicating the soil formation under subtropical conditions. It shows the most differentiated profile, a complexly organized structure, and bright red tones. Its first and main, warmer and wetter phase is associated with the Muchkap Interglacial (MIS 15), and the second phase is associated with the Ikoretsk Interglacial (MIS 13).

What is the reason for the absence of the several Late and Middle Pleistocene paleosols, one should ponder. There are no paleosols formed in MIS 7 (Romny paleosol) and in MIS 9 (Kamenka paleosol), which is obviously due to the palaeogeomorphological position of the section. Second, in MIS 7–8 and in MIS 17, during the transgressions of the Black Sea, there was a depression here, a marine bay or estuary. Despite partial filling with subaerial deposits, the depression continued in the interglacial that followed the transgression. This contributed to a more complete preservation of the soils formed at that time and already buried in the next cold period. At the same time, the elevation sites paleosols were destroyed and not preserved. However, over time, the depression became more and more filled with sediments and no longer served as a reliable repository for paleosols (Sycheva 2008). Therefore, those paleosols formed during subsequent warmings (interglacials and interstadials) after the formation of depressions are better preserved in the studied section – marine bays or estuaries during the transgressions.

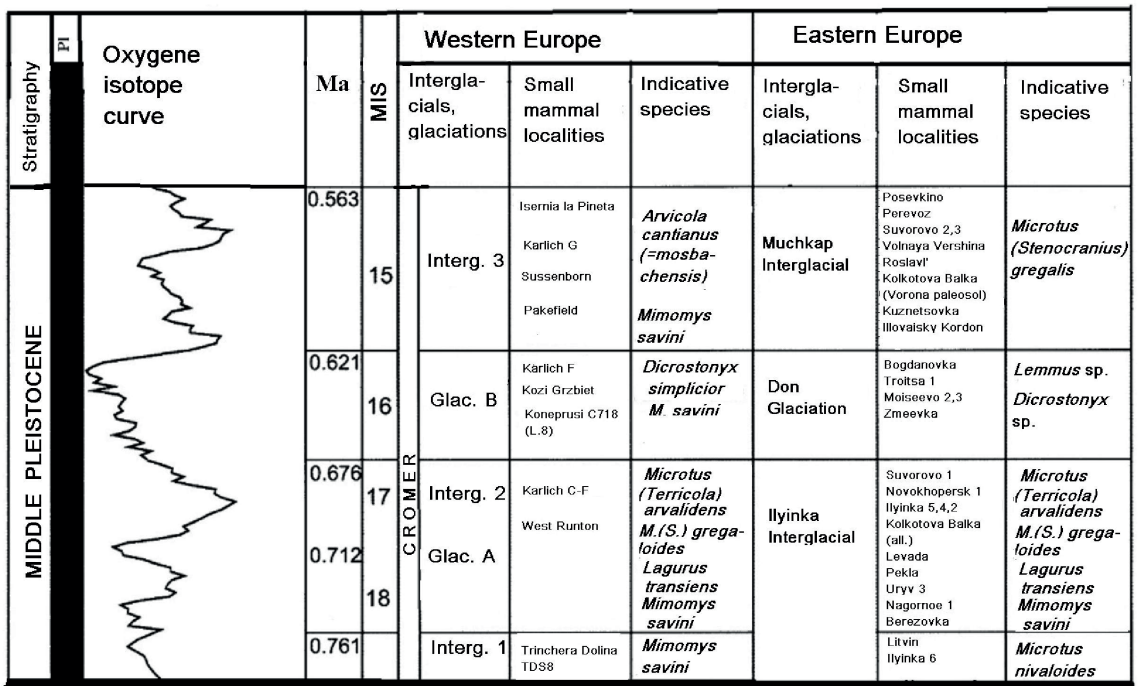

Fig. 5. Biostratigraphical subdivision of the early Middle Pleistocene based on small mammals (after Agadjanian 2009; van Kolfschoten and Turner 1996; Markova 1916; Markova and Puzachenko 2018; Maul and Parfitt 2010; Nadachowski 1985; Stuart 1996; Stuart and Lister 2010 and others)

CONCLUSION

The entire sequence of the Tiraspolian small mammal faunas is correlated with the early Middle Pleistocene (from the Brunhes – Matuyama boundary to the beginning of the Ikoretsk Interglacial (MIS 13), when the first archaic water voles appeared in Eastern Europe (Iosifova et al. 2009; Shik 2014). The evolutionary characteristics of the small mammals from the Pekla section suggests that this fauna could be correlated with faunas from the fluvial deposits of the VI Dniester terrace in Kolkotova Balka, the stratotype section of the Tiraspolian faunal assemblage, situated near the city of Tiraspol (Moldova) and in the Levada section (VI terrace of Dniester River) (Alexandrova 1976; Markova 2016; Markova et al. 2021; Markova and Puzachenko 2018). The Novokhopersk and the Ilyinka 5, 4, 2 faunas (Don basin) possess a similar species composition (Agadjanian 2009). These faunas are correlated with the complicated Ilyinskian Interglacial (MIS 17 and 18) (Shik 2014).

The faunas of this evolutional level are very close to the famous British fauna from the West Runton Freshwater Bed, which includes *Clethrionomys hintonianus, Pliomys episcopalis, Mimomys savini, Microtus* sp. *("arvalinus"), L. (Stenocranius) gregaloides, Microtus "ratticepoides", M. (Terricola) arvalidens,* and *Apodemus* cf. *sylvaticus* (Stuart 1996; Maul and Parfitt 2010). Maul and Parfitt (2010) correlate this fauna with the beginning of the Cromer Interglacial II. The Pekla fauna is also close to the fauna of the German multilayer locality Kärlich C-F (van Kolfschoten and Turner 1996). All faunas of this evolutional level are correlated with the MIS 17 (Fig. 5).

The rodent fauna of Pekla thus has a distinct position on the stratigraphical scale. It is younger than Early Tiraspolian faunas from Litvin (Taman Peninsula) and Shamin (Don R. basin), but older than Late Tiraspolian faunas correlated with the Don Glaciation (MIS 16) and the Muchkap Interglacial (MIS 15), where the first *Lasiopodomys (Stenocranius) gregalis* appear (Markova and Puzachenko 2016, 2018) (Fig. 5).

The characteristics of the paleosols, and the structure of the Pekla section with two loess-soil series (upper and lower, separating and underlying marine sands and clays with OSL dates), made it possible to reconstruct the sequence of events in the Late and the Middle Pleistocene and compare them with marine isotope stages.

The lower soil (PS 5) is the Vorona pedocomplex. It formed in a subtropical climate during the Muchkap Interglacial (MIS 15) and in a temperate climate during the subsequent Interglacial (MIS 13). Its stratigraphic position is in the early Middle Pleistocene, which is in good agreement with the small mammal studies presented in this paper.

The Inzhavino paleosol (PS 4) was formed under the steppe conditions of a temperate climate. The time of its formation falls in the Likhvin interglacial (MIS 11), and its stratigraphic position corresponds to the beginning of the late Middle Pleistocene.

The upper three paleosols belong to the Late Pleistocene: the lower one to the Mikulino Interglacial (MIS 5e), the second to the Early Valdai Interstadial (MIS 5c), and the upper one to the Middle Valdai Interstadial (beginning of MIS 3).

Thus, the upper LPS is the Late Pleistocene ones (PS 3-1), while the lower one is the late Middle Pleistocene (PS 4) and the early one (PS 5) corresponds to the Muchkap and Ikoretsk Interglacials (MIS 15 and MIS 13).

The findings of rodent locality of the evolved Tiraspolian stage (MIS 17) beneath the paleosol 5 (PS5) in the marine-liman deposits of the Pekla section proves the soil's age and the veracity of its correspondence to the Vorona fossil soil (MIS 15 and MIS 13).

A significant contribution to the paleogeography and stratigraphy of this time period has been made by the newly discovered palaeopedological and micromammalian data from the Pekla section. These data allow us to improve our understanding of natural events for a lengthy period of time, from the early Middle Pleistocene to the Holocene.

REFERENCES

A.K. Agadjanian A.K. (2009). Pliocene-Pleistocene mammals of the Russian plain. Paleontol. J. Moscow: Nauka, 45, 474–475 (in Russian).

Alexandrova L.P. (1976). Anthropogene rodents of the European part of the USSR: Moscow, Nauka Press, 98 (in Russian).

Dodonov A.E., Zhou L.P., Markova A.K., Tchepalyga A.L., Trubikhin V.M., Aleksandrovski A.L. and Simakova A.N. (2006). Middle–Upper Pleistocene bio-climatic and magnetic records of the Northern Black Sea Coastal Area. Quaternary International, 149, 44-54, DOI: 10.016/quaint.2005.11.017

Iosifova Yu.I., Agadjanian A.K., Ratnikov V.Yu. and Sycheva S.A. (2009). About the Ikoretsk suite and the horizon in the upper part of Lower Neopleistocene in the Mastyzhenka section (Voronezh region). Bull. of Regional Interdepartmental Stratigraphical Commission on center and south of the Russian Plain. Moscow Interdepartmental Stratigraphical Committee of Russia, 89-105 (in Russian).

Lisiecki L.E. and Raymo M.E. (2005). A Pliocene-Pleistocene stack of 57 globally distributed benthic 18O records. Paleoceanography, 20(1), PA1003, DOI: 10.1029/2004PA001071.

Markova A.K. (1982). Pleistocene rodents of the Russian Plain: Moscow, Nauka Press (in Russian).

Markova A.K. (1990). Pleistocene microtheriofauna of the European part of the USSR. Int. Symp. Evol. Phyl. Biostr. Arvicolids (Ed.- O.Fejfar and W.- D. Heinrich); Praha, 313-338.

Markova A.K. (1992). Pleistocene Microtheriofauna of Eastern Europe. Stratigraphy and Quaternary palaeogeography of Eastern Europe. Inst. of Geography RAS, 50-94 (in Russian).

Markova A.K. (2002). New fossil small mammal localities on the Taman Peninsula. Abstract to III Russian Quaternary Conference: Smolensk, №1, 166-167 (in Russian).

Markova A.K. (2007). Pleistocene mammal faunas of Eastern Europe. Quaternary International, 160(1), 100-111, DOI: 10.1016/j.quaint.2006.09.11.

Markova A.K. (2014). Small mammal faunas from deposits of the Chaudian transgression. Stratigraphy and sedimentology of oil-gas basins. Special issue devoted to IGCP 610 Second Plenary Conference "From the Caspian to Mediterranean: Environmental change and human response during the Quaternary", №1, 95-97.

Markova A.K. (2016). Small mammal faunas related to the Early Middle Pleistocene. Izvestia RAS. Seria geogr. №1, 87-102 (in Russian).

Markova A.K., Chepalyga A.L. and Puzachenko A.Yu. (2021). Middle Pleistocene small mammal and mollusk locality Levada (lower Dniester River basin) and it position in the Tiraspolian faunas of the Russian plain. Quaternary International, 605, 81-92, DOI: 10.1016/j.quaint.2020.08.006.

Markova A.K. and Puzachenko A.Yu. (2016). The European small mammal faunas related to the first half of the Middle Pleistocene. Quaternary International, 420, 378-390, DOI: 10.1016/j.quaint.2015.07.067.

Markova A.K. and Puzachenko A.Yu. (2018). Middle Pleistocene small mammal faunas of Europe: evolution, biostratigraphy, correlation. GES, 11, 21-38, DOI: 10.24057/2071-9388-2018-11-3-21-38.

Maul L.C. and Parfitt S.A. (2010). Micromammals from the 1995 Mammoth Excavation at West Runton, Norfolk, UK: Morphometric data, biostratigraphy and taxonomic reappraisal. Quaternary International, 228, 91-115, DOI: 10.1016/j.quaint.2009.01.005.

Mikhailesku, K.D. and Markova, A.K., 1992. Palaeogeographic stages of fauna development on the south of Moldova during the Anthropogene: Kishinev, Shtiintsa (in Russian).

Nadachowski A. (1985). Biharian voles (Arvicolidae, Rodentia, Mammalia) from Kozi Grzbiet (Central Poland). Acta zool. Cracov. 29/2, 3-28.

Nikiforova K.A., Belyayeva E.I., Vangengeim E.A., Konstantinova N.A. and Negadaev-Nikonov K.N. (Eds.) (1971). Pleistocene of Tiraspol: Kishinev, Shtiintsa (in Russian).

Panin P.G., Timireva S.N., Konstantinov E.A., Kalinin P.I., Kononov Y.M., Alekseev A.O., Semenov V.V. (2019). Plio-Pleistocene paleosols: loess-paleosol sequence studied in the Beregovoye section, the Crimean Peninsula. Catena, 172, 590–618, DOI: 10.1016/j.catena.2018.09.020.

Panin P.G., Timireva S.N., Morozova T.D., Kononov Y.M. and Velichko A.A. (2018). Morphology and micromorphology of the loess-paleosol sequences in the south of the East European Plain (MIS 1-MIS 17). Catena, 168, 79–101, DOI: 10.1016/j.catena.2018.01.032.

Pilipenko O.V., Sharonova Z.V., Trubikhin V.M., Abrahamsen N. And Moerner N.-A., 2005. Paleomagnetic and petromagnetic investigations of rocks of the Pekla loesssoil section (Krasnodar territory) in the interval 240-55 ka. Izvestiya Phys. Solid Earth, 41(6), 492–501 (in Russian).

Pilipenko O.V. and Trubikhin V.M. (2011). Paleomagnetic record in the Late Pleistocene loess-soil deposits of the Pekla section in the time interval 425-50 Ka. Izvestiya Phys. Solid Earth, 47(8), 686–697 (in Russian).

Sedov S., Sycheva S., Targulian V., Pi T., Díaz J. (2013). Last Interglacial paleosols with Argic horizons in Upper Austria and Central Russia: pedogenetic and paleoenvironmental inferences from comparison with the Holocene analogues. Quaternary Science Journal, 62(1), 44–58, DOI: 10.3285/eg.62.1.05.

Shik S.M. (2014). Neopleistocene of central European Russia (the new ideas on stratigraphy and palaeogeography). Stratigraphy. Geol. Correlation, 22(2), 108-120 (in Russian).

Shishov L.L., Tonkonogov V.D., Lebedeva I.I. (2004). Classification and diagnostics of Russian soils. Smolensk: Oikumena (in Russian).

Stuart A.J. (1996). Vertebrate faunas from the Early Middle Pleistocene of East Anglia. The early Middle Pleistocene in Europe: Rotterdam. Balkema, 9-24.

Stuart A.J. and Lister A.M. (2010). The West Runton Freshwater Bed and the West Runton Mammoth. Quaternary International. 228(1-2), 1-7, DOI: 10.1016/j.quaint.2010.07.035.

Svitoch A.A., Selivanov A.O. and Yanina T.A. (1998). Paleogeographic Events of Ponto- Caspian and Mediterranean: Materials on Reconstruction and Correlation. MSU Publishing House: Moscow (in Russian).

Svitoch A.A. and Novichkova T.S. 2001. Lithology and sedimintological condition of Chauda deposits of the Taman Peninsula (key sections Pekla and Tuzla). Lithology and natural resources, №5, 547-553 (in Russian).

Sycheva S.A. (2008). Morpholithopedogenes in accumulative and transaccumulative landscapes as a special mechanism of soil and lithology memory. Soil memory. Chapter 5: Moscow, LKI publishers, 128-160 (in Russian).

Sycheva S., Frechen M., Terhorst B., Sedov S., Khokhlova O. (2020). Pedostratigraphy and chronology of the Late Pleistocene for the extra glacial area in the Central Russian Upland (reference section Aleksandrov quarry). Catena, 194(1), DOI: 10.1016/j.catena.2020.104689.

Sycheva S.A., Khokhlova O.S. and Pushkina P.R. (2021). Structure of the Late Pleistocene Climate Rhythm Inferred from the Detailed Soil-Sedimentation Archive of the Extraglacial Region of the East European Plain (Aleksandrovka Quarry). Stratigraphy and Geological Correlation, 29(3), 368-387.

Sycheva S., Sedov S. (2012) Paleopedogenesis during the Mikulino interglacial (MIS 5e) in the East-European plain: buried toposequence of the key-section "Alexandrov quarry". Boletín de la Sociedad Geológica Mexicana, 64(2), 189-197.

Timireva S.N., Kononov Yu. M., Sycheva S.A., Taratunina N.A., Kalinin P.I., Filippova K.G., Zakharov A.L., Konstantinov E.A., Murray A.S. and Kurbanov R.N. (2022). Revisiting the Taman Peninsula loess-paleosol sequence: Middle and Late Pleistocene record of Cape Pekla. Quaternary International, 620, 36-45, DOI: 10.1016/j.quaint.2021.06.010.

Van Kolfschoten T., Turner E. (1996). Early Middle Pleistocene mammalian faunas from Kärlich and Miesenheim I and their biostratigraphical implications. The early Middle Pleistocene in Europe, Turner ed. J C. Balkema, Rotterdam, 228-253.

Velichko A.A., Gribchenko Yu.N., Gubonina Z.P., Morozova T.D., Nechaev V.P., Sycheva S.A., Timireva S.A., Udartsev V.P., Khalcheva T.A., Tsatskin A.I. and Chikolini N.I. (1977). The main features of loess-paleosol structure. Loess-paleosol formation of East-European Plain. Palaeogeography and stratigraphy. Moscow. Institute of Geography RAS, 5-24 (in Russian).

Velichko A.A., Markova A.K., Pevzner M.A., Udartsev V.P. (1983). The position of Matuyama-Brunhes boundary in the chronostratigraphical scale of continental deposits of Eastern Europe. Doklady AN USSR, 269(5), 1147-1150 (in Russian).

Velichko A.A., Markova A.K., Morozova, T.D. (1992). Loess-paleosol geochronology of the South-West Russian Plain on new data. In: Quaternary Geochronology: Moscow, Nauka, 28–33 (in Russian).

Velichko A.A., Morozova T.D. (2010). Basic features of Late Pleistocene soil formation in the East European Plain and their paleogeographic interpretation. Eurasian Soil Science. 43(13), 1535–1546, DOI: 10.1134/S1064229310130120.

Velichko A.A., Morozova T.D., Pevzner M.A. (1973a). Structure and age of loess and fossil soil horizons on the main terrace levels of the northern Azov region. Paleomagnetic analyses in studies of Quaternary deposits and volcano formations: Moscow, Nauka, 48–70 (in Russian).

Velichko A.A., Morozova T. D., Pevzner M.A., Khalcheva T.A. (1973b). Sequences of loesses and fossil soils on Chaudian-Bakinian deposits in the Taman Peninsula and their paleomagnetic characteristics. Paleomagnetic analyses in studies of Quaternary deposits and volcano formations: Moscow, Nauka, 70–76 (in Russian).

Working Group WRB IUSS. (2015). World Reference Base for Soil Resources 2014, update 2015. International soil classification system for naming soils and creating legends for soil maps. World Soil Resources Reports No. 106. FAO, Rome.

Zubakov V.A. (1988) Climatostratigraphic scheme of the Black Sea Pleistocene and its correlation with the oxygen-isotope scale and glacial events. Quat. Res. 29(1), 1–24, DOI: 10.1016/0033-5894(88)90067-1.

Zubakov V.A. (2005). State of art of climatostratigraphy: about the correlation of European climate with astrochronomentic scale. Bull. of Commission for study of the Quaternary. №66, 42-64 (in Russian).

RESEARCH PAPER

FLOOD SUSCEPTIBILITY MAPPING USING LOGISTIC REGRESSION ANALYSIS IN LAM KHAN CHU WATERSHED, CHAIYAPHUM PROVINCE, THAILAND

Katawut Waiyasusri[1*], Parichat Wetchayont[2], Aekkacha Tananonchai[3], Dolreucha Suwanmajo[4],
[1]Geography and Geo-informatics Program, Faculty of Humanities and Social Sciences, Suan Sunandha Rajabhat University, 1 U-Thong Nok Road, Dusit, Bangkok 10300 Thailand
[2]Department of Geography, Faculty of Social Sciences, Srinakharinwirot University, 114 Sukhumvit 23, Khlong Toei Nuea, Wattana District, Bangkok 10110 Thailand
[3]Bureau of Quality Control of Livestock Products, Department of Livestock Development Ministry of Agriculture and Cooperatives, 91 Moo 4, Tivanont road, Bang Kadi, Pathumthani 12000 Thailand
[4]AAPICO ITS Company Limited, Hitech Industrial Estate, 99 Moo 1, Ban Lane, Bang Pa-in, Ayutthaya 13160 Thailandina
***Corresponding author:** katawut.wa@ssru.ac.th
Received: November 8th, 2022 / Accepted: May 4th, 2023 / Published: July 1st, 2023
https://DOI-10.24057/2071-9388-2022-159

ABSTRACT. Due to Tropical Storm Dianmu's influence in the Lam Khan Chu watershed (LKCW) area, central Thailand saw its worst flood in 50 years from September 23 to September 28, 2021. The flooding lasted for 1-2 months. The objective of this research is to study flood susceptibility using logistic regression analysis in LCKW area. According to the study 11 floods occurred repeatedly between 2005 and 2021, in the southern of Bamnetnarong district and continued northeast to Chaturat district and Bueng Lahan swamp. These areas are the main waterways of the LKCW area, the Lam Khan Chu stream and the Huai Khlong Phai Ngam, for which the dominant flow patterns are braided streams. The main factors influencing flooding are geology, stream frequency, topographic wetness index, drainage density, soil, stream power index, land-use, elevation, mean annual precipitation, aspect, distance to road, distance to village, and distance to stream. The results of the logistic regression analysis shed light on these factors. All such variables were demonstrated by the β value coefficient. The area's susceptibility to flooding was projected on a map, and it was discovered to have extremely high and high levels of susceptibility, encompassing regions up to 148.308 km^2 (8.566%) and 247.421 km^2 (14.291%), respectively, in the vicinity of the two main river sides of the watershed. As a result of this research the flood susceptibility map will be used as a guideline for future flood planning and monitoring.

KEYWORDS: flood susceptibility, logistic regression analysis, Lam Khan Chu watershed, Chaiyaphum, Thailand

CITATION: Waiyasusri K., Wetchayont P., Tananonchai A., Suwanmajo D. (2023). Flood Susceptibility Mapping Using Logistic Regression Analysis In Lam Khan Chu Watershed, Chaiyaphum Province, Thailand. Geography, Environment, Sustainability, 2(16), 41-56
https://DOI-10.24057/2071-9388-2022-159

ACKNOWLEDGEMENTS: Acknowledgments to the U.S. Geological Survey (Earth Explorer Homepage: https://earthexplorer.usgs.gov/), and gratefully acknowledge for Suan Sunandha Rajabhat University Research Grant.

Conflict of interests: The authors reported no potential conflict of interest.

INTRODUCTION

Floods are major natural disasters on a global scale that can cause significant damage to life and property (Faiz et al. 2018; Maleki et al. 2020; Leal et al. 2021). It can be seen from the statistics of The Emergency Event Database (EM-DAT), which has recorded flood events all over the world, found that in 2021 there were 223 flooding events (CRED 2022). There are many factors affecting the occurrence of floods, including the occurrence of thunderstorms caused by low-pressure patches over the terrain, the Intertropical Convergence Zone across the low-latitude tropical region, and low-latitude tropical cyclone formation from turbulence, inevitably causes rain to soak for a long time (Sarjito et al. 2022; Purwanto et al. 2021). There are also additional factors that make territory more vulnerable to flooding, which are all caused by human activities such as building water barriers, urbanization, agricultural expansion, land-use change, including deforestation (Camara et al. 2020; Coetzee 2022; Waiyasusri and Chotpantarat 2022) catalysts the severity of floods and increases the frequency of flooding.

The floods in Thailand occur every year, especially during the monsoon season in May-October of each year (Tomkrtoke and Sirisup 2022; Rojpratak and Supharatid 2022). Tropical Storm Dianmu, which developed in the South China Sea and travelled west towards Vietnam, Laos, and Thailand between September 23 and September 28,

2021, had a significant impact on a catastrophic flood that occurred in central Thailand during that time (Thodsan et al. 2022). Tropical Storm Dianmu has created a massive rainstorm that lasted six days, causing flooding in 30 provinces in Thailand, leaving 6 dead and 2 missing (AHA centre 2021). It makes Lam Khan Chu Watershed (LKCW), which is an upstream area of Chi watershed in Chaiyaphum Province, in the north-eastern region of Thailand, with an area of 1731.289 km^2, prone to frequent flooding during the monsoon season (July-October of every year). This has caused considerable damage to communal and agricultural areas. Tropical Storm Dianmu had an impact on LKCW between September 23 and September 28 of 2021, causing the worst flooding in 50 years. The incident caused damage in the along the Huai Lam Khan Chu stream, affecting riverbank overflows and flooding up to 3-4 meters, affecting communities, agricultural areas, and transport routes in the Bamnetnarong district, Chaturat district, and Chaiyaphum Province, flooded lasting 1-2 months. Another reason for the great flooding is that the topography of LKCW is an upstream area with relatively low slopes and wide plains, coupled with land-use dominated by agriculture. And there is very little forest area upstream, which prevents rainfall from being retained in upstream forests and causes it to quickly become surface runoff into the downstream area.

Application of geo-informatics technology plays an important role in the analysis of current disaster management, especially in flooding. This is because it is a technology that can display spatial data and determine the coordinates and relationships of various variables that affect floods. For this reason, flood susceptibility mapping needs to be designed from a common database of hydrological, meteorological, geological and anthropogenic factors (Khosravi et al. 2016; Waiyasusri et a. 2021; Ghasemlounia and Utlu 2021). Typically, flood susceptible areas are analysed using hydrologic and hydraulic modelling approaches with field-based measurements or remote sensing data is used to feed the database into the analysis model (Maan et al. 2020; Bharath et al. 2021; Chauhan et al. 2022). However, statistical analysis principles were developed based on spatial models to conduct flood susceptibility studies to determine its behaviour (Nguyen et al. 2020; Suharyanto 2021; Khiavi et al. 2022). In terms of statistical principles for finding flood-risk areas, it is important to be able to analyse many variables and to analyse a wide area to see the distribution of flood-risk areas (El-Fakharany et al. 2021). In addition, the progress of geo-informatics technology can analyse and process various database sets compiled from past to present. The technology can effectively assess flood-susceptible areas and show good effectiveness.

The most popular educational approaches for flood susceptibility mapping are univariate models (Zhang et al. 2018; Li et al. 2018), multivariate models (Tosunoglu et al. 2020; Jane et al. 2020), and artificial neural network (ANN) models (Elsafi 2014; Dahri et al. 2022). Still, the technique has limitations on the complexity of database manipulation and processing that requires high levels of computer memory hardware and long analytics when using a large number of variables. Other models such as the Frequency Ratio (Ramesh and Iqbal 2022; Jaiswal et al. 2022), Analytic hierarchy process (Mitra et al. 2022; Ekmekcioğlu et al. 2021), and Logistic Regression (Al-Juaidi et al. 2018; Chowdhuri et al. 2020; Kim et al. 2020) also received attention, but not as much as the ANN model. For this reason, logistic regression analysis (LR) may be a better alternative statistical analysis procedure in flood susceptibility studies. Because it can analyse multiple geographic database sets, and databases that are continuous and categorical data. This can be seen from research that studies flood susceptibility in different regions of the world, such as the assessment of flooded areas in Jamaica that has applied LR. Importantly, the relevant variables are local geology, geomorphology, hydrology and land-use (Nandi et al. 2016). In Fujian Province, China, techniques of geodetector, certainty factor, and logistic regression were applied to establish a frame for the flash flood susceptibility assessment. According to empirical results the model achieves the highest degree of accuracy in terms of the success rates (Cao et al. 2020). Although Iran is an arid region, it experiences flash floods in the Haraz watershed in Mazandaran Province. The research introduced key parameters for assessing flood-sensitive areas: altitude, slope angle, plan curvature, Topographic Wetness Index (TWI), Stream Power Index (SPI), distance from river, rainfall, geology, land-use, and Normalized Difference Vegetation Index (NDVI) are all important variables (Bui et al. 2019). Even in the southern Gaza Strip areas, LR was applied to assess flood susceptible areas until the proposed model is robust with very reasonable accuracy (Al-Juaidi et al. 2018). However, it is crucial that the variables that are being added to the model be moderated before they are used in the study. As a study by (Tehrny et al. 2017), 15 flood conditioning factors were compiled and included geo-databases: altitude, slope, aspect, geology, distance from river, distance from road, distance from fault, soil type, land-use, rainfall, Normalized Difference Vegetation Index, SPI, TWI, STI, and curvature were analysed for LR and the results showed the highest prediction rate of 90.36%. (Hamid et al. 2020) studied the sensitivity of flash flood hazard using geospatial techniques, and analysed key variables such as elevation, slope, distance from the network, land-use, density of the drainage, flow accumulation, surface roughness, SPI, TWI, and curvature were analysed in Khartoum area, Sudan. When considering the variables, geography variables are considered first in the study process in which the data is generated from a digital elevation model (DEM). (Lim and Li 2018) in a study of flood mapping using multi-source remotely sensed data and LR in the heterogeneous mountainous regions in North Korea, found that DEM data that can be analysed for terrain should be of high resolution between 1-30 meters to be able to analyse terrain analysis as well. (Chen et al. 2020) using a machine learning technique for flood mapping in the Yangtze River Delta, China identified rainfall variables that are important for model analysis and can also be a catalyst for flooding. For this reason, LR was applied in this research to find flood susceptibility and mapping for floods in the future, specifically in accordance with the principles of the United Nations Sustainable Development Goals (SDGs), Goal 13 addresses: Take urgent action to combat climate change and its impacts (Department of Economic and Social Affairs 2022). It defined climate change as one of the main causes of natural disasters that are more frequent and likely to intensify, causing enormous losses to people's lives and property, as well as having broad economic and social impacts, especially at the community and local level with limited disaster response capacity.

The objective of this research was to study flood susceptibility using logistic regression analysis in Lam Khan Chu Watershed, Chaiyaphum Province, Thailand, by using spatial database that affects flooding in preparing a flood susceptibility map in LKCW. The study guideline has compiled variables that affect the occurrence of floods, as physical factors such as elevation, slope, aspect, stream power index (SPI), sediment transport index (STI), topographic ruggedness index (TRI), topographic wetness

index (TWI), stream frequency (SF), drainage density (DD), infiltration number (IN), mean annual precipitation, geology, soil, and distance to stream; and the socio-economic factor involved and provide flood, and are important variables that used in flood applications including land-use, distance to village, and distance to road. This study is able to predict the factors of influential flood causing variables on flood occurrence. By developing a geographical database for simple management of flood risk regions for sustainable solutions to probable future flooding, the research results will be applied as a guideline for planning and monitoring in the event of future floods.

MATERIALS AND METHODS

Study area

Lam Khan Chu Watershed is a sub-watershed of the Chi watershed. The study area is located between latitudes 15°15′ N to 15°40′ N and longitude 101°20′ E to 102°E. The total study area is approximately 1731.289 km^2. LKCW area covers Thep Sathit, Bamnetnrong, Chaturat, and Sap Yai districts in Chaiyaphum Province, and covers part of Theparak district, Nakhon Ratchasima province (Fig. 1). The topography in the study area has an altitude of between 186-819 meters above mean sea level. The western part is a high mountain range, with the highest point of the LKCW area in the northwest of the study area. Elevation of 819 meters, located in Pa Hin Ngam National Park, is an important watershed forest area in the study area. An undulating plain with a small slope that slopes of the research area makes up the majority of the study area. It appears that the lowest point of the study area is Bueng Lahan, which is an important wetland in this region. The elevation of the terrain is 186 meters. The drainage pattern of the LKCW is a parallel drainage pattern, i.e., there are tributaries flowing dendritic-parallel to the main waterway. There is a direction of flow from west to east. The geological features in the study area are homogeneous, consisting of sedimentary rock covering the entire study area. The Korat group is a group of rocks that belong to the Jurassic–Cretaceous (210-66.4 million year) period, namely the Phu Kradueng formation, Phra Wihan formation, Sao Khua formation, Phu Phan formation, Khok Kruat formation, and Maha Sarakham formation, respectively, and Alluvial deposits in Quaternary (1.6-0.01 million year) covered the downstream area of LKCW around Bueng Lahan swamp.

The sedimentary rocks are described below: Quaternary deposits (Qa) consists of fluvial deposits, Maha Sarakham formation (KTms) consists of sandstone and rock salt, Khok Kruat formation (Kkk) consists of siltstone and sandstone, Phu Phan formation (Kpp) consists of siltstone and conglomerate, Sao Khua formation (Ksk) consists of siltstone and sandstone, Phra Wihan formation (JKpw) consists of quarzitic sandstone and conglomerate, and Phu Kradueng formation (Jpk) consists of siltstone and claystone.

Data

For the preparation of data in this research, Secondary data from various sources were collected for the analysis of flood recurrence areas in the LCKW, in particular the Actual flood area data for 2005-2021 and spatial data for the analysis of factors contributing to flooding, collecting data as follows: physical factors such as elevation, slope, aspect, SPI, STI, TRI, TWI, SF, DD, IN, mean annual precipitation, geology, soil, and distance to stream. Socio-economic factors that are relevant and provide for flooding, and are considered the most important variables used in flood work are land-use, distance to village, and distance to road (Table 1). All data are generated in raster database format, grid cell size 30x30 m.

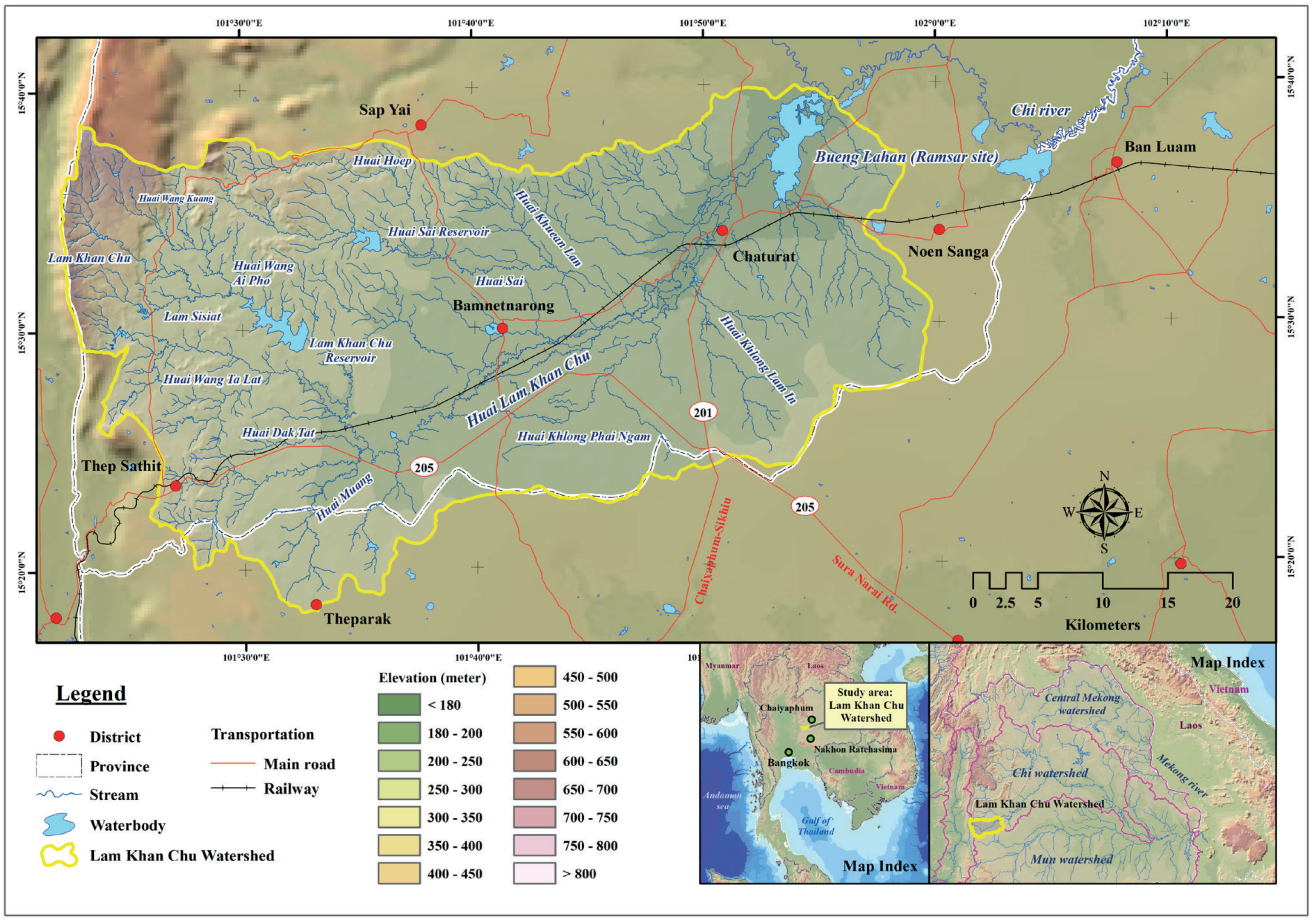

Fig. 1. Geographic map of the Lam Khan Chu Watershed area, Chaiyaphum Province

Table 1. Spatial data layers used in this research

Driving Factor	Variable (Theme)	Year	Source
	Actual flooding area	2005-2021	Derived from Geo-Informatics and Space Technology Development Agency (public organization) (GISTDA)
Physical factor	Elevation (Digital Elevation Model-DEM)	2020	Derived from Royal Thai Survey Department (RTSD)
	Slope	2020	Derived from the DEM
	Aspect	2020	Derived from the DEM
	Stream Power Index (SPI)	2021	Derived from the DEM
	Sediment Transport Index (STI)	2021	Derived from the DEM
	Topographic Ruggedness Index (TRI)	2021	Derived from the DEM
	Topographic Wetness Index (TWI)	2021	Derived from the DEM
	Stream Frequency (SF)	2021	Derived from the DEM
	Drainage Density (DD)	2021	Derived from the DEM
	Infiltration Number (IN)	2021	Derived from the DEM
	Mean annual precipitation	2005-2020	Derived from Thai Meteorological Department (TMD)
	Geology	2017	Derived from Department of Mineral Resources
	Soil	2017	Derived from Land Development Department (LDD)
	Distance to stream	2021	Derived from Department of Water Resource, Thailand
Socio-economic factor	Land-use	2020	Derived from Land Development Department (LDD)
	Distance to village	2021	Derived from Royal Thai Survey Department (RTSD)
	Distance to road	2021	Derived from Department of Public Works and Town &Country Planning.

Method

The research process consists of the following steps, as shown in Fig. 3 (1): flood prone area analysis, (2) spatial database analysis of driving factors, and (3) statistical approach. The details of each step are briefly explained below (Fig. 2).

Flood prone area analysis

The past occurrences records analysis may estimate future flood hazard events (Degiorgis et al. 2012; Tehrany and Kumar 2018). The first step for the analysis of flood susceptible areas is to analyze past events that tend to occur in the same area and the environmental variables that affect the flooding there. The Geo-Informatics and Space Technology Development Agency (public organization) (GISTDA) has analyzed and synthesized flood data from satellite imagery from various sources and compiled into a database system that can be used from the source https://flood.gistda.or.th/. Next, the flood prone area was generated from actual flood area during 2005 to 2019 using overlay analysis tools in GIS, obtained repeated flooding data over the past 16 years and then analyzed to determine the proportion of flooded area in the LKCW area, and those flood prone area data were analyzed for logistic regression in the next step.

Spatial database analysis of driving factors

The selection of factors affecting flooding is important for the flood susceptibility analysis to obtain accurate spatial results. In this study, the most related and repeated flood conditioning factors selection is crucial (Tehrany et al. 2015; Rahmati et al. 2019).

The first important data for this research study is Elevation (DEM) data obtained from the Royal Thai Survey Department (RTSD) in shapefile format, namely elevation point data, contour line data, stream line data, water bodies and watershed boundary. Most of the initial source data from the Royal Thai Survey Department (RTSD) are vector data, and thus are difficult to statistically analyze in research. Therefore, such vector data must be converted into a raster showing the statistical grid, especially digital elevation. The data was analyzed by spatial analysis by Topo to Raster technique in ArcGIS 10.2 software. The result was DEM data of 30x30 m grid cell size (Fig. 3a) for subsequent analysis of other variables. The local topographic slope (Fig. 3b), aspect (Fig. 3c), SPI (Fig. 3d), STI (Fig. 3e), TWI (Fig. 3f), TRI (Fig. 3g), SF (Fig. 3h), DD (Fig. 3i), and IN (Fig. 3j), were then calculated from the DEM. Flood prone areas are generally at low elevation and with a low degree of topographic slope (Kia et al. 2012). Aspect data, spatial data showing the direction of the slope, is an important component in determining the direction of water flow in high-slope terrain (Mojaddadi et al. 2017). The hydrological factors such as SPI, STI, TRI, and TWI also have considerable impacts on flood creation (Tehrany et al. 2017).

Stream power index (SPI) is the most widely used variable in flood susceptibility research. This is because it is a variable that indicates the potential for river currents to cause erosion. For this reason, such variables play a role in altering the surface condition of the terrain. The results show negative values for areas with topographic potential deposition and positive values for potential erosive areas. The SPI analysis can be calculated from Equation 1 (Moore et al. 1991; Tehrany et al. 2017):

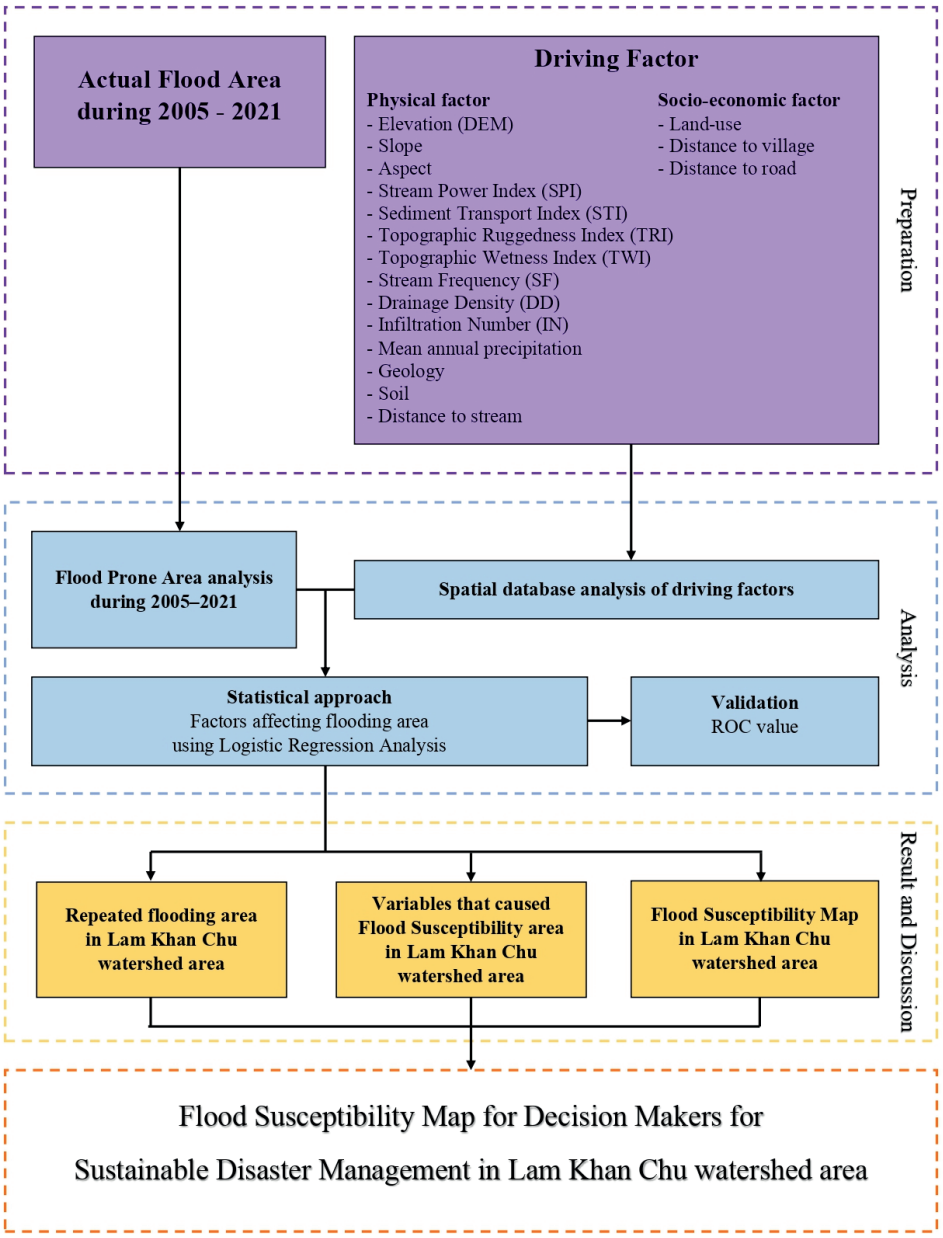

Fig. 2. Flowchart of methodology

$$SPI = A_S \tan\beta \quad (1)$$

Where, A_s indicates the definite catchment area, and β denotes the slope gradient.

Sediment transport index (STI) is another variable that defines the movements of the sediments due to the water movement. The erosion and deposition processes are characterized using STI (Mojaddadi et al. 2017). The results obtained with a high level of STI indicate an area of high sedimentation. Conversely, a low level of STI indicates an area of low sedimentation. STI analysis can be calculated from Equation 2:

$$STI = \left(\frac{A_s}{22.13}\right)^{0.6}\left(\frac{\sin\beta}{0.0896}\right)^{1.3} \quad (2)$$

Where, A_s indicates the definite catchment area, and β denotes the slope gradient.

Topographic wetness index (TWI) is a watershed-forecasting index and an indicator of the tendency for water to flow to a basin based on gravity (Chen and Yu 2011). High TWI values indicate areas prone to water accumulation in the basin, which may occur in lowland, low slope or basin areas. The TWI analysis can be calculated from Equation 3 (Hamid et al. 2020):

$$TWI = \ln\left(\frac{A_S}{\tan\beta}\right) \quad (3)$$

Where, A_s indicates the definite catchment area, and β denotes the slope gradient.

Topographic ruggedness index (TRI) provides a quantitative measure of terrain heterogeneity. TRI is a geomorphological variable that is related between the elevation of the terrain and the flood area (Werner et al. 2005). The results obtained with high levels of TRI indicate areas of high roughness appearing on the terrain, while low levels of TRI indicate relatively flat terrain. The TRI analysis can be calculated from Equation 4 (Tehrany et al. 2017):

$$TRI = Y\left[\sum\left(x_{ij} - x_{00}\right)^2\right]^{1/2} \quad (4)$$

Where, x_{ij} is elevation of each neighbor cell to cell (0,0).

Stream frequency (SF) is the ratio between the numbers of first-order streams to the watershed area. As a result, a high SF indicates an area with a low runoff, refers to the flow of water in a stream from upstream to downstream slowly and takes a long time. A low SF value indicates that the water flow in the stream flows quickly. The SF analysis can be calculated from Equation 5 (Horton 1932):

$$SF = \frac{\sum Ns}{A} \quad (5)$$

Where, N_s is the total number of first order streams and A is the total watershed area (km^2).

Drainage density (DD) is the ratio of the total stream length per watershed area. The result of the DD value, if the DD value is greater than 3, the watershed area has a drainage at the level of well drainage, if the value is between 1 to 3 indicates that the area of the watershed has a moderate drainage pattern, and if the value is less than 1, the area of the watershed has poor drainage. The DD analysis can be calculated from Equation 6 (Horton 1932):

$$DD = \frac{\sum Ls}{A} \quad (6)$$

Where, L_s is the sum of all river basin lengths and A is the total watershed area (km^2).

The Infiltration Number (IN) is the result of the DD and SF analysis of the watershed studied. IN is directly proportional to runoff (Faniran 1968; Das and Mukherjee 2005; Joji et al. 2013; Elewa et al. 2016). As the IN of the watershed shows high, the runoff remains high; and low infiltration number means the runoff is low. The IN analysis can be calculated from Equation 7:

$$IN = DD * SF \quad (7)$$

The additional physical factors applied in this study were mean annual precipitation, geology, soil, and distance to stream (Fig. 4). Mean annual precipitation factors were analyzed using data from the Thai Meteorological Department (TMD) from 2005-2020 to determine average rainfall, then spatial analysis using inverse distance weighted interpolation technique in spatial analysis tools in ArcGIS 10.2 software. The geology and soil variable data as nominal data were converted to raster data format. The distance to stream variable data were analyzed for distance from waterways using the Euclidean distance technique in spatial analysis tools.

The geology, soil, and land-use data are a nominal scale and is represented as categorical as float-number data as follows:

Geology data in the study area consisted of Phu Kradueng formation (Jpk) equal to 1, Phra Wihan formation (JKpw) equal to 2, Sao Khua formation (Ksk) equal to 3, Phu Phan formation (Kpp) equal to 4, Khok Kruat formation (Kkk) is 5, Maha Sarakham formation (KTms) is 6, and Quaternary fluvial deposits (Qa) is 7, according to the Department of Mineral Resources classification criteria.

Soil data in the study area consisted of slightly gravelly sand, coarse sand, loamy coarse sand, loamy fine sand, clay loam, clay, salinity soil, and marl soil. The two types of soils have different drainage potentials as shown in Fig. 4c, thus being represented as 1 and 2. Poorly drained soils are represented as 1 and well drained as 2, according to the classification criteria of the Land Development Department (LDD).

As for the land-use data, the study area has a variety of land uses, so it has been reclassified as follows: Agricultural land represented as 1, Forest land represented as 2, City and village represented as 3, Waterbodies represented as 4, and Miscellaneous area (including grass land, wetland, mineral, and salt pan) represented as 5, according to the classification criteria of the Land Development Department (LDD).

Land-use, distance to village, and distance to road are examples of key socioeconomic factors that affect flooding (Fig. 5). Land-use data is nominal data obtained from the Land Development Department (LDD). The data were converted to a raster data format, and the distance to village and distance to road variable data was obtained by analyzing distance from waterways using the Euclidean distance technique in spatial analysis tools.

Statistical approach

From the sequence of flood prone area analysis and spatial database analysis of driving factors, it was necessary to find factors affecting flooding in order to determine the flood context in LKCW, 17 variables were analyzed including elevation, slope, aspect, SPI, STI, TRI, TWI, SF, DD, IN, Mean annual precipitation, geology, soil, distance to stream, land-use, distance to village, and distance to road. These variables were analyzed together with flood prone area data using LR.

LR is a technique for discovering the empirical relationships between a binary dependent and several independent categorical and continuous variables (Nandi et al. 2016; Tehrany et al. 2017; Kim et al. 2020; Cao et al. 2020). LR is calculated using the following Equation (8).

$$Log\left(\frac{P_i}{1-P_i}\right) = \beta_0 + \beta_1 x_{1,i} + \beta_2 x_{2,i} + \ldots \beta_n x_{n,i} \quad (8)$$

Where, P is the flood prone area, x_i are independent variables and β is the coefficient value.

This statistical method was used to provide the variables that were analyzed to determine which variable had an influence on flooding in that area. It shows the effect of the variable in the β value, to determine the factor affecting the amount of flooding. These statistical principles consider the underlying and dependent variables for all grid cells in the LKCW area. In the conclusion, spatial data obtained from those Logistic regressions can be used to predict flood risk areas in the LCKW area by performing a classification method into 5 classes: very high, high, moderate, low, and very low. It is expressed as Flood Susceptibility Mapping to determine the area that should be addressed in a timely manner for flood disaster management for sustainable spatial development in the future.

RESULTS

Flood Prone Area during 2005–2021 in LKCW area

The flow system in dendritic-parallel drainage pattern of LKCW can divide the branch stream into two banks, on the left side and on the right side of the Lam Khan Chu stream. On the left side are the branch streams Huai Wang Kuang stream, Huai Sai stream, Huai Hoep stream and a short stream that flows into Bueng Lahan swamp. The important right-bank branches of Lam Khan Chu stream are Lam Sisiat stream, Huai Wang Ta Lat stream, Huai Dak Tat stream, Huai Muang stream, Huai Khlong Phai Ngam stream, Huai Khlong Lam In and short streams that flow into Bueng, Lahan swamp. The study of flooding area that occurred during August to October 2021 as Tropical Storm Dianmu hit Thailand, resulting in rainfall that exceeds the water-resistance area, causing overflow in the Lam Khan Chu reservoir. It partially damaged the reservoir, causing massive water inflows to flood the downstream areas, damaging the Bamnetnarong district and Chaturat district covering up to 112.067 km^2 (6.47% of the LKCW area) (Fig. 6a.). Although the flooded area is a narrow area along both banks of the Lan Khan Chu stream, Huai Khlong Phai Ngam, and Huai Khlong Lam In, but it has caused great damage to the area in the city, as most of them are community areas, economic and commercial areas, government offices, and agricultural areas.

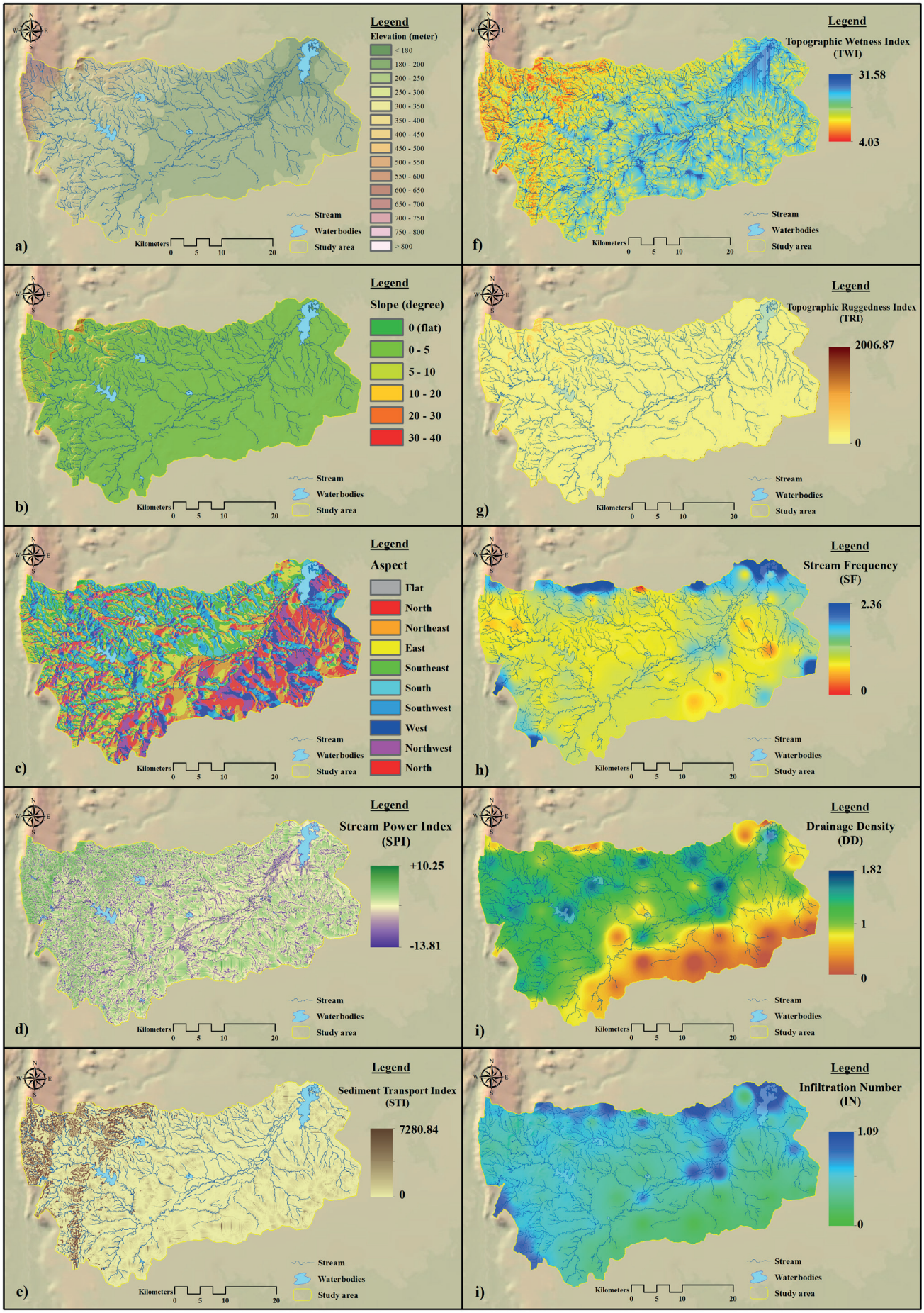

Fig. 3. Spatial database analysis of physical driving factors: elevation (a), slope (b), aspect (c), SPI (d), STI (e), TWI (f), TRI (g), SF (h), DD (i), and IN (j)

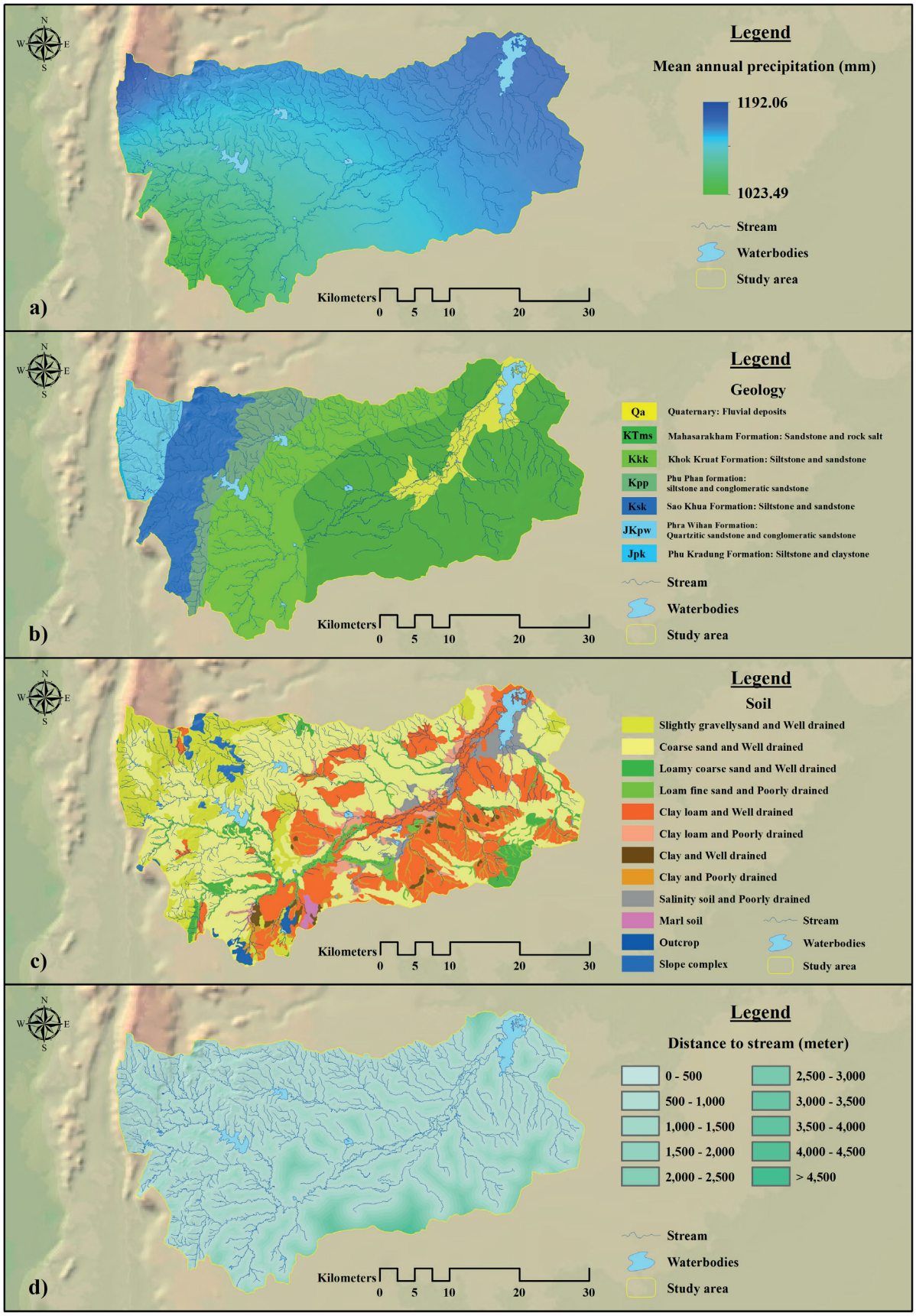

Fig. 4. Spatial database analysis of physical driving factors: mean annual precipitation (a), geology (b), soil (c), and distance to stream (d)

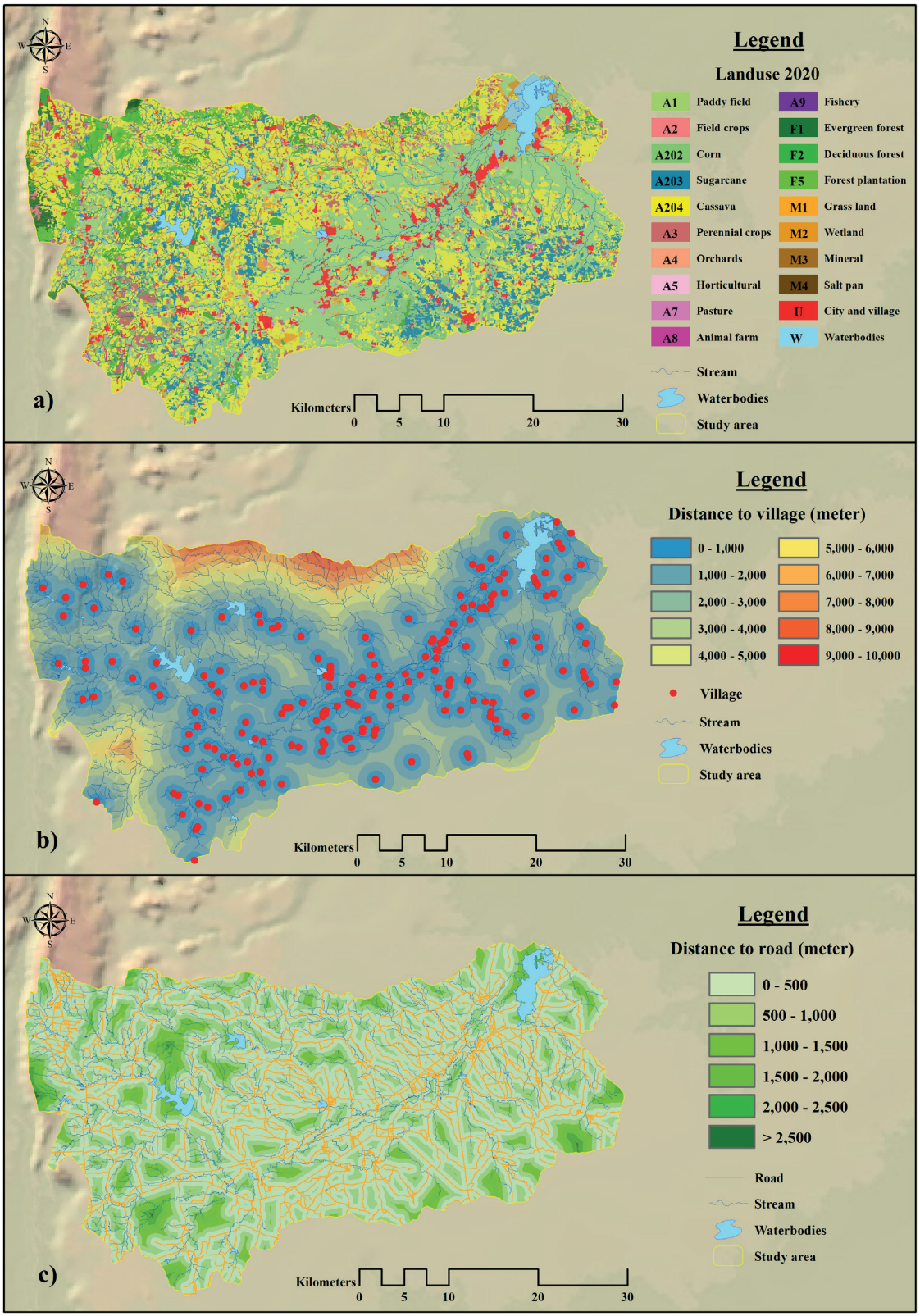

Fig. 5. Spatial database analysis of socio-economic driving factors: land-use (a), distance to village (b), and distance to road (c)

The area has undergone 11 frequent floods since 2005, according to the results of the flood prone area research conducted in LKCW between 2005 and 2021. 2017 was the year when flooding covered the LKCW the most, 127.252 km^2 (7.33% of the total watershed), followed by 2006, found that the flood area covered 118.054 km^2 (6.81 % of the total watershed area), and the years that no flood areas were found in the basin were 2005, 2011, 2015, and 2018, showing the proportion of flooded areas as shown in Table 2. The study of repeated flooding during 2005 – 2021 in LKCW found that most of the repetitive flooding areas occurred in the southern part of the Bamnetnarong district and continued northeast to Chaturat district and Bueng Lahan swamp. These areas are the main waterways of the LKCW area, namely Lam Khan Chu stream and Huai Khlong Phai Ngam, which flow patterns are braided streams, resulting in floodplain landscapes and therefore frequent flooding. As for the repeated flooding area, occurring 11 times in 17 years, it was found that an area of up to 0.543 km^2 (Table 3) appeared around Bueng Lahan swamp, which is northeast of Chaturat district, because it is a lowland terrain where many tributaries flow to the area (Fig. 6b).

Table 2. Flood Prone Area during 2005 – 2021 in LKCW

Year		2005	2006	2007	2008	2009	2010	2011	2012	2013
Area	km^2	-	118.054	68.846	22.327	16.139	101.531	-	11.087	78.854
	%	-	6.81	3.92	1.27	0.92	5.83	-	0.63	4.50
Year		2014	2015	2016	2017	2018	2019	2020	2021	
Area	km^2	10.986	-	82.768	127.252	-	5.370	17.025	112.067	
	%	0.57	-	4.73	7.33	-	0.31	0.98	6.47	

Table 3. Repeated flooding area over a period of 15 years (2005-2021) in LKCW

Repeated flooding (Time)	1	2	3	4	5	6	7	8	9	10	11
Area (km^2)	125.414	64.875	27.919	20.523	16.591	14.445	8.701	5.782	3.298	3.884	0.543

Factors affecting flooding in LKCW area

From the analysis of 17 key variables for determining the susceptibility to flooding in the LCKW area, were analyzed using the LR statistical process and the spatial database variables affecting flooding, the results of the study are shown in Table 4. The results were shown by statistical value β. If the β value of the variable was positive, the higher the variable, the more susceptible to flooding. But if the β value of that variable shows a negative value, it means that the variable with a lower value is more susceptible to flooding. The relative operating characteristic (ROC) shows how the regression equation can be used to predict flood prone risk area based on probability. The ROC values obtained for the probability of flooding area and non-flooding area are 0.899 and 0.865, respectively (Fig. 7), indicating a high value, because a value approaching 1.00 indicates that all 17 variables are effective in analysis of flood prone areas.

All variables were significant at the $p < 0.01$ entry and $p > 0.02$ removal levels (ROC relative operating characteristics)

Table 4. Logistic regression analysis of the flood prone area and affecting factors in LKCW area

Variable	Flooding area		Non-flooding area	
	Coefficient β value	Coefficient Exp β value	Coefficient β value	Coefficient Exp β value
Elevation (digital elevation model-DEM)	-0.032	0.968	0.041	1.040
Slope	-	-	0.018	1.018
Aspect	-0.001	0.999	0.001	1.001
Stream Power Index (SPI)	-0.079	0.924	0.079	1.082
Sediment Transport Index (STI)	-	-	-	-
Topographic Ruggedness Index (TRI)	-	-	-	-
Topographic Wetness Index (TWI)	0.042	1.043	-0.051	0.969
Stream Frequency (SF)	0.795	2.214	-0.785	0.442
Drainage Density (DD)	-0.786	0.456	0.796	2.195
Infiltration Number (IN)	-	-	-	-
Mean annual precipitation	-0.014	0.986	0.014	1.014
Geology	0.845	2.327	-0.855	0.430
Soil	-0.629	0.533	0.639	1.875
Distance to stream	-0.0002	1.000	0.0002	1.000
Land-use	-0.067	0.935	0.067	1.069
Distance to village	-0.001	0.999	0.001	1.001
Distance to road	0.0001	1.000	-	1.000
Constant	20.908		-20.875	
The relative operating characteristic (ROC)	0.899		0.865	

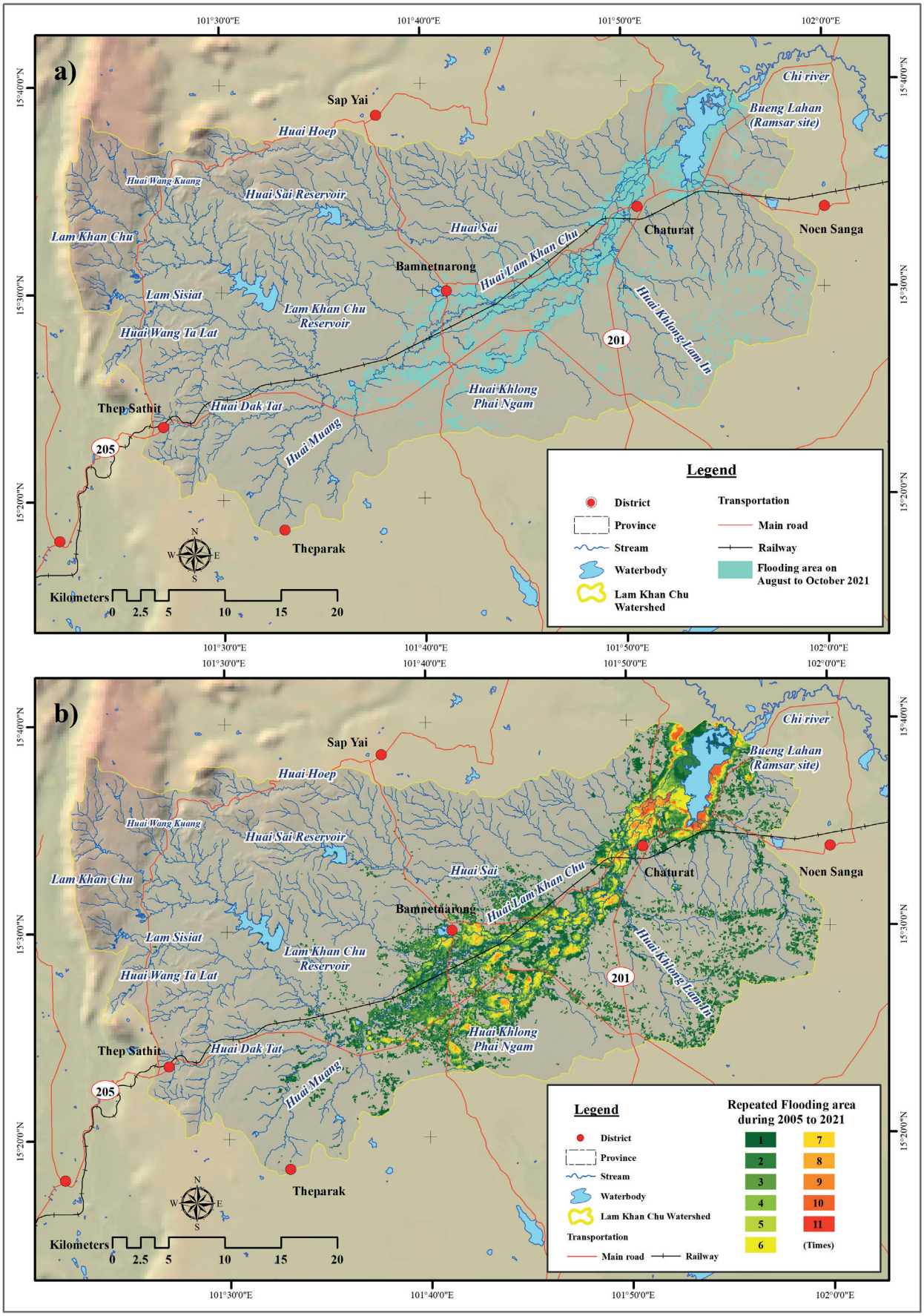

Fig. 6. Flooding area on August to October 2021 in LKCW area (a) and Repeated flooding area during 2005-2021 in LKCW area (b)

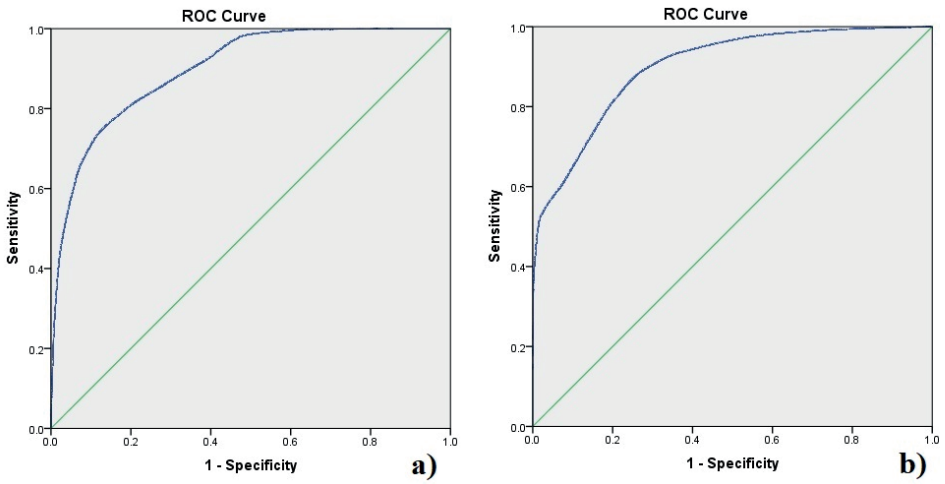

Fig. 7. The relative operating characteristic (ROC) value: flooding area (a) and non-flooding area (b)

The results showed that the flooding area had 4 variables showing high positive β value, namely geology, SF, TWI, and distance to road, respectively. For the variables showing high negative β value, there were 9 variables, namely DD, soil, SPI, land-use, elevation, mean annual precipitation, aspect, distance to village, and distance to stream, respectively. There were 4 variables that did not affect the flooding area in the LKCW area: slope, STI, TRI and IN.

The main reason that four variables (slope, STI, TRI, and IN) did not show β values after logistic regression analysis was due to the physical topography of the study area being largely flat. Only steep slope appeared in a small amount of watershed in the western part of the study area, making slope and TRI variables not statistically significant.

STI levels in the study area were very low, covering the middle and lower parts of the watershed, showing that sediment-carrying was seldom present in the study area. Because there are two important reservoirs, Lam Khan Chu Reservoir and Huai Sai Reservoir, which are sediment banks. In addition, the tributary streams are small and short streams, causing the water mass to not have enough strength to erode the channel until sediment occurs along the waterway, so it is not statistically significant.

As for IN, moderate to low values are found in the area, where IN values are low means, the runoff is low. This is because in the study area there is topography with low potential to store water in the form of surface water. Because most of the waterways are perennial streams, causing them to seep into the ground and collect in the form of groundwater layers, making the IN value not statistically significant.

The flooding area occurred mainly from geology and SF variables, both of which showed high positive β values at 0.845 and 0.795, respectively. It shows that the flooding area is mainly caused by physical factors, as the topography of the LCKW area is supported by soft sedimentary strata, especially modern quaternary sedimentary rocks formed by fluvial deposits. In addition, the area is a low-lying area, resulting in large volumes of water being stored in the area. Most of the LCKW area is also covered by the Mahasarakham Formation, which consists of sandstone and rock salt, soft shale geologic, submerged sedimentary region secondary to Quaternary Neolithic sedimentary rock. The SF variables were the results obtained from the analysis considering the 1st order waterways in the watershed. The SF high value represents an area where the low runoff of the river is defined as the slow flow of water in the river from upstream to downstream over a long period of time, the greater the flooding in the lowland areas for a long time. It can be seen that a high SF value of 2.36 appeared in the surrounding Bueng Lahan swamp. The TWI variable is a predictive index of water accumulation in a watershed area. A high TWI value indicates an area prone to accumulation of water in a basin, making it more prone to flooding in an area. The TWI level shows a high of 31.58 visible on both sides of the main river. High TWI levels can be observed in the vicinity of the Bueng Lahan marsh, the Huai Lam Khan Chu stream, the Huai Sai stream, the Huai Khlong Phai Ngam, and the Huai Dak Tat. As for the distance to road variable, flood-affected areas tend to be far from transport routes.

For variables showing high negative β values affecting flooding area, it can be seen that DD and soil variables showed high negative β values at -0.786 and -0.629, respectively. It shows that the flooding area is mainly caused by physical factors as well. In particular, the DD variable, which was found to be moderate to less than 1, indicates a moderate to low level of drainage. It shows that flood-prone area conditions, especially in the southern and central lowlands of the LKCW area. As for soil variables, the high negative β value was found at the secondary level. The results showed that most of the soil conditions are poorly drained soil found in salinity soil, loam fine sand, and clay loam. As a result, the water volume cannot be drained effectively underground. The SPI variable shows the negative β value as well. It can be seen that the area where the low SPI value found is on both sides of the mainstream where flooding occurs. The land-use variant, floodplains mainly occur in agricultural and lowland areas. Elevation, distance to village, and distance to stream were the three variables that were found to have low negative β values. It represents an area with low elevation of terrain that is susceptible to flooding, including areas near villages and stream.

The results of the study in the non-flooding area consisted of 9 variables showing high positive β value: DD, soil, SPI, land-use, elevation, mean annual precipitation, aspect, distance to village, and distance to stream, respectively. There were four variables showing high negative β value, namely geology, SF, TWI, and distance to road, respectively. It can be seen that it is the reverse of the factors affecting the previous flooding. There are also four variables that do not affect the non-flooding area in the LKCW area: slope, STI, TRI and IN. The results of all variables that were indicators for the occurrence of flood prone areas were subsequently analyzed on the flood susceptibility map in LKCW to form a spatial database for effectively managing flood risk areas.

Flood susceptibility map in LKCW area

The results of the study of flood prone risk area in LCKW by statistical analysis of LR, using the β value as a database and creating a map for disaster management at the watershed level to show it as a flood susceptibility map in LKCW area (Fig. 8) was analyzed spatial using GIS as shown in Equation 9.

$$\begin{aligned} Y = {} & 20.098 + (-0.032 * \text{“}Elevation\text{”}) + (-0.001 * \text{“}Aspect\text{”}) \\ & + (-0.079 * \text{“}SPI\text{”}) + (0.042 * \text{“}TWI\text{”}) + (0.795 * \text{“}SF\text{”}) \\ & + (-0.786 * \text{“}DD\text{”}) + (-0.014 * \text{“}Mean\ annual\ precipitation\text{”}) \\ & + (0.845 * \text{“}Geology\text{”}) + (-0.629 * \text{“}Soil\text{”}) \\ & + (-0.001 * \text{“}Distance\ to\ stream\text{”}) + (-0.067 * \text{“}Land\ use\text{”}) \\ & + (-0.001 * \text{“}Distance\ to\ village\text{”}) + (0.001 * \text{“}Distance\ to\ road\text{”}) \end{aligned} \quad (9)$$

The β value of the variables made the findings a highlight of this study, as it was able to show the level of risk as spatially appropriate data based on the variables involved and affecting specific flooding in the LKCW area. Results of the flood susceptibility study show that flood susceptibility areas are classified into 6 levels: Very high, High, Medium, Low, Very Low, Non-flooding susceptibility respectively (Table 5). A very high flood susceptibility level is discovered in the LKCW region, spanning up to 148.308 km^2 (8.566% of the total area). They appear mainly in the surrounding areas of both main rivers from the downstream to the middle stream of the watershed, especially around the Bueng Lahan swamp and the Huai Lam Khan Chu stream, Huai. Khlong Phai. Ngam, and Huai Muang. The water feature is Braided stream and the terrain is floodplain which makes the area prone to flooding, thus making it a very high level of flood susceptibility. High-risk areas and moderate-risk areas appear close to the very high level of flood susceptibility area as well, but far from the main stream. It covers an area of more than 247.421 km^2 (14.291%) and 310.414 km^2 (17.930%), respectively. The low-risk area, covering an area of 271.594 km^2 (15.687%), was found in the Huai Lam Khan Chu stream, including Huai Khlong Lan In, Huai Khuean Lan, Huai Sai, Huai Wang Ai Pho, Huai Wang Ta Lat, and Huai Dak Tat. Most of the above areas are upstream of the LKCW area. The very low-risk area covers most of the LKCW area, up to 725.153 km^2 (41.885%). Nearly half of the watershed is prone to flood disasters at very low levels, but the likelihood is relatively low. Most of them are upstream of secondary waterways in the northern region, south and west of the basin. Non-flooding susceptibility, appearing in the Northwestern region of the LCKW area, is 28.399 km^2 (1.640% of the total area) considered to be non-flooding susceptibility. Mountainous area can be found in Pa Hin Ngam National Park, a significant watershed forest area in the research area.

DISCUSSION

Floods can be caused by a number of factors and future major floods cannot be accurately predicted (Khosravi et al. 2016). Therefore, it is imperative to collect as many variables affecting flooding as possible, and to select an analysis model that is consistent and timely in response to future flood disasters. It can be seen that from this research, we have tried to select factors that affect flooding, i.e., physical factor and socio-economic factor, with 17 variables related to flooding in the LKCW area as follows: elevation, slope, aspect, SPI, STI, TRI, TWI, SF, DD, IN, mean annual precipitation, geology, soil, and distance to stream. Land-use, distance to village, and distance to road. All 17 variables were created in a geo-database for analysis along with actual flooding area data. The data is then analysed in a geographic information system (GIS) to assess flood susceptibility assessment in the LKCW area. Finally, a flood susceptibility map was created, yielding satisfactory and reliable results, which can be used as a geospatial database for decision-making for flood risk management.

The study of recurrent flooding in the LKCW area yielded interesting data. Over the past 17 years, GISTDA data on flooding from 2005 to 2021 found that 11 recurrent flooding areas occurred mainly in the central region and continued to outlet area, surrounding Bueng Lahan swamp, northeast of the study area, especially the main waterways such as Lam Khan Chu stream and Huai Khlong Phai Ngam stream. The terrain is floodplain with a vast marshland and a braided stream system. Therefore, the area is prone to repeated flooding. This is consistent with the results of a study by (Izumida et al. 2017), studied the repeated flooding area in the Kinu river, Central region in Japan by applying UAV-SfM photogrammetry and aerial lidar to assess the damage caused by flooding. The Piave River in Italy also found that the landscape of the basin was a braided river. It is similar to the floods in the Piave River in northern Italy, which appear braided rivers with strongly impacted flow and sediment regimes (Ziliani et al. 2020). Like the results of a study by (Rajbanshi et al. 2022) in the braided Brahmaputra River in Assam, India, it was found that the 2019 major floods in the Brahmaputra River affected sediment changes in the river, whether it is the movement or accumulation of sediments in the river. It can be concluded that watersheds with floodplain morphology and braided river systems tend to experience repeated flooding almost every year. The communities and agricultural areas in these areas are often affected by floods.

Factors affecting flooding in LKCW area were analysed using LR statistical process. The results showed that

Table 5. Flood susceptibility area in LKCW area (km^2)

Flood susceptibility level	Area	
	km^2	%
Very high	148.308	8.566
High	247.421	14.291
Medium	310.414	17.930
Low	271.594	15.687
Very Low	725.153	41.885
Non-flooding susceptibility	28.399	1.640
Total	1731.289	100.000

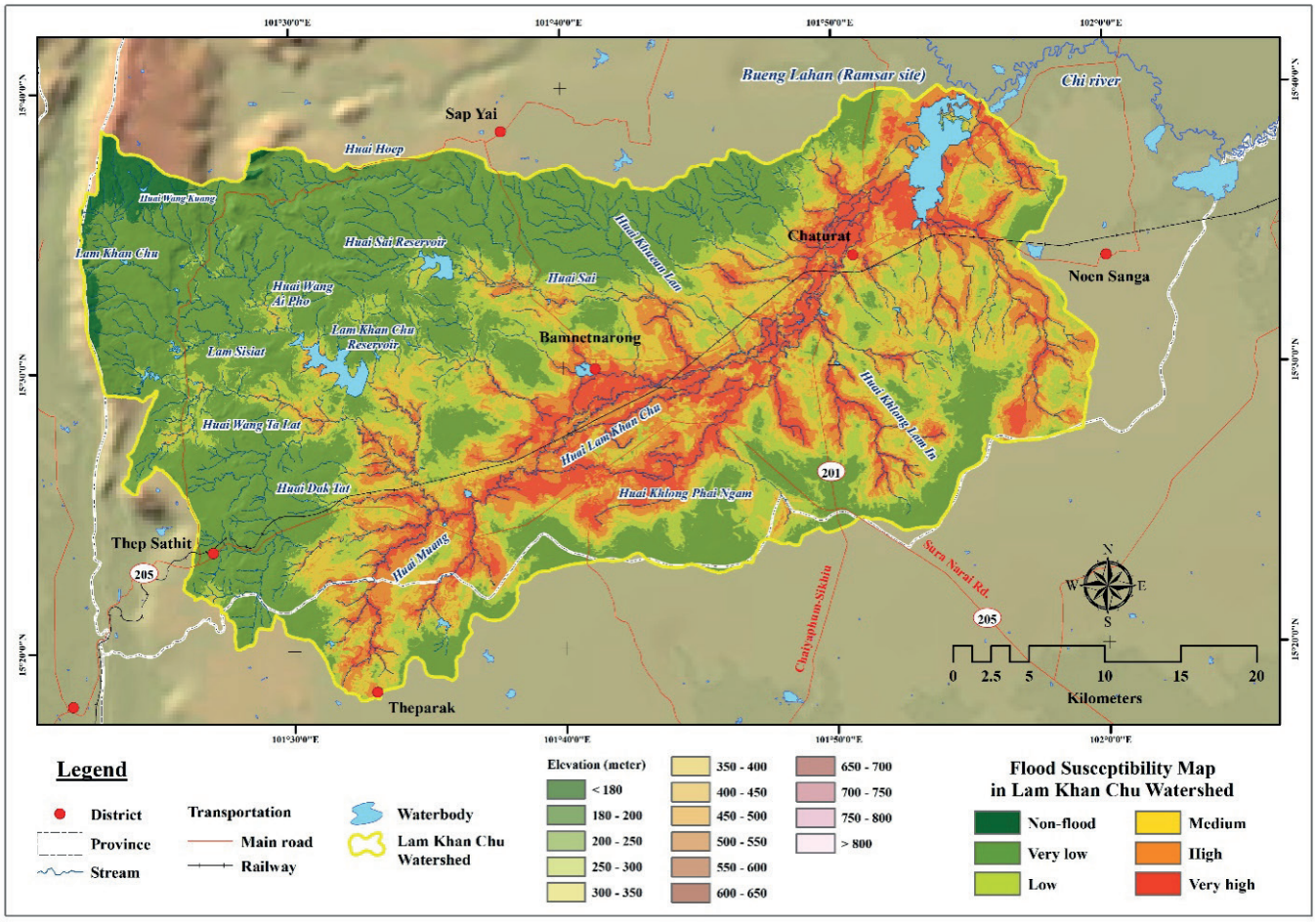

Fig. 8. Flood susceptibility map in LKCW area

the physical factor variables were the most important flooding probability indicators. Specifically, a study in the LKCW area found that geology and SF variables showed high positive β values at 0.845 and 0.795, respectively. Meanwhile, DD and Soil variables showed high negative β values at -0.786 and -0.629. respectively. Geological conditions are supported by an important sedimentary rock group, the Korat group. The rocks of the Jurassic to Cretaceous period are Phra Wihan formation, Sao Khua formation, Phu Phan formation, Khok Kruat formation, and Maha Sarakham formation, respectively (Rattana et al. 2022). Alluvial deposits in the Quaternary era were the most susceptible variables to flooding in the study area, as soft rock contributes to the erosion of water systems on the terrain surface (Prasanchum et al. 2022). Those are located in the valley bottoms which are most prone to flooding in terms of relative elevation. This creates a cuesta topography landscape with steep edges in the west and gradually slopes to the east, resulting in a dendritic-parallel drainage pattern i.e., several tributaries such as Huai Muang, Huai Dak Tat, Huai Wang Ta Lat, LamSisiat, Huai Wang Ai Pho, Huai Sai, Huai Khuean Lan and the short streams surrounding Bueng Lahan flow to the main line, Huai Lam Khan Chu stream. In addition, the SF variables in the study area show the SF high value, indicating the area where the low runoff is the flow of water in the river from the upstream area to the downstream area moving slowly, causing enormous volumes of water flooded in Huai Lam Khan Chu stream for over a month. The DD variable found at a moderate to the level less than 1, showing a moderate to low level drainage system, indicating that the area is prone to flooding, especially in the southern and central lowlands of the LCKW area. The soil variable found a high negative β value at a lower level. The results showed that most of the soil conditions were poorly drained soils found in Salinity soil, Loam fine sand, and Clay loam, which were more consistent with the results of the SF and geology variables. It can be seen that the results of the study in the LKCW area revealed different variables that affect the susceptibility to flooding from other areas. As a case study of (Tehrany et al. 2017) of flood susceptibility mapping in the Xing guo area, China, it was found that the slope variable was the most important variable affecting the top susceptibility to flooding, as did (Al-Juaid et. al. 2018) found high logistic regression coefficient values for Topographic slope variable as high as 1.0483. (Cao et al. 2020) studied flood susceptibility from the Fujian Province, located in south-eastern China, and found that the top influencing variables were land-use and topographic relief. Unlike this study, it was found that the slope variable did not show the coefficient β value in the LKCW area, since most of the area, more than 80 percent, has a low slope of 0–5 degree, but other physical variables that affect susceptibility to flooding were found, including geology, SF, TWI, DD, soil, and SPI, which showed high β value coefficients. In summary, the overall picture from the discussion results shows the difference of factors affecting flooding. It is evident that the LKCW area has different topography and geomorphology from other areas, resulting in β value coefficient of the variables studied changes according to the physical characteristics of the area. Therefore, flood susceptibility studies in other areas should be aware of the causal factors to be studied first in the study of flood risk areas.

Flood susceptibility mapping, that has been generated after obtaining a flood susceptibility variable in the LCKW area, can be indicated sensitivity into 6 levels. It was found that 8.566% of the study areas showed a very high flood

susceptibility level, and 14.291% of the study areas showed a high flood susceptibility level. It can be seen that one-fifth of the basin is at high risk of flooding, particularly in the surrounding areas of Bueng Lahan swamp, Huai Lam Khan Chu stream, Huai Khlong Phai Ngam, and Huai. Muang. It should be especially vigilant if being in the Inter-tropical convergence zone or a tropical cyclone moving into the watershed area, because of the physical nature of the area that is a large basin with slow drainage. For this reason, flood susceptibility mapping is therefore essential, in order for people in the area to understand the spatial context, to understand the geography and limitations of the area, especially at the community and local level that still have the limited capacity to cope with disasters and be prepared to cope and reduce the loss of life and property of people in the LKCW area in the event of the next major disaster.

CONCLUSIONS

Flooding is a catastrophic event that occurs almost every year during Thailand's monsoon season and is particularly severe during the tropical cyclone moving into the area, especially in the watershed areas of northeastern Thailand where this problem is often encountered. This research aims to solve the problems and mitigate such impacts by analyzing individual factors to find answers to the causes of flooding in the study area, by using logistic regression analysis together with GIS to create a Flood susceptibility mapping in LKCW. The results of the study identified important variables affecting flooding including geology, SF, TWI, DD, soil, SPI, land-use, elevation, mean annual precipitation, aspect, distance to road, distance to village, and distance to stream. All such variables are represented by the β value coefficient, which is analyzed to create a flood susceptibility mapping in LCKW. Recommendations for physical research in the basin where high-resolution DEM data can clearly detect the physical characteristics of the stream channel. Stream channel gradient and stream channel depth/width ratio should be added. This research shows that the utilization of flood prone risk map is a useful basis in taking preventive actions to mitigate floods, and relevant agencies should be expedited to assist the most vulnerable areas to mitigate floods. Also, planning and preparing for future floods in high- to very high-risk areas in the LKCW area must be performed. However, this risk map is suitable for alluvial terrain. If used in other areas, other relevant factors should be examined, including the flood context, to make logistic regression analysis more effective.

REFERENCES

Al-Juaidi A.E.M., Nassar A.M. and Al-Juaidi, O.E.M. (2018). Evaluation of flood susceptibility mapping using logistic regression and GIS conditioning factors. Arabian Journal of Geosciences, 11, 765, DOI: 10.1007/s12517-018-4095-0.

AHA Centre, (2021). Tropical Cyclone Dianmu (21W), Lao PDR, Thailand and Viet Nam. [online] Available at: https://reliefweb.int/report/viet-nam/tropical-cyclone-dianmu-21w-lao-pdr-thailand-and-viet-nam-flash-update-2-28-sep-2021 [Accessed 28 Feb. 2022].

Bharath A., Kumar K.K., Maddamsetty R., Manjunatha M., Tangadagi R.B. and Preethi S. (2021). Drainage morphometry based sub-watershed prioritization of Kalinadi basin using geospatial technology. Environmental Challenges, 5, 100277, DOI: 10.1016/j.envc.2021.100277.

Bui D.T., Ngo P.T.T., Pham T.D., Jaafari A., Minh N.Q., Hoa P.V. and Samui P. (2019). A novel hybrid approach based on a swarm intelligence optimized extreme learning machine for flash flood susceptibility mapping. Catena, 179, 184-196, DOI: 10.1016/j.catena.2019.04.009.

Camara M., Jamil N.R.B., Abdullah A.F.B. and Hashim R.B. (2020). Integrating cellular automata Markov model to simulate future land-use change of a tropical basin. Global Journal of Environmental Science and Management, 6(3), 403-414, DOI: 10.22034/gjesm.2020.03.09.

Cao Y., Jia H., Xiong J., Cheng W., Li K., Pang Q. and Yong Z. (2020). Flash Flood Susceptibility Assessment Based on Geodetector, Certainty Factor, and Logistic Regression Analyses in Fujian Province, China. ISPRS International Journal of Geo-Information, 9(12), 748, DOI: 10.3390/ijgi9120748.

Chauhan N., Paliwal R., Kumar V., Kumar S. and Kumar R. (2022). Watershed Prioritization in Lower Shivaliks Region of India Using Integrated Principal Component and Hierarchical Cluster Analysis Techniques: A Case of Upper Ghaggar Watershed. Journal of the Indian Society of Remote Sensing, 50, 1051–1070, DOI: 10.1007/s12524-022-01519-6.

Chen C. and Yu F. (2011). Morphometric analysis of debris flows and their source areas using GIS. Geomorphology, 129(3-4), 387–397, DOI: 10.1016/j.geomorph.2011.03.002.

Chen J., Li Q., Wang H. and Deng M. (2020). A Machine Learning Ensemble Approach Based on Random Forest and Radial Basis Function Neural Network for Risk Evaluation of Regional Flood Disaster: A Case Study of the Yangtze River Delta, China. International Journal of Environmental Research and Public Health, 17(1), 49, DOI: 10.3390/ijerph17010049.

Chowdhuri I., Pal S.C. and Chakrabortty R. (2020). Flood susceptibility mapping by ensemble evidential belief function and binomial logistic regression model on river basin of eastern India. Advances in Space Research, 65(5), 1466-1489, DOI: 10.1016/j.asr.2019.12.003.

Coetzee C. (2022). Change Detection of Vegetation Cover Using Remote Sensing and GIS – A Case Study of the West Coast Region of South Africa. Geography, Environment, Sustainability, 2(15), 91-102, DOI: 10.24057/2071-9388-2021-067.

CRED, (2022). 2021 Disasters in numbers. [online] Available at: http://reliefweb.int/report/world/2021-disasters-numbers [Accessed 28 Jul. 2022].

Dahri N., Yousfi R., Bouamrane A., Abida H., Pham Q.B. and Derdous O. (2022). Comparison of analytic network process and artificial neural network models for flash flood susceptibility assessment. Journal of African Earth Sciences, 193, 104576, DOI: 10.1016/j.jafrearsci.2022.104576.

Das A.K. and Mukherjee S. (2005). Drainage morphometry using satellite data and GIS in Raigad District, Maharashtra. Journal of the Geological Society of India, 65(5), 577–586.

Degiorgis M., Gnecco G., Gorni S., Roth G., Sanguineti M. and Taramasso A.C. (2012). Classifiers for the detection of flood-prone areas using remote sensed elevation data. Journal of Hydrology. 470–471, 302–315, DOI: 10.1016/j.jhydrol.2012.09.006.

Department of Economic and Social Affairs, (2022). Sustainable Development, Goals 13 Take urgent action to combat climate change and its impacts. [online] Available at: https://sdgs.un.org/topics/climate-change [Accessed 6 Mar. 2022].

Ekmekcioğlu Ö., Koc K. and Özger, M. District based flood risk assessment in Istanbul using fuzzy analytical hierarchy process. Stochastic Environmental Research and Risk Assessment, 35, 617–637, DOI: 10.1007/s00477-020-01924-8.

El-Fakharany M.A., Hegazy M.N., Mansour N.M. and Abdo A.M. (2021). Flash flood hazard assessment and prioritization of sub-watersheds in Heliopolis basin, East Cairo, Egypt. Arabian Journal of Geosciences, 14, 1693, DOI: 10.1007/s12517-021-07991-7.

Elewa H.H., Ramadan E.M. and Nosair A.M. (2016). Spatial-based hydro-morphometric watershed modeling for the assessment of flooding potentialities. Environmental Earth Sciences, 75, 906–927, DOI: 10.1007/s12665-016-5692-4.

Elsafi S.H. (2014). Artificial Neural Networks (ANNs) for flood forecasting at Dongola Station in the River Nile, Sudan. Alexandria Engineering Journal, 53(3), 655-662, DOI: 10.1016/j.aej.2014.06.010.

Faiz M.A., Liu D., Fu Q., Uzair M., Khan M.I., Baig F., Li T. and Cui. S. (2018). Stream flow variability and drought severity in the Songhua River Basin, Northeast China. Stochastic Environmental Research and Risk Assessment, 32, 1225-1242, DOI: 10.1007/s00477-017-1463-3.

Faniran A. (1968). The index of drainage intensity—a provisional new drainage factor. Australian Journal of Science, 31, 328–330.

Ghasemlounia R. and Utlu M. (2021). Flood prioritization of basins based on geomorphometric properties using principal component analysis, morphometric analysis and Redvan's priority methods: A case study of Harşit River basin. Journal of Hydrology, 603(part C), 127061, DOI: 10.1016/j.jhydrol.2021.127061.

Hamid H.T.A., Wenlong W. and Qiaomin L. (2020). Environmental sensitivity of flash flood hazard using geospatial techniques. Global Journal of Environmental Science and Management, 6(1), 31-46, DOI: 10.22034/gjesm.2020.01.03.

Horton R.E. (1932). Drainage basin characteristics. Eos, Transactions American Geophysical Union, 13(1), 350–361, DOI: 10.1029/TR013i001p00350.

Izumida A., Uchiyama S. and Sugai T. (2017). Application of UAV-SfM photogrammetry and aerial lidar to a disastrous flood: repeated topographic measurement of a newly formed crevasse splay of the Kinu River, central Japan. Natural Hazards and Earth System Sciences, 17(9), 1505–1519, DOI: 10.5194/nhess-17-1505-2017, 2017.

Jaiswal R.K., Nayak T.R., Lohani A.K. and Galkate R.V. (2022). Regional flood frequency modeling for a large basin in India. Natural Hazards, 111, 1845–1861, DOI: 10.1007/s11069-021-05119-4.

Jane R., Cadavid L., Obeysekera J. and Wahl T. (2020). Multivariate statistical modelling of the drivers of compound flood events in south Florida. Natural Hazards and Earth System Sciences, 20, 2681-2699, DOI: 10.5194/nhess-20-2681-2020.

Joji V.S., Nair A.S.K. and Baiju K.V. (2013). Drainage basin delineation and quantitative analysis of Panamaram watershed of Kabani RiverBasin, Kerala using remote sensing and GIS. Journal of the Geological Society of India, 82, 368–378, DOI: 10.1007/s12594-013-0164-x.

Khiavi A.N., Vafakhah M. and Sadeghi S.H. (2022). Comparative prioritization of sub-watersheds based on Flood Generation potential using physical, hydrological and co-managerial approaches. Water Resources Management, 36, 1897–1917, DOI: 10.1007/s11269-022-03114-3.

Khosravi K., Pourghasemi H.R. Chapi K. and Bahri, M. (2016). Flash flood susceptibility analysis and its mapping using different bivariate models in Iran: A Comparison between Shannon's entropy, statistical index, and weighting factor models. Environmental Monitoring and Assessment, 188(12), 656, DOI: 10.1007/s10661-016-5665-9.

Kia M.B., Pirasteh S., Pradhan B., Mahmud A.R., Sulaiman W.N.A. and Moradi A. (2012). An artificial neural network model for flood simulation using GIS: Johor River Basin, Malaysia. Environmental Earth Sciences, 67, 251–264, DOI: 10.1007/s12665-011-1504-z.

Kim H.I., Han K.Y. and Lee J.Y. (2020). Prediction of Urban Flood Extent by LSTM Model and Logistic Regression. KSCE Journal of Civil and Environmental Engineering Research, 40(3), 273–283, DOI: 10.12652/KSCE.2020.40.3.0273.

Leal M., Reis E., Pereira S. and Santos P.P. (2021). Physical vulnerability assessment to flash floods using an indicator-based methodology based on building properties and flow parameters. Journal of Flood Risk Management, 14, e12712, DOI: 10.1111/jfr3.12712.

Li J., Lei Y., Tan S., Bell C.D., Engel B.A. and Wang Y. (2018). Nonstationary Flood Frequency Analysis for Annual Flood Peak and Volume Series in Both Univariate and Bivariate Domain. Water Resources Management, 32, 4239–4252, DOI: 10.1007/s11269-018-2041-2.

Lim J. and Lee K. (2018). Flood Mapping Using Multi-Source Remotely Sensed Data and Logistic Regression in the Heterogeneous Mountainous Regions in North Korea. Remote Sensing. 10(7), 1036, DOI: 10.3390/rs10071036.

Maan G.S., Patra J.P. and Singh R. (2020). A Hydro-Informatic Approach For Estimation Of Design Flash-Flood In Bargi Dam Cross-Section Of Narmada River, India. Geography, Environment, Sustainability, 13(2), 104-114, DOI: 10.24057/2071-9388-2019-178.

Maleki J., Masoumi Z., Hakimpour F. and Coello C. A. (2020). A spatial land-use planning support system based on game theory. Land Use Policy, 99, 105013, DOI: 10.1016/j.landusepol.2020.105013.

Mitra R., Saha P. and Das J. (2022). Assessment of the performance of GIS-based analytical hierarchical process (AHP) approach for flood modelling in Uttar Dinajpur district of West Bengal, India. Geomatics, Natural Hazards and Risk, 13(1), 2183-2226, DOI: 10.1080/19475705.2022.2112094.

Mojaddadi H., Pradhan B., Nampak H., Ahmad M. and Ghazali A.H.B. (2017). Ensemble machine-learning-based geospatial approach for flood risk assessment using multi-sensor remote-sensing data and GIS. Geomatics, Natural Hazards and Risk, 8(2), 1080-1102, DOI: 10.1080/19475705.2017.1294113.

Moore I.D., Grayson R.B. and Ladson A.R. (1991). Digital terrain modelling: A review of hydrological, geomorphological, and biological applications. Hydrological Processes, 5(1), 3-30, DOI: 10.1002/hyp.3360050103.

Nandi A., Mandal A., Wilson M. and Smith D. (2016). Flood hazard mapping in Jamaica using principal component analysis and logistic regression. Environmental Earth Sciences, 75, 465, DOI: 10.1007/s12665-016-5323-0.

Nguyen B., Minh D., Ahmad A. and Nguyen Q. (2020). The Role of Relative Slope Length in Flood Hazard Mapping Using AHP And GIS (Case Study: Lam River Basin, Vietnam). Geography, Environment, Sustainability, 13(2), 115-123. DOI: 10.24057/2071-9388-2020-48.

Prasanchum H., Tumma N. and Lohpaisankrit W. (2022). Establishing Spatial Distributions of Drought Phenomena on Cultivation Seasons using the SWAT Model. Geographia Technica, 17(2), 1-13, DOI: 10.21163/GT_2022.172.01.

Purwanto P., Sugianto D. N., Zainuri M., Permatasari G., Atmodjo W., Rochaddi B., Ismanto A., Wetchayont P. and Wirasatriya A. (2021). Seasonal Variability of Waves Within the Indonesian Seas and Its Relation with the Monsoon Wind. ILMU KELAUTAN: Indonesian Journal of Marine Sciences, 26(3), 189-196, DOI: 10.14710/ik.ijms.26.3.189-196.

Rajbanshi J., Das S. and Patel P.P. (2022). Planform changes and alterations of longitudinal connectivity caused by the 2019 flood event on the braided Brahmaputra River in Assam, India. Geomorphology, 403, 108174, DOI: 10.1016/j.geomorph.2022.108174.

Ramesh V. and Iqbal S.S. (2022). Urban flood susceptibility zonation mapping using evidential belief function, frequency ratio and fuzzy gamma operator models in GIS: a case study of Greater Mumbai, Maharashtra, India. Geocarto International, 37(2), 581-606, DOI: 10.1080/10106049.2020.1730448.

Rattana P., Choowong M., He M., Tan L., Lan J., Bissen R. and Chawchai S. (2022). Geochemistry of evaporitic deposits from the Cenomanian (Upper Cretaceous) Maha Sarakham Formation in the Khorat Basin, northeastern Thailand. Cretaceous Research, 130, 104986, DOI: 10.1016/j.cretres.2021.104986.

Rhmati O., Samadi M., Shahabi H., Azareh A., Rafiei-Sardooi E., Alilou H., Melesse A.M., Pradhan B., Chapi K. and Shirzadi A. (2019). SWPT: An automated GIS-based tool for prioritization of sub-watersheds based on morphometric and topo-hydrological factors. Geoscience Frontiers, 10(6), 2167-2175, DOI: 10.1016/j.gsf.2019.03.009.

Rojpratak S. and Supharatid S. (2022). Regional extreme precipitation index: Evaluations and projections from the multi-model ensemble CMIP5 over Thailand. Weather and Climate Extremes, 37, 100475, DOI: 10.1016/j.wace.2022.100475.

Sarjito S., Ammaria H., Helmi M., Prayitno S. B., Nurdin N., Setiawan R. Y., Wetchayont P. and Wirasatriya A. (2022). Identification of Potential Locations for Kappaphycyus alvarezii Cultivation for Optimization of Seaweed Production Based on Geographic Information Systems in Spermonde Archipelago Waters, South Sulawesi, Indonesia. ILMU KELAUTAN: Indonesian Journal of Marine Sciences, 27(3), 253-266, DOI: 10.14710/ik.ijms.27.3.253-266.

Suharyanto A. (2021). Estimating Flood Inundation Depth Along the Arterial Road Based on the Rainfall Intensity. Civil and Environmental Engineering, 17(1), 66-81, DOI: 10.2478/cee-2021-0008.

Tehrany M.S., Pradhan B., Mansor S.H. and Ahmed N. (2015). Flood susceptibility assessment using GIS-based support vector machine model with different kernel types. Catena, 125, 91–101, DOI: 10.1016/j.catena.2014.10.017.

Tehrany M.S., Shabani F., Jebur M.N., Hong H., Chen W. and Xie A. (2017). GIS-based spatial prediction of flood prone areas using standalone frequency ratio, logistic regression, weight of evidence and their ensemble techniques, Geomatics, Natural Hazards and Risk, 8(2), 1538-1561, DOI: 10.1080/19475705.2017.1362038.

Thodsan T, Wu F, Torsri K, Cuestas EMA, and Yang G. (2022). Satellite Radiance Data Assimilation Using the WRF-3DVAR System for Tropical Storm Dianmu (2021) Forecasts. Atmosphere, 13(6), 956, DOI: 10.3390/atmos13060956.

Tomkratoke S. and Sirisup S. (2022). Influence and variability of monsoon trough and front on rainfall in Thailand. International Journal of Climatology, 42(1), 619-634, DOI: 10.1002/joc.7263.

Tosunoglu F., Gürbüz F. and İspirli, M.N. (2020). Multivariate modeling of flood characteristics using Vine copulas. Environmental Earth Sciences, 79, 459, DOI: 10.1007/s12665-020-09199-6.

Waiyasusri K. and Chotpantarat S. Spatial Evolution of Coastal Tourist City Using the Dyna-CLUE Model in Koh Chang of Thailand during 1990–2050. ISPRS International Journal of Geo-Information. 2022; 11(1), 49, DOI: 10.3390/ijgi11010049.

Waiyasusri K., Kulpanich N., Worachairungreung M., Sae-ngow P. and Chaysmithikul P. (2021). Flood Prone Risk Area Analysis during 2005–2019 in Lam Se Bok Watershed, Ubon Ratchathani Province, Thailand. Geographia Technic, 16(1), 141–153, DOI: 10.21163/GT_2021.161.12.

Werner M.G.F., Hunter N.M. and Bates P.D. (2005). Identifiability of distributed floodplain roughness values in flood extent estimation. Journal of Hydrology, 314(1-4), 139–157, DOI: 10.1016/j.jhydrol.2005.03.012.

Zhang T., Wang Y., Wang B., Tan S. and Feng P. (2018). Nonstationary Flood Frequency Analysis Using Univariate and Bivariate Time-Varying Models Based on GAMLSS. Water, 10(7), 819, DOI: 10.3390/w10070819.

Ziliani L., Surian N., Botter G. and Mao L. (2020). Assessment of the geomorphic effectiveness of controlled floods in a braided river using a reduced-complexity numerical model, Hydrology and Earth System Sciences, 24(6), 3229–3250, DOI: 10.5194/hess-24-3229-2020.

RESEARCH PAPER

FLASH FLOOD HAZARD MAPPING USING LANDSAT-8 IMAGERY, AHP, AND GIS IN THE NGAN SAU AND NGAN PHO RIVER BASINS, NORTH-CENTRAL VIETNAM

Tien-thanh Nguyen[1*], Anh-huy Hoang[2], Thi-thu-huong Pham[1], Thi-thu-trang Tran[1]

[1]Faculty of Surveying, Mapping, and Geographic Information, Hanoi University of Natural Resources and Environment, 41A, Phu Dien Road, North-Tu Liem District, Hanoi, 100000, Vietnam

[2]Faculty of Environment, Hanoi University of Natural Resources and Environment, 41A, Phu Dien Road, North-Tu Liem District, Hanoi, 100000, Vietnam

***Corresponding author:** ntthanh@hunre.edu.vn

Received: July 21st, 2022 / Accepted: May 4th, 2023 / Published: July 1st, 2023

https://DOI-10.24057/2071-9388-2022-117

ABSTRACT. Flash floods have been blamed for significant losses and destruction all around the world are widely, including Vietnam, a developing nation that has been particularly hard hit by climate change. Therefore, flash flood hazards are essential for reducing flood risks. The topographic wetness index (TWI), altitude, slope, aspect, rainfall, land cover, normalized difference vegetation index (NDVI), distances to rivers and roads, and flow length were used in this study to create a spatial database of ten exploratory factors influencing the occurrence of flash floods in the Ngan Sau and Ngan Pho river basins (North-Central Vietnam). Subsequently, the analytic hierarchy process (AHP) was applied to calculate the weights of these influencing factors. The flood threat was then mapped using GIS techniques. The validation of the flash flood hazards involved 151 flood inventory sites in total. The findings demonstrate that (i) distance from rivers (0.14) and TWI (0.14) factors have the greatest influence on flash flooding, whereas distance from roads (0.06) and NDVI (0.06) factors were found to have the least influence; (ii) a good conformity of 84.8 percent between flood inventory sites and moderate to very high levels of flash flood hazard areas was also discovered; (iii) high and very high flood hazard levels covering areas of 275 and 621.1 km^2 were mainly detected along and close to the main rivers and streams, respectively. These results demonstrated the effectiveness of GIS techniques, AHP, and Landsat-8 remote sensing data for flash flood hazard mapping.

KEYWORDS: flash floods, hazard mapping, GIS techniques, AHP, remote sensing, Ngan Sau and Ngan Pho river basin (Vietnam)

CITATION: Tien-thanh Nguyen, Anh-huy Hoang, Thi-thu-huong Pham, Thi-thu-trang Tran (2023). Flash Flood Hazard Mapping Using Landsat-8 Imagery, Ahp, And Gis In The Ngan Sau And Ngan Pho River Basins, North-Central Vietnam. Geography, Environment, Sustainability, 2(16), 57-67

https://DOI-10.24057/2071-9388-2022-117

ACKNOWLEDGEMENTS: The authors appreciate the help with manuscript suggestions from the editor and anonymous reviewers. We are grateful to Dr. Van-dai Hoang (Vietnam Institute of Meteorology, Hydrology, and Climate Change, Ministry of Natural Resources and Environment, Vietnam) for providing the road network data. The flood inventory datasets were provided by the project (grant number: TNMT.2016.05.12) funded by the Ministry-level Scientific and Technological Key Programs of the Ministry of Natural Resources and Environment of Vietnam.

Conflict of interests: The authors reported no potential conflict of interest.

INTRODUCTION

Flood represents the excess flow that inundates the conveying or holding medium when its capacity has been exceeded (Getahun and Gebre 2015). This is the most frequently occurring natural disaster in the world (Jonkman 2005), which has caused millions of fatalities in the twentieth century, tens of billions of dollars of direct economic loss each year, and serious disruption to global trade (Merz et al. 2021). Recently, Kvočka et al. (2016) generally characterized four types of flood events as extreme flood events, including dam-break floods, storm surges, flash floods, and extreme/large river floods. Among these types of extreme flood events, flash floods are one of the most significant natural hazards that cause serious risk to life and destruction of buildings and infrastructure (Gaume et al. 2009) and pose the greatest flood risk to the general population (Kvočka et al. 2016). According to a research by Chatzichristaki et al. (2015), areas with increased housing development such as tourist destinations and places near city centres, where the stream bed is severely affected by human pressure, are more likely to experience flood fatalities. Due to the increasingly devastating effects of floods, the recent year's scientific community has drawn attention for the identification of flood-exposed areas and particularly critical infrastructure and assets in flood hazard zone (Qiang 2019; Stefanidis et al. 2022). Therefore, flood risk assessment, including three approaches of hazard, exposure, and vulnerability assessment as proposed by Field et al. (2012), plays a vital role in flood prevention and

flood risk management. Among these approaches, flood hazard assessment usually receives the most attention as flood hazard maps are used for estimating the danger to people due to flooding (Koks et al. 2015).

Over the years, a lot of work has gone into developing methods for effective flood hazard mapping. Teng et al. (2017) summarizes flood hazard mapping can be carried out based on three major approaches, namely the physically-based, empirical, and physical modelling methods. A review of the most recent studies by Mudashiru et al. (2021) has indicated an application rate of 43.8% for physically based, 10% for physical, and 46.2% for the empirical modelling methods in flood hazard mapping. This shows that the use of empirical modelling methods has received a lot of attention in flood hazard mapping. The empirical models are data-driven models, popularly referred to as black-box models that rely on observation data and characteristics and mechanisms of the hydrological cycle Mudashiru et al. (2021). Chen et al. (2019) divided empirical models for flood modeling and mapping into qualitative and quantitative methods. The quantitative-based empirical models depend upon data analysis targeted at evaluating the relationship between flood occurrence and flood-causing/contributing factors, while the qualitative approach relies upon experts' opinions of the same (Mudashiru et al. 2021). With the help of a Geographic Information System (GIS), one of the main advantages of empirical models is their operability with various statistical and data-driven approaches through the use of different types of data such as Digital Elevation Model (DEM), terrain, hydrological and geomorphology data, and remotely sensed images. These data-driven approaches for flood hazard mapping are categorized into multi-criteria decision-making modelling methods (Arabameri et al. 2019; Mudashiru et al. 2022), statistical modelling methods (Arabameri et al. 2019; Malik et al. 2021), artificial intelligence (Chang et al. 2020; Chapi et al. 2017), machine learning models (Hosseini et al. 2020; Rahman, Chen, et al. 2021), and the state-of-the-art deep learning models (Costache et al. 2022; Satarzadeh et al. 2022). Among these approaches, a combination of GIS with a multi-criteria decision-making modelling method-based analytic hierarchy process (GIS-AHP) has proved its effectiveness in many recent studies on flood hazard mapping (Aydin and Sevgi Birincioğlu 2022; Daneshparvar et al. 2022; Pathan et al. 2022). In addition, a recent study of Şahin (2021) has revealed that the most important benefit of AHP over other multi-criteria decision-making modelling methods is that it not only allows pairwise comparisons, which increase the accuracy of judgments compared to evaluating all the alternatives simultaneously, but also permits consistency checking. Despite numerous studies, there hasn't been much research done on mapping flash flood hazards using a combination of remote sensing, GIS, and AHP techniques. To fill this literature gap, this paper aims to investigate the use of Landsat-8 imagery, AHP, and GIS in identifying the flash flood influencing factors and map flood hazards.

Disastrous flooding is projected to increase in many regions, particularly in Africa and Asia (Merz et al. 2021). As a country situated in Asia, Vietnam frequently experiences extreme weather-related natural disasters (Noy and Vu 2010), of which flooding in North-Central Vietnam is the most serious (Bich et al. 2011). The Ngan Sau and Ngan Pho river basins, which are in North-Central Vietnam, are frequently the area most affected by floods (Kha et al. 2018; Long and Dung 2009; Nguyen and Ha 2017). Therefore, the objective of this study is to investigate the integration of Landsat-8 imagery, AHP, and GIS in mapping flash flood hazards in the study area.

STUDY AREA AND DATA USED

Study area

Geographically, the study area of the Ngan Sau and Ngan Pho river basins is located between 17°50´00´´N to 18°37´58´´N latitudes and 105°07´00´´E to 106°56´00´´E longitudes, covering an area of approximately 4,274 square kilometers (Fig. 1). Politically, the Ngan Sau and Ngan Pho river basins consist of Huong Son, Duc Tho, Vu Quang, and Huong Khe districts, which are located in Ha Tinh administrative province (Fig. 1-b), North-Central Vietnam (Fig. 1-a). The Ngan Pho river basin covers an area of 1,060 km^2 with a river and stream density of 0.91 km/km^2 and a total volume of water of 1.40 km^3 corresponding to an average flow of 45.6 m^3/s (Tran et al. 2020). Whereas the Ngan Sau river system is the second largest tributary of the Ca river,

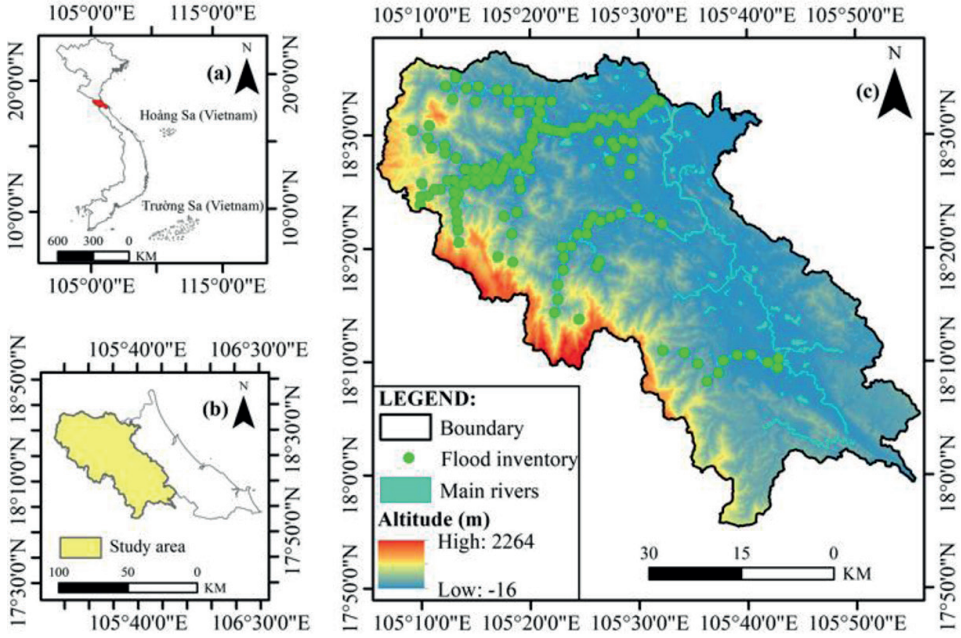

Fig. 1. Location of the study area: (a) location of Ha Tinh province (North-Central Vietnam), (b) location of Ngan Sau-Ngan Pho River basin, (c) altitude of Ngan Sau-Ngan Pho River basin overlaid by flood inventory sites and main rivers and streams

extending 135 km (Hoang et al. 2020). The study area's relief is low in the north and northeast, increasing towards the west and southwest at as high as 2264 m (Fig. 1-c).

In the Ngan Sau and Ngan Pho river basins, which were among the floodplains in central Vietnam that were most severely affected (Kha et al. 2018; Long and Dung 2009; Nguyen and Ha 2017; Nguyen 2017), flash floods have been blamed for several fatalities and significant environmental and societal harm. Typically, ten deaths, 16,200 households flooded, 177 houses washed away, and 5,026 hectares of winter-spring rice crops were damaged by a flash flood in the upstream area of the Ngan Pho River basin in 1989 (Hoang et al. 2020). Also in this upstream area, heavy rain caused another flash flood in 2002. A total of 77 deaths, hundreds of injuries, and 70,694 houses flooded were also reported in a recent study of Hoang et al. (2020). In addition, loss of life, social-economic and environmental damages caused by other flash floods were also confirmed in recent years (Hoang and Tran 2018; Nguyen and Ha 2017).

Data used

In this study, Landsat-8 Collection 2 Level 2 Science Product (L2SP) (paths of 126 and 127, rows of 47 and 48) recently distributed by the United States Geological Survey (USGS) website (www.usgs.gov) was acquired on April 8, 2022. Landsat-8 L2SP with a spatial resolution of 30 meters provides surface reflectance data that is already atmospherically corrected (Marzouki and Dridri 2022). These Landsat-8 L2SP images were used to extract land cover types and NDVI. Thirty-meter resolution DEM datasets downloaded from the USGS were used to calculate topographic and hydrologic parameters (slope, aspect, TWI, flow length, flow direction, flow accumulation, and stream networks). Rainfall data was obtained from the CRU (Climate Research Unit) website (https://crudata.uea.ac.uk). The road network layer and 151 flood inventory sites were obtained from the project (grant number: TNMT.2016.05.12), which was financially supported by the Ministry-level Scientific and Technological Key Programs of the Ministry of Natural Resources and Environment of Vietnam. The road network layer was used to calculate the distance to roads, whereas flood inventory sites were used for the validation of the flash flood hazards.

METHODOLOGY

Data from Fig. 2 demonstrates the workflow of this study. The input data (flood inventory and ten exploratory factors) was first collected and prepared in ArcGIS. Among these factors, land cover types and NDVI were extracted from Landsat-8 OLI imagery in ENVI. Subsequently, the weights of the flood conditioning factors were calculated using the AHP technique. Then, GIS techniques were applied to categorize flash flood hazards into five levels: very low, low, moderate, high, and very high. Finally, the validation of flash flood hazards was carried out based on the test data values of 151 flood inventory sites.

Selection of influencing factors

In this study, based on the causes of flash floods reported previously and the important characteristics of the Ngan Sau and Ngan Pho river basins such as natural conditions, topography and hydro-meteorology, a total

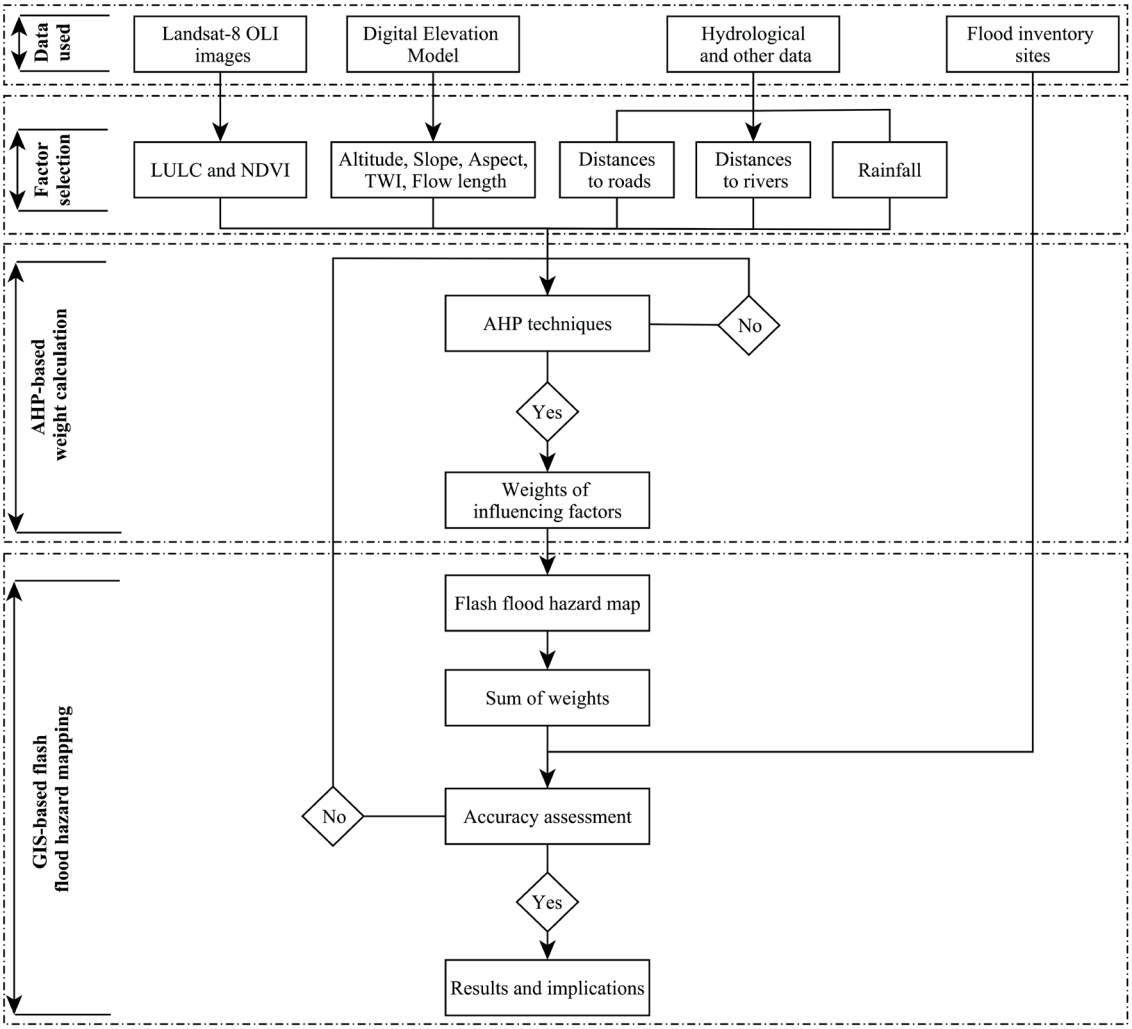

Fig. 2. Workflow of this study

of ten major flash flood hazard-influencing factors were chosen to investigate the effectiveness of the proposed method. These factors include altitude, slope, aspect, TWI, land cover, NDVI, distances to rivers and roads, rainfall, and flow length.

The topographic factors, including altitude, slope, aspect, and TWI, play significant roles in flood hazard mapping. The altitude of the Ngan Sau and Ngan Pho river basins varies from 16 meters to 2264 meters (Fig. 3-b) and was derived from DEM (acquired from the USGS). Flood hazard and altitude are inversely proportional, which indicate that relatively more elevated areas are relatively less susceptible to floods (Rahman and Ningsheng et al. 2021). Aspect and slope were derived from DEM data. Aspect reflects the direction of the terrain and then the direction of floodwater flow (Bui et al. 2020), whereas, the slope is a significant factor in flood mapping. The TWI factor measures the direction and accumulation of water flow due to the gravity of the place (Tehrany et al. 2015) and is calculated by equation (1):

$$TWI = \ln\left(\frac{A_s}{\tan\beta}\right) \quad (1)$$

where: A_s is the upslope area per unit of contour length (m^2/m) and β measures the topographic gradient or local slope gradient in degrees (Park and Kim 2019).

Rainfall is the main factor contributing to flooding in the Ngan Sau and Ngan Pho river basins. Most of the rainfall occurs in the monsoon season from August to October. Rainfall data was first obtained from the CRU (Climate Research Unit) website. The inverse distance weighted interpolation method in ArcGIS software was then applied to obtain the thirty-meter resolution rainfall data of the Ngan Sau and Ngan Pho river basins.

Land cover-related factors such as land cover types and NDVI are crucial factors in flood hazard mapping because areas with relatively less vegetation are often more prone to flooding (Rahman and Ningsheng et al. 2021). In this study, both land cover types and NDVI were generated from Landsat-8 OLI images in ENVI software. Based on the supervised method of maximum likelihood supervised classification, the land cover in the study area was classified into five categories: water bodies, built-up, bare land, agricultural land, and forest, respectively. Whereas the NDVI is calculated using bands 4 (red band) and 5 (near infrared band) in a Landsat-8 OLI image. The NDVI can be expressed in equation (2) (Alvarez-Mendoza et al. 2019):

$$NDVI = \frac{Band5 - Band4}{Band5 + Band4} \quad (2)$$

Distances to rivers and roads also play significant roles in the mapping of flash flood hazards. These distances can be calculated using the Euclidean distance. Areas close to main channels are more likely to be flooded (Chowdhuri et al. 2020), whereas impermeable surfaces (roadways, pavements, and parking spaces) increase the rainfall-runoff process (Mukherjee and Singh 2020).

Flow length is considered to be an important factor in flood susceptibility assessment. Flow length would be used to extract the surface runoff (Abou El-Magd et al. 2010). High surface runoff increases flood risk (Prokešová et al. 2022). Based on DEM data, it was possible to calculate the flow length within each cell, which is either equal to the grid cell length (L) in the case of orthogonal or L√2 in the case of diagonal (Abou El-Magd et al. 2010).

Analytic hierarchy process (AHP)

The AHP, first introduced by Saaty (1988), is a geospatial technique for determining the weights of the influencing factors (Rehman et al. 2022). Numerous studies have successfully applied the AHP for hazard mapping (Gigović et al. 2017; Koem and Tantanee 2021; Neji et al. 2021). In particular, AHP assembled with GIS (GIS-AHP) not only effectively provides a wide range of geographically spatial data manipulation costs and time, but also offers procedures and techniques to evaluate, to analyze, to design, and to prioritize value judgments (Rehman et al. 2022). Therefore, GIS-AHP was used in this study for the calculation of the weights of the ten flash flood hazard influencing factors.

AHP evaluates two influencing factors simultaneously, and gives preference to one factor over another based on experienced judgments. These judgments are measured using a preference scale of 1 to 9, in which a lower number (1) indicates a lesser preference and a higher number (9) shows more importance of that particular factor over another (Rehman et al. 2022). The accuracy and consistency of the obtained weights can be assessed based on the Consistency Ratio (*CR*). The *CR* is calculated by equation (3):

$$CR = \frac{CI}{RI} \quad (3)$$

where: *CR* is the consistency ratio of a particular AHP matrix, the Consistency Index (**CI**) can be calculated from equation (4), and *RI* is the random index.

$$RI = \frac{\lambda_{max} - n}{n - 1} \quad (4)$$

where: λ_{max} is the consistency vector, and "n" represents the number of influencing factors (n = 10 in this study). The CR should be within the limits of 10% (CR < 0.01), otherwise the assigned score values should be reconsidered (Arabameri et al. 2019; Lootsma 1999).

GIS-based flash flood hazard mapping

After weights of influencing factors were obtained, the weighted sum tool in ArcGIS software was used to multiply the designated field values for each input raster by the obtained weight. The overall weight for the final map of flash flood hazards was then synthesized using equation (5):

$$FFHI = \sum_{i=1}^{n} H_i \times W_i \quad (5)$$

where: *FFHI* is the flash flood hazard index, n represents the number of influencing factors, H_i is the rescaled values of influencing factor i, and W_i is the weight of the influencing factor *i*.

FFHI ranges from 0 to 5. Based on values of *FFHI*, levels of flash flood hazards in the Ngan Sau and Ngan Pho river basins were classified into five classes: very low (less than 1), low (between 1 and 2), moderate (between 2 and 3), high (between 3 and 4), and very high (more than 4).

Accuracy assessment

The areas of flash flood hazards were finally validated based on 151 flood inventory sites collected from the field survey. The accuracy assessment was performed using ArcGIS software. The layer of flood inventory sites is laid over that of flash flood hazard

areas which were obtained from the above-discussed method. The degree of spatial correlation or conformity between the areas of medium-to-high hazard levels and flood inventory is the basis for evaluating the accuracy of the proposed method. In this case, the accuracy of the proposed method increases with the increasing spatial correlation or conformance.

RESULTS AND DISCUSSIONS

Analysis of influencing factors

After datasets were collected, based on the maximum and minimum values of ten factors affecting flash flood hazards, the values of these factors were divided into 5 equal intervals or classes. The degree of these influencing factors affecting flooding was then ranked using a 1 to 5 scale or class. Class 1 represents the factor having the least influence, whereas class 5 represents the factor having the most influence. Data from Table 1 illustrates the degree of influence on flash floods of ten influencing factors in the Ngan Sau and Ngan Pho river basins.

The TWI ranged from 2 to 24.9 (Fig. 3-a). The TWI ranged between 11 and 15, and between 15 and 24.9 had the highest weight, demonstrating high and very high flood susceptibility at this range of TWI (Fig. 4-a). Whereas very low and low flood susceptibility were found with the TWI of between 2 and 5.8, and between 5.8 and 7.9. Low altitude areas, such as flat areas, foothills, and valley floors, are more susceptible to flooding (Rahman and Chen et al. 2021). The altitude ranging from -16 to 2264 meters (Fig. 3-b), was accordingly classified into five classes (Table 1). The altitude ranging between -16 and 145, 145 and 379, 379 and 717, 717 and 1155, and 1155 and 2264 meters, indicates very low, low, moderate, high, and very high influence on floods, respectively (Fig. 4-b). A low slope gradient, usually flat areas, is more susceptible to flooding (Rahman and Chen et al. 2021). The slope gradient ranged from 0 to 86.8 degrees (Fig. 3-c), and five classes of 0-6.8, 6.8-14.6, 14.6-22.1, 22.1-31, and 31-86.8 were classified (Fig. 4-c). In the case of aspect, based on the flow of main streams and rivers, the eastern-facing slopes (east, northeast, and southeast) showed a positive correlation with the flooding, hence these aspects were classified as class numbers 5 and 4 (Fig. 4-h). In contrast, the western-facing slopes (northwest, southwest, and west) indicated a weaker relationship with the flooding, with class numbers of 2 and 1, respectively. Whereas the flat areas showed the strongest relationship with flooding, therefore the flat area was classified as class 5.

Areas close to rivers and roads are more likely to be flooded (Chowdhuri et al. 2020), hence distances close to rivers and roads were assigned high-class numbers. In the case of distance to rivers, class numbers 5 and 4 were found within distances of below 778 and 778-1622 meters, followed by 1622-2587, 2587-4070, and above 4070 meters as class numbers 3, 2, and 1, respectively (Fig. 4-f). As for the factor of distance to roads, class numbers 5 and 4 were found within distances of below 3402 and 3402-7793 meters, followed by the 7793-12842, 12842-18769, and above 18769 meters as class numbers 3, 2, and 1, respectively (Fig/ 4-g). In this study, three types of land cover (Fig. 3-d), namely, water bodies, agricultural and bare lands, were found to be more susceptible to flood occurrence, whereas, other land cover types were found to have a weaker relationship with flooding. Therefore, the highest-class numbers 5 and 4 were assigned to water bodies and agricultural land, followed by bare soil, built-up, and forest as class numbers 3, 2, and 1, respectively (Fig. 4-d). The derived NDVI ranges between -0.11 and 0.65 (Fig. 3-e). The low values of NDVI indicate the less dense vegetated areas, which are more susceptible to flooding. Accordingly, the high-class numbers 5 and 4 were assigned to NDVI in the range between -0.1 and 0.14, 0.14 and 0.25, followed by the NDVI in the range of 0.25-0.3, 0.3-0.4, and 0.4-0.65 as class numbers 3, 2 and 1, respectively (Fig. 4-e).

Rainfall is an important factor that is positively correlated with flooding in the Ngan Sau and Ngan Pho river basins. In this study, the high rainfall areas were classified as high-class numbers. In this case, high-class numbers 5 and 4 were assigned to rainfall between 1736 and 1772, and between 1717 and 1736 mm, followed by the rainfall between 1697-1717, 1675-1697, and 1646-1675 mm, assigned as class numbers of 3, 2 and 1, respectively. The flow length ranged between 0 and 120594 (Fig. 3-i). High-class numbers 5 and 4 were assigned to flow length between 93272-120594 and 70189-93272, followed by the rainfall between 50875-70189, 27793-50875, and below 27793 were assigned as class numbers 3, 2, and 1, respectively.

Analysis of weights of influencing factors

In this study, the experts give their opinions and compare the pairwise influencing factors either jointly or individually. It is, accordingly, based on the experienced judgments of the

Table 1. Flash flood hazard influencing factors

No	Influencing factors	Classes (degree of influence)				
		1 (very low)	2 (low)	3 (moderate)	4 (high)	5 (very high)
1	Altitude (m)	-16-145	145-379	379-717	717-1155	1155-2264
2	Slope (degree)	0-6.8	6.8-14.6	14.6-22.1	22.1-31	31-86.8
3	Aspect	West	Northwest, Southwest	North, South	Northeast, Southeast	Flat, East
4	TWI	2-5.8	5.8-7.9	7.9-11	11-15	15-24.9
5	Flow length	0-27793	27793-50875	50875-70189	70189-93272	93272-120594
6	Distance to streams (m)	4070-9321	2587-4070	1622-2587	778-1622	0-778
7	Distance to roads (m)	18769-27989	12842-18769	7793-12842	3402-7793	0-3402
8	Rainfall (mm)	1646-1675	1675-1697	1697-1717	1717-1736	1736-1772
9	LULC	Forest	Agriculture	Built-up	Bare soil	Water
10	NDVI	0.4-0.65	0.3-0.4	0.25-0.3	0.14-0.25	-0.1-0.14

* Notes: Class numbers 1, 2, 3, 4, and 5 indicate the degree of very low, low, moderate, high, and very high influence on flash floods.

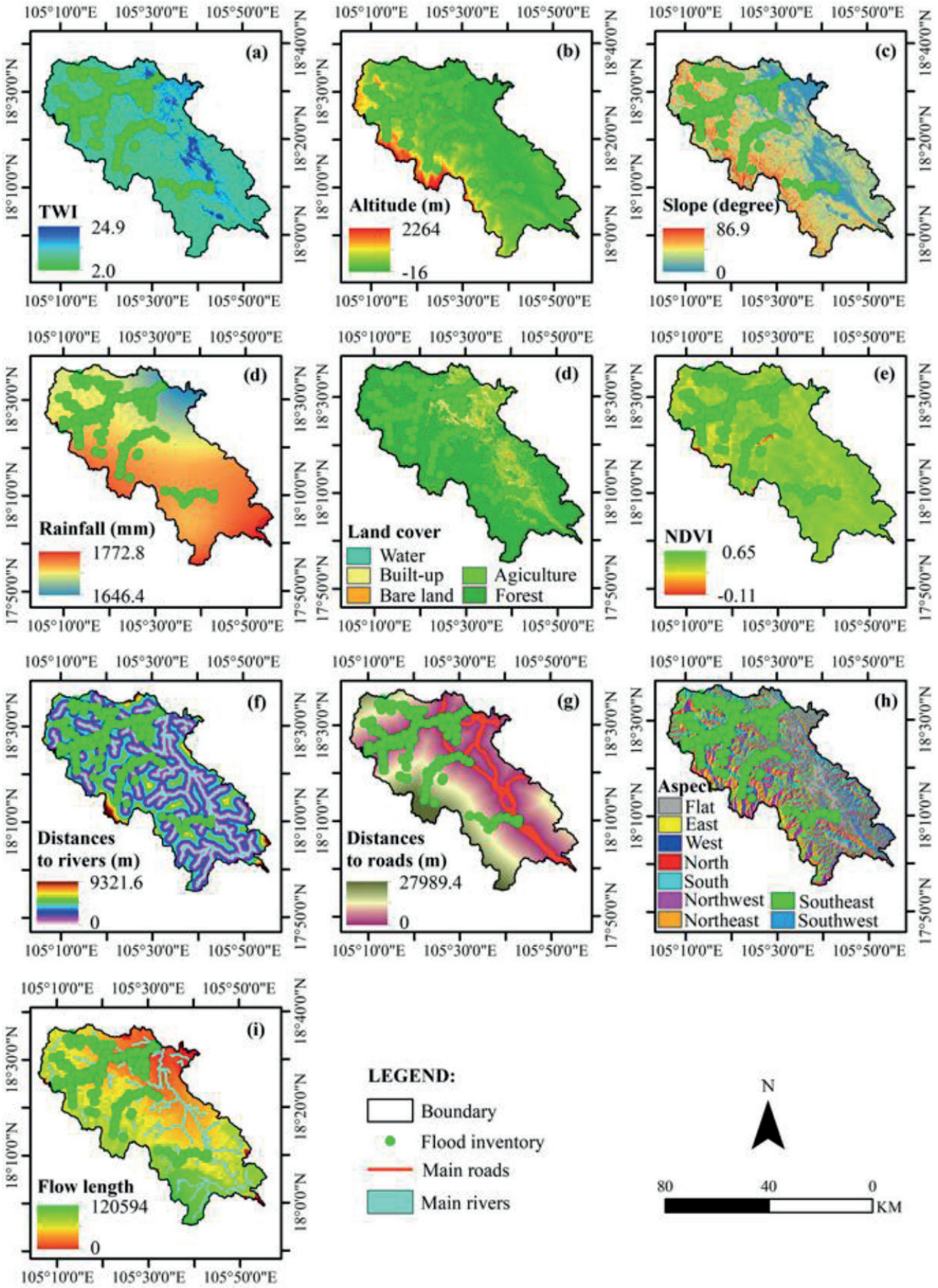

Fig. 3. Maps of 10 influencing factors

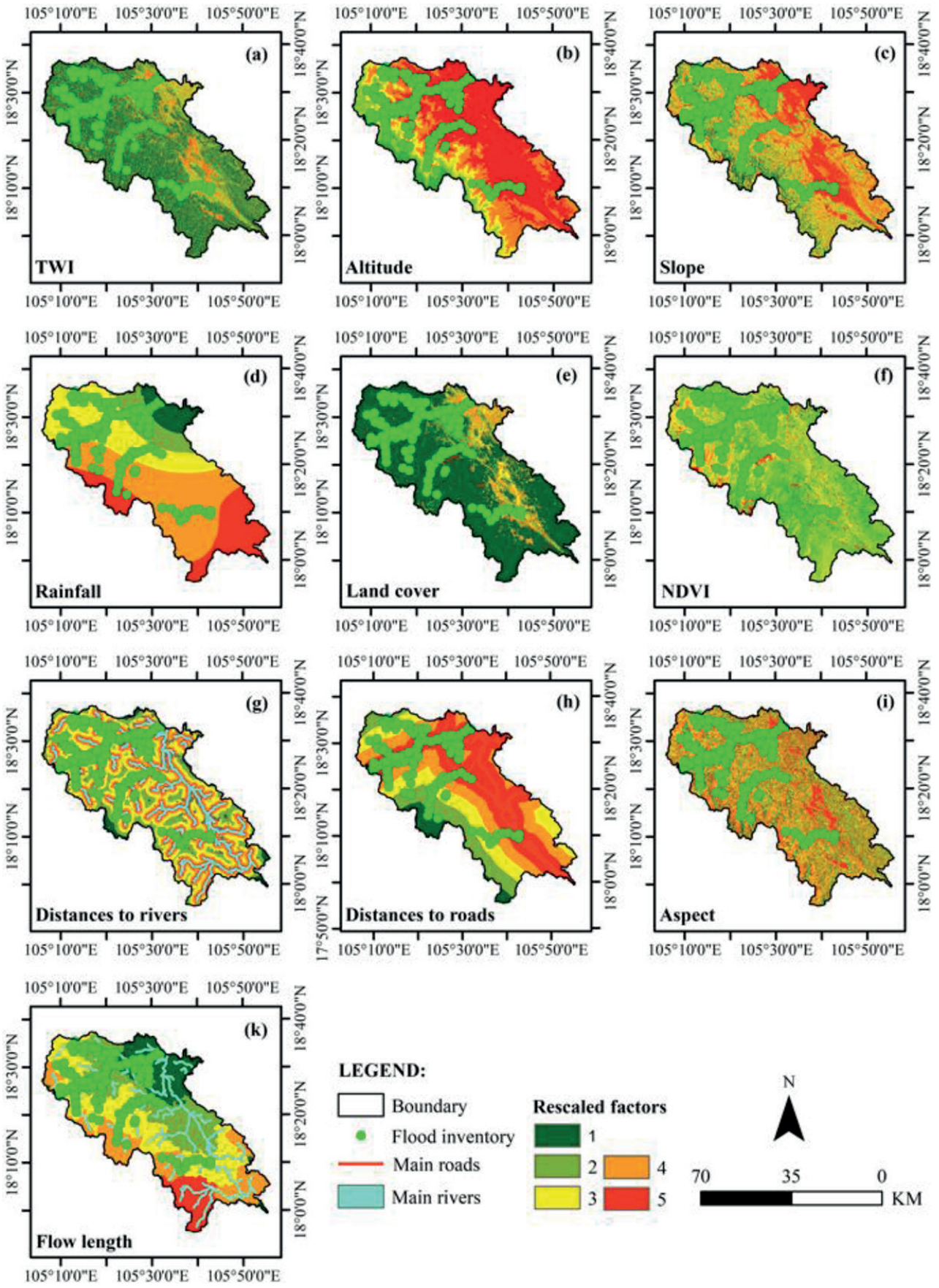

Fig. 4. Maps of ten rescaled influencing factors

experts, the pairwise comparison matrix was formed (Table 2). The AHP technique was then employed to identify the corresponding weight of each influencing factor. Data from Table 2 illustrates the weight values of influencing factors that were obtained from AHP. The Consistency Ratio (CR) of 5.5% was within the limits of 10% (CR < 0.01). This proves the expert's consistency and the validity of the computed weights. Therefore, there is no need to repeat the evaluations. A higher weight value of the factors represents the corresponding factors having more influence on flash floods than others within the Ngan Sau and Ngan Pho study area. Data from Table 2 demonstrates that, with the highest weights of 0.14, two factors, namely distance from rivers and TWI, have the greatest influence on flooding in the study area. These two factors are characterized by the position, the direction, and the accumulation of water flow. It is followed by the rainfall and altitude factors with corresponding weights of 0.13 and 0.12, respectively. This implies that after distance from rivers and TWI factors, rainfall and altitude make more of a contribution to flooding in the area as compared to the remaining factors. This rainfall factor-related result was consistent with those reported by Nguyen (2017) that rainfall duration and intensity in the period of 1990-2012 caused floods in 2002 2007, and 2010 in this area (Hoang et al. 2020; Nguyen 2017). Slope, aspect, flow length, and LULC, with the corresponding weights of 0.1, 0.09, 0.09, and 0.07, respectively, are factors having less influence as compared with the factors discussed above. The lowest weight values of 0.06 were found for both the distance from roads and NDVI factors. This indicates that these two factors have the least influence on flooding in the study area.

Analysis of flash flood hazards

The use of 151 flood inventory sites for the validation of the flash flood hazards in the Ngan Sau and Ngan Pho river basins has revealed that a total of 84.8 percent of flood inventory sites were in good conformity with moderate to very high levels of flash flood hazard areas. This indicates a high degree of strong spatial correlation. In particular, a higher degree of correlation between flood inventory areas and moderate-to-high level flash flood hazard areas obtained from the proposed method was found in the Ngan Sau River basin, in the northern and northwestern study areas (Fig. 5). This result suggests that the integration of Landsat-8 imagery, GIS and AHP allows for accurate and reliable flash flood hazard mapping in this study area.

The areas of flash flood hazards in the Ngan Sau and Ngan Pho river basins were statistically summarized in Table 3 and their corresponding spatial distribution was shown in Fig. 5, respectively. Data from Table 3 illustrates the areas of very high and high flash flood hazard levels were 275 and 621.1 km^2, accounting for 19.5 and 8.6 percent of the total areas of the river basin, respectively. Moderate, low, and very low flash flood hazard levels were extracted with areas of 923.2, 889.1, and 477.8 km^2, accounting for most of the total area with 29, 27.9, and 15 percent, respectively. Data from Fig. 5 demonstrates the very high and high flash flood hazard levels. They were mainly located in the areas along and close to the main Ngan Sau and Ngan Pho rivers and streams, whereas the moderate, low, and very low flood hazard levels were mostly detected in the areas of high and very high altitudes and far from rivers and roads. It is clear that there was a strong correlation between areas of high, very high flash flood hazard levels and close distances to rivers and high TWI areas. In particular, the results on high and very high levels of flash flood hazard areas are in good agreement with the locations of floods recorded and reported in recent studies in the districts of Huong Son in 2016 and 2017 (Hoang et al. 2020; Nguyen and Ha 2017; Nguyen 2017; PSN 2016) and of Duc Tho in 2017 (Group 2016; Thien 2017) in the northwest and northeast of the river basin. High and very high levels of flash flood hazard areas were also identified in Vu Quang district in the west of the basin where flash floods often hit in flood seasons such as in 2011 (Minh Thu 2011) and 2017 (Tien 2017). In addition, moderate-to-very high levels of flash flood hazards were found in the area of Huong Khe district, southwest of the river basin. These areas of flash flood hazards were in good conformity with flash flood sites reported in recent studies such as in 2013 (VT 2019). A negative correlation between low and very low flash flood hazard areas and flood inventory sites. This is consistent with the fact that no floods in history were reported and occurred in very low and low-flash flood hazard areas.

Table 2. Ranking of flash flood influencing factors to obtain the pairwise comparison matrix and their corresponding weights

Comparison Matrix											Weights
Influencing factors	1	2	3	4	5	6	7	8	9	10	
TWI	1	1	1	1	3	5	1	3	1	1	0.14
Altitude	1	1	1	1	2	3	1	3	1	1	0.12
Slope	1	1	1	1	3	1	1/2	1	1	1	0.10
Rainfall	1	1	1	1	3	2	2	3	1	1	0.13
LULC	1/3	1/2	1/3	1/3	1	1	1/3	3	1	1	0.07
NDVI	1/5	1/3	1	1/2	1	1	1/5	1	1	1	0.06
Distance from rivers	1	1	2	1/2	3	5	1	3	1	1	0.14
Distance from roads	1/3	1/3	1	1/3	1/3	1	1/3	1	1	1	0.06
Aspect	1	1	1	1	1	1	1	1	1	1	0.09
Flow length	1	1	1	1	1	1	1	1	1	1	0.09
	Consistency Ratio = 5.5% (< 10%)										

Table 3. Areas of flash flood hazard levels

Levels of flash flood hazards	Areas [km^2]	Percentage [%]	Accumulated percentage [%]
Very low	477.8	15.0	15.0
Low	889.1	27.9	42.9
Moderate	923.2	29.0	71.9
High	621.1	19.5	91.4
Very high	275.0	8.6	100.0

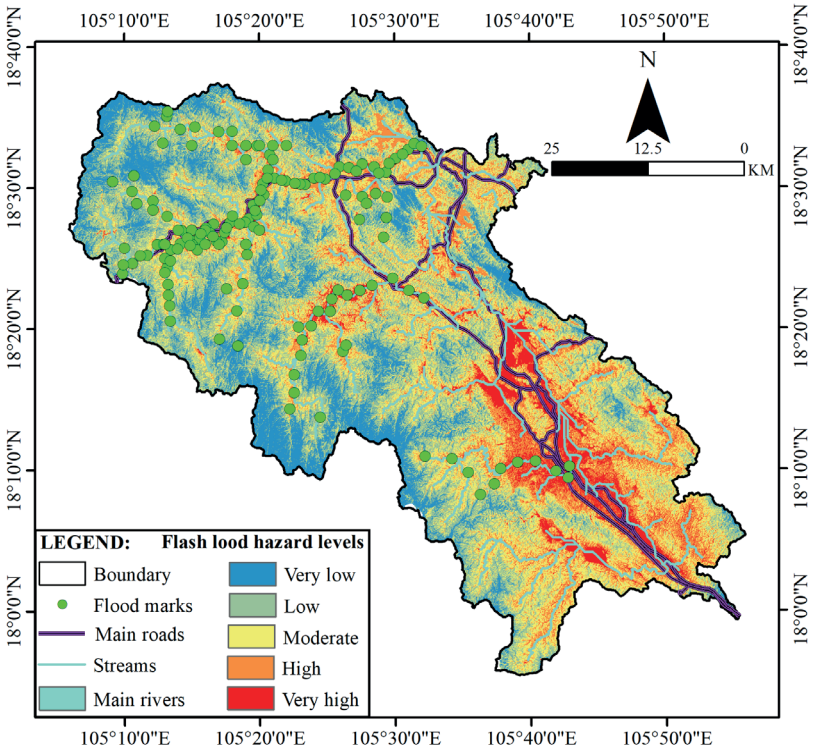

Fig. 5. Map of flash flood hazards

CONCLUSIONS

This study set out to investigate the integration of Landsat-8 imagery, AHP, and GIS in mapping flash flood hazards in the Ngan Sau and Ngan Pho river basins, in north-central Vietnam. A total of ten exploratory factors influencing the flash flood hazards occurrence, namely TWI, altitude, slope, aspect, rainfall, land cover, NDVI, distances to rivers and roads, and flow length, were used to calculate the weights with the help of the AHP technique. Land cover and NDVI were extracted from Landsat-8 OLI imagery. Methods for spatial analysis in GIS were then applied to map the flood hazard. Finally, the validation was carried out using 151 flood inventory sites. The study's results indicated that flash flood hazards are mainly associated with distance from rivers, TWI, and rainfall factors. In addition, a high degree of spatial correlation between 128 flood inventory sites and moderate to very high levels of flash flood hazard areas were also revealed. Last but not least, high and very high flood hazard levels were mainly detected along and close to the main rivers and streams, with areas of 275 and 621.1 km^2, respectively. All these results confirm the effectiveness of the Landsat-8 imagery, AHP, and GIS combination in providing practical flash flood hazard maps. These findings from this study not only enable better watershed management but also effectively reduce the likelihood of future flooding. One source of weakness in this study which could have affected the accuracy of the proposed method was the lack of the factor of rainfall threshold for flash floods. Therefore, more research is required to fully understand how this aspect affects the identification of flash flood hazards.

AUTHOR CONTRIBUTIONS

Tien-thanh Nguyen designed the research, processed and analyzed the data, analysed the findings, and produced the report. Thi-thu-huong Pham and Thi-thu-trang Tran collected the data. The authors revised the manuscript under the supervision of Anh-huy Hoang. All authors discussed the findings and offered feedback on the manuscript at all stages.

REFERENCES

Abou El-Magd I., Hermas E. and El Bastawesy M. (2010). GIS-modelling of the spatial variability of flash flood hazard in Abu Dabbab catchment, Red Sea Region, Egypt. The Egyptian Journal of Remote Sensing and Space Science, 13(1), 81–88, DOI: 10.1016/j.ejrs.2010.07.010.

Alvarez-Mendoza C.I., Teodoro A. and Ramirez-Cando L. (2019). Improving NDVI by removing cirrus clouds with optical remote sensing data from Landsat-8–a case study in Quito, Ecuador. Remote Sensing Applications: Society and Environment, 13, 257–274, DOI: 10.1016/j.rsase.2018.11.008.

Arabameri A., Rezaei K., Cerdà A., Conoscenti C. and Kalantari Z. (2019). A comparison of statistical methods and multi-criteria decision making to map flood hazard susceptibility in Northern Iran. Science of the Total Environment, 660, 443–458, DOI: 10.1016/j.scitotenv.2019.01.021.

Aydin M.C. and Sevgi Birincioğlu E. (2022). Flood risk analysis using gis-based analytical hierarchy process: a case study of Bitlis Province. Applied Water Science, 12(6), 122, DOI: 10.1007/s13201-022-01655-x.

Bich T.H., Quang L.N., Thanh Ha L.T., Duc Hanh T.T. and Guha-Sapir D. (2011). Impacts of flood on health: epidemiologic evidence from Hanoi, Vietnam. Global Health Action, 4(1), 6356, DOI: 10.3402/gha.v4i0.6356.

Bui D.T., Hoang N.-D., Martínez-Álvarez F., Ngo P.-T.T., Hoa P.V., Pham T.D., Samui P. and Costache R. (2020). A novel deep learning neural network approach for predicting flash flood susceptibility: A case study at a high frequency tropical storm area. Science of The Total Environment, 701, 134-413, DOI: 10.1016/j.scitotenv.2019.134413.

Chang D.-L., Yang S.-H., Hsieh S.-L., Wang H.-J. and Yeh K.-C. (2020). Artificial intelligence methodologies applied to prompt pluvial flood estimation and prediction. Water, 12(12), 35-52, DOI:10.3390/w12123552.

Chapi K., Singh V.P., Shirzadi A., Shahabi H., Bui D.T., Pham B.T. and Khosravi K. (2017). A novel hybrid artificial intelligence approach for flood susceptibility assessment. Environmental Modelling and Software, 95, 229–245, DOI: 10.1016/J.ENVSOFT.2017.06.012.

Chatzichristaki C., Stefanidis S., Stefanidis P. and Stathis D. (2015). Analysis of the flash flood in Rhodes Island (South Greece) on 22 November 2013. Silva, 16(1), 76–86.

Chen W., Hong H., Li S., Shahabi H., Wang Y., Wang X. and Ahmad B. Bin. (2019). Flood susceptibility modelling using novel hybrid approach of reduced-error pruning trees with bagging and random subspace ensembles. Journal of Hydrology, 575, 864–873, DOI: 10.1016/j.jhydrol.2019.05.089.

Chowdhuri I., Pal S.C. and Chakrabortty R. (2020). Flood susceptibility mapping by ensemble evidential belief function and binomial logistic regression model on river basin of eastern India. Advances in Space Research, 65(5), 1466–1489, DOI: 10.1016/j.asr.2019.12.003.

Costache R., Tin T.T., Arabameri A., Crăciun A., Ajin R.S., Costache I., Islam A.R.M.T., Abba S.I., Sahana M. and Avand M. (2022). Flash-flood hazard using deep learning based on H2O R package and fuzzy-multicriteria decision-making analysis. Journal of Hydrology, 609, 127-747, DOI: 10.1016/j.jhydrol.2022.127747.

Daneshparvar B., Rasi Nezami S., Feizi A. and Aghlmand R. (2022). Comparison of results of flood hazard zoning using AHP and ANP methods in GIS environment: A case study in Ardabil province, Iran. Journal of Applied Research in Water and Wastewater, 9(1), 1–7, DOI: 10.22126/ARWW.2022.6667.1218.

Field C.B., Barros V., Stocker T.F. and Dahe Q. (2012). Managing the risks of extreme events and disasters to advance climate change adaptation: special report of the intergovernmental panel on climate change. Cambridge University Press, DOI: 10.13140/2.1.3117.9529.

Gaume E., Bain V., Bernardara P., Newinger O., Barbuc M., Bateman A., Blaškovičová L., Blöschl G., Borga M. and Dumitrescu A. (2009). A compilation of data on European flash floods. Journal of Hydrology, 367(1–2), 70–78, DOI: 10.1016/J.JHYDROL.2008.12.028.

Getahun Y.S. and Gebre S.L. (2015). Flood hazard assessment and mapping of flood inundation area of the Awash River Basin in Ethiopia using GIS and HEC-GeoRAS/HEC-RAS model. Journal of Civil and Environmental Engineering, 5(4), 1, DOI: 10.4172/2165-784X.1000179.

Gigović L., Pamučar D., Bajić Z. and Drobnjak S. (2017). Application of GIS-interval rough AHP methodology for flood hazard mapping in urban areas. Water, 9(6), 360, DOI: 10.3390/w9060360.

Group B. (2016). Golden heart fund relieved flood victims in Ha Tinh province. Bitexco Group [online]. Available at: http://bitexco.com.vn/newdetail/golden-heart-fund-relieved-flood-victims-in-ha-tinh-province-115.html [Accessed 6 Nov. 2021].

Hoang L.T.T. and Tran T.M. (2018). Climate Change Vulnerability Assessment Fortourism Sector in Ha Tinh Province. VNU Journal of Science: Earth and Environmental Sciences, 34(1), DOI: 10.25073/2588-1094/vnuees.4230.

Hoang V., Tran H.T. and Nguyen T.T. (2020). A GIS-based spatial multi-criteria approach for flash flood risk assessment in the ngan sau-ngan PHO mountainous river basin, north central of Vietnam. Environment and Natural Resources Journal, 18(2), DOI: 10.32526/ennrj.18.2.2020.11.

Hosseini F.S., Choubin B., Mosavi A., Nabipour N., Shamshirband S., Darabi H. and Haghighi A.T. (2020). Flash-flood hazard assessment using ensembles and Bayesian-based machine learning models: Application of the simulated annealing feature selection method. Science of the Total Environment, 711, 135-161, DOI: 10.1016/j.scitotenv.2019.135161.

Jonkman S.N. (2005). Global perspectives on loss of human life caused by floods. Natural Hazards, 34(2), 151–175, DOI: 10.1007/s11069-004-8891-3.

Kha D.D., Nhu N.Y. and Anh T.N. (2018). An approach for flow forecasting in ungauged catchments–A case study for Ho Ho reservoir catchment, Ngan Sau River, Central Vietnam. Journal of Ecological Engineering 19(3), 74–79, DOI: 10.12911/22998993/85759.

Koem C. and Tantanee S. (2021). Flash flood hazard mapping based on AHP with GIS and satellite information in Kampong Speu Province, Cambodia. International Journal of Disaster Resilience in the Built Environment, 12(5), 457–470, DOI: 10.1108/IJDRBE-09-2020-0099.

Koks E.E., Jongman B., Husby T.G. and Botzen W.J.W. (2015). Combining hazard, exposure and social vulnerability to provide lessons for flood risk management. Environmental Science and Policy, 47(2), 42–52, DOI: 10.1016/j.envsci.2014.10.013.

Kvočka D., Falconer R.A. and Bray M. (2016). Flood hazard assessment for extreme flood events. Natural Hazards, 84(3), 1569–1599, DOI: 10.1007/s11069-016-2501-z.

Long B.D. and Dung P.T. (2009). Flash floods, hydrometeorological forecasting and warning systems in Viet Nam. Proceedings of the 7th Annual Mekong Flood Forum: Integrated Flood Risk Management in the Mekong River Basin, 229–240.

Lootsma F.A. (1999). Multi-criteria decision analysis via ratio and difference judgement. Springer, DOI: 10.1007/b102374.

Malik S., Pal S.C., Arabameri A., Chowdhuri I., Saha A., Chakrabortty R., Roy P. and Das B. (2021). GIS-based statistical model for the prediction of flood hazard susceptibility. Environment, Development and Sustainability, 23, 16713–16743, DOI: 10.1007/s10668-021-01377-1.

Marzouki A. and Dridri A. (2022). Normalized Difference Enhanced Sand Index for desert sand dunes detection using Sentinel-2 and Landsat 8 OLI data, application to the north of Figuig, Morocco. Journal of Arid Environments 198, 104-693, DOI: 10.1016/j.jaridenv.2021.104693.

Merz B., Blöschl G., Vorogushyn S., Dottori F., Aerts J.C.J.H., Bates P., Bertola M., Kemter M., Kreibich H. and Lall U. (2021). Causes, impacts and patterns of disastrous river floods. Nature Reviews Earth and Environment, 2(9), 592–609.

Minh Thu C.T. (2011). Spring buds after floods [online]. Nhan Dan Online. Available at: https://en.nhandan.vn/spring-buds-after-floods-post15790.html [Accessed 6 Nov. 2021].

Mudashiru R.B., Sabtu N., Abdullah R., Saleh A. and Abustan I. (2022). A comparison of three multi-criteria decision-making models in mapping flood hazard areas of Northeast Penang, Malaysia. Natural Hazards, 112(3) 1903–1939, DOI: 10.1007/s11069-022-05250-w.

Mudashiru R.B., Sabtu N., Abustan I. and Balogun W. (2021). Flood hazard mapping methods: A review. Journal of Hydrology, 603, 126846.

Mukherjee F. and Singh D. (2020). Detecting flood prone areas in Harris County: a GIS based analysis. GeoJournal, 85(3), 647–663, DOI: 10.1007/s10708-019-09984-2.

Neji N., Ayed R. Ben and Abida H. (2021). Water erosion hazard mapping using analytic hierarchy process (AHP) and fuzzy logic modeling: a case study of the Chaffar Watershed (Southeastern Tunisia). Arabian Journal of Geosciences, 14, 1–15, DOI: 10.1007/s12517-021-07602-5.

Nguyen D. and Ha H.Q. (2017). Flash floods potential area mapping at Huong Khe District, Ha Tinh prov. VNUHCM Journal of Natural Sciences, 1(T4), 249–254, DOI: 10.32508/stdjns.v1iT4.487.

Nguyen H. (2017). Thousands of households violated by a flood in Ha Tinh province [online]. Dai Doan Ket Newspaper. Available at: http://daidoanket.vn/xa-hoi/ha-tinh-hang-nghin-ho-dan-bi-ngap-lut-tintuc382249 [Accessed 6 Nov. 2021].

Noy I. and Vu T.B. (2010). The economics of natural disasters in a developing country: The case of Vietnam. Journal of Asian Economics, 21(4), 345–354, DOI: 10.1016/j.asieco.2010.03.002.

Park S. and Kim J. (2019). Landslide susceptibility mapping based on random forest and boosted regression tree models, and a comparison of their performance. Applied Sciences, 9(5), 942, DOI: 10.3390/app9050942.

Pathan A.I., Girish Agnihotri P., Said S. and Patel D. (2022). AHP and TOPSIS based flood risk assessment-a case study of the Navsari City, Gujarat, India. Environmental Monitoring and Assessment, 194(7), 509.

Prokešová R., Horáčková Š. and Snopková Z. (2022). Surface runoff response to long-term land use changes: Spatial rearrangement of runoff-generating areas reveals a shift in flash flood drivers. Science of the Total Environment, 815, 151-591, DOI: 10.1016/j.scitotenv.2021.151591.

PSN. (2016). People's Police College 5 supports people in flood-hit localities [online]. Public Security News. Available at: http://en.cand.com.vn/Public-security-forces/People-s-Police-College-5-supports-people-in-flood-hit-localities-414865/ [Accessed 6 Nov. 2021].

Qiang Y. (2019). Flood exposure of critical infrastructures in the United States. International Journal of Disaster Risk Reduction, 39, 101-240, DOI: 10.1016/j.ijdrr.2019.101240.

Rahman M., Chen N., Islam M.M., Mahmud G.I., Pourghasemi H.R., Alam M., Rahim M.A., Baig M.A., Bhattacharjee A. and Dewan A. (2021). Development of flood hazard map and emergency relief operation system using hydrodynamic modeling and machine learning algorithm. Journal of Cleaner Production, 311, 127594, DOI: 10.1016/j.jclepro.2021.127594.

Rahman M., Ningsheng C., Mahmud G.I., Islam M.M., Pourghasemi H.R., Ahmad H., Habumugisha J.M., Washakh R.M.A., Alam M. and Liu E. (2021). Flooding and its relationship with land cover change, population growth, and road density. Geoscience Frontiers, 12(6), 101224, DOI: 10.1016/j.gsf.2021.101224.

Rehman A., Song J., Haq F., Mahmood S., Ahamad M.I., Basharat M., Sajid M. and Mehmood M.S. (2022). Multi-hazard susceptibility assessment using the analytical hierarchy process and frequency ratio techniques in the Northwest Himalayas, Pakistan. Remote Sensing, 14(3), 554, DOI: 10.3390/rs14030554.

Saaty, T.L. (1988). What is the Analytic Hierarchy Process? Mathematical Models for Decision Support. NATO ASI Series, Springer, Berlin, Heidelberg, 48, DOI: 10.1007/978-3-642-83555-1_5.

Şahin M. (2021). A comprehensive analysis of weighting and multicriteria methods in the context of sustainable energy. International Journal of Environmental Science and Technology, 18(6), 1591–1616, DOI: 10.1007/s13762-020-02922-7.

Satarzadeh E., Sarraf A., Hajikandi H. and Sadeghian M.S. (2022). Flood hazard mapping in western Iran: assessment of deep learning vis-à-vis machine learning models. Natural Hazards, 1–19, DOI: 10.1007/s11069-021-05098-6.

Stefanidis S., Alexandridis V. and Theodoridou T. (2022). Flood exposure of residential areas and infrastructure in Greece. Hydrology, 9(8), 145, DOI: 10.3390/hydrology9080145.

Tehrany M.S., Pradhan B. and Jebur M.N. (2015). Flood susceptibility analysis and its verification using a novel ensemble support vector machine and frequency ratio method. Stochastic Environmental Research and Risk Assessment, 29, 1149–1165, DOI: 10.1007/s00477-015-1021-9.

Teng J., Jakeman A.J., Vaze J., Croke B.F.W., Dutta D. and Kim S. (2017). Flood inundation modelling: A review of methods, recent advances and uncertainty analysis. Environmental Modelling and Software, 90 201–216, DOI: 10.1016/J.ENVSOFT.2017.01.006.

Thien D. (2017). Flash flood in Duc Tho distric, Ha Tinh province [online]. Ha Tinh Newspaper. Available at: https://baohatinh.vn/xa-hoi/hung-lu-thuong-nguon-ve-vung-ngoai-de-duc-tho-ngap-bang/141928.htm [Accessed 6 Nov. 2021].

Tien D. (2017). Police forces help people overcome floods. Ministry of Public Security of Socialist Republic of Vietnam [online]. Available at: https://en.bocongan.gov.vn/social-ativities/police-forces-help-people-overcome-floods-t4209.html [Accessed 6 Nov. 2021].

VT H. (2019). Emergency response to flood in Huong Son, Ha Tinh. [online]. Available at: https://www.oxfamblogs.org/vietnam/2014/01/29/emergency-response-to-flood-in-huong-son-ha-tinh/ [Accessed 6 Nov. 2021].

RESEARCH PAPER

EFFECT OF LAND-USE CHANGES ON LANDSCAPE FRAGMENTATION: THE CASE OF RAMALLAH AREA IN CENTRAL PALESTINE

Mohammad Muhsen[1*], Ahmad Abu Hammad[1], Mustapha Elhannani[2]
[1]Department of Geography, Birzeit University, PO Box 14, Birzeit, Palestine
[2]Faculté des lettres, langues et science humaines, Université d'Angers-France
***Corresponding author:** mmohsin@birzeit.edu
Received: September 18th, 2022 / Accepted: May 4th, 2023 / Published: July 1st, 2023
https://DOI-10.24057/2071-9388-2022-136

ABSTRACT. The urban sprawl of cities periphery is one of such changes that has led to drastic land-use changes, which resulted in landscape fragmentation. The objective of this study is to understand the process of landscape fragmentation because of urban expansion; identifying the most influential drivers that have changed the land-use. To achieve the objectives due to changes in land use, a study had conducted in Ramallah area of Palestine. The study utilized Fragstat software to quantify the landscape changes with regard to its pattern and structure through a number of indices, also using Geographic Information System tool to draw up different landscape parcels spatially with its characteristics.

The spatial analysis carried out on the land-use change used the 1997 and 2017 aerial photos to quantify the landscape fragmentation, which included a variety of land-uses. Over 52% of the study area underwent noticeable urbanization process, resulting in appreciable landscape changes to the area, especially after 1993. The statistical analysis of the landscape fragmentation revealed significant changes in land-use during the period from 1997 to 2017; the green landscape has been fragmented at a large scale by increasing the number of landscape patches (from 71 to 148 patches). As a result, there was an obvious reduction in agricultural lands, such as olive groves and grassland. At the same time, the urban surface areas increased from 654 patches in 1997 to 2019 patches in 2017. These results indicate that the landscape has become more fragmented due to geopolitical and socio-economic drivers since mid-1995 after Oslo accord.

KEYWORDS: land-use, landscape fragmentation, pattern, Fragstat

CITATION: Muhsen M., Hammad A. A., Elhannani M. (2023). Effect Of Land-Use Changes On Landscape Fragmentation: The Case Of Ramallah Area In Central Palestine. Geography, Environment, Sustainability, 2(16), 68-76
https://DOI-10.24057/2071-9388-2022-136

Conflict of interests: The authors reported no potential conflict of interest.

INTRODUCTION

The process of fragmentation involves splitting the green areas into smaller patches whereas in some areas becoming isolated (Flowers et al. 2020) that called it unravelling. Landscape has fragmented all over the world due to the disintegration of wildlife and the ecosystem (Mumu 2016). The landscape fragmentations were also affected by socioeconomic factors (Luo et al. 2015). Landscape fragmentation is subjected to land-use change, the main driver of environmental change, which caused by intensive urban expansion due to population growth, unplanned land use shift and poor land management, in addition to urban and infrastructure developments are considered main drivers of landscape changes and fragmentation (Jaeger and Raumer 2006).

The analysis of landscape fragmentation requires an analysis of the driving factors influencing the land use changes from green to urban areas. Recent studies addressed the role of land use on the fragmentation of forests and agricultural land that has been linked to a number of environmental consequences (Bryon et al. 2020). (Antonio et al. 2019) included the role of human activities in landscape fragmentation, the transportation networks, urbanized area and suburban and rural sprawl in Natura area of Sardinia-Italy as influential factors that affected landscape and caused fragmentation.

Urban growth and transportation networks are rapidly encroaching on the peripheral and rural areas that led to a high urbanization rate around the world, which is one of the most important drivers of landscape fragmentation besides other socioeconomic factors. Over the recent decades, urbanized areas have extremely expanded and associated with the growth of transportation networks, deforestation and decreasing of cultivated land areas. Gradually, as a result, the landscape pattern has dramatically changed over time (Weng Yc 2007).

The demand for new infrastructure and houses has pushed toward the conversion of the agricultural land to urban land-use (Radad and Samat 2016). Hence, in 1943, the land-use map showed that agricultural land had been the dominating land-use. The declining importance of traditional culture of agrarian society and the farming system (Nazer 2009) is proof of the agricultural terraces degradation.

The land-use of the Palestinian communities has changed in the last two decades. During this period between 1997 and 2017, Ramallah area underwent one

of its greatest changes, due to the geopolitical and socio-economic situation (Bilgin 2016; Hilal and Saka 2015; Bimlom 2014; UN-Habitat 2015 and Shaheen 2013).

Ramallah as the study area of this paper has experienced a noticeable growing population coupled with rapid urban area growth. Nowadays, Ramallah area ranks as the first condensed area in the West Bank, and functions as one of the urban centres. Moreover, Ramallah is experiencing significant building units, particularly in the duration between 2007 and 2017, including suburbs-style (out-skirt) landscape that characterized the current de facto.

However, the spatial analysis in the study focused on the changes in the green areas that occurred because of the development of built-up area, considering it as one aspect depicting the changes in the landscape. Hence, the study area faces land-use changes, fragmentation of its landscape, and such changes is associated with socio-economic transformation processes (Abu Helu 2012; Noubani 2010; Taraki 2008 and Khamaisi 2006). The implications of this issue are not fully being taken into consideration.

The random urban model characterizes the study area based on the de facto situation. Many studies related to the landscape have demonstrated landscape change due to urban development and its effect on other elements of the landscape through spatial and temporal analysis (Riitters et al. 1995 and Baker 1989).

Evidence from several studies, including (Muhsen and Abu Hammad 2017) and (Hammad and Sharkas 2008), showed the research area's landscape pattern had changed significantly throughout that time period. The Palestinian authority onset is a significant part of the process of transformation from rural landscape into new urban landscape model (Al-Houdalieh and Suader 2009). The onset of the authority caused internal migration, thereby creating a dire need for residential areas in the first stage of the development process.

According to (Muhsen and Abu Hammad 2017) studies revealed that the urban area extended over 300 hectares during the periods of 1997 and 2017; most of the land converted to built-up area with a 52-percentage increase in the same period. However, Ramallah area has faced a new situation within the past two decades, connected to the high demand for dwellings to meet the high need of newcomers to the study area (Harker 2014). The high need for dwellings connected with a high completion and demand on lands, services, and other uses, which affected adversely agricultural land, and other green areas causing a change in land-use. In later stages, this process is associated with raising value and prices of land.

In addition, number of studies (Zaho et al. 2020; Zambrano et al. 2019; Kong and Kakagoshi 2006), the effects of the landscape's fragmentation mainly had negative consequences on species richness and animals in the ecosystem. Indeed, they have reduced the space of the green area (forest, natural grassland and agricultural land). In addition, the fragmentation has substantial adversely effects on the landscape due to the limited green areas in some regions. That means more threats on the natural ecosystem, biodiversity and water resources by reduction, loss habitat or in some areas replaced by invasion habitat, wildlife diversity devastation and changing the natural landscape pattern etc.

According to Samsuri the area of the forest in Batang Toru watershed has fragmented between 1989 and 1993 because of the anthropogenic activities in the area, the study has conducted by using Fragstat to generate landscape metrics to quantify the fragmentation rate (Samsuri et al. 2014). Concurrently, in all over the world, forests and agricultural areas are the most affected areas where process of fragmentation occurred due to deforestation and other accompanied human activities, which is similar to what has been found by (Jane et al. 2004) in their study about Honduras region.

According to (Jochen A. et al. 2007) and (Chen 2003) it is an important environmental indicator in assessing the sustainable land use, biodiversity and urban growth by quantitative methods (i.e., size perimeter). While according to (Davidson 2006), landscape fragmentation index can be defined as the breaking up of continuity such as habitat, decreasing or increasing number of patches, and decreased average patches size. This study aims to identify the land-use changes and the scale of landscape fragmentation; analyzing the new urban landscape based on the evaluation of the new development; and understanding its implications through landscape fragmentation index.

The high pace of urbanization in the Palestinian territory in general, and specifically in the study area after 1993, and the land changes are responsible for the beginning of landscape fragmentation with its associated negative outcomes, which was characterized by a period of rapid changes according to a number of studies such as (Samar et al. 2018). Samar study focused on the landscape changes in Ramallah City by using Fragstat tool and found that Ramallah city landscape has been changed during the period between 1994 and 2014 because of the rapid urban growth at the expense of greenery areas (i.e., trees and shrub).

In the same track, few studies have addressed the influence of urban expansion on landscape fragmentation in the study area. For example (Samer 2015) has analyzed land use changes in Ramallah metropolitan during 1990 and 2003; the analysis based on urban expansion increase and utilized aerial photos analysis to quantify the changes by using GIS and Remote Sensing. The study revealed that the impact of the Israeli limitations and obstacles on Palestinian urban expansion, which accelerated fragmentation more into the greenery areas.

However, increasing the urbanized areas and the anthropogenic activities resulted to landscape fragmentation that has converted larger areas of natural landscape into smaller and isolated areas.

Though, the lack of spatial statistical analysis on the land use as well as landscape changes are considered as one of most important field information of urban studies for Ramallah area. This study has fostered the spatial statistical analysis to bridge the gap lack of spatial analysis for the study area, but more studies need to be achieved in the near future about the urban development and its implications.

Moreover, not many researches and studies have focused on addressing the main drivers that led to the landscape fragmentation. Therefore, more studies need to interlinked these drivers to give an answer for the rapid pace of urbanization that affected adversely on the study area landscape.

Precisely, the critical questions of the study are: what is the land use is and landscape changes that happened on the study area the last two decades, and what are the drivers that led to those changes. Towards this, the study aims to quantify the landscape fragmentation of the study area based on land use changes, the landscape patterns change over the time, and to identify the main drivers responsible for the fragmentation process.

MATERIALS AND METHODS

Study Area

The study area is comprised of three adjacent cities: Ramallah, Al-bireh, and Betunia. The total area is about 188,2 hectares (Fig. 1) and the population is 200,000 (Ramallah Area Municipality 2017), or nearly two-thirds of the 328,861 inhabitants who live in the Ramallah district (PCBS 2018). The study area experienced land use changes, which fragmented the landscape and affected the vegetation cover through human-driven changes such as urban development.

A number of Israeli colonies and military bases are surrounding the study area. The area is about 800 meters above sea level. This area has a Mediterranean climate, with an average annual rainfall of about 600 mm, between the months of December and February. The average annual temperature is about 17 c°, and the warmest months are July and August. In addition, the area is characterized by topographic variation in terms of elevation and slope aspects, which are western and eastern slopes. Terrarosa soil with limestone and dolomite origin covered the study area. The fertile soils combined with the Mediterranean Sea climate, makes most of the land in the study area suitable for agriculture.

The region had a mixed vegetation cover including olive groves, forest, agricultural land…etc. Historically, the number of populations has been affected by internal migration due to political conflicts between the Israelis and the Palestinians (1948 and 1967 war).

The population of the area increased about three times from 9,250 in 1945 to 31,485 inhabitants in 1961. This increase coincided with the return of the Palestinian Authority in 1993, as well as, the emerging trend of internal migration due to the centralization of Palestinian governmental institutions and the private sectors in this area. In addition, the number of the population increased to be 103,335 inhabitants in 2015 (PBCS 2015), but if compared with the number provided by the municipalities of the three cities, it is estimated to be more than 200,000 inhabitants.

In 2017, the number increased rapidly, due to the high pace of internal migration after 1997, which accompanied a high rate of urban development that changed agricultural landscape into urban landscape.

Methodology

The study used two sets of aerial photos (1997: cell size 1.25 and 2017: 0.25) to detect changes in urban area, supervised aerial photo analysis of different land use elements in 1997 and 2017. The different land use elements were extracted from aerial photos. Urban land is classified as (Unattractive Indicators) which includes residential dwelling and excludes yards, sidewalks, transportation, and industrial areas. While, agriculture/Natural vegetation land, Natural grassland, Forest and olives groves are classified as (Attractive Indicators). This classification is according to the Ministry of Local Government.

The study used geographic information system (GIS-ArcMap 10.5) tool to detect the past and the actual land use changes that have occurred over the specific period to quantify different land use pattern and characteristics (size, shape, perimeter etc…). The Ministry of Local Government has provided the researcher with the tow aerial photos.

The land-use maps production of the study area depended on the direct and visual interpretation of the 1997 and 2017 aerial photos by digitizing the completely targeted area for two class of land-use urban area and green area, where the extracted data was manually transferred to base maps of

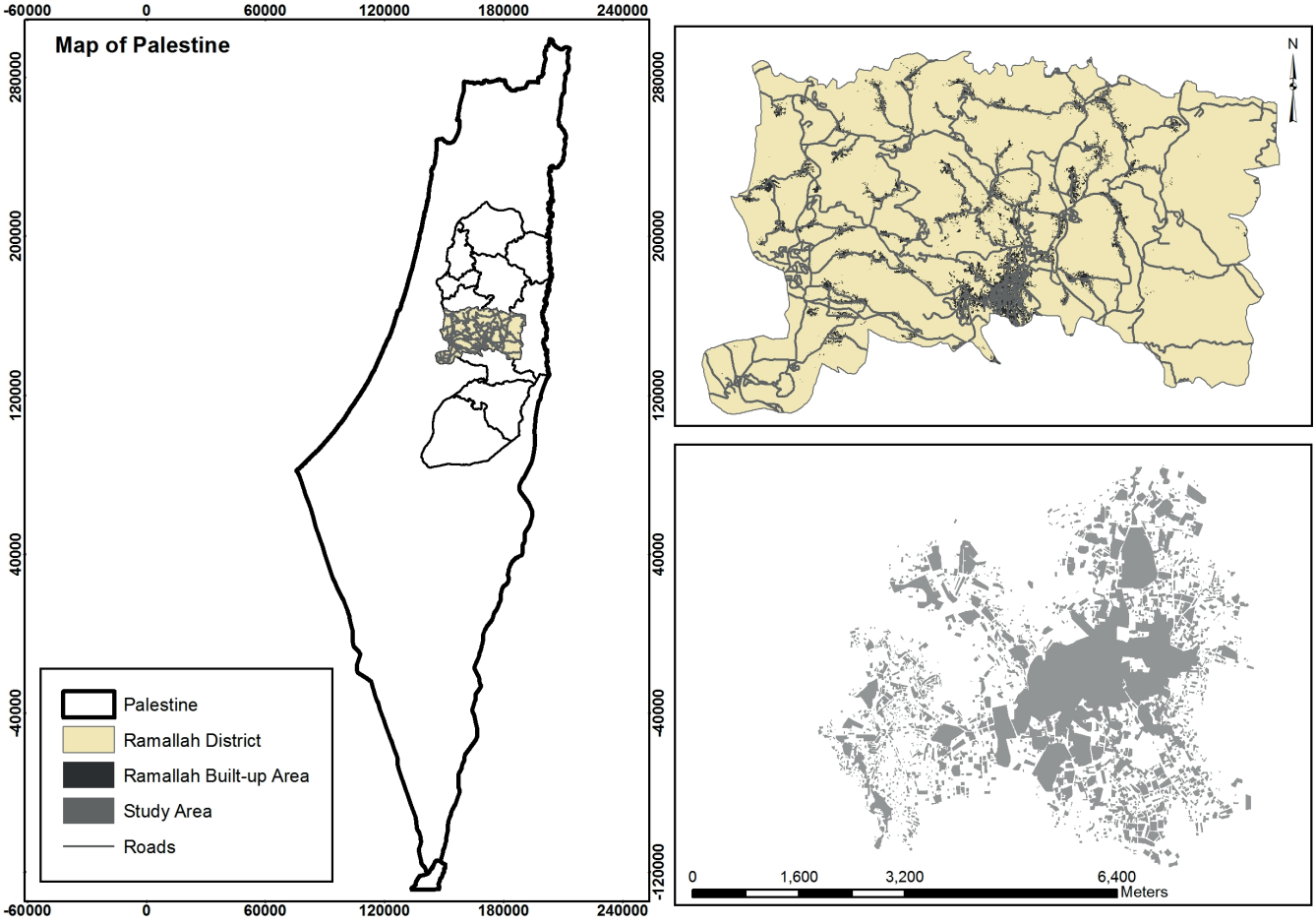

Fig. 1. Location of the study area (source: Department of Geography-Birzeit University)

the previous land-use classes. The ground truth verification method used through three field visits were conducted to ensure accuracy of the process of land-use analysis, and to obtain more data about the land use classes. The attribute data was used for the spatial pattern analysis and to produce several maps.

Generally, the research carried out by three stages: Data collection (Literature review, aerial photos and feature class), Data processing (digitizing, tabulation…) and Data analysis (landscape metrics…) (Table 1).

The land-use maps of the study area interpreted using the ground truth visual interpretation of the 1997 and 2017 aerial photos, where the extracted data was manually transferred to base maps of the various land-use classes. In this technique of ground truth verification, the number of field visits were done to ensure accuracy of the process of land-use analysis, and to obtain more data. The attribute data was used for the spatial pattern analysis and to produce several maps.

In order to follow up on the land-use changes and facilitate analysis, the study area was divided into two main classes: Green and Urban land-use. The green area was classified to four sub-classes as mentioned previously. The Fragstats program which is regarded as a spatial statistical program to measure the landscape fragmentation (Batty 1999) and (Baker 1989) and its characteristics by landscape metrics (Keles et al. 2008) and (Li X et al. 2001), was used to measure the landscape fragmentation using the patches-dynamics approach. These metrics and their acronyms are as follows:

NP: Number of Patches
PD: Patch Density
ED: Edge Density
LPI: large patch index
LSI: Landscape Shape Index
P.M: Perimeter Mean
F-Index: Fraction Dimension Index

RESULTS AND DISCUSSION

Land-use Aggregation

In 1997 the agriculture land use covered about 40 percent of the total study area (Fig. 1). The agricultural/natural vegetation cover has been badly changed in correspondence to the increase of the urban land-use, as it decreased from 40 percent of the total surface area in 1997 to 32 percent in 2017, whereas natural grassland decreased from 10.4 percent in 1997 to 8.3 percent in 2017 (Fig. 2). Thus, urban land-use increased from 38.75 percent in 1997, to about 51 percent in 2017. Generally, land-use showed a general trend of increasing urban land-use and decreasing agricultural area between 1997 and 2017. As a result, 2017 is dominated by mixed agricultural/non-agricultural land and urban/sub urban agglomerations.

This analysis indicates that the mean area of the urban agglomeration significantly increased due to the urban development that converted agricultural land to urban land in a short span of time, which also characterized the new pattern in the past two decades. The accelerated process of urbanization helped in decreasing the residents' awareness towards the importance of the agricultural land. 82 percent of respondents ensured that this change is connected to the anthropogenic driver that is related to the high value of land for a commercial purpose rather than an agricultural purpose, for example the price of 1m^2 of commercial land is estimated to be more than $500 in some part of the study area.

Table 1. The Study Data

Data Collection	Format	Data Processing	Data Analysis
Aerial Photo 1997, 1.25*1.25	Raster	Input Data	-
Aerial Photo 2017, 0.25*0.25	Raster	Input Data	-
Land use feature class: 1997 and 2017	Vector	Digitizing ArcGIS	Visual Interpretation
Land use feature class: 1997 and 2017	Vector	Tabulation ArcGIS	Classification
Land use feature class: 1997 and 2017	Raster	Rasterization ArcGIS	Raster Map of land use
Land use Map: 1997, 2017	Raster	Fragstat Software	Output file: Landscape Metrics, PN, PD i.e….

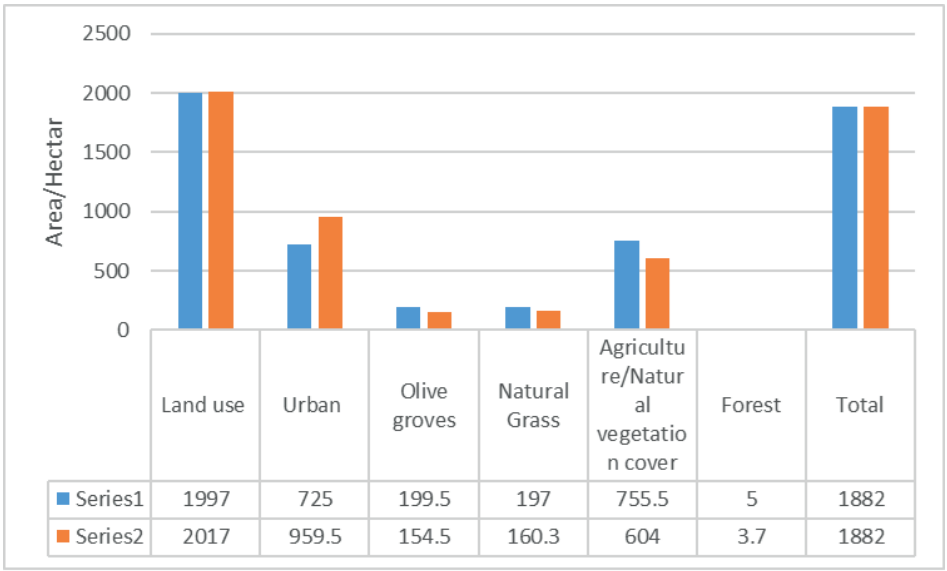

Fig. 2. Area of different Land-uses (Hectare) in 1997 and 2017

Forested land decreased by about 0.05 percent due to the urban development; particularly in some areas, that has biodiversity. Forest area also decreased by about 26 percent in favor of urban areas. Despite these negative changes in the green areas, the municipality has attempted to save the rest of the forest part by creating a public park for local residents.

Fragmentation Analysis

Spatial analysis of the landscape from 1997 to 2017 indicates that there is a trend of increasing urban area and at the same time decreasing green area. Agricultural land experienced the largest decrease of about 25 percent, with an increase of urban area of about 13 percent. Urban area constitutes the dominant class of landscape with about 51 percent in 2017 compared to 38.5 percent in 1997.

According to the spatial analysis of Fragstat, the number of patches of urban area has increased from 654 patches in 1997 to 2,019 in 2017, whereas the green area increased from 71 patches in 1997 to 148 patches in 2017. The increase in the number of green area patches could indicate that the landscape has fragmented even more than before. The raising number of patches could also mean an increase in the urban development through increasing patches of the built-up area surface that adversely impacted on the green landscape, which has been linked to a number of environmental consequences, particularly on the agricultural system of the area, such as land degradation due to dividing the land (Fig. 3 and Fig. 4).

However, in depth, analysis shows that the degree of fragmentation of the green area has increased, merely due to the urban expansion. Therefore, the number of patches of the green area has increased to about 148 patches, which is considered to be of high level regardless of the surface area. The fragmentation index was 0.8712 in 1997 against 1.0826 in 2017. In addition, the edge density has decreased from 7.34.6 in 1997 to 6.28 in 2017, in relation to the declines of the largest patch index from 24.6 in 1997 to 21.4 in 2017. The analysis shows also a relative increase in landscape shape index from 21.7 in 1997 to 30 in 2017, which is linked with the increasing number of patches accompanied with an increase into the perimeter and its shapes of the green areas. All these metrics indicate that the green area has fragmented, because of the urban development process. While the increase in heterogeneity of the urban landscape by an incremental rise has taken the urban sprawl pattern. This is obvious from the fragmentation index of urban area that has decreased from 1.0405 in 1997 to 1.0251 in 2017, and at the same time becoming more dominant. Hence, all these indices indicate that there is a decline in the green landscape heterogeneity and it has become more dispersion (Fig. 5 and Fig. 6). The

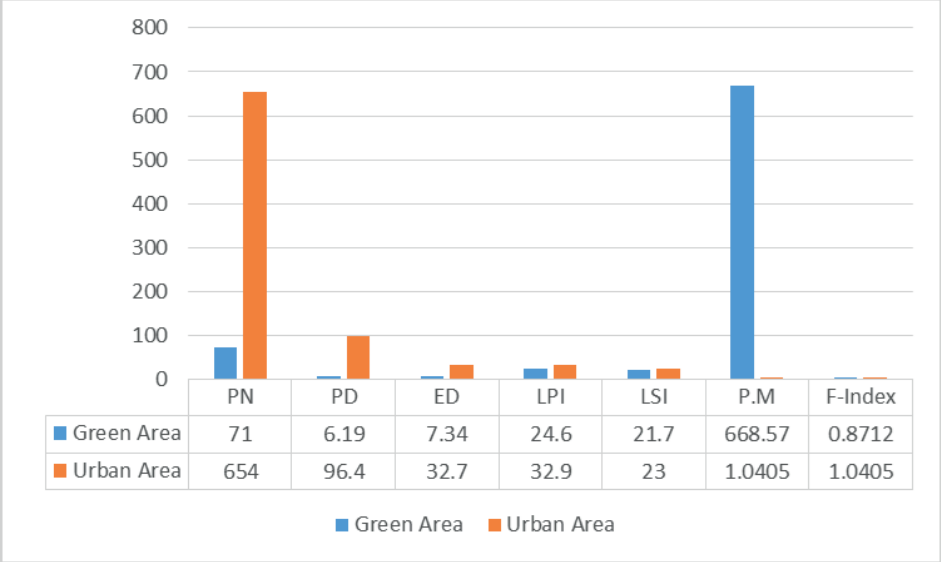

	PN	PD	ED	LPI	LSI	P.M	F-Index
Green Area	71	6.19	7.34	24.6	21.7	668.57	0.8712
Urban Area	654	96.4	32.7	32.9	23	1.0405	1.0405

Fig. 3. Spatial landscape analysis for 1997

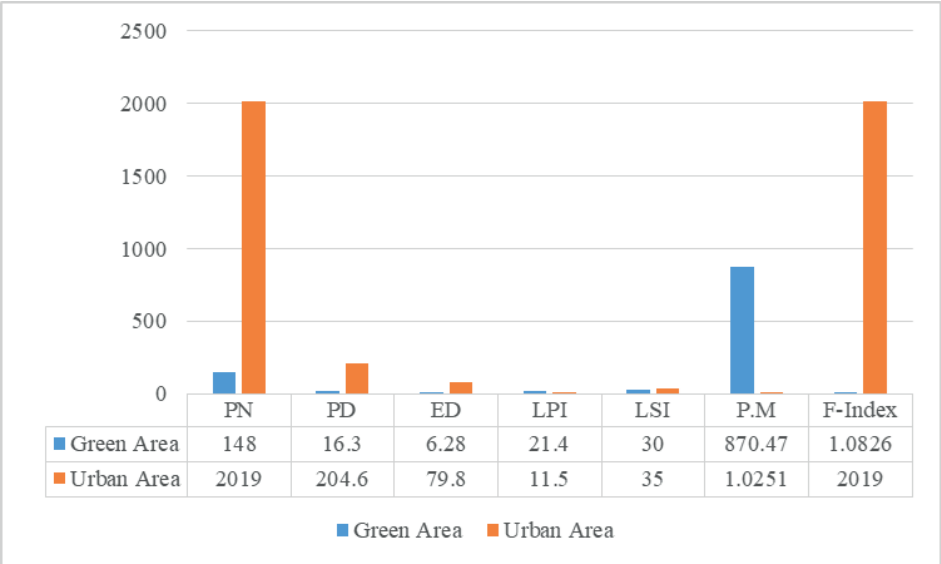

	PN	PD	ED	LPI	LSI	P.M	F-Index
Green Area	148	16.3	6.28	21.4	30	870.47	1.0826
Urban Area	2019	204.6	79.8	11.5	35	1.0251	2019

Fig. 4. Spatial Landscape Analysis for 2017

patch perimeter (area ratio) also increased from 668.57 to 870.47 in the same period 1997 and 2017. This increase is strongly correlated to an increase in landscape shape index of the green area that reached 30 in 2017, considering it as another indicator for the landscape fragmentation that is strongly related to the decline of green land, especially the agriculture/natural vegetation land with 112 percent increase, which can be attributed to dividing large patches into smaller ones. These indices asserted that the decrease of the green land was driven by high rate of urban development.

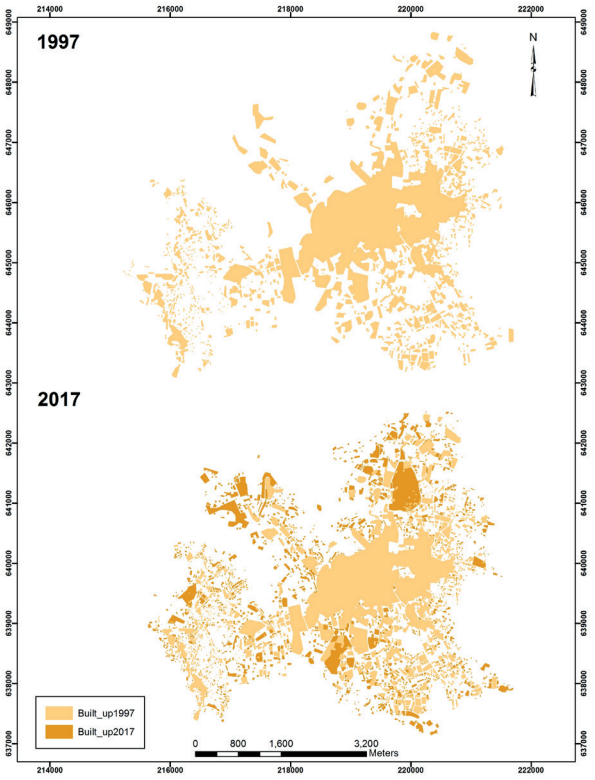

Fig. 5. Urban Area Distribution 1997-2017

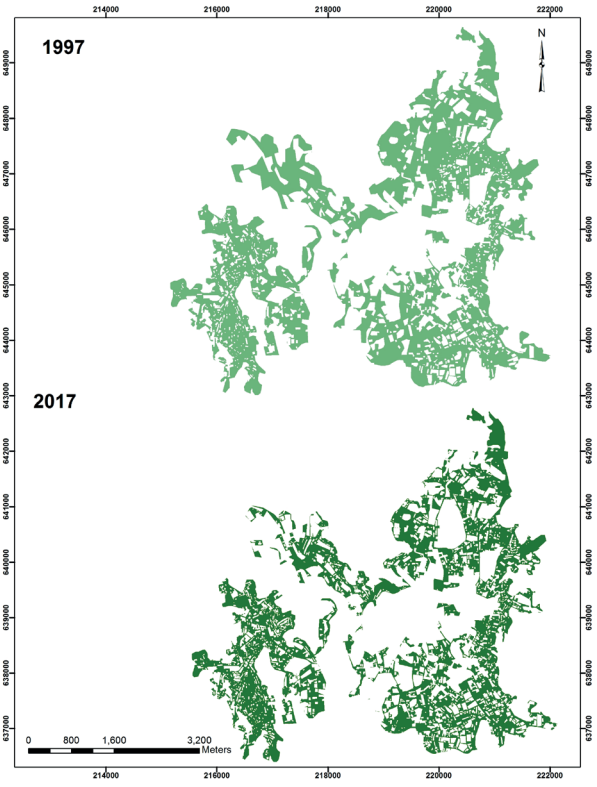

Fig. 6. Green Area Distribution 1997-2017

The analysis also showed that the patches density (PD) increased in the urban area from 96.4 in 1997 to 204.6 in 2017, this indicates that the landscape fragmentation is at a higher level. At the same time, there was an increase in PD for the green area from 6.19 in 1997 to 16.03 in 2017. In addition, the landscape Patch Index (LPI) was 32.9 in 1997, while 11.5 in 2017, and the landscape shape index (LSI) was 23 in 1997 and it increased to 35 in 2017. The main conclusion is that the combination of these analysis of indices (an increase in NP, PD and LSI, whereas a decrease in LPI) lead to a more fragmented landscape between 1997 and 2017, as well as smaller patches. While the increase in patches density indicates a more fragmented landscape Forman and Gordon (1981) Furthermore, the edge density ED is also related to the patch area; it was recorded 32.7 in 1997 and increased to 79.8 in 2017 for urban area. This increase in ED strongly supported the assumption of the fragmentation of landscape. As a result of this landscape fragmentation, the landscape fragmentation index affirmed increased from 1.0498 in 1997 to 1.0554 in 2017 (Fig. 7).

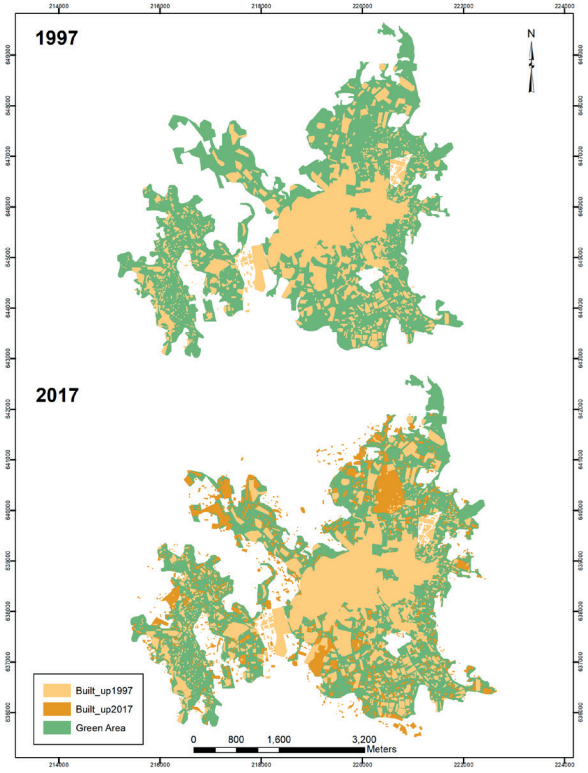

Fig. 7. Land-use Distribution during 1997 and 2017

Acceleration of urban expansion is the main trend that led to the dominance of urban landscape. Due to the increase of the number of edges through increasing LSI to 23, the landscape became more complex. However, as mentioned previously, the current urban landscape is characterized by urban sprawl pattern and leapfrog pattern towards the fringes, more dispersed alongside the transportation arteries, surrounding the core (centre) area and in adjacent rural areas.

Moreover, the landscape fragmentation has affected adversely the environment of the study area. For example, the abandonment of agricultural land, especially in sloppy areas, has increased the risk of soil erosion, which is evident from field visits. This resulted in a decrease in soil fertility that affected the natural vegetation, where some plants have either disappeared or decreased (i.e., Salvia officinalis, Thymus vulgaris, and Matricaria chamomile).

Generally speaking, the landscape of the study area has shown an increase in the urban land at the expense of a decrease in each class of green land, and the continuity and unity pattern of urban land-use indicates that this land-use has become dominant in the study area. Thus, rapid rate of urban development resulted in rapid rate of landscape fragmentation with associated decrease in the green area that was replaced with the urban surfaces.

Drivers of landscape Fragmentation

Agricultural and natural vegetation classes were more affected than other class. The surface area decreased from 755.5 hectare in 1997 to 604 hectare in 2017. The number of patches and fragmentation index are both divided into smaller units. This could refer to a number of drivers, which can be consider as key driver of landscape fragmentation: as following

Ramallah's strategic and unique geographical location, along with its closeness to Jerusalem, were among the strongest reasons for choosing Ramallah to be administrative and political centre for the Palestinian Authority in the mid-1990s (Harker 2014). This is accompanied with the increasing rate of population due to returnees and inside immigration. The increase in population necessitated dramatic increase in the number of residential dwellings that have been built the last 20 years. All of these changes have confronted unduly with the available land.

The rise of population was a primary driver of land use change in this period. Statistics revealed, the population number of the Ramallah area was about 55,380 inhabitants in 1997 (PCBS 2011 (while it reached 200,000 inhabitants in 2017 (Municipalities statistics 2018). The rapid population increase followed a high demand on land to accommodate people created an increase of about 54 percent in the built-up area which occurred during the 1997 to 2017.

Furthermore, the political conditions are an important driver that reshaped the landscape of the study area through restrictions to different lands that is being exerted by the Israelis, resulting in either accelerating or decelerating the changes in landscape. The analysis revealed that there are two colonies adjacent to the study area on northeast direction, a military base on south-west direction and the separation wall on south-west and south direction. These political restrictions enhanced building in certain direction and prevented in other directions, hence, created a densely urban area in certain directions more than others at the expense of agricultural lands.

One the main driver of Ramallah's urban development came from the 1993 peace prosses of Oslo. The Oslo Accord allowed Palestinian members of the PLO (Palestinian Liberation Movement), who were exiled, to return to Palestine and allowed them authority over the West Bank and Gaza Strip. The Palestinian Authority choose Ramallah as the core center amongst the other cities of the West Bank that let it grow.

The urbanization rate in the city increased from 37.3% in 1950, to more than 60% in 2005. Studies also had shown that Ramallah area had 32% of the total governorate population resided. Ramallah has become a very crowded due to the large increase and its limited area. The city is a main urbanized and political center in Palestine as well as having the first highest rate of internal migration, which makes it geographically, economically and centralized important in the West Bank (MAS 2008).

This rapid suburb expansion appeared between 1993 and 2015, and it is known as the boom years. More than other directions in the city, the northwest has seen the most growth. Furthermore, the population of Ramallah area has soared due to the urban-urban and rural-urban internal migration. Some of the benefits of this rapid growth was for land traders and to the real estate sector, not to forget profitable and rapid income all in which accelerated the pace of the urban development process.

The Oslo Accord had stated that the Palestinian areas are to be divided into three geopolitical areas (A, B and C). Ramallah area is divided under area 'A', which gives full control by Palestinian Authority.

However, the restrictions that are imposed by the Israelis in area 'C' (the Israeli have full control, which is 60% of the total land of the West Bank) have significant consequences for both areas 'A' and 'B' where over 90% of the Palestinians reside (The World Bank 2013), also according to the World Bank report; the Palestinian side has a scarcity on land affordability to meet the urban growing need due to the prevention of urban expansion into area 'C' that ended with further strain on land in area 'A' and 'B'.

Furthermore, the political conditions are an important driver that reshaped the landscape of the study area through restrictions to different lands that is being exerted by the Israelis, resulting in either accelerating or decelerating the changes in landscape. The analysis revealed that there are two colonies adjacent to the study area on northeast direction, a military base on south-west direction and the separation wall on south-west and south direction. These political restrictions enhanced building in certain direction and prevented in other directions, hence, created a densely urban area in certain directions more than others at the expense of agricultural lands.

Moreover, due to the lack of awareness of the rapid process of urbanization in the West Bank generally and in the study area particularity, adding the absence of legislations or its implementation, landscape fragmentation had noticeably increased.

CONCLUSIONS

This study represents a process of utilizing Fragstat method to measure the land-use changes, from green areas to urban aggregate, which caused landscape fragmentation. This work was achieved by comparing between two aerial photos during the periods between 1997 and 2017. The visual interpretation of aerial photos found that different agricultural land-use has decreased as a green area, against the increase in the urban land-use. During 1997 and 2017, the spatial statistical analysis indicates that the area has fragmented even more.

In the case of the Ramallah area, the observed pattern became the white stone landscape. The geopolitical factor after 1993 followed by high rate of cadastral investments may have provided the main factors for urban development of the study area, thus fragmented the landscape.

However, the process of urban development (Urbanization) was associated with the decrease of general vegetation cover. This finding asserted that the urban development affects adversely on the vegetation cover during 1997 and 2017, at an unpresented scale and more than ever.

It is concluded that there has been a considerable landscape fragmentation by land-use changes. Due to different factors, as well as, the most important population growth, that have posed many challenges at the scale of land-use management and planning, proper planning might have helped to limit the agricultural land decrease.

REFERENCES

Baker W.L. (1989). A review of models in landscape change, Landscape Ecology, 2, 111-133.

Bimlom (2014). Trapped by Planning: Isreali Policy, Planning and Development in the Palestinian Neighborhoods of East Jerusalem. Planners for Planning Rights, 13 Ibn Ezra St. Jerusalem.

B'Tselm (2013). Acting the Landlord: Israel's Policy in Area C, the West Bank. ISBN 978-965-7613-05-4.

Batty M., Xie Y. and Sun Z. (1999). Modeling urban dynamics through GIS-based cellular automata. Computers, Environment and Urban Systems, 23, 205-233.

Cheng J. and Masser I., (2003). Urban growth modeling: a case study of Wuhan city, PR

China. Landscape and Urban Planning, 62, 199-217.

Davidson C. (2006). Issues in Measuring Landscape Fragmentation. Wildlife Society Bulletin, 26(1), 27-32.

Flowers B., Huang K.T. and Aldana G.O. (2020). Analysis of the Habitat Fragmentation of Ecosystem in Belize Using Landscape Metrics. Sustainability, 3024, DOI: 10/3390/su12073024.

Forman R.T.T. and Godron, M. (1981). Patches and structural components for a landscape ecology. BioScience, 31, 733–740.

Hammad A., Ahmad and Sharkas, Othman (2008). Urban Encroachment on Agricultural land: Factors and Causes in Ramallah suburbs area as a case study, Edition Presses Department of Geography, Birzeit University, Palestine.

Harker C. (2014). The Only Way Is Up? Ordinary Topologies of Ramallah, International Journal of Urban and Regional Research, 38(1), 318-335.

Helu M.A. (2012). Urban Sprawl in Palestinian Occupied Territories Causes, Consequences and Future. Environment and Urbanization ASIA, 3(8), 121-141.

Hilal J. and El-Sakka (2015). A reading on the socio Urban Changes in Ramallah and Kufur Aqab. The Centre for Development Studies. Birzeit University.

Jaeger J. and Schwarz-v.Raumer H.-G. (2006). Time Series of Landscape Fragmentation Caused by Transportation Infrastructure and Urban Development: A Case Study from Baden-Wurttemberg, Germany. Ecology and Society 12(1).

Jaeger J., Schwarz-v.Raumer H.-G., Esswein H., Muller M. and Schmidt-Luttmann M. (2007). Time Series Landscape Fragmentation Caused by Transportation Infrastructure and Urban Development a Case Study from Baden-Wurttemberg, Germany. Ecology and Society, 12(1).

Keles S., Sivrikaya F., Cakir G. and Kose S (2008). Urbanization and forest cover change in regional directorate of Trabzon forestry from 1975 to 2000 using landsat data. Environmental Monitoring and Assessment, 140, 1-14.

Kong F., Nakagoshi N. (2006). Spatial-temporal gradient analysis of urban green spaces in Jinan, China. Landscape and Urban Planning, 78(3), 147-164.

Ledda A., Serra V. and Andrea de Montis (2019). The Effect of Rural Buildings on Landscape Fragmentation in Natura 2000 Sites: A case Study in Sardinia. Sustainability, 11(4695), DOI: 10.3390/su11174695.

Li X., Lu L., Cheng G, Xiao H. (2001). Quantifying landscape structure of the Heihe River Basin, north-west China using FRAGSTATS. Journal Arid Environment, 48, 521-535.

Luo T., Zhang T., Wang Z. Gan Y. (2015). Driving Forces of Landscape Fragmentation due to Urban Transportation Networks: Lessons from Fujian, china. Journal of Urban Planning and Development, DOI: 10.1061/(ASCE)UP.1943-5444.0000292.

Maitima J., Olson J.M., Mugatha S.M., Mugisha S. and Mutie I.T. (2010). Journal of Sustainable Development in Africa, 12(3), ISSN: 1520-5509.

Mulu D. (2016). A Review on the Effect of Habitat Fragmentation on Ecosystem. Journal of Natural Science Research, 6(15), ISSN 2225-0921.

Muhsen M., Hammad A. (2017). Urban Expansion Effects on Landscape Pattern: The case of Ramallah area. The International Journal of the Environment and Water, 6(2), ISSN: 2052-3408.

Nazer S., Abughannam R. and Khasib S. (2018). Landscape change in Ramallah-Palestine (1994-2014). Landscape Research, DOI: 10.1080/01426397.2018.1495184.

Noubani A. (2010). Dynamics of land-Use and Land-Cover: The Case of the Palestinian West Bank. Unpublished PhD Thesis. University of Washington.

Palestinian Central Bureau of Statistics (2011). Ramallah and Al Bireh Governorate Statistical Yearbook, (3), Ramallah, Palestine.

Palestinian Central Bureau of Statistics (2015). Data and Projections. Ramallah, Palestine.

Palestinian Central Bureau of Statistics (2019). Population, Housing and Establishments Census 2017: Census Final Results-Summary-Ramallah and Al-Bireh Governorate. Ramallah, Palestine.

Raddad S. (2015). Assessing land use/cover changes under political transition using remote sensing and Geographic Information Systems. International Journal of Environment. Society and Space, 3(1), 57-68.

Raddad S. and Samat N. (2016). Urban development and expansion trends under the political instability in Palestine: Jerusalem-Ramallah case study. International Journal of Development Research, 06(08), 8940-8947.

Rassem K. (2006). Planning and development a new Palestinian urban core under conditional Israeli Occupation: Ramallah City, 42nd IsoCaRP Congress.

Riitters K.H., Neill R.V., Hunsaker C.T., Wickham J.D., Yankee D.H., Timmins S.P., Johns K.B., Jackson B.L. (1995). A factor analysis of landscape pattern and structure metrics. Landscape ecology, 23-39.

Salah Al-H. and Sauder R. (2009). Buildings Destruction: The consequences of Rising Urbanization on Cultural Heritage in the Ramallah Province. International Journal of Cultural Property, 16(01), 1-23.

Samsuri S., Surati J.I.N., Kusmana C., Murtilaksono K. (2014). Analysis of Tropical Forest Landscape Fragmentation in Batang Toru Watershed, North Sumatra. JMHT, XX(2), 77-85, DOI: 10.7226/jtfm.20.2.77.

Shaheen L. (2013). Rapid Urbanization and the challenges of Sustainable Urban Development in Palestinian Cities. International Journal of Social, Behavioral, Educational, Business and Industrial Engineering, 7(3), 643-649.

Southworth J., Munore D. and Nagendra H. (2004). Land cover change and landscape fragmentation-comparing the utility of continuous and discrete analyses for a Western Honduras region. Agriculture. Ecosystem and Environment, 101, 185-205.

Taraki L. (2008). Enclave Micropolis: The Paradoxical Case of Ramallah/Al-Bireh. Journal Palestinian Studies, 37(4), 6-20.

Taraki L. (2006). Living in Palestine, Family survival, Resistance, and Mobility under Occupation. Syracuse University Press, New York.

Tomlin C. D. (1990). Geographic Information System and Cartographic Modeling. Prentice-Hall, Englewood Cliffs New Jersey.

UN-Habitat (2015). Right to Develop: Planning Palestinian Communities in East Jerusalem. United Nation Human Settlements Programme. East Jerusalem.

Weng Y.C. (2007). Spatiotemporal Changes of Landscape Pattern in Response to Urbanization. Landscape and Urban Planning, 8(4), 341-353.

Zambrano L., Aronson M., Fernadez T. (2019). The consequences of Landscape Fragmentation on Socio-Ecological Pattern in a Rapidly Developing Urban Areas: A Case Study of the national Autonomous University of Mexico. Frontiers in Environmental Science, DOI: 10.3389/fenvs.2019.00152.

Zhao X., Wen X., Chen S., Ding J., Zhang Y. (2020). Quantifying Land Use/Land Cover and Landscape Pattern Changes and Impacts on Ecosystem Services. International Journal of Environmental Research and Public Health, 17(1), 126, DOI: 10.3390/ijerph17010126.

RESEARCH PAPER

CENDERAWASIH HOT POOL: THE FREQUENT HIGH SEA SURFACE TEMPERATURE PHENOMENA AT CENDERAWASIH BAY, PAPUA

Abd. Rasyid Jalil[1*], Anindya Wirasatriya[2,3], Abdul Malik[4], Fatwa Ramdani[5,6], Puji Rahmadi[7], Gentio Harsono[8,9], Riza Yuliratno Setiawan[10]

[1]Department of Marine Science, Faculty of Marine Science and Fisheries, Hasanuddin University, Makassar, Indonesia
[2]Department of Oceanography, Faculty of Fisheries and Marine Science, Diponegoro University, Indonesia
[3]Coastal and Ocean Remote Sensing Laboratory, Center for Coastal Rehabilitation and Disaster Mitigation Studies, Diponegoro University, Indonesia
[4]Department of Geography, Faculty of Mathematics and Natural Sciences, Universitas Negeri Makassar, Indonesia
[5]Department of International Public Policy, Faculty of Humanities and Social Sciences, University of Tsukuba, Tsukuba, Ibaraki, Japan
[6]Program in Economic and Public Policy, Graduate School of Humanities and Social Sciences, University of Tsukuba, Tsukuba, Ibaraki, Japan
[7]Research Center for Oceanography, National Research and Innovation Agency, Jakarta, Indonesia
[8]Faculty of Science and Defense Technology, Republic Indonesia Defense University, Bogor, Indonesia
[9]Hydro-Oceanography Service Center, Indonesian Navy
[10]Department of Fisheries, Faculty of Agriculture, Gadjah Mada University, Yogyakarta, Indonesia.
***Corresponding author:** abdulrasyid.fayufi@gmail.com
Received: October 30th, 2022 / Accepted: May 4th, 2023 / Published: July 1st, 2023
https://DOI-10.24057/2071-9388-2022-156

ABSTRACT. The term "warm pool" refers to a body of water with the characteristic of SST exceeding 28°C within a particular area and a relatively long period in an annual circle. However, there are regions with an annual mean SST measured above 30°C, and we classified them as hot pools because of the conditions of intense solar radiation and low wind speed. One of the Hot Pool spots was found in Indonesia, in Cenderawasih Bay. The present study examines the existence of the Cenderawasih Hot Pool using long-term observation of satellite SST data. In order to learn more about their mechanisms, we also analyzed surface wind, surface heat flux, and surface current data. The results show that SSTs in Cenderawasih Bay have a 50% chance of exceeding 30°C within the 13 years of study (2013-2015). Heat input comes from strong solar radiation, i.e., 50% of solar radiation is more than 200 W/m^2. The location is also dominated by low wind speed, i.e., 80% wind speed of lower than 4 m/s, which caused the low latent loss in Cenderawasih Bay. Cenderawasih Bay is fully separated from surface currents during the dry and wet seasons since the easterly subsurface water flow does not enter the bay. The absence of strong currents prevents the mixing process, maintaining the high temperature in the surface layer. Those processes are discovered and they serve as compelling evidence to support Cenderawasih Bay as one of the Hot Pool areas within the Indonesian seas.

KEYWORDS: global climate; sea surface temperature; Hot Pool spot; Cenderawasih Bay

CITATION: Jalil Abd. R., Wirasatriya A., Malik A., Ramdani F., Rahmadi P., Harsono G., Setiawan R. Y. (2023). Cenderawasih Hot Pool: The Frequent High Sea Surface Temperature Phenomena At Cenderawasih Bay, Papua. Geography, Environment, Sustainability, 2(16), 77-83
https://DOI-10.24057/2071-9388-2022-156

ACKNOWLEDGEMENTS: We thank the Program of Indonesia Collaborative Research run by Hasanuddin University and Diponegoro University, for financing this research, with the number of contracts: 1269/UN4.22/PT.01.03/2020 and 193.07/UN7.6.1/PP/2020.

Conflict of interests: The authors reported no potential conflict of interest.

INTRODUCTION

The western equatorial Pacific has a big impact on the climate. The Earth's circulation is specifically affected by the warm pool, an area with average sea surface temperatures (SST) exceeding 28°C (e.g., Wyrtki 1989; Yan et al. 1992; Clement and Seager 1999; Chongyin et al. 1999; Pierrehumbert 2000; Clement et al. 2005; Thoron et al. 2005; Herweijer et al. 2005).

On the other hand, high SST in tropical regions has attracted researchers to investigate the mechanisms since the formation of high SST requires a particular atmospheric process (e.g., Ramanathan and Collins 1991; Wallace 1992; Arking and Ziskin 1994). This process is depicted by (Waliser

and Graham 1993), which shows the relation between SSTs and deep convection. They utilized highly reflective cloud information from an arbitrary examination of monthly SST data with a grid spacing of 2º (produced from combined satellite observation and in situ data) and daily visible and infrared satellite image data. The highly reflective cloud increases along with the SST as it rises from 26ºC to 29.5ºC. In contrast, the highly reflective cloud diminishes with increased SST in the temperature from 29.5ºC to 32ºC. As a result, the analysis proved that several atmospheric processes impacted SSTs below and above 29.5°C.

By taking advantage of high temporal and spatial resolution SST products derived from satellite observations (i.e., daily and ≤ 25 km×25 km), several studies (Kawamura et al. 2008; Qin et al. 2007, 2008; Qin and Kawamura 2009, 2010; Wirasatriya et al. 2015, 2016, 2017a, 2020) were able to identify high SST events (i.e., more than 30°C) in specific areas and at certain periods and define them as Hot Event (HE). In summary, they concluded that considerable daily heat gains characterize the production of HE under high solar radiation and low wind speed brought on by "remote convection" mechanisms.

(Wirasatriya et al. 2015) elaborated on the climatology of HEs in the western equatorial Pacific using the SST dataset derived from satellite microwave sensors. Throughout nine years of observation (2003-2011), they discovered 71 HE cases in the western equatorial Pacific, with the majority centered on the Solomon Islands and New Guinea Island's northern coasts, which extend eastward up to 160∞W. According to the climatology, the region has solar radiation of more than 200 W/m^2 and wind speeds of less than 4 m/s. Low wind speeds heavily influence the mechanism for HE incidence in the western equatorial Pacific. Much of the equatorial region experiences sun radiation above 200 W/m^2 during the HE periods. Low wind speeds minimize latent heat loss, which results in high SSTs and HEs in specific locations. (Wirasatriya et al. 2015) also emphasized that high solar radiation and low wind speed are much more common during the development stage and less common during the decay stage. This study also demonstrated that a rise in the long-term mean SST in the western equatorial Pacific is correlated with an increase in the frequency of HE events. HEs were responsible for 51.5% of the SSTs >30°C in the warm pool region bounded by the 29.5 °C isotherms of the climatological SST. Thus, statistically, there is a relation between the occurrence of HE and the formation of the western Pacific warm pool. Moreover, (Wirasatriya et al. 2020) demonstrated the role of HE in maintaining the warm mixed layer in the western Pacific warm pool. The frequent occurrence of HE transports heat from the surface layer to the deeper layer above the thermocline to maintain the warm mixed layer in the warm pool. Since the Pacific warm pool influences the global climate's variability through coupled ocean-atmosphere dynamics and thermodynamics (e.g., Clement and Seager 1999; Herweijer et al. 2005), this becomes an example of the contribution of high SST phenomena to regulate the global climate.

Within the Indonesian seas, the frequent appearance of high SST > 30°C has been reported by (Tita et al. 2020) in Tomini Bay and by (Swandiko et al. 2021) in the Malacca Strait. Their appearances also the high solar radiation and weak wind. The morphology of the semi-enclosed waters causes the high-frequency occurrence of low wind speed by less than 4 m/s in both areas. Besides these two areas, there is no more study on the high SST phenomena within the Indonesian Seas.

The present study demonstrates the frequent high SST occurrence (more than 30°C) in Cenderawasih Bay. Cenderawasih Bay is in northern Papua Island, part of the western Pacific warm pool. It is semi-enclosed water with a deep basin, surrounded by mountain chains (Fig. 1). Cenderawasih Bay is the habitat for whale sharks (Ihsan et al. 2018). Since the area determines warm pool definition with SST climatology higher than 28°C, we call the high-frequency occurrence of SSTs higher than 30°C in the Cenderawasih Bay the Cenderawasih Hot Pool. (Wirasatriya et al. 2015) found that the duration of HE occurrence in the western equatorial Pacific is no longer than two months since HE requires a typical condition of high solar radiation and low wind speed. Thus, it is interesting to understand the mechanisms of the high-frequency occurrence of high SST in the Cenderawasih Hot Pool.

MATERIALS AND METHODS

We used the semi-daily 11 µm SST products from Moderate Resolution Imaging Spectroradiometer (MODIS) Aqua Lv3 with a spatial resolution of 0.04º×0.04º (Esaias

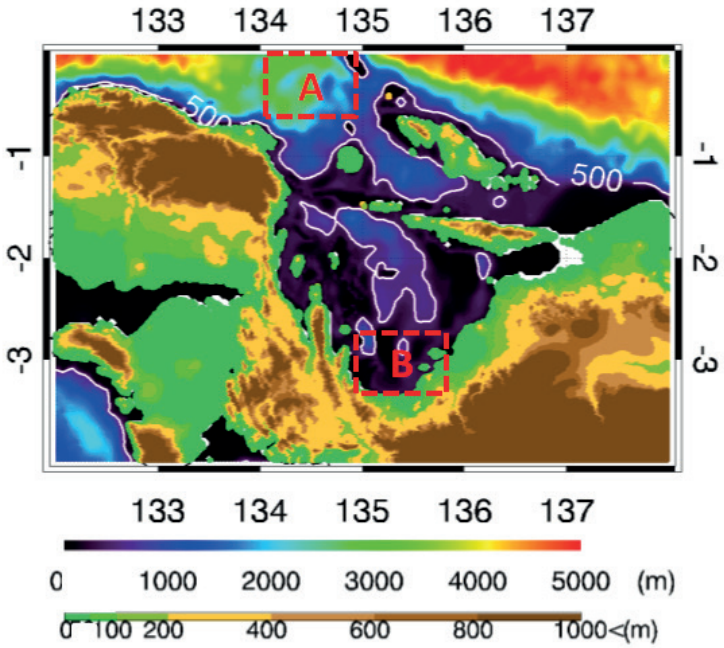

Fig. 1. Bathymetry and topography of Cenderawasih Bay. The dashed boxes A and B represent the sampling area for outside and inside Cenderawasih Bay, respectively, as shown in Fig. 5

et al. 1998) and observation period from 2003 to 2015. The MODIS SST 11 μm the Multi-Channel SST algorithm generates m by using brightness temperatures at 11 μm and 12 μm (Brown and Minnet 2009). The best accuracy was achieved by validating and testing this data against in-situ measurements (e.g., Lee et al. 2010; Qin et al. 2014; Ghanea et al. 2015).

We can obtain the Cross-Calibrated Multi-Platform (CCMP) gridded surface vector winds version 2.0 from the following website: www.remss.com, and use it to calculate surface winds. As a result, CCMP is regarded as a Level-3 ocean vector wind analysis product. They are created utilizing data from moored buoys, satellites, and model winds. The surface wind data for spatial and temporal resolutions is 0.25°×0.25° respectively and quarter daily. This wind product has greater accuracy than other wind reanalysis data.

We used a 0.5° grid from the Objectively Analyzed Air-Sea Fluxes project to analyze daily latent heat fluxes and solar radiation (Yu and Weller 2007). The period of observation for latent heat flux is from 2003 to 2015, but for solar radiation is only from 2003 to 2009 due to the availability of the data. Global 30 Arc-Second Elevation data was used to obtain topography. Global 30 Arc-Second Elevation (GTOPO30) data was used to obtain topography[1]. ETOPO, a one-arc-minute global relief model of Earth's surface that combines land topography and ocean bathymetry[2], provides bathymetry. For oceanic parameters, we used the current reanalysis data from http://marine.copernicus.eu/ to obtain the seasonal variation of the current pattern at 100 m depth in the Cenderawasih Hot Pool.

To calculate the frequency occurrence of SST within 13 years of observation, we calculate the percentage of SST > 30°C occurrence in each grid. Since high SST of more than 30°C occurs during the condition of low wind speed (i.e., < 4 m/s) and high solar radiation (i.e., > 200 W/m^2) (Wirasatriya et al. 2015), we calculated the percentage of low wind speed and high solar radiation in the Cenderawasih Bay. Furthermore, we also calculated the percentage of low latent heat release (<120 W/m^2) to explain how wind speed influences the variability of SST. The equation for calculating the percentage is as follows:

$$\%\,(x,y) = \frac{1}{n}\sum_{i=1}^{n} pi\,(x,y) \times 100\,\% \qquad (1)$$

where *%(x,y)* is percentage the percentage of high SST > 30°C or percentage of weak wind speed < 4 m/s or percentage of solar radiation > 200 W/m^2 or percentage of latent heat flux < 120W/m^2 at position (x,y); p*i* is the amount of SST data > 30°C or the amount of weak wind speed < 4 m/sec or the amount solar radiation > 200 W/m2 or the amount of latent heat flux < 120W/m^2 at position (x,y). Furthermore, we also analyze the climatological mean of each parameter. To create monthly and monthly climatology, all geophysical parameters are incorporated as follows (Wirasatriya et al. 2017b):

$$\overline{X}\,(x,y) = \frac{1}{n}\sum_{i=1}^{n} xi\,(x,y,t) \qquad (2)$$

where $\overline{X}$ is monthly mean value or monthly climatology value at position (x,y), is ith value of the data at (x,y) position and time t. Next, n is the number of data in 1 month and the number of monthly data in 1 period of climatology (i.e., from 2003 to 2016 = 13 data) for monthly calculation and monthly climatology calculation, respectively. Moreover, if pixel xi is a hollow pixel, it is not included in the calculation.

RESULTS AND DISCUSSION

Cenderawasih Hot Pool

The definition of the Cenderawasih Hot Pool is described in Fig. 2, which shows the climatological mean of SST and the percentage of daily SSTs more than 30°C from 2003 to 2015 (13 years). In Cenderawasih Bay, the mean SST at the southern part of 2°S is more than 30°C, and the high SSTs are more than 50%. It means that the mean SST in Cenderawasih Bay is higher than the definition of the western Pacific warm pool which is 28°C (Wyrtki 1989), and more than 3.5 years within 2003-2015, SSTs in Cenderawasih Bay can reach more than 30°C. At the southernmost of the bay, the mean SST reaches 30.5°C, with the percentage of high SSTs being more than 70%. It has become the hottest area of Cenderawasih Bay.

In contrast, in the area outside Cenderawasih Bay, i.e., the western Pacific warm pool's offshore seas, the percentage is less than 30%. Thus, this evidence supports the definition of Cenderawasih Bay as the Cenderawasih Hot Pool. The high-frequency occurrence of high SST in Cenderawasih Bay may correspond to whale sharks' yearly appearance. (Ihsan et al. 2018) indicated the tolerance of whale sharks in high SST conditions.

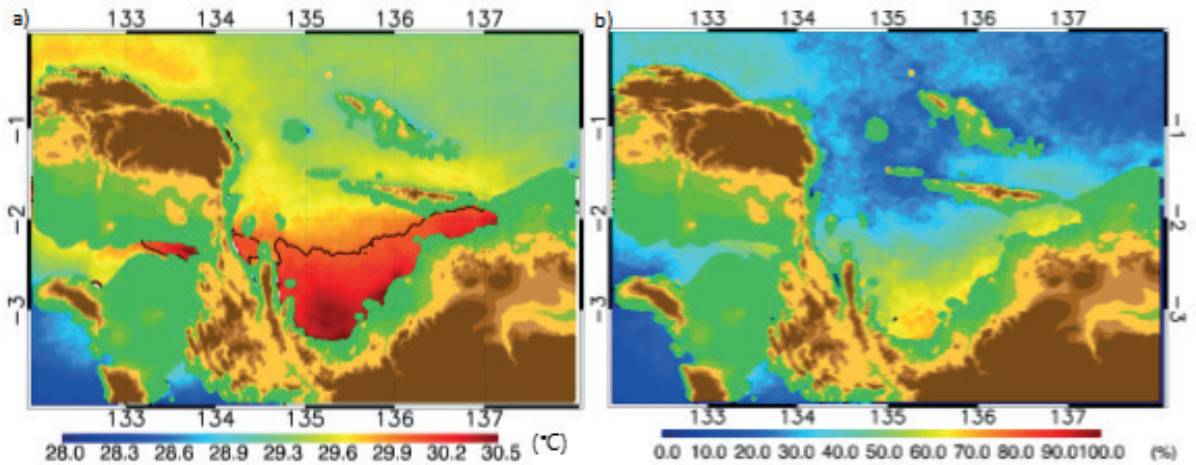

Fig. 2. Climatological mean of SST (a) and percentage of daily SSTs > 30°C during thirteen years of observation (2003-2015) (b). The black contour is 30°C

[1]https://www.usgs.gov/centers/eros/science/usgs-eros-archive-digital-elevation-global-30-arc-second-elevation-gtopo30?qt-science_center_objects=0#qt-science_center_objects

[2] https://www.ngdc.noaa.gov/mgg/global/

Atmospheric Aspect of Cenderawasih Hot Pool

Fig. 3 clearly shows that low wind speed dominates Cenderawasih Bay, i.e., 80% wind speed < 4 m/s occurred during 2003-2015. This causes low latent loss in Cenderawasih Bay. For solar radiation, the percentage of high solar radiation inside and outside Cenderawasih Bay is almost similar i.e., nearly 50%, indicating that high solar radiation is not dominant in both areas. This means that, although high solar radiation does not frequently occur, the absence of strong wind speed may maintain the latent heat loss to keep the SST in Cenderawasih Bay higher than 30°C.

To investigate how low wind speed occurs in the study area, we show the monthly climatology map of surface wind during summer and winter (Fig. 4). For both seasons, Cenderawasih Bay is protected from high wind speed due to high mountain chains in the western, southern, and eastern parts. In the northern part, small islands at the mouth of the bay prevent the strong wind speed from entering the bay. Thus, the role of topography is crucial for the occurrence of constant high SSTs in Cenderawasih Bay. The same tendencies are also found at the Tomini Bay and Malacca Strait, as indicated by (Tita et al. 2020) and (Swandiko et al. 2021).

The influence of wind speed and solar radiation on the SST variation is further examined by plotting the monthly climatology of wind speed, solar radiation, and SST at areas A and B (Fig. 1), representing the areas outside and inside Cenderawasih Bay. Seasonal variations of SSTs are observed in both areas. The minimum SSTs occur during the wet and dry seasons, while the maximum SSTs during the transition season. This seasonal SST variability is similar to the other areas in the Indonesian seas, such as the Java Sea (Wirasatriya et al. 2018), Maluku Sea (Wirasatriya et al. 2019), Halmahera Sea (Setiawan et al. 2019), etc.

For the area outside Cenderawasih Bay, SST ranges from 28.2°C to 30.6°C. It is seen that the variability of SST is controlled by wind speed and solar radiation. From January to June, when wind speed decreases from 2.2 m/s to 0.3 m/s and solar radiation is more than 200 W/m2, SST increases from 28.2°C to 30.5°C. From June to October, wind speed is lower than 1 m/s. In the absence of strong wind, the low SST in July is caused by the decrease of solar radiation to a minimum.

For the area inside Cenderawasih Bay, persistent high SST is observed as the SST ranges from 30.2°C to 31.1°C. It may be due to the low wind speed of fewer than 1 m/s for years. Thus, the variability of SST is seen as ruled by solar radiation. The minimum solar radiation causes the minimum SST in July. However, the absence of strong wind prevents latent heat loss that maintains the high SST inside Cenderawasih Bay.

The oceanic aspect of Cenderawasih Hot Pool

To investigate the oceanic aspect of the Cenderawasih Hot Pool, we plotted the current patterns at 100 m depth shown in Fig. 6. A northwestward current has been identified north of Cenderawasih Bay. During the wet season (January), the speed of this current ranges from 0.5 m/s to 0.7 m/s. During the dry season (August), when the northwesterly wind disappears (Fig. 4b), the speed of the northwestward current increases. This northwestward current is known as the New Guinea Coastal Under Current (NGCUC). NGCUC is a permanent current feature at 200 m depth regardless of the wind reversals (Tsuchiya et al. 1989). Inside Cenderawasih Bay, strong currents are absent in this area, preventing the mixing process from maintaining the high temperature in the surface layer. During the dry and wet seasons, Cenderawasih Bay is fully isolated since the westward subsurface water flow does not enter Cenderawasih Bay. Thus, this isolated basin causes the Cenderawasih Bay area to be influenced mainly by the air-sea interaction process mentioned in the previous section creating Cenderawasih Hot Pool.

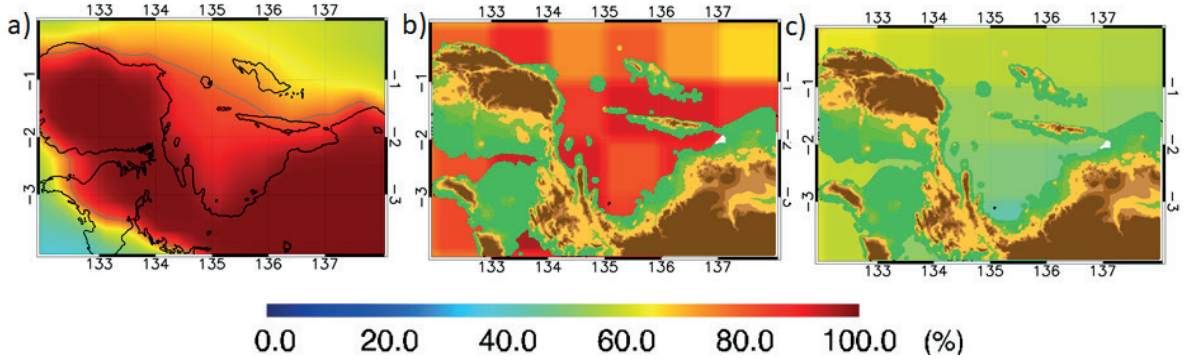

Fig. 3. The percentage of wind speed less than four m/s (a), latent heat release less than 120 W/m² (b), and solar radiation more than 200 W/m² (c)

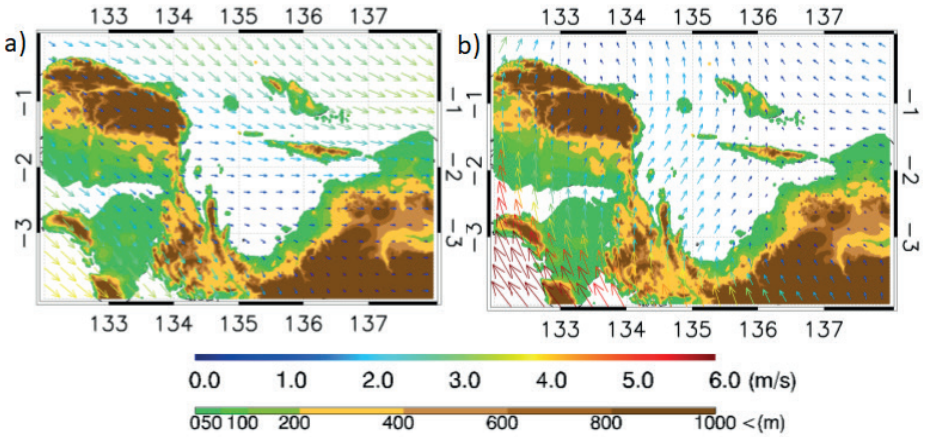

Fig. 4. Monthly climatology of surface wind speed during a) wet season (January) and b) dry season (August)

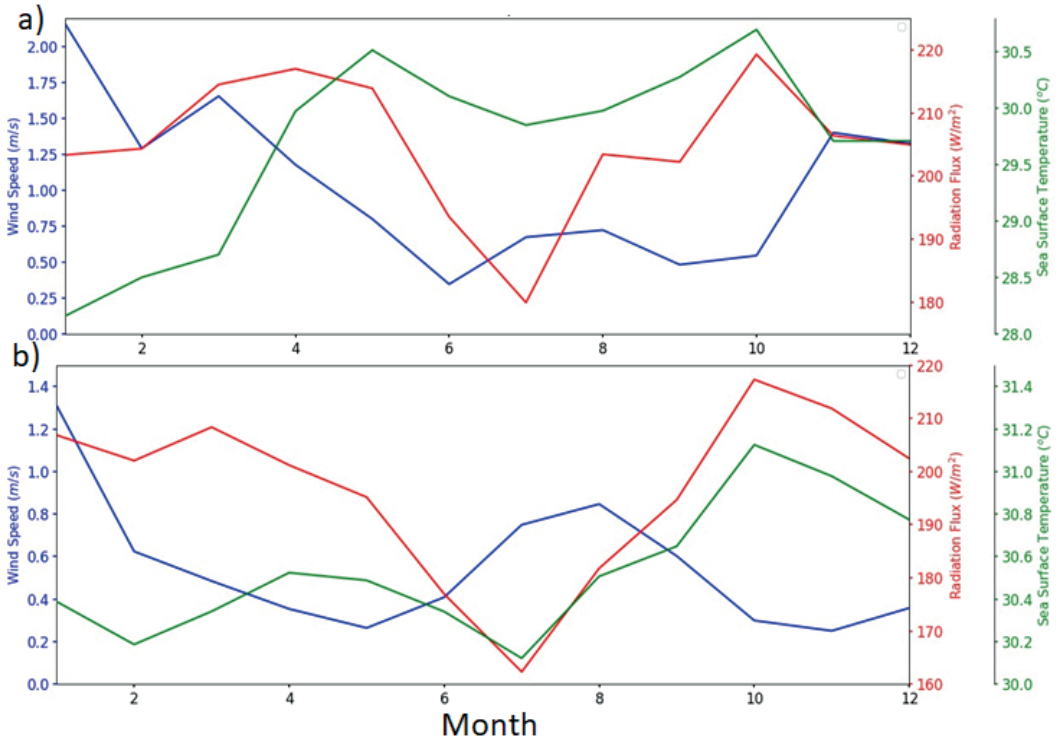

Fig. 5. Monthly climatology of SST, wind speed, and solar radiation at a) area outside and b) area inside Cenderawasih Bay, as shown in Fig. 1

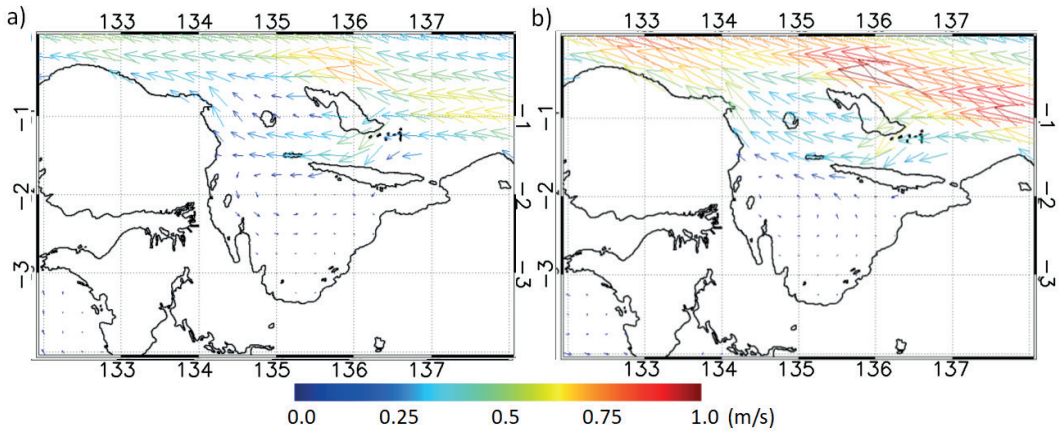

Fig. 6. Monthly climatology of current at 100 m depth in January (a) and August (b)

CONCLUSIONS

The hot Pool is used to categorize high SST episodes (>30°C) in particular areas and during specific periods (relatively long periods). Since the term "warm pool" has been used to define an area with the annual average SST distributed below 30°C in dominant, therefore "hot pool" was taken to represent the area with SST dominated above 30°C.

Under high solar radiation and low wind speed, this event is characterized by considerable daily heat gains. The constant high SST occurrence in Cenderawasih Bay, which is more than 50% of 13 years, SSTs can reach more than 30°C and are dominated by the condition of low wind speed, i.e., 80% wind speed is less than m/s along the years, also 50% solar radiation measured is more than 200 W/m^2. The current pattern at 100 m depth also shows that NGCUC does not enter Cenderawasih Bay. Thus, this indicates that Cenderawasih Bay is an isolated water. Those are the solid evidence for defining Cenderawasih Bay as the "Cenderawasih Hot Pool."

REFERENCES

Arking A. and Ziskin D. (1994). Relationship between clouds and sea surface temperatures in the western tropical Pacific. Journal of Climate, 7(6), 988-1000, DOI: 10.1175/1520-0442(1994)007%3C0988:RBCASS%3E2.0.CO;2.

Brown O.B. and Minnett P.J. (2009). MODIS infrared sea surface temperature algorithm theoretical basis document, ver 2.0, [online] Available at: https://modis.gsfc.nasa.gov/data/atbd/atbd_mod25.pdf [Accessed 25 October 2022].

Chongyin L., Mingquan M., and Guangqing Z. (1999). The variation of warm pool in the equatorial western Pacific and its impacts on climate. Advances in Atmospheric Sciences, 16(3), 378-394, DOI: 10.1007/s00376-999-0017-0.

Clement A. and Seager R. (1999). Climate and the tropical oceans. Journal of Climate, 12(12), 3383-3401, DOI: 10.1175/1520-0442(1999)012%3C3383:CATTO%3E 2.0.CO;2.

Clement A.C., Seager R., and Murtugudde R. (2005). Why are there tropical warm pools? Journal of Climate, 18(24), 5294-5311, DOI: 10.1175/JCLI3582.1.

Esaias W.E., Abbott M.R., Barton I., Brown O.B., Campbell J.W., Carder K.L., ... and Minnett P.J. (1998). An overview of MODIS capabilities for ocean science observations, IEEE Transactions on Geoscience and Remote Sensing, 36(4), 1250-1265, DOI: 10.1109/36.701076.

Ghanea M., Moradi M., Kabiri K., and Mehdinia A. (2015). Investigation and validation of MODIS SST in the northern Persian Gulf, Advances in Space Research, 57(1), 127-136, DOI: 10.1016/j.asr.2015.10.040.

Harweijer C., Seager R., Winton M., and Clement A.M.Y. (2005). Why ocean heat transport warms the global mean climate. Tellus, 57(4), 662-675, DOI: 10.3402/tellusa.v57i4.14708.

Hosoda K. (2013). Empirical method of diurnal correction for estimating sea surface temperature at dawn and noon. Journal of Oceanography, 69, 631-646, DOI: 10.1007/s10872-013-0194-4.

Ihsan E.N., Enita S.Y., and Wirasatriya, A. (2018). Oceanographic factors in fishing ground location of Anchovy at Teluk Cenderawasih National Park, West Papua: Are these factors have an effect of Whale Sharks appearance frequencies? In IOP Conference Series: Earth and Environmental Science, 116(1), 012-017, DOI: 10.1088/1755-1315/116/1/012017.

Kawamura H., Qin H., and Ando, K. (2008). In-situ diurnal sea surface temperature variations and near-surface thermal structure in the tropical hot event of the Indo-Pacific warm pool. Journal of Oceanography, 64, 847-857, DOI: 10.1007/s10872-008-0070-9.

Ming-An L., Tzeng M. T., Hosoda K., Sakaida F., Kawamura H., Shieh W. J., Yang Y., and Chang, Y. (2010). Validation of JAXA/MODIS sea surface temperature in water around Taiwan using the Terra and Aqua satellites. TAO: Terrestrial, Atmospheric and Oceanic Sciences, 21(4), 727-736, DOI: 10.3319/TAO.2009.09.07.01(Oc).

Pierrehumbert R.T. (2000). Climate change and the tropical Pacific: The sleeping dragon wakes. Proceedings of the National Academy of Sciences, 97(4), 1355-1358, DOI: 10.1073/pnas.97.4.1355.

Qin H., Kawamura H., and Kawai Y. (2007). Detection of Hot Event in the equatorial Indo-Pacific warm pool using advanced satellite sea surface temperature, solar radiation, and wind speed. Journal of Geophysical Research: Oceans, 112 (C7), DOI: 10.1029/2006JC003969.

Qin H., Kawamura H., Sakaida F., and Ando K. (2008). A case study of the tropical hot event in November 2006 (HE0611) using a geostationary meteorological satellite and the TAO/TRITON mooring array. Journal of Geophysical Research: Oceans, 113(C8), DOI: 10.1029/2007JC004640.

Qin H. and Kawamura H. (2009). Atmosphere response to a hot SST event in November 2006 as observed by AIRS instrument. Advances in space research, 44(3), 395-400, DOI: 10.1016/j.asr.2009.03.003.

Qin H. and Kawamura H. (2010). Air-sea interaction throughout the troposphere over a very high sea surface temperature. Geophysical research letters, 37(1), 1-4, DOI: 10.1029/2009GL041685.

Qin H., Chen G., Wang W., Wang D., and Zeng L. (2014). Validation and application of MODIS-derived SST in the South China Sea. International journal of remote sensing, 35(11-12), 4315-4328, DOI: 10.1080/01431161.2014.916439.

Ramanathan V. and Collins W. (1991). Thermodynamic regulation of ocean warming by cirrus clouds deduced from observations of the 1987 El Niño. Nature 351 (6321), 27-32, DOI: 10.1038/351027a0.

Setiawan R.Y., Wirasatriya A., Hernawan U., Leung S., and Iskandar I. (2020). Spatio-temporal variability of surface chlorophyll-a in the Halmahera Sea and its relation to ENSO and the Indian Ocean Dipole. International Journal of Remote Sensing, 41(1), 284-299, DOI: 10.1080/01431161.2019.1641244.

Swandiko M., Wirasatriya A., Marwoto J., Muslim, Indrayanti E., Subardjo P., Ismunarti D.H. (2021). Studi persistensi suhu permukaan laut tinggi (>30°C) di perairan Selat Malaka. Buletin Oseanografi Marina, 10(2), 162-170, [online] Available at: https://ejournal.undip.ac.id/index.php/buloma/article/download/31554/19352 [Accessed 25 October 2022] (in Indonesian).

De Garidel-Thoron T., Rosenthal Y., Bassinot F., and Beaufort L. (2005). Stable sea surface temperatures in the western Pacific warm pool over the past 1.75 million years. Nature, 433(7023), 294-298, DOI: 10.1038/nature03189.

Tita A.D.C., Wirasatriya A., Sugianto D.N., Maslukah L., Handoyo G., Helmi M., and Avianto P. (2020). Persistence of high sea surface temperature (> 30°C) in Tomini Bay. In IOP Conference Series: Earth and Environmental Science, 530(1), 012-038, DOI: 10.1088/1755-1315/530/1/012038.

Waliser D.E. and Graham N.E. (1993). Convective cloud systems and warm-pool sea-surface temperatures: Coupled interactions and self-regulation. Journal of Geophysical Research: Atmospheres, 98(D7), 12881-12893, DOI: 10.1029/93JD00872.

Wallace J.M. (1992). Effect of deep convection on the regulation of tropical sea surface temperature. Nature, 357(6375), 230-231, DOI: 10.1038/357230a0.

Wirasatriya A., Kawamura H., Shimada T., and Hosoda K. (2015). Climatology of hot events in the western equatorial Pacific. Journal of Oceanography, 71, 77-90, DOI: 10.1007/s10872-014-0263-3.

Wirasatriya A., Kawamura H., Shimada T., Hosoda K. (2016). Atmospheric structure favoring high sea surface temperatures in the western equatorial Pacific. Journal of Geophysical Research, 121(19), 11-368, DOI: 10.1002/2016JD025268.

Wirasatriya A., Sugianto D.N., and Helmi M. (2017). The Influence of Madden Julian Oscillation on the Formation of the hot event in the western equatorial pacific. In IOP Conference Series: Earth and Environmental Science, 55(1), 012-006, DOI: 10.1088/1755-1315/55/1/012006.

Wirasatriya A., Setiawan R.Y., and Subardjo P. (2017). The effect of ENSO on the variability of chlorophyll-a and sea surface temperature in the Maluku Sea, IEEE Journal of Selected Topics in Applied Earth Observations and Remote Sensing, 10(12), 5513-5518, DOI: 10.1109/JSTARS.2017.2745207.

Wirasatriya A., Prasetyawan I.B., Triyono C.D., Muslim, and Maslukah L. (2018). Effect of ENSO on the variability of SST and chlorophyll-a in Java Sea. In IOP Conference. Series: Earth and Environmental Science, 116(1), 012-063, DOI: 10.1088/1755-1315/116/1/012063.

Wirasatriya A., Sugianto D.N., Helmi M., Setiawan R.Y., and Koch M. (2019). Distinct characteristics of SST variabilities in the Sulawesi Sea and the northern part of the Maluku Sea during the southeast monsoon. IEEE Journal of Selected Topics in Applied Earth Observations and Remote Sensing, 12(6), 1763-1770, DOI: 10.1109/JSTARS. 2019.2913739.

Wirasatriya A., Kawamura H., Helmi M., Sugianto D.N., Shimada T., Hosoda K., Handoyo G., Putra Y.D.G., and Koch M. (2020). Thermal structure of Hot Events and their possible role in maintaining the warm isothermal layer in the Western Pacific warm pool. Ocean Dynamics, 70, 771–786, DOI: 10.1007/s10236-020-01362-8.

Wyrtki K. (1989). Some thoughts about the West Pacific warm pool. In Proceedings of the Western Pacific International Meeting and Workshop on TOGA COARE, Noumèa, New Caledonia: 99-109, [online] Available at: https://horizon.documentation.ird.fr/exl-doc/pleins_textes/doc34-08/30195.pdf#page=114 [Accessed 26 October 2022].

Yan X.H., Ho C.R., Zheng Q., and Klemas V. (1992). Temperature and size variabilities of the western Pacific warm pool. Science, 258 (5088), 1643-1645, DOI: 10.1126/science.258.5088.1643.

Yu L. and Weller R.A. (2007). Objectively Analyzed air-sea heat fluxes for the global ice-free oceans (1981–2005). Bulletin of the American Meteorological Society, 88(4), 527-540, DOI: 10.1175/BAMS-88-4-527.

RESEARCH PAPER

AEROPALYNOLOGICAL PROFILE OF CHEREPOVETS AND VOLOGDA, THE CITIES OF VOLOGDA REGION, NW RUSSIA

Alexandra Kamygina[1,2*], Yulia Tabunova[1], Natalia Afanasyeva[1,2], Nadezhda Poddubnaya[1]
[1]Cherepovets State University, Lunacharskogo av., 5, Cherepovets, 162600, Russia
[2]Lomonosov Moscow State University, Leninskiye Gory, 1, Moscow, 119991, Russia
***Corresponding author:** camygina@yandex.ru
Received: October 10th, 2022 / Accepted: May 4th, 2023 / Published: July 1st, 2023
https://DOI-10.24057/2071-9388-2022-140

ABSTRACT. The article presents data on the composition and seasonal dynamics of airborne pollen in Cherepovets and Vologda. The study was carried out from April 10 to September 30, 2014 and from April 16 to August 31, 2015 in Cherepovets, and from June 3 to September 30, 2019 in Vologda. Pollen data were obtained from the Durham gravimetric samplers. Samples were collected daily. Twenty-one types of pollen have been identified, ten of which are the most common allergenic types (*Alnus, Artemisia, Betula, Fraxinus, Salix, Plantago,* Poaceae, *Quercus, Rumex, Urtica*), which account for more than 50% of all pollen that has been registered. The article contains pollen calendars showing two peaks of pollen grain quantity: spring (from last decade of April to May), summer (from the end of June to the middle of July). *Betula* (30%) and Asteraceae (28%) pollen dominate in the pollen spectrum. *Pinus* (20%), *Plantago* (6%) and Poaceae (5%) also play an important role in the regional spectrum. The results show the presence of allergenic pollen from different taxa throughout the study. The proportion of damaged pollen grains is approximately 2%, which corresponds to the norm in natural population in normal condition. This data can become the basis for developing recommendations for reducing the level of pollinosis in the Vologda Region.

KEYWORDS: aerobiology, airborne pollen types, allergenic taxa, Vologda Region

CITATION: Kamygina A., Tabunova Y., Afanasyeva N., Poddubnaya N. (2023). Aeropalynological Profile Of Cherepovets And Vologda, The Cities Of Vologda Region, Nw Russia. Geography, Environment, Sustainability, 2(16), 84-92
https://DOI-10.24057/2071-9388-2022-140

ACKNOWLEDGEMENTS: The study was funded by Cherepovets State University. The work is done using equipment Regional shared services centre of Cherepovets State University.

Conflict of interests: The authors reported no potential conflict of interest.

INTRODUCTION

More than half of the world's population lives in urban ecosystems. These ecosystems differ from natural ones and are often characterized by rapid changes in parameters caused by both intentional and unintentional actions of people as well as by the management of ecosystem components in the interest of creating a comfortable life (Gil and Brumm 2014). Maintaining high air quality is an immense problem as the atmosphere contains many particles of various origins. Among them, pollen grains and plant fragments play a significant role. Spores of various plants, fungi, bacteria, etc. are also important components of aerial plankton. Many of them, primarily pollen grains of plants, have long been known as an etiological factor of pollinosis — a classic allergic disease associated with human intolerance to plant pollen antigens that can significantly affect the quality of life (Malygina et al. 2010; Piotrowska-Weryszko and Weryszko-Chmielewska 2015; Posevina 2011).

In recent years, the necessity for aeropalynological research has been growing due to the widespread increase in the number of diseases caused by aeroallergens. Currently, "allergy" is one of the main public health problems in the Russian Federation. According to the results of the research conducted by the NRC Institute of Immunology FMBA of Russia, 17.5% to 30% of the population suffers from various forms of allergic diseases (Allergy. Statistics in Russia 2017; Federal Clinical Guidelines… 2015). A distinctive feature of allergic diseases caused by pollen is their seasonal nature. The severity of symptoms in patients with pollinosis is directly proportional to the concentration of allergens in the atmosphere (Kruczek et al. 2015).

The pollen of many plants is a strong allergen in itself, but in many large cities its effect can be enhanced by the influence of polluting gases (nitrogen oxide, sulfur oxide, ozone, and others) and solid particles. Pollen grains can deform and their allergenic properties may increase (Wang et al. 2009; Namork et al. 2006; Guedes et al. 2009; Bryce at al. 2010; Sénéchal et al. 2015). Seasonal airborne pollen content maxima often coincide with an increased presence of non-biological particles in the atmosphere (Barck et al. 2002, 2005; Dziuba 2006; Hajkova et al. 2015; Nenasheva 2013; Puc et al. 2015).

In a study conducted in Poland, Puc and co-authors (2015) established a correlation between weather and air pollutants (for example, nitrogen oxides), giving a new understanding of the mechanisms of respiratory allergic diseases. Air pollution increases symptoms in people with pollen allergies. Evidently, in this case there is a

manifestation of the law of cumulative action of the factors of the Mitscherlich-Baule equation. Therefore, Puc and co-authors (2015) suggests simultaneous monitoring of the amount of pollen and air pollutants.

In general, the amount of pollen in the atmosphere, the dynamics, and the duration of pollen seasons are determined by many factors; therefore, long-term observations are required to obtain the information necessary for management, and data analysis should include various aspects. Long-term observations are also important for detecting phenological shifts in pollen seasons due to global climatic changes (Haselhorst et al. 2017; Van Vliet et al. 2002; Zhang et al. 2022).

In terms of the prevention and treatment of allergic diseases, pollen calendars prepared in a certain region are a valuable source of information for predicting the concentration and dynamics of pollen rain. Since effective advice for the prevention and treatment of pollinosis can only be based on local data, such calendars are particularly significant for a given area due to the variability of vegetation cover and weather conditions of the regions.

Currently, the monitoring of the aeropalynological situation is carried out on the territory of all continents. The key monitoring points with the highest concentration of volumetric traps include the majority of European countries, the United States of America, several South American countries, the southeastern territory of Australia, and the Japanese Islands (Worldwide Map of Pollen Monitoring Stations 2022). On the territory of Russia, similar observations are conducted in Moscow, Ryazan, Stavropol, Tyumen, St. Petersburg, Krasnodar, Yekaterinburg, and some other cities (ZAUM… 2022).

The purpose of the study was to obtain an aeropalynological calendar for the major cities of the Vologda Oblast — Cherepovets and Vologda — for the purpose of developing recommendations for reducing the level of pollinosis in the region.

MATERIALS AND METHODS

Study area

The research was carried out in the Vologda Region of the North-Western Federal District of European Russia (Fig. 1). The region is located in the boreal climate zone of the Eastern European taiga. Spruce and pine forests dominate the vegetation cover; in the southern part of the region, the share of broad-leaved trees is noticeable. The main tree species are spruce (41%), pine (24%), birch (28%), and aspen (6%) (Antipov et al. 1957; Vorobyov 2007). There are also larch, elm, alder, and arborescent willows. The duration of the growing season is 150 days (Report on the State… 2019; Skupinova 2007).

Vologda (59°13′26″ N, 39°53′02″ E, 120-130 m a.m.s.l.) is the administrative, transportation, industrial, and cultural center of the Vologda Region. Cherepovets (59°07′59″ N, 37°53′59″ E, 130-140 m a.m.s.l.) is the transportation, scientific, and industrial center of the region, in which the enterprises of ferrous metallurgy and chemical industry are the largest. The area of Cherepovets is 122 km^2 (Official website of the city of Cherepovets. Architecture 2022), the population is 309445 (Official website of the city of Cherepovets. Population of Cherepovets 2022). As of 2012, there were 500 hectares of green space in the city's residential area (Shvetsov 2012). The area of Vologda is 116 km^2, the population is 320566 (Official website of the Administration of the city of Vologda 2022). Green spaces cover an area of 413 hectares as of 2019 (Official website of the Administration of the city of Vologda. Decision of the Vologda City… 2022).

The level of atmospheric air pollution in Cherepovets during the study period was categorized as elevated, and in Vologda as low (Report on the State… 2016; Report on the State… 2019). The atmospheric pollution index is expressed in units (standard index — the average annual concentration of various pollutants divided by the maximum permissible concentration and reduced to the

Fig. 1. Study area (http://yandex.ru/maps/)

harmfulness of sulfur dioxide), which correspond to the level of atmospheric air contamination (Documents on the state… 2006).

The atmospheric pollution index was estimated at 9.9-3.9 units in 2014 and 4 units in 2015 in Cherepovets. In Vologda the atmospheric pollution index was estimated at 2.5 units in 2018. The index was determined by the concentrations of benzo[a]pyrene, formaldehyde, nitrogen dioxide, suspended solids, and ammonia. The volume of emissions of pollutants into the atmosphere from stationary sources in 2015 in Cherepovets reached 316.797 tones (Report on the State… 2016).

Meteorological data

The region is located in a zone of excessive humidification, where the annual amount of precipitation exceeds the evaporation rate. The average amount of precipitation is 588 mm per year, of which 171 mm falls during the cold period of the year (November-March), 417 mm falls during the warm period (April-October) (Vorobyov 2007). Western and southern winds at a speed of 3–5 m/s prevail (Report on the State… 2019; Skupinova 2007), characterized by a long cold, snowy winter, a short spring, a relatively short moderately warm humid summer, and a long and wet autumn (Skupinova 2007). The average temperature in January is -12.6 °C, the average temperature in July is 16.8 °C, the frost-free period is 116 days (Vorobyov 2007).

The aerobiological method

The study was conducted from April 10 to September 30, 2014 and from April 16 to August 31, 2015 in Cherepovets, and from June 3 to September 30, 2019 in Vologda.

To establish the taxonomic composition of pollen spectrum and its daily quantity, Durham gravimetric pollen samplers were used (Durham 1946), which were installed in the open roof space in the central districts of Cherepovets and Vologda at an altitude of about 15 m. Samples were collected daily. The collection of samples had started after the beginning of the growing season due to legal difficulties in accessing the roof.

The trapping surface in the pollen trap is a glass slide coated with a glycerin–gelatin mixture. The composition of the mixture and the method of preparation are based on standard methodological guidelines described in the work of N.R. Meyer-Melikyan and co-authors (1999). Determination and counting of pollen grains were carried out using a light microscope with a magnification of ×640 on the total area of the cover glass (3.24cm^2).

Fifteen pollen types dominating in pollen spectra and possessing strong allergenic properties were selected for the pollen calendar according to the list of the most important (allergenic or abundant) types (Meyer-Melikyan et al. 1999; Nilsson and Spieksma 1994). According to the recommendations (Nilsson and Spieksma 1994), the list was supplemented with other species whose pollen causes outbreaks of pollinosis in the study area. Taxa not found in the airborne spectrum of the locality were excluded. The current list for the region is presented in the Table 1.

Pollen calendars were created using 'AeRobiology' R package.

RESULTS

Results of aeropalynological monitoring of Cherepovets

As a result of the study conducted in 2014 and 2015, 21 pollen types were identified in the aeropalynological spectrum (*Acer, Alnus, Betula, Fraxinus, Picea, Pinus, Populus,* Rosaceae, *Quercus, Salix, Tilia, Ulmus, Artemisia,* Asteraceae, Chenopodiaceae, *Plantago,* Poaceae, *Rumex, Taraxacum* and Apiaceae, *Urtica* (Fig. 2).

Pollen of seven taxa of arboreal plants accounted for 75% of the total number of pollen grains found, and pollen of six

Table 1. Significant allergenic taxa for the Vologda Region (according to the recommendations (Nilsson and Spieksma 1994))

№	Recommended	Excluded	Relevant	Additional
1.	Alnus	—	—	Asteraceae
2.	Ambrosia	Ambrosia	—	Populus
3.	Artemisia	—	—	Rosaceae
4.	Betula	—	—	Salix
5.	Castanea	Castanea	—	Tilia
6.	Chenopodiaceae	—	—	Apiaceae
7.	Corylaceae	Corylaceae	—	—
8.	Cupressaceae	Cupressaceae	—	—
9.	Oleaceae	—	Fraxinus	—
10.	Pinaceae	—	Picea, Pinus	—
11.	Plantago	—	—	—
12.	Poaceae	—	—	—
13.	Quercus	—	—	—
14.	Rumex	—	—	—
15.	Urticaceae	—	—	—

taxa of herbaceous plants accounted for 25%. These taxa were the most dominant in the pollen rain.

In 2015, four more taxa appeared in the aeropalynological calendar: *Populus, Rumex, Quercus, Tilia* (Fig. 3).

Two peaks in quantity were determined in the calendars for both years. First peak occurred in spring (from the last ten days of April to May) due to the flowering of anemophilic arboreal and shrubby plants, and the second peak occurred in summer (from late June to early and mid-July) due to the flowering of herbaceous plants.

Alnus (~7%) and *Betula* (~41%) were the absolute dominants in the spring spectrum. The summer and autumn dominants were *Pinus* (~21%) among the trees and *Plantago* (~4%) among the herbaceous plants. Chenopodiaceae (~3%) and Poaceae (~3%) were also very significant in the summer-autumn spectrum.

The share of damaged grains (characterized by traces of physical destruction: in the form of ruptures and cracks on the shell, torn off wings of gymnosperm pollen, deformation of the body of pollen grains, etc.) in the aeropalynological spectrum was approximately 2%. The occurrence of such grains is approximately the same during the observation period.

Results of aeropalynological monitoring of Vologda

The study of the pollen rain in the atmosphere of Vologda conducted in 2019 showed that 21 types of pollen are found in the aeropalynological spectrum (*Acer, Alnus, Betula, Fraxinus, Picea, Pinus, Populus, Quercus, Salix, Tilia, Ulmus,* Rosaceae, *Artemisia, Plantago, Rumex, Typha, Urtica,* Asteraceae, Chenopodiaceae, Poaceae, Apiaceae). Single spores of *Lycopodium* were also found. However, the most significant taxa determined in the summer and autumn period were six taxa of arboreal plants (*Acer, Betula, Picea, Pinus, Populus, Tilia*), the pollen of which constitutes to approximately 30% of the total number of pollen grains recorded and eight taxa of herbaceous plants (*Artemisia*, Asteraceae, Chenopodiaceae, *Plantago*, Poaceae, *Rumex*, Apiaceae, *Urtica*), the pollen of which constitutes to approximately 70%. These taxa were included in the pollen calendar (Fig. 4).

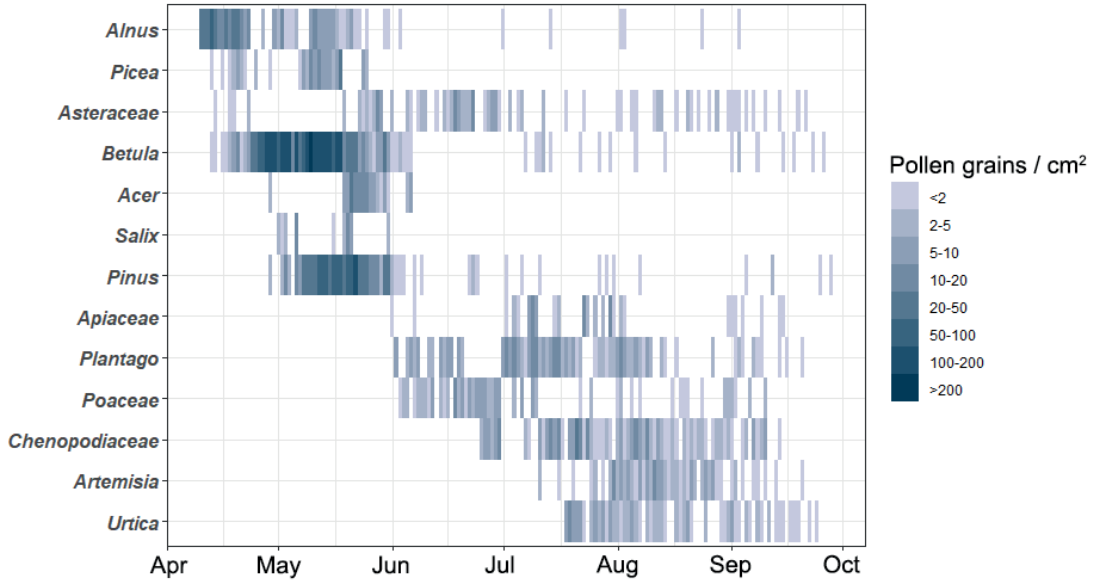

Fig. 2. Pollen calendar of Cherepovets's aeropalynological spectrum in 2014

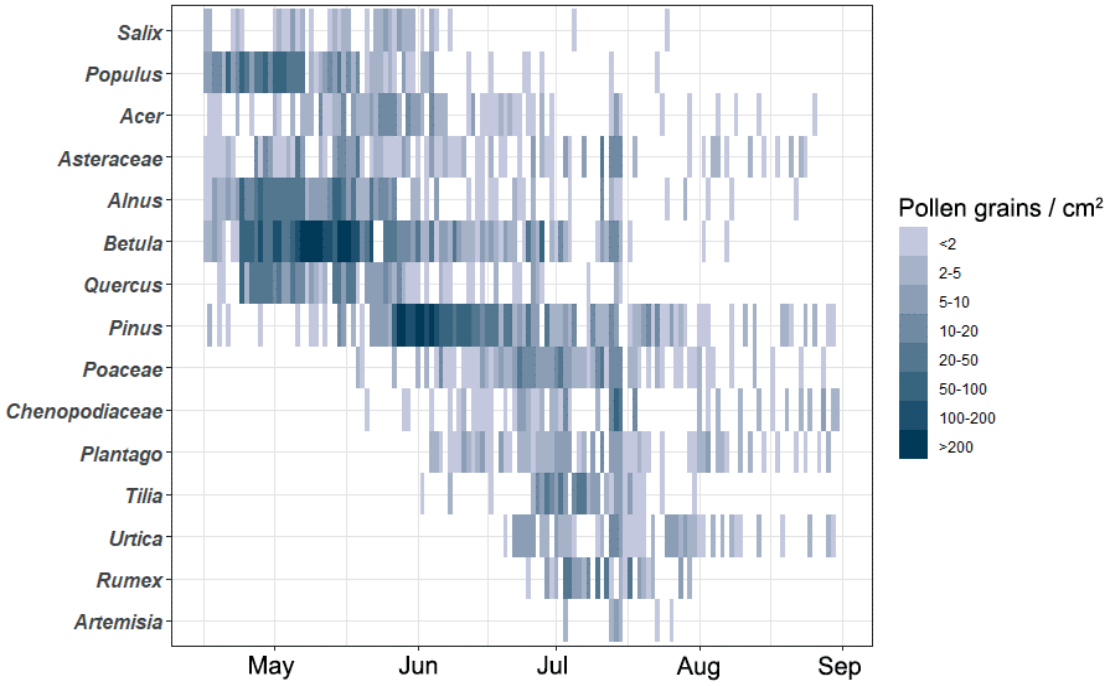

Fig. 3. Pollen calendar of Cherepovets's aeropalynological spectrum in 2015

Fig. 4. Pollen calendar of Vologda's aeropalynological spectrum in the summer-autumn of 2019

Since spring samples were not collected in 2019, we can clearly trace only the early-summer peak of pollination on the calendar: from late June to early July.

The calendar shows that in the first ten days of June, the influence of the spring peak of pollination periods of arboreal plants is still very noticeable. In general, in the summer and autumn period, there is a gradual decrease in the amount of arboreal plants' pollen in the air.

In the second decade of June, number of pollen grains of herbaceous plants increases until the first decade of July and then pollination decreases by the end of the month. The autumn maximum, due to late flowering Asteraceae species, was at the same level during the whole September. The predominance of pollen grains of herbaceous taxa indicates that herbaceous plants are the basis for the formation of summer and autumn pollen rains. Asteraceae pollen dominates the aeropalynological spectrum among herbaceous plants. These pollen grains account for about 28% and play a significant role in the summer and autumn peaks. In summer *Pinus* pollen was most common among arboreal plants (~18%).

The proportion of damaged grains in the pollen spectrum was approximately 1%.

Thus, observations in the two cities showed a fundamentally similar pattern of pollination, a small feature was the presence of an autumn maximum in pollination of herbaceous plants in Vologda.

DISCUSSION

The study showed that *Acer, Alnus, Betula, Fraxinus, Picea, Pinus, Populus, Quercus, Salix, Tilia, Artemisia,* Asteraceae, Chenopodiaceae, *Plantago*, Poaceae, *Rumex*, Apiaceae, and *Urtica* are the main airborne pollen types in large cities of the Vologda Region. These taxa are also typical of the boreal zone of Europe (Sofiev and Bergmann 2013).

Earlier, similar studies were also conducted in the north-west of European Russia in Petrozavodsk and showed that the dominant taxa in this region are *Betula, Pinus*, Poaceae, *Urtica, Artemisia* (Elkina 2007). In other Russian cities, such as Moscow, Ryazan, Smolensk, aeropalynological studies have revealed the same dominant taxa (Posevina et al. 2010, 2011; Posevina and Severova 2017; Slabkaya et al. 2012).

The differences in pollen rain are related to the regional peculiarities of flora and landscaping in different countries. For instance, in Ukraine, in addition to *Betula* and *Urtica*, one of the most important dominants is *Ambrosia*, a dangerous allergenic plant (Rodinkova 2015). In Denmark, *Corylus*, Cupressaceae/Taxaceae, *Fagus, Sambucus,* and Cruciferae also play a significant role in pollen spectra (Goldberg et al. 1988), and in Switzerland *Carpinus, Platanus,* and *Castanea* (Clot 2003). Poland is characterized by a significant presence of *Betula, Alnus, Corylus, Fraxinus, Populus, Carpinus,* and Cupresaceae/Taxaceae in aerospectrums (Malkiewicz et al. 2017). On the East of European Russia, in the Perm region, the most important pollens for monitoring are of *Betula*, Poaceae, and *Artemisia* (Novoselova and Minaeva 2015). According to the results of the study, the most significant taxa for the Vologda Region are *Betula, Alnus* and *Pinus* among the trees, as well as Asteraceae, *Plantago* and Poaceae among the herbaceous plants.

Two pollination periods were distinguished: spring (from the last decade of April to May) coincides with the flowering of generally anemophilous trees with *Betula* as the dominant pollen type and summer (from late June to early and mid-July) due to the flowering of herbaceous plants (pollen shed of Poaceae, Asteraceae, *Artemisia* and other weeds). The results of many Russian and European studies turn out to be similar, but the pollination periods differ in duration for several weeks. In Croatia, pollen concentrations also showed two peaks, one in April and one in August (Peternel et al. 2005). Similar results have also been reported from central Italy and south France (Clot 2001; Emberlin et al. 1993; Jäger et al. 1991; Spieksma and Frenguelli 1991). There were two principal periods of the increase in the pollen concentration in Vinnitsa (central Ukraine) in late April and from mid-June until the end of August (Rodinkova 2015). In contrast to the Vologda Region, researches in the Perm Region (Russia) and Ryazan have shown three pollen shed periods in mid-spring, early summer, and late summer, which might be explained by regional peculiarities of vegetation and climate (Posevina et al. 2010; Novoselova and Minaeva 2015).

The most allergenic, according to (Sofiev and Bergmann 2013), is pollen of 18 taxa, of which ten (*Alnus, Artemisia, Betula, Fraxinus, Salix, Plantago*, Poaceae, *Quercus, Rumex, Urtica*) account for about 50% of all pollen grains detected in the atmosphere of Cherepovets and Vologda.

Birch pollen dominates (30%) in the pollen spectrum of arboreal taxa in the Vologda Region, which coincides with the results of other researchers in Russia (Posevina et al. 2010, 2011; Posevina and Severova 2017; Elkina 2007; Slabkaya et al. 2012), and also in the Northern and Central Europe (Adams-Groom et al. 2002; Sofiev and Bergmann 2013; Spieksma et al. 1995). We have detected the presence of birch and pine pollen in the spectrum of the second half of the growing season, which does not coincide with the period of its flowering. This phenomenon was noted earlier in the Czech Republic, Poland, and Germany (Estrella et al. 2006; Hajkova et al. 2015; Szczepanek 1994). It can be caused by the secondary lifting of pollen grains from the ground by the wind, or the transfer of pollen grains over long distances from other territories. (Skjøth et al. 2009), comparing data from Poland and the UK, showed that long-distance transport is an important source of *Betula* pollen grains in both countries, indicating that sensitization and symptoms of pollinosis may occur in areas remote from the pollen source.

Among herbaceous plants, attention should be paid to the species of the Poaceae and Asteraceae families, especially *Artemisia* (Posevina et al. 2010; Novoselova and Minaeva 2015). Studies by Grewling and co-authors (2015) in Poland, Câmara Camacho and co-authors (2015) in Portugal, and Ianovici (2015) in Romania showed trends toward a significant increase in the pollination period of Poaceae although with a relatively low concentration compared to arboreal plants. Poaceae pollen is among the main causes of pollen allergy in Europe, a long pollination period can be harmful for patients with allergies (Ianovici 2015; D'Amato et al. 2007; Sanchez-Mesa et al. 2003). In Russia grass pollen is also considered as one of the most important allergen (Posevina et al. 2010; Posevina and Severova 2017; Elkina 2007; Slabkaya et al. 2012).

Despite the fact that many plant species of the Asteraceae family are pollinated by insects and do not have a high potential for spreading pollen grains by wind, pollen allergens of plants of the genus *Artemisia* are an important cause of pollinosis in Europe and Russia (Kazlauskas et al. 2006; Shamgunova and Zaklyakova 2010). In this context, it is worth noting that although *Artemisia* species belong to anemophilic plants, their pollen grains are not as well adapted for wind transport as other lighter and smaller ones (Grewling et al. 2015); however, they cause on average a stronger allergic reaction in patients at a lower concentration compared, for example, with birch (Sofiev and Bergmann 2013).

In recent years, an increased prevalence of allergy to ragweed pollen from the Asteraceae family has been estimated in Europe, especially in Hungary, Austria, France, Italy, and several other countries (Asero 2002, 2007; Bottero et al. 1990; Corsico et al. 2000; Déchamp et al. 1995; Dervaderics et al. 2002; Járai-Komlódi and Juhász 1993; Rybnicek and Jäger 2001; Thibaudon et al. 2003). In North America, ragweed is one of the strongest sensitizing pollen types causing the main symptoms of pollinosis during its pollination in late summer and autumn (White and Bernstein 2003). In Austria, it has been demonstrated that there is a high correlation between an increase in the amount of ragweed pollen and sensitization rates (Jäger 2000). Pollen grains of ragweed have not been detected in the Vologda Region; however, because this plant continues to spread throughout Europe moving northward, it is necessary to closely monitor the presence of its pollen in the spectra, especially in connection with the trend of increasing temperatures (Gleisner et al. 2022).

In a few studies, opinions are expressed that the proportion of damaged pollen grains increases with environmental pollution (Dziuba 2007); however, researchers do not usually record the presence of damaged pollen and its quantity (Bicakci et al. 2003; Erkara et al. 2009). We were able to show that in the aeropalynological spectra of Cherepovets and Vologda the amount of damaged pollen reached 2%. But in general, according to numerous works of Dziuba (Dziuba 1993, 2006, 2007; Dziuba et al. 1996, 1999, 2001, 2005), in natural population in normal condition without any pollutions the percentage of damaged pollen can reach up to 7-10% because of mistakes in microsporogenesis. Thus, according to the results of our study, we have not identified a clear effect of air pollution on pollen in the Vologda Region.

CONCLUSIONS

Thus, as a result of the conducted studies, the data of monitoring the airborne pollen diversity and its seasonal dynamics in Cherepovets and Vologda were obtained, as well as the pollen grains with allergenic potential were detected and a pollen calendar was compiled.

Twenty-one types of pollen have been identified, ten of which are the most common allergenic types (*Alnus, Artemisia, Betula, Fraxinus, Salix, Plantago,* Poaceae, *Quercus, Rumex, Urtica*), which in total amount to more than 50% of all registered pollen. The results show the presence of allergenic pollen from different taxa throughout the study. Pollen calendars show two peaks of pollen grain quantity: spring (from last decade of April to May) and summer (from the end of June to the middle of July). *Betula* (~30%) and Asteraceae (~28%) pollen dominate in the pollen spectrum in the Vologda Region. *Pinus* (~20%), *Plantago* (~6%) and Poaceae (~5%) also play an important role in the regional spectrum, that generally correlates with the data of neighboring regions.

Despite the mostly elevated level of atmospheric air pollution during the study period, the proportion of damaged pollen grains was approximately 2%, which corresponds to the norm in natural population in normal condition without any pollutions.

This new data can become the basis for developing recommendations for reducing the level of pollinosis in the Vologda Region.

REFERENCES

Adams-Groom B., Emberlin J., Corden J., Millington W. and Mullins J. (2002). Predicting the start of the birch pollen season at London, Derby and Cardiff, United Kingdom, using a multiple regression model, based on data from 1987 to 1997. Aerobiologia, 18, 117–123, DOI: 10.1111/aec.12296.

Allergymask (2016). Allergymask. Statistics in Russia, [online] Available at: http://allergy-mask.ru/articles/allergiya-statistika-v-rossii.html [Accessed 6 Nov. 2017] (in Russian).

Antipov N., Bobrocskiy R., Butuzova O., Voropanova T., Lebedev V., Savinov V., Sadokov K., Serditov N. and Sokolov N. (1957). Nature of the Vologda Oblast: Digest of articles. Vologda: Regional book publishing house (in Russian).

Asero R. (2002). Birch and ragweed pollinosis north of Milan: A model to investigate the effects of exposure to "new" airborne allergens. Allergy, 57(11), 1063–1066, DOI: 10.1034/j.1398-9995.2002.23766.x.

Asero R. (2007). The changing pattern of ragweed allergy in the area of Milan, Italy. Allergy, 62(9), 1097–1099, DOI: 10.1111/j.1398-9995.2007.01436.x.

Barck C., Lundahl J., Halldén G. and Bylin G. (2005). Brief exposures to NO2 augment the allergic inflammation in asthmatics. Environmental Research, 97(1), 58–66, DOI: 10.1016/j.envres.2004.02.009.

Barck C., Sandström T., Lundahl J., Halldén G., Svartengren M., Strand V., Rak S. and Bylin G. (2002). Ambient level of NO2 augments the inflammatory response to inhaled allergen in asthmatics. Respiratory Medicine, 96(11), 907–917, DOI: 10.1053/rmed.2002.1374.

Bicakci A., Tatlidil S., Sapan N., Malyer H. and Canitez Y. (2003). Airborne pollen grains in Bursa, Turkey, 1999-2000. Annals of Agricultural and Environmental Medicine, 10(1), 31–36.

Bottero P., Venegoni E., Riccio G., Vignati G., Brivio M., Novi C. and Ortolani C. (1990). Pollinosi da Ambrosia artemisiifolia in Provincia di Milano. Folia Allergologica et Immunologica Clinica, 37(2), 99–105.

Bryce M., Drews O., Schenk M.F., Menzel A., Estrella N., Weickenmeier I., Smulders M.J.M., Buyers J., Ring J., Görg A., Behrendt H. and Traidl-Hoffmann C. (2010). Impact of urbanization on the proteome of birch pollen and its chemotactic activity on human granulocytes. International Archives of Allergy and Immunology, 151, 46–55, DOI: 10.1159/000232570.

Clot B. (2001). Airborne birch pollen in Neuchâtel (Switzerland): Onset, peak and daily patterns. Aerobiologia, 17(1), 25–29, DOI: 10.1023/A:1007652220568.

Clot B. (2003). Trends in airborne pollen: An overview of 21 years of data in Neuchâtel (Switzerland). Aerobiologia, 19(3), 227–234, DOI: 10.1023/B:AERO.0000006572.53105.17.

Corsico R., Falagiani P., Ariano R., Berra D., Biale, Bonifazi F., Campi P., Feliziani V., Frenguelli G., Galimberti M., Gallesio M. T., Liccardi G., Loreti A., Marcer G., Marcucci F., Meriggi A., Minelli M., Nardelli R., Nardi G., Negrini C. A., Papa G., Piu G., Pozzan M., D'Ambrosio F. P., Riva G. (2000). An epidemiological survey on the allergological importance of some emerging pollens in Italy. Journal of Investigational Allergology and Clinical Immunology, 10(3), 155–161.

D'Amato G., Cecchi L., Bonini S., Nunes C., Annesi-Maesano I., Behrendt H., Liccardi G., Popov T., Van Cauwenberge P. (2007). Allergenic pollen and pollen allergy in Europe. Allergy, 62, 976–990, DOI: 10.1111/j.1398-9995.2007.01393.x.

Déchamp C., Le Gal M. and Deviller P. (1995). Prevalence of ragweed hayfever in the south and east of the greater Lyon region in 1993. Allergie et Immunologie, 27(9), 323–325.

Dervaderics M., Fust G. and Otos M. (2002). Differences in the sensitisation to ragweed and occurrence of late summer allergic symptoms between natives and immigrant workers of the nuclear power plant of Hungary. Immunological Investigations, 31(1), 29–40, DOI: 10.1081/IMM-120003220.

Documents on the state of atmospheric pollution in cities for informing government agencies, the public and the population. General requirements for the development, construction, presentation and content. Guidance document 52.04.667-2005. (2006). Electronic fund of legal and regulatory documents, [online] Available at: https://docs.cntd.ru/document/1200067118 [Accessed 30 Nov. 2022] (in Russian).

Durham O.C. (1946). The volumetric incidence of atmospheric allergens: IV. A proposed standard method of gravity sampling, counting, and volumetric interpolation of results. Journal of Allergy, 17(2), 79–86, DOI: 10.1016/0021-8707(46)90025-1.

Dziuba O.F. (1993). Pollen Angyosperms Teratomorphs as the Result of an Ecological Stress under Conditions of a Large City. XV Int. Botanical Congress, Abstr. Yokohama, Japan. 247, 287.

Dziuba O.F. (2006). Palinoindication of environmental quality. St. Petersburg: Nedra (in Russian).

Dziuba O.F. (2006). Study of pollen from surface samples to assess the quality of the environment. Oil and Gas Geology. Theory and Practice, 1, Article 1 (in Russian).

Dziuba O.F. (2007). Teratomorphic pollen grains in modern and paleopalinological spectra and some problems of palinostratigraphy. Oil and Gas Geology. Theory and Practice, 2, Article 2 (in Russian).

Dziuba O.F. and Kudrina A.N. (1996). The main trends in the change in the sculpture of the surface of angiosperm pollen under the influence of industrial emissions. Palynology in biostratigraphy, paleoecology and paleogeography, p. 46 (in Russian).

Dziuba O.F., Kulikova N.K. and Tokarev P.I. (2005). Natural polymorphism of Pinus sylvestris L. pollen in connection with some problems of paleopalinology. Proceedings of the International Paleobotanical Conference, Modern problems of paleofloristics, paleophytogeography and phytostratigraphy, 84-88 (in Russian).

Dziuba O.F., Yakovleva T.L., Kudrina A.N. and Tarasevich V.F. (1999). Pollen as a model for quality control of the male generative sphere of plants, animals and humans. Current problems of palynology at the turn of the third millennium, Abstracts of the IX All-Russian Palynological Conference, 61-80 (in Russian).

Elkina N.A. and Markovskaya E.F. (2007). Experience of palynological studies of the air environment of cities in the taiga zone. Proceedings of the Karelian Scientific Center of the Russian Academy of Sciences, 11, 20-27 (in Russian).

Emberlin J., Savage M. and Woodman R. (1993). Annual variations in the concentrations of Betula pollen in the London area, 1961–1990. Grana, 32(6), 359–363, DOI: 10.1080/00173139309428965.

Erkara I.P., Cingi C., Ayranci U., Gurbuz K.M., Pehlivan S. and Tokur S. (2009). Skin prick test reactivity in allergic rhinitis patients to airborne pollens. Environmental Monitoring and Assessment, 151(1), 401–412, DOI: 10.1007/s10661-008-0284-8.

Estrella N., Menzel A., Krämer U. and Behrendt H. (2006). Integration of flowering dates in phenology and pollen counts in aerobiology: Analysis of their spatial and temporal coherence in Germany (1992–1999). International Journal of Biometeorology, 51(1), 49–59, DOI: 10.1007/s00484-006-0038-7.

Federal Clinical Guidelines for the Diagnosis of Allergic Diseases. (2015). The Russian Association of Allergology and Clinical Immunology, [online] Available at: https://nrcii.ru/specialistam/klinrecommend/ [Accessed 15 Feb. 2022] (in Russian).

Gil D. and Brumm H. (Eds.). (2014). Avian Urban Ecology: Behavioural and Physiological Adaptations edited by Diego Gil and Henrik Brumm. Oxford University Press, [online] Available at: https://bioone.org/journals/the-condor/volume-117/issue-4/CONDOR-15-75.1/Avian-Urban-Ecology-Behavioural-and-Physiological-Adaptations-edited-by/10.1650/CONDOR-15-75.1.full.

Gleisner H., Ringer M. A. and Healy S.B. (2022). Monitoring global climate change using GNSS radio occultation. Npj Climate and Atmospheric Science, 5(1), 1–4, DOI: 10.1038/s41612-022-00229-7.

Goldberg C., Buch H., Moseholm L. and Weeke E.R. (1988). Airborne Pollen Records in Denmark, 1977–1986. Grana, 27(3), 209–217, DOI: 10.1080/00173138809428928.

Government of the Vologda Oblast, Department of Natural Resources and Environmental Protection of the Vologda Region. (2016). Report on the state and environmental protection of the Vologda Oblast in 2015, [online] Available at: http://vologda-oblast.ru/periodic/FILE%20RUS/10381.pdf [Accessed 15 Feb. 2022] (in Russian).

Government of the Vologda Oblast, Department of Natural Resources and Environmental Protection of the Vologda Region. (2019). Report on the state and environmental protection of the Vologda Oblast in 2018, [online] Available at: http://vologda-oblast.ru/periodic/FILE%20RUS/10381.pdf [Accessed 15 Feb. 2022] (in Russian).

Grewling Ł., Kasprzyk I., Borycka K., Chłopek K., Kostecki Ł., Majkowska-Wojciechowska B., Malkiewicz M., Myszkowska D., Nowak M., Piotrowska-Weryszko K., Puc M., Stawińska M., Balwierz Z., Szymańska A., Smith M., Sulborska A. and Weryszko-Chmielewska E. (2015). Searching for a trace of Artemisia campestris pollen in the air. Acta Agrobotanica, 68(4), 399–404, DOI: 10.5586/aa.2015.040.

Guedes A., Ribeiro N., Ribeiro H., Oliveira M., Noronha F. and Abreu I. (2009). Comparison between urban and rural pollen of Chenopodium alba and characterization of adhered pollutant aerosol particles. Journal of Aerosol Science, 40, 81–86, DOI: 10.1016/j.jaerosci.2008.07.012.

Hajkova L., Kožnarová V., Možný M. and Bartošová L. (2015). Changes in flowering of birch in the Czech Republic in recent 25 years (1991–2015) in connection with meteorological variables. Acta Agrobotanica, 68(4), 285–302, DOI: 10.5586/aa.2015.043.

Haselhorst D.S., Tcheng D.K., Moreno J.E. and Punyasena S.W. (2017). The effects of seasonal and long-term climatic variability on Neotropical flowering phenology: An ecoinformatic analysis of aerial pollen data. Ecological Informatics, 41, 54–63, DOI: 10.1016/j.ecoinf.2017.06.005.

Ianovici N. (2015). Relation between Poaceae pollen concentrations and meteorological factors during 2000–2010 in Timisoara, Romania. Acta Agrobotanica, 68(4), 373–381, DOI: 10.5586/aa.2015.033.

Jäger S. (2000). Ragweed (Ambrosia) sensitisation rates correlate withthe amount of inhaled airborne pollen. A 14-year studyin Vienna, Austria. Aerobiologia, 16(1), 149–153, DOI: 10.1023/A:1007603321556.

Jäger S., Spieksma E.T.M. and Nolard N. (1991). Fluctuations and trends in airborne concentrations of some abundant pollen types, monitored at Vienna, Leiden, and Brussels. Grana, 30(2), 309–312, DOI: 10.1080/00173139109431985.

Járai-Komlódi M. and Juhász M. (1993). Ambrosia elatior (L.) in Hungary (1989–1990). Aerobiologia, 9(1), 75–78, DOI: /10.1007/BF02311373.

Kazlauskas M., Šauliene I. and Lankauskas A. (2006). Airborne Artemisia pollen in Siauliai (Lithuania) atmosphere with reference to meteorological factors during 2003–2005. Acta Biologica Universitatis, 6, 1–2.

Kruczek A., Puc M., Stacewicz A. and Wolski T. (2015). The threat of allergenic airborne trees pollen to pollinosis sufferers in a rural area (Western Pomerania, Poland). Acta Agrobotanica, 68(4), 325–331, DOI: 10.5586/aa.2015.039.

Malkiewicz M., Lipiec A., Dąbrowska-Zapart K., Chłopek K., Ziemianin M., Piotrowska-Weryszko K., Weryszko-Chmielewska E., Rapiejko A., Jurkiewicz D. and Rapiejko P. (2017). Birch pollen season in southern Poland in 2017. Alergoprofil, 13(3), 118–123, DOI: 10.24292/01.ap.200917.

Malygina K., Minaeva N., Koriukina I. and Komarova E. (2010). Features of anamnesis and clinical characteristics of pollinosis in children. Perm Medical Journal, 27(5), Article 5 (in Russian).

Meyer-Melikyan N., Severova E., Gapochka G., Polevova S., Tokarev P. and Bovina Iy. (1999). Principles and methods of aeropalynological research. Moscow.

Namork E., Johansen B.V. and Løvik M. (2006). Detection of allergens adsorbed to ambient air particles collected in four European cities. Toxicology Letters, 165, 71–78, DOI: 10.1016/j.toxlet.2006.01.016.

Nenasheva G. (2013). Aeropalynological monitoring of allergenic plants of Barnaul: Monograph. SB RAS (in Russian).

Nilsson S. and Spieksma F.T.M. (Eds.). (1994). Allergy Service Guide in Europe. Swedish Museum of Natural History.

Novoselova L.V. and Minaeva N. (2015). Pollen monitoring in Perm Krai (Russia) – experience of 6 years. Acta Agrobotanica, 68(4), 343–348, DOI: 10.5586/aa.2015.042.

Official website of the Administration of the city of Vologda. (2022). According to the results of the latest All-Russian population census, more than 320 thousand people live in Vologda, [online] Available at: http://vologda-portal.ru/novosti/index.php?ID=472464&SECTION_ID=151 [Accessed 29 Nov. 2022] (in Russian).

Official website of the Administration of the city of Vologda. Decision of the Vologda City Duma of June 27, 2019 No. 1852. [online]. Available at: http://vologda-portal.ru/oficialnaya_vologda/index.php?ID=414897&SECTION_ID=173 [Accessed 29 Nov. 2022] (in Russian).

Official website of the city of Cherepovets. Architecture, [online] Available at: https://cherinfo.ru/36 [Accessed 29 Nov. 2022] (in Russian).

Official website of the city of Cherepovets. Population of Cherepovets, [online] Available at: https://cherinfo.ru/18 [Accessed 29 Nov. 2022] (in Russian).

Orlova N.I. (1997). Determinant of higher plants of the Vologda Oblast. Vologda: Rus. (in Russian).

Peternel R., Čulig J., Mitić B., Hrga I. and Vukušić I. (2005). Airborne pollen spectra at three sites in inland Croatia, 2003. Botanical Bulletin of Academia Sinica, 46(1), 53–59.

Piotrowska-Weryszko K. and Weryszko-Chmielewska E. (2015). Spatial differentiation of airborne arboreal pollen in Lublin (Poland). Acta Agrobotanica, 68(4), 333–341, DOI: 10.5586/aa.2015.035.

Posevina Y. (2011). Palynoecological monitoring of atmospheric air in the city of Ryazan: Abstract of the dissertation for the degree of candidate of biological sciences. RUDN University (in Russian).

Posevina Y.M. and Severova E.E. (2017). Dynamics of pollen rain in Ryazan: the first volumetric data. Bulletin of the Moscow Society of Naturalists. Department of Biology, 122(4), 102-108 (in Russian with English summary).

Posevina Y.M., Ivanov E.S. and Severova E.E. (2010). Palynoecological assessment of atmospheric air quality. RUDN Journal of Ecology and Life Safety, 5, 15-22 (in Russian with English summary).

Posevina, Y.M., Severova E. E. and Ivanov E. S. (2011). Interseasonal rhythmic of dusting of early-flowering tree taxa of the aeropalynological spectrum in Ryazan. Bulletin of the Moscow Society of Naturalists. Department of biology, 4, 48-54 (in Russian).

Puc M., Wolski T., Camacho I.C., Myszkowska D., Kasprzyk I., Grewling Ł., Nowak M., Weryszko-Chmielewska E., Piotrowska-Weryszko K., Chłopek K., Dąbrowska-Zapart K., Majkowska-Wojciechowska B., Balwierz Z., Malkiewicz M., Grinn-Gofroń A., Stacewicz A., Kruczek A. and Borycka K. (2015). Fluctuation of birch (Betula L.) pollen seasons in Poland. Acta Agrobotanica, 68(4), 303–313, DOI: 10.5586/aa.2015.041.

Rodinkova V.V. (2015). Airborne pollen spectrum and hay fever type prevalence in Vinnitsa, central Ukraine. Acta Agrobotanica, 68(4), 383–389, DOI: 10.5586/aa.2015.037.

Rybnicek O. and Jäger S. (2001). Ambrosia (ragweed) in Europe. Allergy and Clinical Immunology International, 13, 60–66.

Sanchez-Mesa J.A., Smith M., Emberlin J., Allitt U., Caul-ton E. and Galan C. (2003). Characteristics of grass pollen seasons in areas of southern Spain and the United Kingdom. Aerobiologia, 19, 243–250, DOI: 10.1023/B:AERO.0000006597.44452.a3.

Sénéchal H., Visez N., Charpin D., Shahali Y., Peltre G., Biolley J.P., Lhuissier F., Couderc R., Yamada O., Malrat-Domenge A., Pham-Thi N., Poncet P. and Sutra J.P. (2015). A Review of the Effects of Major Atmospheric Pollutants on Pollen Grains, Pollen Content, and Allergenicity. The Scientific World Journal, 2015, DOI: 10.1155/2015/940243.

Shamgunova B.A. and Zaklyakova L.V. (2010). Aeropalynological aspects of hay fever. Astrakhan Medical Journal, 1, 27-35.

Shvetsov V. (2012). "Clean City" gathers ideas, [online] Official website of the city of Cherepovets. Available at: https://cherinfo.ru/news/51552-cistyj-gorod-sobiraet-idei [Accessed 29 Nov. 2022] (in Russian).

Skupinova E. (2007). Atlas of the Vologda Oblast (O. Zolotova, Ed.). Aerogeodesia: Port-April (in Russian).

Slabkaya E.V., Meshkova R.Y. and Aksyonova S.A. Aeropalynological control of the environment and results of pollen monitoring in Smolensk in 2009-2010 (2012). Bulletin of the Smolensk State Medical Academy, 2, 40-42 (in Russian with English summary).

Sofiev M. and Bergmann K.-C. (2013). Allergenic Pollen: A Review of the Production, Release, Distribution and Health Impacts. Springer, DOI: 10.1007/978-94-007-4881-1.

Spieksma F.Th.M. and Frenguelli G. (1991). Allergenic significance of Alnus (Alder) pollen. In Allergenic Pollen and Pollinosis in Europe (pp. 36–44). Blackwell Scientific Publications.

Spieksma F.Th.M., Emberlin J.C., Hjelmroos M., Jäger S. and Leuschner R.M. (1995). Atmospheric birch (Betula) pollen in Europe: Trends and fluctuations in annual quantities and the starting dates of the seasons. Grana, 34(1), 51–57, DOI: 10.1080/00173139509429033.

Szczepanek K. (1994). Pollen calendar for cracow (southern Poland), 1982–1991. Aerobiologia, 10(1), 65–70, DOI: 10.1007/BF02066749.

Thibaudon M., Lachasse C. and Finet F. (2003). [Ragweed in France and the Rhône-Alpes region (Lyon, Bourgoin, Grenoble, Roussillon]. European Annals of Allergy and Clinical Immunology, 35, 87–91.

Van Vliet A.J.H., Overeem A., De Groot R.S., Jacobs A.F.G and Spieksma F.Th.M. (2002). The influence of temperature and climate change on the timing of Pollen release in the Netherlands. International Journal of Climatology, 22(14), 1757–1767, DOI: /10.1002/joc.820.

Vorobyov G. (Ed.). (2007). Nature of the Vologda Oblast. Vologda: Vologzhanin (in Russian).

Wang X., Gong S., Nakamura S., Kurihara K., Suzuki M., Sakamoto K., Miwa M. and Lu S. (2009). Air pollutant deposition effect and morphological change of Cryptomeria japonica pollen during its transport in urban and mountainous areas of Japan. WIT Transactions on Biomedicine and Health, 11, 77–89, DOI: 10.2495/EHR090081.

White J. and Bernstein D. (2003). Key pollen allergens in North America. Annals of Allergy, Asthma and Immunology: Official Publication of the American College of Allergy, Asthma, and Immunology, 91(5), 425–435, DOI: 10.1016/S1081-1206(10)61509-8.

ZAUM. Worldwide Map of Pollen Monitoring Stations. (2022), [online] Available at: https://www.zaum-online.de/pollen/pollen-monitoring-map-of-the-world.htm [Accessed 24 Feb. 2022].

Zhang Y. and Allison L. Steiner A.L. (2022). Projected climate-driven changes in pollen emission season length and magnitude over the continental United States. Nature Communications, 13, 1234, DOI: 10.1038/s41467-022-28764-0.

RESEARCH PAPER

ASSESSMENT OF AIR POLLUTION AND ITS ASSOCIATION WITH POPULATION HEALTH: GEO-STATISTICAL EVIDENCE FROM PAKISTAN

Munazza Fatima[1], Ibtisam Butt[2], Muhammad Nasar-u-Minallah[3*], Asad Atta[4], Gong Cheng[4]
[1]Department of Geography, the Islamia University of Bahawalpur, Pakistan
[2]Institute of Geography, University of the Punjab Lahore, Pakistan
[3]Department of Geography, Govt. Graduate College Gojra, Pakistan
[4]School of Geosciences and Info-Physics, Central South University, Changsha, China
***Corresponding author:** Nasarbhalli@gmail.com
Received: October 27th, 2022 / Accepted: May 4th, 2023 / Published: July 1st, 2023
https://DOI-10.24057/2071-9388-2022-155

ABSTRACT. Human health is harmed by air pollution. The objective of this research was to show that air pollution in Pakistan is getting worse and is negatively impacting people's health. IQ Air and the Institute for Health Metrics and Evaluation provided the data for this descriptive research. Monthly data of $PM_{2.5}$ μg/m^3 from ten different localities across Pakistan are used to show spatial distribution through the geospatial technique of interpolation. The findings show that two third of the country has high $PM_{2.5}$ concentration, with Lahore as the most polluted city. In Pakistan, solid fuel use has decreased, leading to a decline in associated mortality and morbidity. However, there have been significant increases in $PM_{2.5}$ and ozone levels, resulting in a rise in the country's overall health burden caused by air pollution. Furthermore, the number of deaths attributed to air pollution has also increased since 1990. A total of 57% of chronic obstructive pulmonary disease, 40% of lower respiratory infections, 36% of ischemic stroke, 35% of ischemic heart diseases, 32% of lung cancer, 25% of diabetes, and 20% of neonatal outcomes are directly attributed to air pollution in Pakistan. The main contributors to air pollution are population growth, growing motorization, and unsustainable energy usage. The main challenges due to air pollution control and monitoring in Pakistan include a lack of awareness, poor policy creation and implementation, the use of improper fuel, rising energy demands, and an absence of pollution monitoring stations in most cities. Therefore, there is a need for a robust air pollution monitoring system, increased public awareness, and the implementation of clean and sustainable policies to regulate this environmental health issue.

KEYWORDS: air pollution, health effects, interpolation, Pakistan, $PM_{2.5}$

CITATION: Munazza Fatima, Ibtisam Butt, Muhammad Nasar-u-Minallah, Asad Atta, Gong Cheng (2023). Assessment Of Air Pollution And Its Association With Population Health: Geo-Statistical Evidence From Pakistan. Geography, Environment, Sustainability, 2(16), 93-101
https://DOI-10.24057/2071-9388-2022-155

Conflict of interests: The authors reported no potential conflict of interest.

INTRODUCTION

An important environmental health problem around the world is air pollution, both outdoors and indoors. In developing countries, urban centers have poor air quality due to population growth, degradation of vegetation cover, broad industrialization and urbanization (Colbeck et al. 2010; Tabinda et al. 2020). With 207.9 million inhabitants Pakistan has the fifth-highest population in the world. Pakistan is bordered by the most populated countries of China and India as well. The average $PM_{2.5}$ concentration in Pakistan in 2022 was 14.2 times higher than the annual air quality guideline value recommended by the World Health Organization (WHO). In 2019, Pakistan recorded a $PM_{2.5}$ reading of 65.81 μg/m^3, placing it in the 'unhealthy' ratings category. This category typically includes readings between 55.5 to 150.4 μg/m^3. Similarly, neighboring countries like India and Afghanistan also exhibited high $PM_{2.5}$ concentrations, with readings of 68.78 μg/m^3 and 55.14 μg/m^3 respectively (IQAir 2023). Similar to Pakistan, where only 49.1 percent of the population consumes clean fuel such as natural gas for cooking, the remaining half of the population uses alternative fuels such as wood, dung, agricultural waste etc. that contribute to indoor air pollution (WHO 2018). The combined health effects of ambient and household air pollution are significant in Pakistan. According to the World Health Organization (WHO), ambient and household air pollution are responsible for around 113 deaths per 100,000 people in Pakistan (WHO 2021a).

Population growth, unmonitored industrialization, and rapid urbanization are the key driving forces for environmental problems such as noise and air pollution, drinking water scarcity, poor sanitation and waste management, especially in urban areas of Pakistan (Mir et al. 2016). Anjum et al. (2021) stated in their recent review that major air pollutants including NO_x, O_3 and SO_2 have been increasing in Pakistan for two decades. But

the country's air quality monitoring system hasn't kept up with the problem. There are numerous causes of air pollution in Pakistan, some are constant throughout the year, such as automobiles, factories, and brick kilns, while others are seasonal or occasional, such as stubble burning during winters and openly burning waste in the streets. In addition, poorly maintained construction sites and dust storms also add silt, dust and silica, which ultimately make the concentration of $PM_{2.5}$ and PM_{10} in the air. Large-scale loss of trees is also one of the main reasons for high pollution. On the other hand, exposure to smoke inside, from smoking or using solid fuels for cooking is the main contributor to household air pollution and may have negative effects on health. Despite the fact that there is research on the effects of air pollution on health in Pakistan, most of them are based on the case studies of big urban centres such as Karachi, Lahore, Peshawar, Quetta, Rawalpindi and Islamabad (Anjum et al. 2021).

Contamination caused by toxic gases, dust, fumes, smoke or any other substance in the atmosphere may vary in quantities and duration. It is injurious to human health referred to as air pollution. The human respiratory system is mainly exposed to air pollution, hence breathing in these pollutants causes inflammation, oxidative stress, immunosuppression, and mutagenicity in cells throughout our body impacting the lungs, heart, and brain among other organs and eventually leading to disease (Kampa and Castanas 2008; WHO 2021a). According to the World Health Organization (WHO), indoor and outdoor air pollution causes seven million premature deaths due to stroke, heart disease, chronic obstructive pulmonary disease, lung cancer and acute respiratory infections (WHO 2021a). Outdoor or ambient air pollution includes mainly particulate matter (PM_{10} and $PM_{2.5}$), Carbon Mono oxide CO, Nitrogen dioxide NO_2, and ground ozone O3. However, there are two categories of indoor air pollution: combustion sources (CO, PM_{10}, and $PM_{2.5}$) and non-combustion sources (Volatile organic compound VOCs, Lead, Radon, mould, bacterial growth etc.) (WHO 2021b). The major outdoor pollution sources include residential energy for cooking and heating, combustion of fossil fuel, vehicles, power generation, agriculture/waste burning, and industrial smoke and forest fires. Although air pollution affects developed and developing counties equally, low and middle-income countries show a maximum health burden. The reason includes widespread industrialization, unmonitored environmental planning, urbanization and high population growth, especially in urban areas (Mannucci and Franchini 2017). Nine out of ten people worldwide breathe air that exceeds WHO guideline limits, according to recent reports from the WHO.

Air pollution can have both immediate and long-term negative impacts on a person's health (Saldiva et al. 1994). This is especially true for the elderly, children, and those who already have cardiovascular and respiratory problems (Lee et al. 2014). These problems varied from slight upper respiratory irritation to chronic respiratory and heart disease, lung cancer, acute respiratory infections in children and chronic bronchitis in adults, provoking pre-existing heart and lung disease, or asthmatic attacks (Kampa and Castanas 2008). In a study, Fiordelisi et al. (2017) stated that PM_{10} with a diameter <10 μm reaches the lung and $PM_{2.5}$ with a diameter <2.5 μm penetrates deeper into the lung, and exposure to these pollutants increases the rate of cardiovascular deaths. Similarly, indoor air pollution is equally injurious to human health. The main indoor air pollution source is the use of biomass fuels such as coal, wood, animal dung, crop residues and their incomplete combustion. This incomplete combustion produces suspended particulate matter, carbon monoxide, formaldehyde, nitrogen dioxide, polycyclic aromatic hydrocarbons, etc. in the indoor air. There is several evidence that exposure to such pollutants can raise the risk of developing disorders including respiratory infections (e.g., pneumonia, tuberculosis and chronic obstructive pulmonary disease (COPD), lung cancer, and asthma), low birth weight, cataracts, and cardiovascular events (Kim et al. 2011).

There are several studies focusing health impacts of air pollution in Pakistan. Khwaja et al. (2012) proved that extremely elevated concentrations of $PM_{2.5}$ are associated with significantly raised rates of cardiovascular disease in Karachi. In another study based in Lahore, Sughis et al. (2012) found that 8–12-year-old children, who are exposed to (traffic-related) air pollution were associated with higher systolic and diastolic blood pressure. Similarly in a self-reported study students of Malakand Division Pakistan, reported that exposure to air pollution significantly affected their physical health, behaviour, and psychology (Ullah et al. 2021). Khan and Lohano (2018) analyzed that children in households using polluting fuels are 1.5 times more likely to have symptoms of acute respiratory infection (ARI) than children in households using cleaner fuels in Pakistan. Likewise, another study relates indoor air pollution to childhood pneumonia (Naz and Ghimire 2020). In addition, there are several reviews available explaining the health effects of air pollution on human health in Pakistan (Ilyas et al. 2010; Colbeck et al. 2010; Anjum et al. 2021). But almost all of these studies focus on the big cities, and none of them gives an updated and comprehensive insight into the overall health impacts of air pollution in Pakistan. Thus, this descriptive research article aims to present the geo-statistical evidence of air pollution through spatial distribution of $PM_{2.5}$ and cumulative health effects of different air pollutants since 1990 in Pakistan.

STUDY AREA

The Islamic Republic of Pakistan is a country situated in South Asia. Pakistan's total population is almost 220.9 million making it the fifth most populated country in the world (UNODC 2022). It is situated at 30.3753° N, and 69.3451° E covering an area of 881,913 square kilometers (Riaz et al. 2021). In terms of relative location, Pakistan is bounded by Afghanistan to the north and northeast, by China to the northeast and by India to the east and southeast. The Arabian Sea makes its southern border (Burki et al. 2021). Baluchistan, Khyber Pakhtunkhwa (KPK), Punjab and Sindh are the four main provinces of Pakistan. However, Azad Jammu, Kashmir (AJK) and Gilgit Baltistan are regarded as autonomous regions (Fig. 1). Geographically, Pakistan is a part of the Indo-Gangetic Plain, with mountains and plateaus making up three-fifths of its total land area and a level plain making up remaining two fifths. Pakistan's climate, which is predominantly dry and continental in origin, is marked by hot summers and chilly to frigid winters. Pakistan lies at the edge of the monsoonal system. Precipitation received varies greatly throughout the country (Burki et al. 2021). The degradation of all environmental components (air, water, and land) is frighteningly escalating and continues to be a serious concern in Pakistan due to growing industrial and agricultural operations, energy demands, urbanization, traffic density, and population expansion (Khwaja et al. 2012). These degraded environmental problems cause serious health issues in Pakistan (Khan et al. 2014).

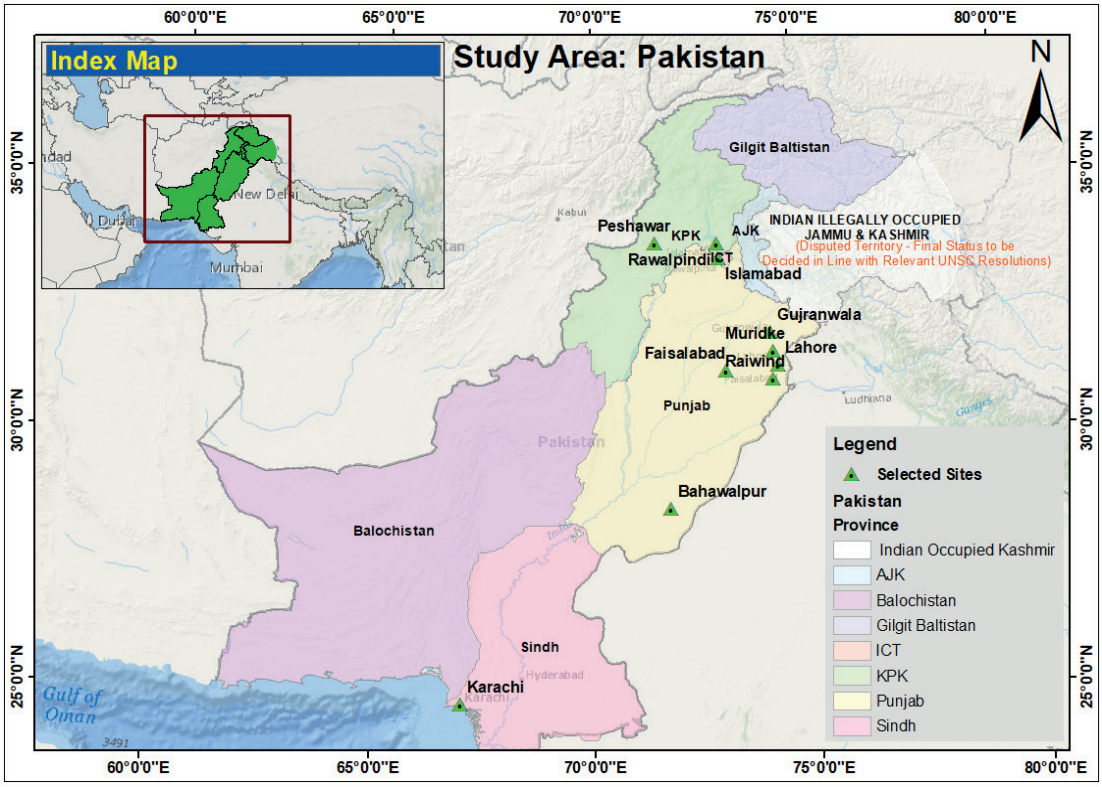

Fig. 1. Map of Pakistan showing the Provinces and Selected sites for IDW of $PM_{2.5}$

MATERIALS AND METHODS

For this study, air quality data about $PM_{2.5}$ µg/m^3 was taken from the online data resource of IQAir[1]. This data is available for each month of 2020 for ten different cities across Pakistan. On the other side, health impact statistics are taken from the Global Burden of Disease Study published in 2019 by the Institute for Health Metrics and Evaluation (IHME)[2]. Health data is presented in total deaths attributed to air pollution, disability-adjusted life-years (DALYs) attributed to each type of air pollution (ozone, solid fuel and $PM_{2.5}$), cause-specific mortality and morbidity, and age-standardize rates. DALYs can be defined as the sum of the years of life lost from early deaths plus the years lived with a disability, such as paralysis from a stroke related to air pollution exposure. However, the age-standardized rates are the total number of deaths or DALYs per 100,000 people, calculated based on a standard distribution of the population across age categories. Higher air pollution-attributable and age-standardized rates of disease reflect directly a combination of higher air pollution intensities and/or sicker populations (IHME 2021). The methodology of this study is shown in Fig. 2. As the study is based on secondary sources of data, hence no primary data has been collected for this descriptive research.

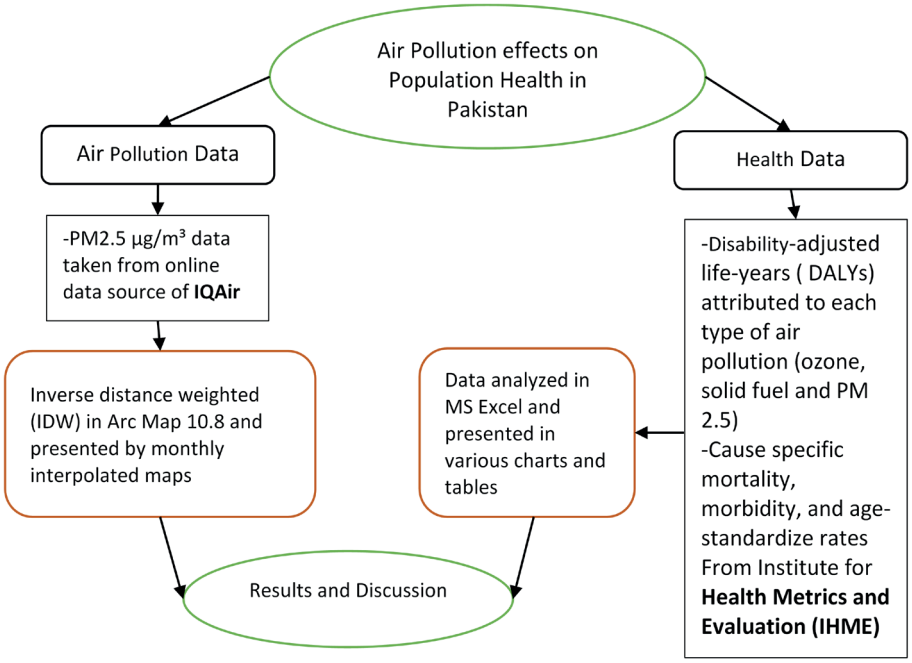

Fig. 2. Methodology Flowchart

[1]https://www.iqair.com
[2]http://www.healthdata.org

Chronic obstructive pulmonary disease (COPD) is the only disease for which the health burden of ozone is estimated. Neonatal deaths and DALYs are estimated only for $PM_{2.5}$, household air pollution, or the two combined (air pollution). Neonatal outcomes include complications from being born too small (low birth weight) or too early (pre-term) and lower respiratory infections. Facts and numbers about air pollution and health are also taken from the websites of the WHO, the Pakistan Environmental Protection Agency (EPA) and various published articles in addition to these two main sources (IHME 2021).

The main technique used to show the spatial distribution of $PM_{2.5}$ is interpolation. The distance between the observed sample sites and the site at which the prediction must be made is used to calculate the interpolation weights in inverse distance weighted (IDW) models (Wong et al. 2004). Hence, IDW from the Geo-statistical Interpolation Tool of Arc Map was used to predict the spatial distribution pattern of $PM_{2.5}$ concentrations across Pakistan. The weights are calculated through the following equation:

$$\hat{v} = \frac{\sum_{i=1}^{n} \frac{1}{d_i^p} v_i}{\sum_{i=1}^{n} \frac{1}{d_i^p}}$$

where $\hat{v}$ is the interpolated value at the target location
n is the number of sample points (known values) used in the interpolation
v_i is the value of the i^{th} sample
$1/d_i^p$ is the weight assigned to the i^{th} sample point, which is inversely proportional to its distance from the target location.

This technique is based on the idea that adjacent will share more characteristics than distant ones. It provides an air pollution probability distribution in Pakistan that is more precise. Hence, IDW uses point data of $PM_{2.5}$ in numeric values and resulted in a raster buffered image according to to strengthen the points and values across the country. For this reason, interpolated maps of air pollution are generated by using Arc Map 10.8 software developed by ESRI to analyze and evaluate geospatial, spatial-statistical and remotely sensed data. The trend of air pollutants and the deaths, DALYs, and age-standardized rates attributed to air pollution are shown with the help of charts and graphs. Microsoft Excel is used to chart the health effects of air pollution in Pakistan.

RESULTS

Spatial Interpolation of $PM_{2.5}$ µg/m³ over Pakistan

Fig. 3 shows the interpolated maps of $PM_{2.5}$ µg/m³ concentration from high values (red) to low values (blue) over Pakistan during 2020. This interpolation is based on a total of ten cities around the country including Lahore, Bahawalpur, Faisalabad, Gujranwala, Muridke, Raiwind, Karachi, Rawalpindi, Islamabad, and Peshawar (Fig. 1). The interpolation of each month shows the different distributions. During January, $PM_{2.5}$ values are higher around Peshawar, Faisalabad and Lahore and lower values spread out from Rawalpindi and Karachi. The map of February also depicts almost similar distribution to January but with high values (dark colour) distributed widely in the central parts of Pakistan.

March and April show red contours around Peshawar and Bahawalpur, with relatively low values at the rest of the sample sites. During May and June, southern Punjab, western KPK and most of the Baluchistan province show comparatively higher values than other parts of the country. July, August and September show high values toward the northwestern part of the country generally around Peshawar. October pinpoint red contours only around Peshawar and Lahore, and blue contours around Islamabad and nearly the whole south of the country. Interpolation maps of November and December show a high concentration of $PM_{2.5}$ in most of the parts, except the north and south of the country (Fig. 4).

Fig. 3 shows the average annual interpolation of $PM_{2.5}$ in Pakistan, which clearly shows higher values > 60 in almost

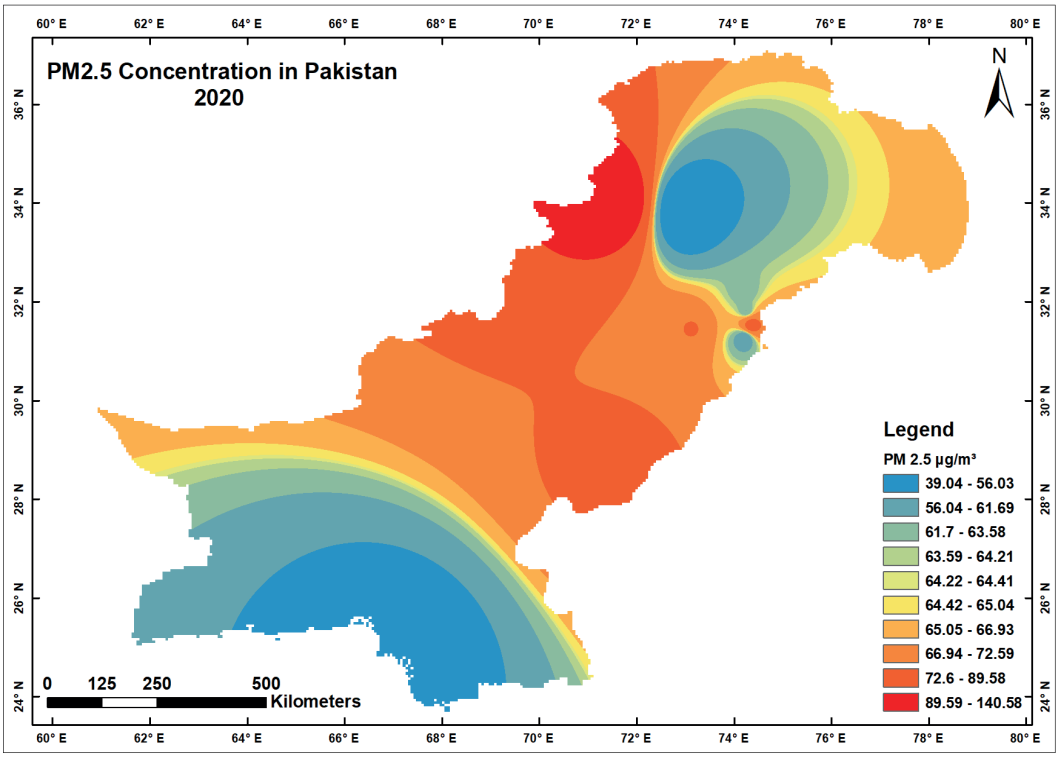

Fig. 3. Interpolated Map of Pakistan showing average PM2.5 concentration (2020)

two third areas of the country. Blue zones can only be seen in the extreme south and north of the country.

In comparison to these maps, the actual values of $PM_{2.5}$ concerning WHO air quality standards are shown in Table 1. According to these values, major cities like Peshawar, Lahore, Bahawalpur, Faisalabad, and Gujranwala showed high values of $PM_{2.5}$ µg/m^3 concentration making them unhealthy and sometimes very unhealthy according to the WHO air quality standards; however, Karachi, Rawalpindi and Islamabad show comparatively low concentration and moderate air quality. Besides this, a higher concentration of these pollutants is persistent between November to February.

Use of Solid Fuel in Pakistan

Fig. 5 compares the population-weighted ozone concentration, population-weighted $PM_{2.5}$µg/m^3, and people utilizing solid fuel since 1990. Analyzing the historic data from 1990 to 2019, it is revealed that the proportion of the population using solid fossil fuels decreased from 0.83 in 1990 to 0.53 in 2019. Though $PM_{2.5}$ reached its maximum of 70.9µg/m^3 in 2014 followed by a slight decrease, ozone remained persistently increased since 1990. However, collectively the population-weighted $PM_{2.5}$ µg/m^3 and ozone concentration showed an increasing trend.

Health Impacts of Air Pollution in Pakistan (1990-2019)

Deaths Attributed to Air Pollution

Fig. 6 shows the number of deaths attributed to each pollutant such as $PM_{2.5}$, ozone and solid fuel between 1990 and 2019. It can be observed that the total number of deaths attributed to $PM_{2.5}$ increased exponentially since 1990; however, deaths due to ground ozone remained constant at a low number with a slight increase. On the other hand, for thirty years, the total number of deaths due to fossil fuels decreased.

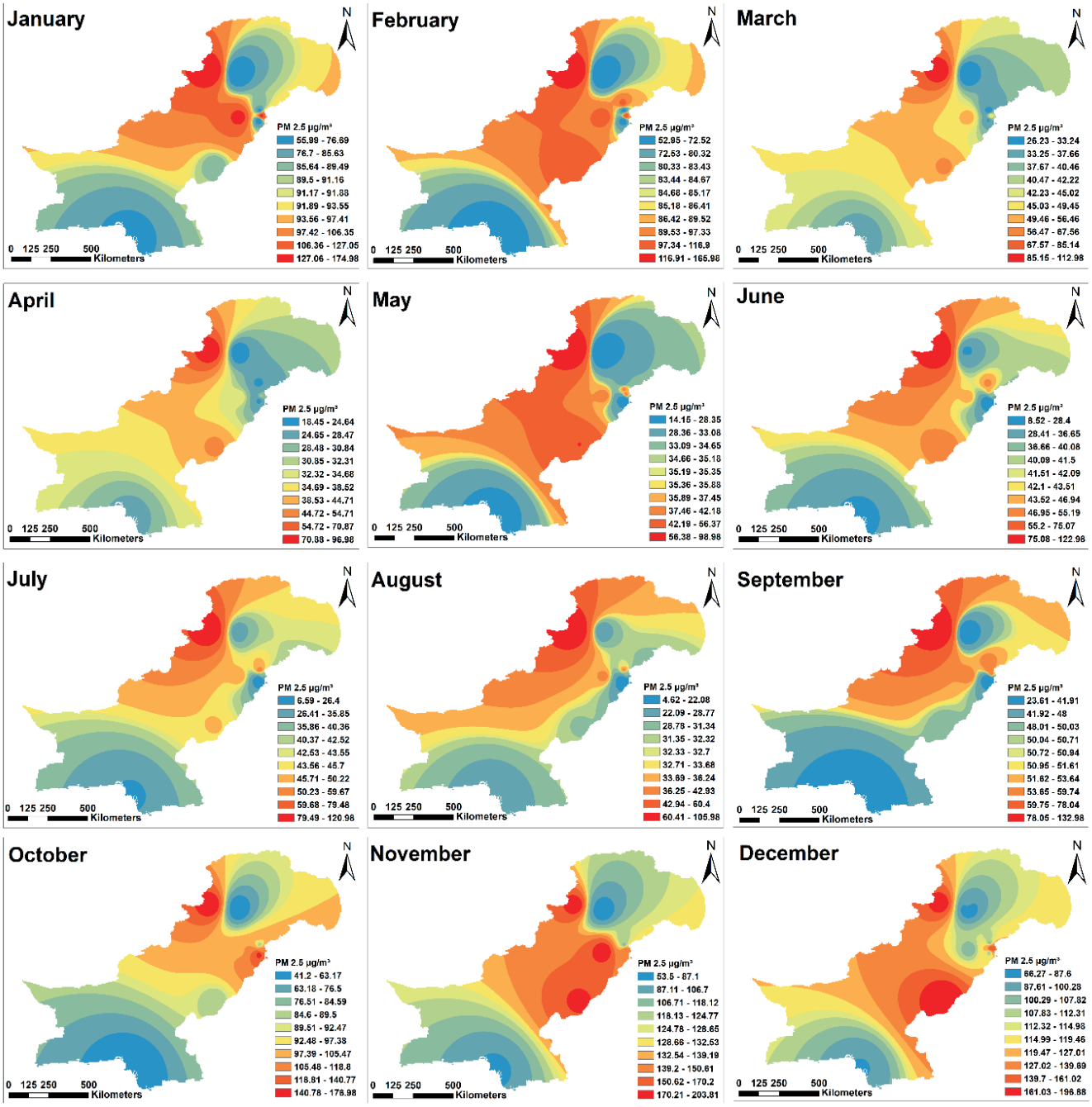

Fig. 4. Map Showing Monthly Spatial Distribution of Pm2.5 µg/m^3 in Pakistan for 2020

Table 1. $PM_{2.5}$ µg/m^3 Concentration in Major Cities of Pakistan during 2020 (Source: IQ Air 2020).

Cities	2020 mean	Jan	Feb	Mar	Apr	May	Jun	Jul	Aug	Sep	Oct	Nov	Dec
Lahore	79.2	138	107.3	47	31.4	38.9	39.9	39.7	30.8	56	109.9	151.3	161
Bahawalpur	78.7	86.7	112.8	57.8	46.6	56.5	49.8	46	31	48.8	85.5	177.2	196.9
Faisalabad	73.2	146.3	108.2	54.7	34.6	39.2	45.7	50	38.3	56.7	103.9	203.9	101.5
Gujranwala	62.1	86.6	104.4	35.6	22.4	30.7	49.8	46.6	32.4	57	98.6	118	110
Muridke	61.6	70.4	63.7	27.8	27.7	38.4	45.5	55.5	37.4	57.7	84.8	114.8	105.1
Raiwind	56.6	62	60.8	32.3	23.1	18.5	7.9	5.9	4.1	23	152.7	145.3	107.6
Karachi	43.8	70.9	60	35.4	26.9	24.1	25.6	24.6	24.6	29.7	41.2	80.9	86
Rawalpindi	42.4	55.9	55.5	26.2	18.4	14.1	24	29.2	22.8	35	51.1	82.9	93.7
Islamabad	39	63.5	52.9	26.7	22.4	18.8	29.8	33.2	27.2	32	42.4	53.3	66.1
Peshawar	140.6	175	166	113	97	99	123	121	106	133	177	193	185

WHO target | Good | Moderate | Unhealthy sensitive | Unhealthy | Very unhealthy | Hazardous

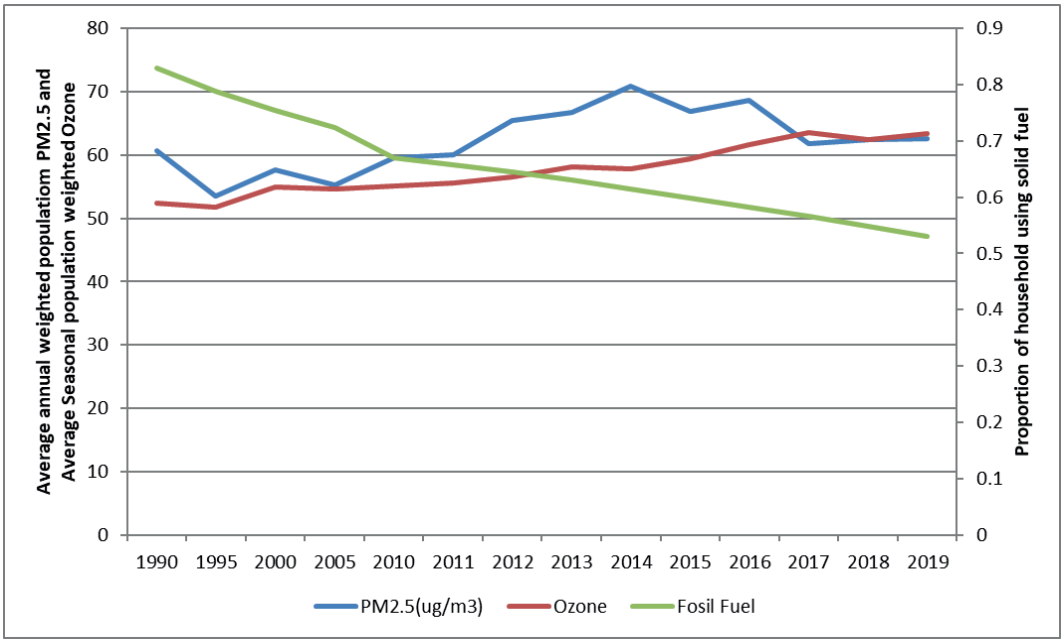

Fig. 5. The trend in the Proportion of the Population Using Solid Fuels, Average Annual Population-Weighted $PM_{2.5}$ (ug/m^3) and Average seasonal population-weighted Ozone in Pakistan (1990 to 2019)

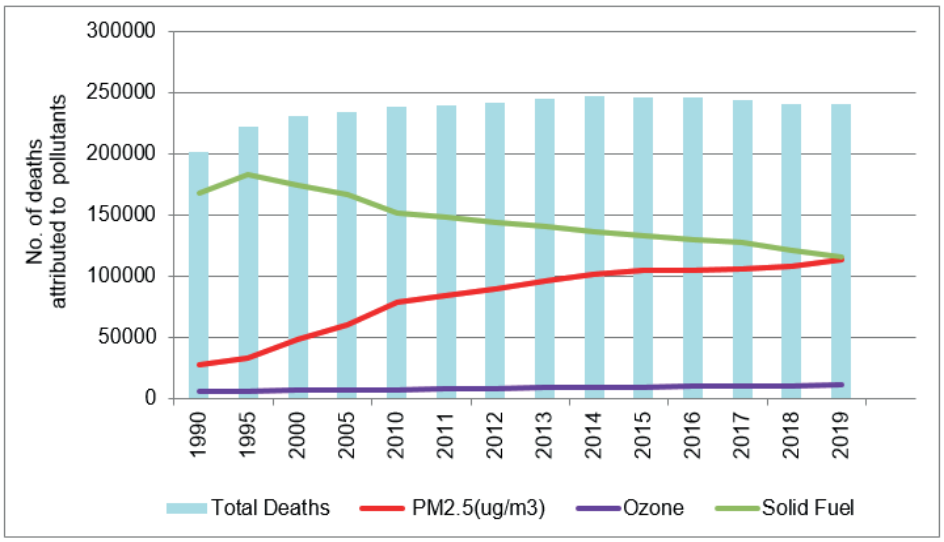

Fig. 6. The trend in the number of deaths attributed to major Pollutants in Pakistan (1990-2019)

Age Standardized DALYS attributed to Air Pollutants

Age-standardized DALYs/100,000 persons in Pakistan are shown in Fig. 7. The cumulative DALYs attributed to air pollution show a decreasing trend, but DALYs attributed to $PM_{2.5}$ increased since 1990. DALYs attributed to solid fuel decreased sharply, however, DALYs attributed to ozone remained constant as low as <500 DALYs/100,000 persons.

Cause-Specific Deaths

Fig. 8 shows the estimates of State of Global Air 2020, during 2019 in terms of case-specific deaths in Pakistan. COPD shows the highest burden with 57% of total deaths it causes during 2019. Similarly, among other respiratory diseases, lower respiratory infections (LRI) 40 % and Lung cancer 32% of total deaths can be attributed to air pollution. Besides this, ischemic heart disease and ischemic stroke constitute 36 and 35 per cent of their total deaths respectively. Almost 25% of diabetes deaths and 20% of neonatal outcomes deaths are also because of air pollution.

Cause-specific Burden of Diseases

Similar to mortality, morbidity due to air pollution can be measured by the cause-specific burden of diseases. Fig. 9 shows the cause of a specific burden of various diseases due to air pollution in Pakistan. Among these diseases, 53% of total COPD, 40% of LRI and 32% of lung cancer can be attributed to air pollution. Ischemic heart disease and ischemic stroke also show a high burden of 38 and 39 percent respectively. Diabetes and neonatal outcomes disease burden are < 25 per cent.

DISCUSSION

This research gives an overview of Pakistan's potential health outcomes related to air pollution. In 2019, Pakistan became the second most polluted country in the world. According to IDW, the majority of cities in Punjab and KPK have air quality levels that are about a year over the recommended limit which must not be more than 5 µg/m3 (WHO 2021c). Results also revealed that the northern and southern parts of the country show comparatively low concentrations of $PM_{2.5}$. In terms of seasonal variations, $PM_{2.5}$ concentration is more persistent between winters i.e., November to February. Time trends show that the proportion of the population using solid fuel decreased but the average annual weighted PM of 2.5 and average seasonal proportion weighted ozone kept on increasing since 1990. As a result, the mortality and morbidity attributed to solid fuel declined in comparison to $PM_{2.5}$ and ozone which increased massively causing the overall

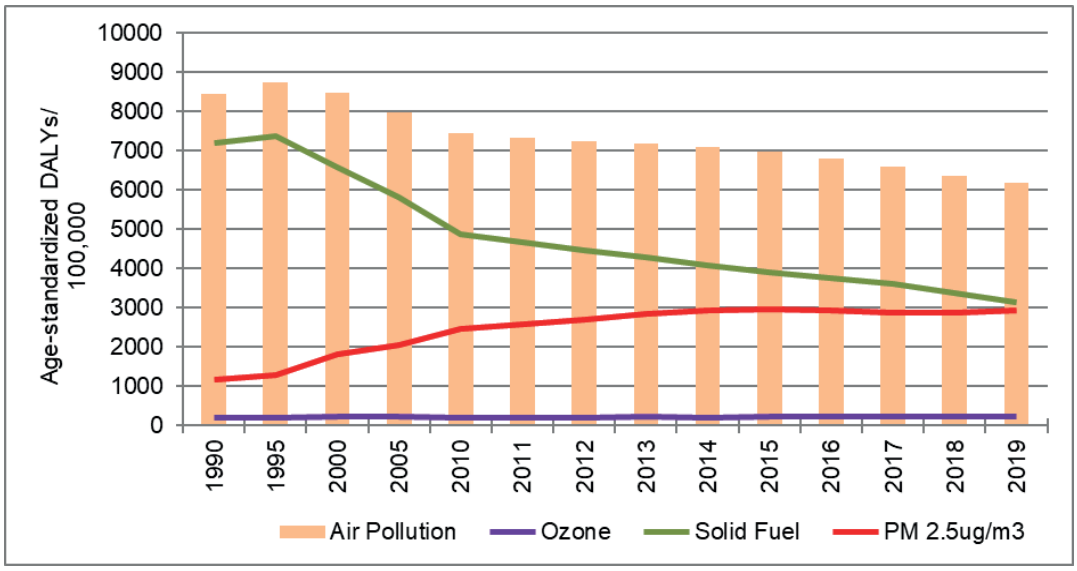

Fig. 7. The trend in Age-Standardized DALYs/100,000 attributed to major Pollutants in Pakistan (1990-2019)

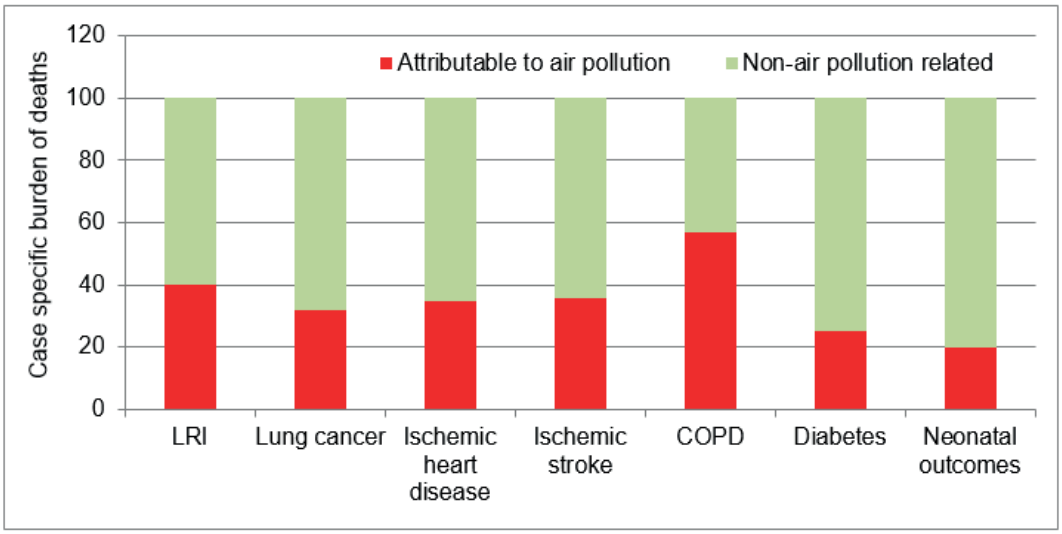

Fig. 8. Cause-specific Burden of Deaths in Pakistan (2019)

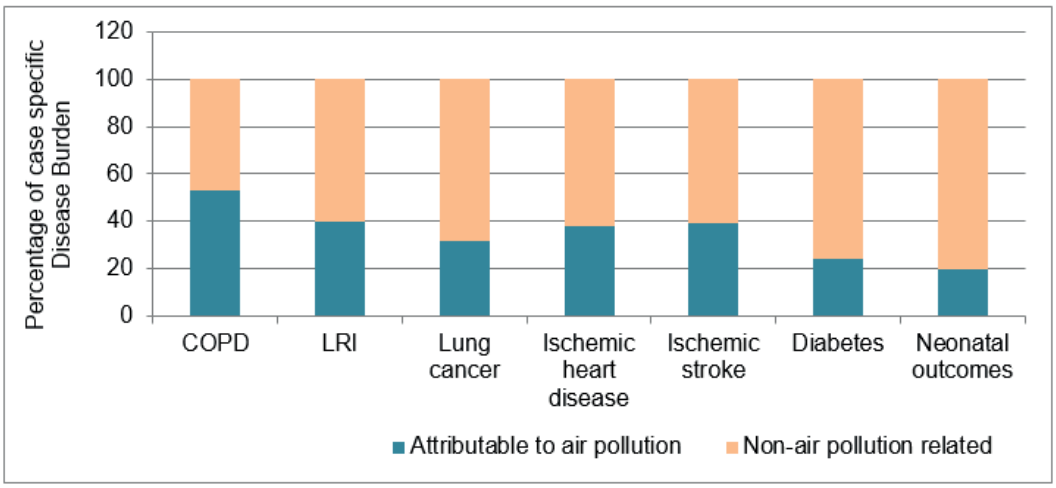

Fig. 9. Percentage of Case-Specific Burden of Diseases and Air Pollution

increase in health burden due to air pollution in Pakistan. COPD has the highest mortality and morbidity burden attributed to air pollution. LRI, lung cancer, ischemic heart diseases, ischemic stroke, diabetes and neonatal outcomes are also the main health problems relatable to air pollution in this country.

The ecosystem, biodiversity, human communities, animal habitations, forests, lands, and oceans are continually threatened by Pakistan's low adaptive capacity as a result of its high poverty rate, limited financial resources, lack of physical resources, and continual extreme climatic events such as varying temperatures, continuous flooding, melting glaciers, a saturation of lakes, earthquakes, hurricanes, storms, avalanches, droughts, scarcity of water, pest diseases, human healthcare issues, and seasonal and lifestyle changes (Hussain et al. 2019). The levels of $PM_{2.5}$ in all of Pakistan's major cities are above the legal limit. There are no facilities for continuous monitoring in the country. Lack of emission inventories, political will, and awareness are the greatest challenges (Anjum et al. 2021). Pakistan is the most urbanized country in the region, and it is undergoing fast motorization and increased energy demand, which is the cause of this terrible scenario. The main health effects of air pollution are associated, mainly, with increased premature mortality and learning disabilities (Sánchez-Triana et al. 2014). The uncontrolled urban population, increasing the number of vehicles, industries, and poor implementation of air quality standards have made the problem of air pollution even worst (Ali et al. 2017). Air pollution, particularly in large urban centres, harms the populations' health and quality of life, and contributes to environmental degradation (Sánchez-Triana et al. 2014). Pakistan's rapid growth in motor vehicle activity in cities has brought in its wake a range of serious socioeconomic, environmental, health, and welfare impacts (Ilyas 2007). The main challenges relating to air pollution control and monitoring in Pakistan include lack of awareness, failure of policy making and implementation, use of improper fuel, increasing energy demands and a smaller number of pollution monitoring stations. The establishment of a better monitoring system, developing of emission inventories and benchmarks, raising awareness and promoting sustainable policies and practices are all urgently needed to address these challenges (Anjum et al. 2021).

This research article has a few restrictions. Air pollution data of $PM_{2.5}$ is only available for the year 2020, which can represent results, that deviated from normal years due to the Covid-19 pandemic and the suspension of most of the transport and industrial activity in Pakistan. In addition, there was no data available on any site from the Baluchistan province. There is a lack of air pollution monitoring stations across Pakistan; hence no real-time data is used for this research. Despite these limitations, this research provides a spatial overview of air pollution across the country. Moreover, it provides evidence of the intense effects of air pollution causing different diseases in Pakistan. The research's findings can serve as a foundation for future studies that examine the relationship between numerous other social, economic, and environmental determinants of health as well as their regional differences across the country.

CONCLUSION

This descriptive research article is unique as it provides strong pieces of evidence of air pollution and its association with population health in terms of various disease burdens in Pakistan. The evidence relating to air pollution and its association with health outcomes has been presented in this research a clear picture of how bad the situation is in Pakistan. Air pollutants especially $PM_{2.5}$ and ozone are on the rise causing various health issues, particularly respiratory diseases. Thus, the current air pollution condition is not suitable for health in Pakistan, hence needed a strong monitoring system and implementation of clean and sustainable policies to regulate this environmental health issue. Government should initiate rapid action not only to minimise ambient air pollution but also to sensitize and aware public to adopt preventive measures. Furthermore, to support the nation's sustainable aims, this issue needs to be explored on a more scientific basis. This study also provides valuable facts and figures that provide the foundation for further scientific research linking each air pollutant with different diseases in Pakistan.

REFERENCES

Ali M.U., Rashid A., Yousaf B. and Kamal A. (2017). Health outcomes of road-traffic pollution among exposed roadside workers in Rawalpindi City, Pakistan. Human and Ecological Risk Assessment: An International Journal, 23, 1330-1339, DOI: 10.1080/10807039.2017.1308814.

Anjum M.S., Ali S.M., Subhani M.A., Anwar M.N., Nizami A.S., Ashraf U. and Khokhar M. F. (2021). An emerged challenge of air pollution and ever-increasing particulate matter in Pakistan; a critical review. Journal of Hazardous Materials, 402, 123-943, DOI: 10.1016/j.jhazmat.2020.123943.

Burki S.J., Ziring L., Ludin M., Qadir P., Rahman N., and Ilyas Q. (2021). Pakistan. Encyclopaedia Britannica.

Colbeck I., Nasir Z. A. and Ali Z. (2010). The state of indoor air quality in Pakistan — a review. Environmental Science and Pollution Research, 17(6), 1187-1196, DOI: 10.1007/s11356-010-0293-3.

Fiordelisi A., Piscitelli P., Trimarco B., Coscioni E., Iaccarino G. and Sorriento D. (2017). The mechanisms of air pollution and particulate matter in cardiovascular diseases. Heart Failure Reviews, 22, 337-347, DOI: 10.1007/s10741-017-9606-7.

Hussain M., Butt A.R., Uzma F., Ahmed R., Irshad S., Rehman A. and Yousaf B. (2019). A comprehensive review of climate change impacts, adaptation, and mitigation of environmental and natural calamities in Pakistan. Environmental Monitoring and Assessment, 192, 48, DOI: 10.1007/s10661-019-7956-4.

IHME. (2021). How We Estimate Burden of Disease [online]. Institute for Health Metrics and Evaluation. Available at: https://www.stateofglobalair.org/data/estimate-burden [Accessed 6 Nov. 2021].

Ilyas S.Z. (2007). A review of transport and urban air pollution in Pakistan. Journal of Applied Sciences and Environmental Management, 11, 35-45, DOI: 10.4314/jasem.v11i2.55004.

Ilyas S.Z., Khattak A.I., Nasir S.M., Qurashi T. and Durrani R. (2010). Air pollution assessment in urban areas and its impact on human health in the city of Quetta, Pakistan. Clean Technologies and Environmental Policy, 12, 291-299, DOI: 10.1007/s10098-009-0209-4.

IQAIR. (2020). World's most polluted countries 2020 (PM2.5) [online]. IQAir. Available at: https://www.iqair.com/world-most-polluted-countries [Accessed 29 Oct. 2021].

IQAIR. (2023). Air quality in Pakistan, [online] IQAir. Available at: https://www.iqair.com/pakistan [Accessed 19 May 2023].

Kampa M. and Castanas E. (2008). Human health effects of air pollution. Environmental Pollution, 151, 362-367, DOI: 10.1016/j.envpol.2007.06.012.

Khan M.S.B. and Lohano H.D. (2018). Household air pollution from cooking fuel and respiratory health risks for children in Pakistan. Environmental Science and Pollution Research, 25, 24778-24786, DOI: 10.1007/s11356-018-2513-1.

Khan A.A., Fatima M., Khan K. (2014). Spatial analysis of environmental health risks: A case of Bahawalpur district, Pakistan. Pakistan Journal of Commerce and Social Sciences, 8, 238-257.

Khwaja H.A., Fatmi Z., Malashock D., Aminov Z., Kazi A., Siddique A., Qureshi J. and Carpenter D.O. (2012). Effect of air pollution on daily morbidity in Karachi, Pakistan. Journal of Local and Global Health Science, 2012(3), DOI: 10.5339/jlghs.2012.3.

Kim K.H., Jahan S.A. and Kabir E. (2011). A review of diseases associated with household air pollution due to the use of biomass fuels. Journal of Hazardous Materials, 192, 425-431, DOI: 10.1016/j.jhazmat.2011.05.087.

Lee B.J., Kim B. and Lee K. (2014). Air Pollution Exposure and Cardiovascular Disease. Toxicological Research, 30(2), 71-75, DOI: 10.5487/TR.2014.30.2.071.

Mannucci P.M. and Franchini M. (2017). Health Effects of Ambient Air Pollution in Developing Countries. International Journal of Environmental Research and Public Health, 14, 1048, DOI: 10.3390/ijerph14091048.

Maqsood N., Younes I., and Nasar-u-Minallah M. (2019) Industrial Noise Pollution and Its Impact on the Hearing Capacity of Workers: A Case Study of Gujranwala City, Pakistan. International Journal of Economic and Environmental Geology, 10(2), 45-49, DOI: 10.46660/ijeeg.Vol10.Iss2.2019.261.

Mir K.A., Purohit P., Goldstein G.A. and Balasubramanian R. (2016). Analysis of baseline and alternative air quality scenarios for Pakistan: An integrated approach. Environmental Science and Pollution Research, 23, 21780-21793, DOI: 10.1007/s11356-016-7358-x.

Naz L. and Ghimire U. (2020). Assessing the prevalence trend of childhood pneumonia associated with indoor air pollution in Pakistan. Environmental Science and Pollution Research, 27, 44540-44551, DOI: 10.1007/s11356-020-10346-6.

Riaz K., Aziz N. and Riaz H. (2021). Estimating the Extreme Temperature Occurrence Over Pakistan Using Interannual and Interdecadal Temperature Variation and Teleconnections During 1901-2018. International Journal of Climate Research, Conscientia Beam, 5, 15-24, DOI: 10.18488/journal.112.2021.51.15.24.

Saldiva P.H.N., Lichtenfels A.J.F.C., Paiva P.S.O., Barone I.A., Martins M.A., Massad E., Pereira, J.C.R., Xavier V.P., Singer J.M. and Bohm G.M. (1994). Association between Air Pollution and Mortality Due to Respiratory Diseases in Children in São Paulo, Brazil: A Preliminary Report. Environmental Research, 65, 218-225, DOI: 10.1006/enrs.1994.1033.

Sánchez-Triana E., Enriquez S., Afzal J., Nakagawa A. and Khan A.S. (2014). Cleaning Pakistan's Air Policy Options to Address the Cost of Outdoor Air Pollution. Washington, DC: International Bank for Reconstruction and Development / The World Bank.

Sughis M., Nawrot T.S., Ihsan-ul-haque S., Amjad A. and Nemery B. (2012). Blood pressure and particulate air pollution in schoolchildren of Lahore, Pakistan. BMC Public Health, 12, 378, DOI: 10.1186/1471-2458-12-378.

Tabinda, A.B., Ali, H., Yasar, A., Rasheed, R., Mahmood, A. and Iqbal, A. (2020). Comparative Assessment of Ambient Air Quality of Major Cities of Pakistan. MAPAN, 35, 25-32.

Ullah S., Ullah N., Rajper S.A., Ahmad I. and Li Z. (2021). Air pollution and associated self-reported effects on the exposed students at Malakand division, Pakistan. Environmental Monitoring and Assessment, 193, 708, DOI: 10.1007/s10661-021-09484-2.

UNODC. (2022). Country Profile: Pakistan [online]. United Nations Office on Drugs and Crimes. Available at: https://www.unodc.org/pakistan/en/country-profile-pakistan.html [Accessed 12 Mar. 2023].

WHO. (2018). Household air pollution and health, [online] World Health Organization. Available at: https://www.who.int/news-room/fact-sheets/detail/household-air-pollution-and-health [Accessed 21 Jun. 2021].

WHO. (2021a). Air Pollution, [online] World Health Organization. Available at: https://www.who.int/health-topics/air-pollution#tab=tab_1 [Accessed 22 Jun. 2021].

WHO. (2021b). Air quality and health, [online] World Health Organization. Available at: https://www.who.int/teams/environment-climate-change-and-health/air-quality-and-health/health-impacts/types-of-pollutants [Accessed 23 Jun. 2021].

WHO (2021c). WHO global air quality guidelines: particulate matter (PM2. 5 and PM10), ozone, nitrogen dioxide, sulfur dioxide and carbon monoxide: executive summary.

Wong D.W., Yuan L. and Perlin S.A. (2004). Comparison of spatial interpolation methods for the estimation of air quality data. Journal of Exposure Science and Environmental Epidemiology, 14, 404-415, DOI: 10.1038/sj.jea.7500338.

Zia S., Yaqoob S., Nasar-u-Minallah M., Hanif A., and Aslam A. (2021). Relationship Analysis between Vegetation and Traffic Noise Pollution: A Case Study of Lahore, Pakistan. International Journal of Economic and Environmental Geology, 12(3), 65-69, DOI: 10.46660/ijeeg.Vol12.Iss3.2021.624.

RESEARCH PAPER

CO_2 EXCHANGE OF SEEDLINGS OF *RHIZOPHORA APICULATA BL.* IN ARTIFICIAL AND NATURAL MANGROVE FORESTS OF SOUTHERN VIETNAM

Nikolay G. Zhirenko[1,2], Van Thinh Nguyen[2], Juliya A. Kurbatova[1*]

[1]A.N. Severtsov Institute of Ecology and Evolution, Russian Academy of Sciences, Moscow, Russia

[2]Joint Russian–Vietnamese Tropical Scientific Research and Technological Center, Southern Branch, Ho Chi Minh City, Vietnam

***Corresponding author:** kurbatova.j@gmail.com

Received: July 14th, 2022 / Accepted: May 4th, 2023 / Published: July 1st, 2023

https://DOI-10.24057/2071-9388-2022-111

ABSTRACT. Mangrove forests are an important part of tropical coastal ecosystems. Until recently, these forests were intensively exterminated. Currently, the issue of mangrove conservation is being discussed at a number of symposiums due to their significant role in reducing the effects of greenhouse gas emissions. However, there has recently been uncertainty in estimation of CO_2 fluxes in mangrove forests due to a lack of field research.

The results of studies of photosynthesis at the leaf level in-situ in seedlings of *Rhizophora apiculata* Blume, 1827 of both natural and artificial origin are presented. The studies were carried out on a mangrove plantation growing in Can Gio Mangrove Biosphere Reserve, which is 50 kilometres from Ho Chi Minh City (South Vietnam). CO_2 gas exchange during photosynthesis was measured using a gas analysing system called the LI-6800 (USA).

Photosynthetically active radiation (PAR) is the main factor affecting the photosynthesis of the studied seedlings. Artificial seedlings that were grown in open areas had higher productivity and greater photosynthetic rates. It has been determined that the measured photosynthesis are scattered over three clearly marked zones, which correspond to the measurements of photosynthesis made in the pre-noon, noon and afternoon hours. The water reserves used up before noon were not fully replenished in the afternoon by the seedlings. Based on the results obtained, it has been suggested that the main inhibitory factor affecting the photosynthesis of *R. apiculata* (if PAR is not taken into account) is a violation of the water balance of the leaves.The optimum air temperature for photosynthesis processes in seedlings is (35 ± 2) °C. The intensity of photosynthesis also increases with an increase in the concentration of CO_2 in the air. The increases of photosynthesis continue until the concentration of CO_2 reaches ~1000 μmol·mol^{-1} and then do not increase. We associate this circumstance with the maximum possibilities of the photosynthetic apparatus of the leaf of the studied plant.

The obtained research results will contribute to a better theoretical understanding of the productivity of plants of this species in the respective ecosystems, and will also allow us to move from photosynthesis at the leaf level to photosynthesis at the planting level. The work's mathematical models can be used to model changes in *R. apiculata* photosynthesis from the point of view of climate change.

KEYWORDS: *Rhizophora apiculata*, air temperature, CO_2 concentration, diurnal dynamics, the intensity of photosynthesis, light response curve

CITATION: Zhirenko N. G., Nguyen Van Th., Kurbatova J. A. (2023). CO_2 Exchange Of Seedlings Of *Rhizophora Apiculata Bl.* In Artificial And Natural Mangrove Forests Of Southern Vietnam. Geography, Environment, Sustainability, 2(16), 102-109
https://DOI-10.24057/2071-9388-2022-111

Conflict of interests: The authors reported no potential conflict of interest.

INTRODUCTION

Mangrove forests are one of the unique forest ecosystems. They are an important part of tropical coastal ecosystems. Mangroves play important ecological roles as well as serving as a source of income (Donato et al. 2011; Hogarth 2007; Hogarth 2008; Simard et al. 2019; Saintilan et al. 2020).

However, the degradation of mangrove ecosystems is currently being observed (Alongi 2002; Valiela et al. 2001; Nguyen 2000). This is a result of economic activity, which primarily entails the clearing of these forests (Luong 2014), as well as ongoing global warming (Desherevskaya et al. 2013), which causes sea levels to rise, flooding of mangrove forests, and the drying up of specific mangrove ecotopes (FAO 2007; Simard et al. 2019).

Scientists are therefore undoubtedly interested in studying mangrove ecosystems. Studying the physiological properties of mangroves is one of the main foci of this type of research. The studies pertaining to their gas exchange are the most relevant of these (Clough 1997). Nevertheless, despite having enough knowledge in this area of research, many unanswered questions still exist. In particular, this applies to the mangroves of Vietnam.

Our estimates place *Rhizophora apiculata* Blume, 1827 as one of the most common tree species in the mangrove forests of South Vietnam. This species is widely used in reforestation

activities (Hogarth 2007). Forming grandiose plantations due to its stilted roots, *R. apiculata* plays an important role in the ecology of mangrove forests (Thongjoo et al. 2018; Wenfang et al. 2020). Of undoubted interest is the fact that *R. apiculata* belongs to plants with C4 photosynthesis, which allows the plant to better adapt when growing in conditions of high temperatures and lack of water (Ehleringer and Björkman 1977; Slack and Hatch 1967). Therefore, it is not accidental that many researchers pay attention to this species (Christensen 1978; Ong et al. 1995).

Our previous studies on mature *R. apiculata* trees showed that photosynthesis depression in these trees began to appear at noon and persisted until the end of the day (Đô Phong Lủu et al. 2021). Based on this, we hypothesized that the parameters characterizing the photosynthetic abilities of *R. apiculata* should differ at different times of the day. We found no studies to support or refute our hypothesis. We also assumed that plants growing in various environments should have varying values for these characteristics.

The proposed hypothesis, which was to investigate the daily change of the indicators of the photosynthetic capacity of *R. apiculata* seedlings of artificial and natural origin, determined the goal of the study.

The following tasks were established in accordance with the study's goal: 1) to obtain daily dynamics of the intensity of photosynthesis for seedlings of artificial and natural origin; 2) to model the response curves of photosynthesis to light according to the Michaelis-Munten equation (1); 3) to obtain the dependence of photosynthesis on temperature and CO_2 concentration in the air; 4) to analyze the obtained results.

The results of our research of the photosynthetic exchange of CO_2 at the leaf level in-situ of seedlings of *R. apiculata* of natural and artificial origin are presented in this article. These results can be used to recalculate photosynthesis at the leaf level, down to the planting level. Also, the results will help in predicting how plants of this species will grow in the future in relation to climatic changes around the world. The results of the study will be helpful in creating reforestation strategies.

MATERIALS AND METHODS

Study site, plant material and growing conditions

The research was carried out in July 2020 in a mangrove plantation located in the Can Gio Biosphere Reserve, located 50 km from Ho Chi Minh City (10°28´36´´N, 106°54´17´´E) (South Vietnam). As the test subject, 5-year-old seedlings of *Rhizophora apiculata* Blume, 1827, both of artificial and natural origin, were selected.

Artificial seedlings grew in an open area and were intended for reforestation activities (Fig. 1a). The number of studied seedlings n = 27, their average height h = 57 cm (Standard Deviation, SD = 7 cm), the average number of leaves per seedling N = 35 (SD = 16).

Natural seedlings grew along the edge of the water channel on its northern side (Fig. 1b). The seedlings were formed as a result of the germination of floating fruits that were washed ashore. At noon, the seedlings were shaded by the trees and shrubs growing behind them. Seedling parameters: n = 14, h = 88 cm (SD = 8 cm), N = 10 (SD = 5). Twice a day, both sites were flooded with water as a result of sea tides.

Measurement of photosynthetic gas exchange and experimental design

Photosynthesis processes were considered from the standpoint of CO_2 gas exchange. The rate of photosynthesis (photosynthesis) was measured using a Portable Photosynthesis System LI-6800 (Li-Cor Inc., USA). For artificial illumination of the investigated part of the sheet, a 3 × 3 cm light source was used, supplied by the LI-6800 manufacturer as an addition to the device. The emission spectrum of the light source consists of red (λ = 660 nm) and blue (λ = 453 nm) colours. When using it, the object was illuminated with light, consisting of red and blue colours in a ratio of 9: 1. During measurements under natural light, photosynthetically active radiation (PAR) was measured using a sensor located in the LI-6800 measuring chamber.

During measurements, the required microclimate parameters were set in the LI-6800 measuring chamber – object illumination, air temperature and humidity, CO_2 concentration.

For the study, we used the formed intact leaves, as a rule, located on the penultimate node of the shoot. The measurements were carried out in the middle part of the leaf, bounded by the frame of the LI-6800 measuring chamber with an aperture of 3x3 cm. Current measurements of photosynthesis were carried out on 2–4 randomly selected seedlings. To construct the diurnal graphical dependencies, the average values of the measured values were used.

Studies of the dependence of photosynthesis on temperature were carried out on artificial seedlings. During measurements, the following microclimate parameters were set in the LI-6800 measuring chamber: illumination

Fig. 1. Studied seedlings of *R. apiculata* of artificial (a) and natural (b) origins

1000 μmol·m^{-2}·s^{-1}, CO_2 concentration 400 μmol·mol^{-1}, humidity ~ 60%. The measurements were carried out in an automatic mode in the temperature range from 24 to 46 °C.

Studies of the dependence of photosynthesis on CO_2 concentration were also carried out on artificial seedlings. During measurements, the following microclimate parameters were set in the LI-6800 measuring chamber: illumination 1000 μmol·m^{-2}·s^{-1}, temperature 30 °C, humidity ~ 70%. The measurements were carried out in an automatic mode in the CO_2 concentration range from 350 to 1000 μmol·mol^{-1} with a step of 50 μmol·mol^{-1}.

The work used meteorological data obtained from a meteorological station located on the territory of the reserve.

Diurnal curves of photosynthesis and PAR

The data for plotting the diurnal dynamics of photosynthesis and PAR were obtained over two days: July 4, 2020, from 15:00 to 19:00 and July 27, 2020, from 05:00 to 14:30. The total solar radiation these days differed by 6% (the cloudiness on July 4, 2020, in the first half of the day was slightly higher). The average air temperature during the daylight hours on July 4, 2020, was 34 °C, and on July 27, 2020 – 36 °C.

The measurements were carried out with an interval of ~20 min with the following microclimate parameters in the LI-6800 measuring chamber: CO_2 content 400 μmol·mol^{-1}, humidity ~65%, temperature ~32 °C.

In order to conduct a more detailed analysis of the obtained dependences, daily measurements were divided into three time periods: pre-noon time – from 06:00 to 09:30, noon – from 09:30 to 15:30 and afternoon – from 15:30 to 18:30.

The total values of PAR and CO_2 gas exchange were calculated for a full day, as well as in the pre-noon time – from 00:00 to 12:00 and in the afternoon – from 12:00 to 24:00.

Light-response curves

The Michaelis–Munten equation served as the foundation for the mathematical explanation of the photosynthetic light response curves (Michaelis and Menten 1913). We used this equation in a modified form (Kaipiainen 2009):

$$A = A_m \times Q / \left(Q + K_M\right) + A_d \quad (1)$$

where A is the intensity of photosynthesis, μmol·m^{-2}·s^{-1};
A_m – is the maximum intensity of photosynthesis, μmol·m^{-2}·s^{-1};
Q – PAR, μmol·m^{-2}·s^{-1}; A_d - respiration rate at $Q = 0$, μmol·m^{-2}·s^{-1};
K_M – Michaelis constant (K_M is numerically equal to PAR, at which the intensity of photosynthesis is half of the maximum $A = 0.5A_m$). K_m values are often used by researchers when comparing the physiological characteristics of plants (Hieke et al. 2002). According to (1), the light compensation point (*LCP*) was determined, μmol·m^{-2}·s^{-1}, which shows at what intensity of PAR photosynthesis becomes zero.

To assess the efficiency of photosynthesis, we propose to use the slope of the tangent *a* (italic font) to the function curve of (1) at the point corresponding to K_M. From a physical point of view, this coefficient reflects the rate of change in the intensity of photosynthesis with a change in PAR by one unit.

Statistical analysis

Data processing was carried out using the MS Excel "Descriptive statistics" package ($p < 0.05$). The degrees of association of the studied datasets were determined using Pearson's correlation coefficients, *r*. To determine the statistical significance of the coefficient *r*, *p*-values were calculated. *P*-values were calculated using the T.TEST function and corresponded to a paired Student's t-test with a two-tailed distribution at a significance level of α = 0.05. The parameters of equation (1) were selected using the MS Excel package "Parameters of the solution search" (the limiting number of iterations is 100, the relative error is 0.00001, the permissible deviation is 5%, the convergence is 0.0001). The slope *a* of the tangent, the coefficients of the equation for this tangent, as well as the extremum points of the graphical dependencies, were determined using differentiation methods. The total values of the investigated quantities were determined by the integration method. Graphing was carried out using the MS Excel environment.

RESULTS

Diurnal dynamics of photosynthesis and PAR

Fig. 2 shows the daily dynamics of the intensity of photosynthesis and PAR, obtained as a result of measurements on seedlings of artificial origin.

Fig. 3 shows the daily dynamics of the intensity of photosynthesis and PAR, obtained as a result of measurements on seedlings of natural origin.

The indicators characterizing the degree of association *r* between the intensity of photosynthesis *A* and PAR, as well as the values of total PAR and CO_2 gas exchange for daily dynamics of the intensity of photosynthesis and PAR of seedlings of artificial and natural origin, are summarized in Table 1.

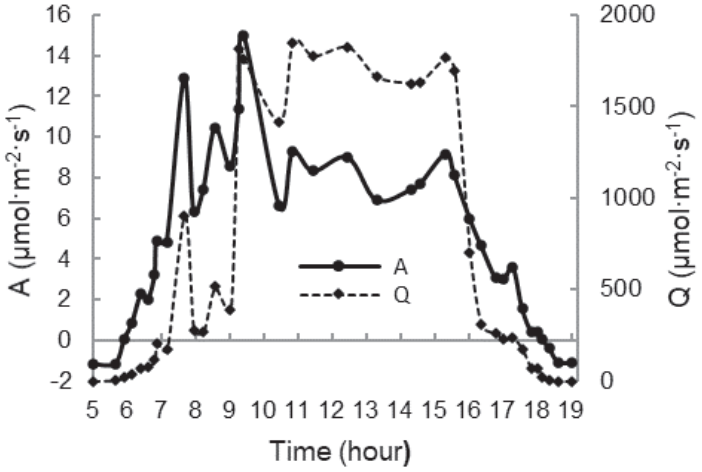

Fig. 2. Daily dynamics of the intensity of photosynthesis – *A*, and PAR – *Q*, of artificial seedlings

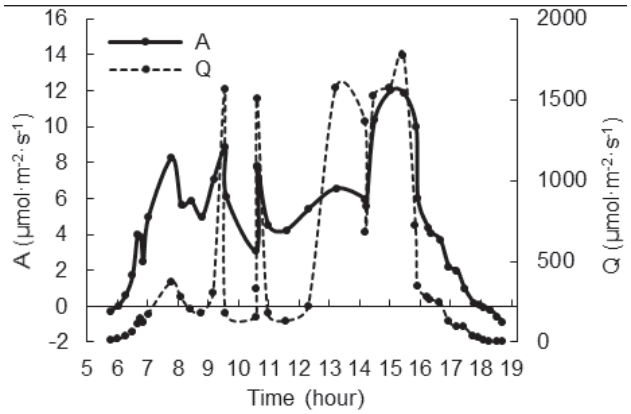

Fig. 3. Daily dynamics of the intensity of photosynthesis – *A*, and PAR – *Q*, seedlings of natural origin

Table 1. Indicators characterizing daily dynamics of photosynthesis and PAR in seedlings of artificial and natural origin

Index	Seedlings of artificial origin / Seedlings of natural origin			
	Whole day	Pre-noon time	Noontime	Afternoon time
r / *p*	0.78 / 4.7E-06 0.78 / 2.1E-05	0.85 / 0.012 0.96 / 0.002	0.50 / 5.0E-09 0.77 / 0.006	0.87 / 0.044 0.90 / 0.006
Total PAR, mol·m^{-2}	46.9±2.4 24.2±1.3	24.2±1.3 5.8±0.3		22.8±1.2 18.4±1.0
Total gas exchange CO_2, mol·m^{-2}	0.304±0.016 0.241±0.013	0.154±0.008 0.103±0.006		0.151±0.008 0.138±0.007

Light-response curves

Fig. 4 shows the values of photosynthesis depending on PAR, measured on seedlings of artificial (Fig. 4a) and natural (Fig. 4b) origin. The figures also show the curves approximating these values, constructed according to (1) for the values obtained in the pre-noon (curves 1) and in the afternoon (curves 2) and tangents to these curves at the points corresponding to the K_M values.

The indicators characterizing the photosynthetic characteristics of seedlings obtained according to (1), as well as the R^2 values for the curves plotted and the number of measurements n, are summarized in Table 2.

Dependence of photosynthesis on temperature and on CO_2 concentration

The obtained values of the intensity of photosynthesis for seedlings of artificial origin, as a function of the temperature *T* of the air surrounding the leaf, are approximated by a quadratic equation (R^2=0.97, n=20):

$$A(T) = -0.0889T^2 + 6.2453T - 100.84 \quad (2)$$

The extremum of this function corresponds to a value of T = 35 °C. Therefore, taking into account measurement errors, the optimal temperature for photosynthesis of *R. apiculata* seedlings is T_{opt} = 35 ± 2 °C.

The dependence of the intensity of photosynthesis of *R. apiculata* on the concentration of CO_2 in the air is described by a quadratic equation (R^2=1.00, *n*=13):

$$A(CO_2) = -8E-06(CO_2)^2 + 0.016(CO_2) - 0.599 \quad (3)$$

DISCUSSION

Effect of PAR on photosynthesis

The following unique patterns can be seen in the diurnal dynamics of the intensity of photosynthesis in seedlings of artificial origin (Fig. 2, Table 1):

1) an increase in photosynthesis to maximum values in the pre-noon time, up to 09:30, in proportion to an increase in PAR (*r* = 0.85);

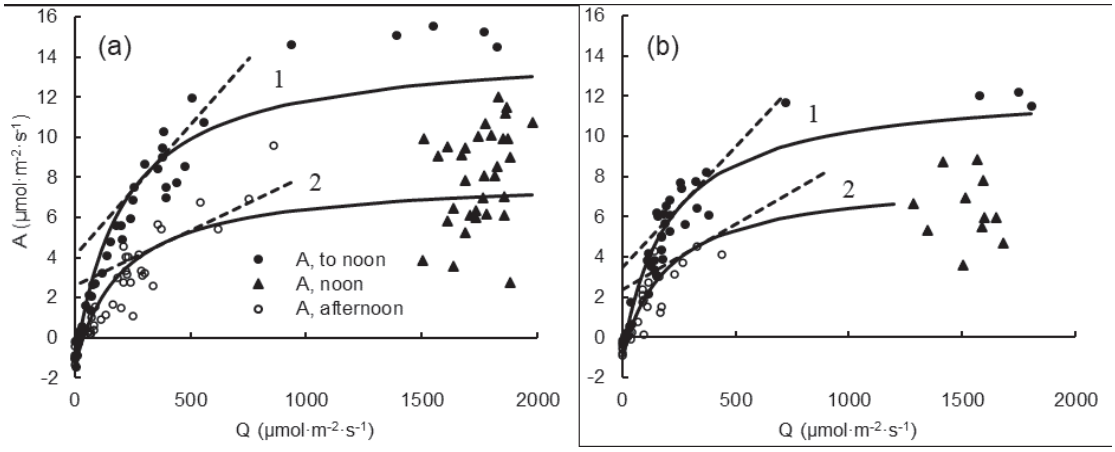

Fig. 4. Dependences of the intensity of photosynthesis – *A*, on PAR – *Q*, obtained on seedlings of artificial (a) and natural (b) origins

Table 2. Indicators characterizing photosynthetic characteristics of seedlings

Index	Seedlings of artificial origin		Seedlings of natural origin	
	Pre-noon time	Afternoon time	Pre-noon time	Afternoon time
R^2	0.97	0.90	0.95	0.89
n	124		94	
A_m, μmol·m^{-2}·s^{-1}	16.0	9.5	13.5	8.9
a	0.013	0.006	0.012	0.007
K_M	202.5	202.7	204.2	204.6
Ad, μmol·m^{-2}·s^{-1}	-1.5		-1.0	
LCP, μmol·m^{-2}·s^{-1}	21.0	38.0	16.3	25.9

2) a decline in photosynthesis from maximum values to values corresponding on average to 8.0 μmol·m^{-2}·s^{-1} (SD = 2.4 μmol·m^{-2}·s^{-1}), and the exit of the photosynthesis curve to a kind of plateau at noon, from 09:30 to 15:30, with a weak dependence of photosynthesis on PAR ($r = 0.50$);

3) a decline in photosynthesis in the afternoon, from 15:30, in proportion to a decrease in PAR ($r = 0.87$);

4) negative values, indicating the processes of respiration occurring in the leaf, at night.

It is interesting to note that the same diurnal dynamic was obtained for the light leaves of *Rhizophora mucronata* Poir. growing in Indian red mangroves (Kumar et al. 2017).

In order to give a more detailed interpretation of the listed patterns, let us turn to the dependences of photosynthesis on PAR (Fig. 4a) and indicators characterizing the photosynthetic characteristics of seedlings (Table 2).

The markers representing the obtained photosynthesis values are distributed in three clearly marked zones: 1 – in the zone corresponding to the photosynthesis values obtained in the pre-noon (markers in the form of circles); 2 – in the zone corresponding to the values obtained at noontime (triangular markers); 3 – in the zone corresponding to the values obtained in the afternoon (markers in the form of open circles) (Fig. 4a).

The curves plotted according to (1) for the photosynthesis values obtained in the pre-noon and afternoon (Fig. 4a) have a high degree of association (Table 2). The K_M coefficients characterizing the physiological characteristics of plants are approximately the same, which is obvious since we examined plants of the same type. However, the maximum intensity of photosynthesis, Am, in seedlings in the pre-noon time was significantly higher than in the afternoon. The same applies to the slopes *a*. Thus, in artificial seedlings, the efficiency of photosynthesis in the pre-noon time was 2.2 times higher than in the afternoon.

On the other hand, the *LCP* for these seedlings in the afternoon was 1.8 times higher than that in the pre-noon. That is, in the afternoon, at a PAR of 38.0 μmol·m^{-2}·s^{-1}, the absorption of CO_2 by the leaf was compensated by its release. Such processes are caused by respiration, as a rule, associated with metabolic processes occurring in the leaf. In addition to the foregoing, it should be mentioned that these seedlings' photosynthesis, is sated when the PAR is about 1800 μmol·m^{-2}·s^{-1}, as shown in Fig. 2 and Fig. 4a.

Similar patterns in the dynamics of photosynthesis, indicating its different behaviour in the pre-noon and daytime hours, in similar studies by other researchers, the authors of this work did not reveal. However, it should be noted that the authors of the work (Ball et al. 1997), when conducting similar studies, noted a very large scatter of data. With the exception of measurements taken around noon, this was not noticed in our research.

The daily dynamics of photosynthesis in seedlings of natural origin (Fig. 3, Table 1), in general, is characterized by the same regularities as in seedlings of artificial origin. Distinctive features of these dynamics are somewhat large values of r obtained before and afternoon (0.96 and 0.90), as well as the presence of a relationship between photosynthesis and PAR at noon ($r = 0.77$).

A similar situation emerges when analyzing the features of photosynthesis of seedlings according to Fig. 4b – the obtained values of photosynthesis are also distributed in the three zones indicated above.

The plotted curves (1) for the values of photosynthesis obtained before and afternoon also have a high degree of association (Table 2). The K_M coefficients are approximately the same. The maximum intensity of photosynthesis, A_m, in seedlings in the pre-noon time is significantly higher than in the afternoon. The same applies to the slopes *a*. Thus, in seedlings of natural origin, the efficiency of photosynthesis in the pre-noon time was 1.7 times higher than in the afternoon. The *LCP* for these seedlings in the afternoon was 1.6 times higher than that in the pre-noon time. In the afternoon, *LCP* was 25.9 μmol·m^{-2}·s^{-1}.

Summarizing what has been said, we can present a comparative analysis of the characteristics of the growth of seedlings of artificial and natural origin.

On the one hand, these seedlings have similar characteristics. Thus, the diurnal dynamics of seedlings are characterized by an increase in photosynthesis in the pre-noon and a decrease in photosynthesis in the afternoon, with strong degrees of connection with PAR (Fig. 2, Fig. 3, Table 1). The obtained values of photosynthesis are distributed in three clearly marked zones, corresponding to the values of photosynthesis obtained in the pre-noon, noon and afternoon (Fig. 4a and Fig. 4b). Photosynthesis values obtained in the pre and afternoon time are described with a high degree of association.

Slope coefficients *a* obtained for seedlings during the pre-noon and during the afternoon are identical (Table 2). Accordingly, the efficiency of photosynthesis during pre-noon and during the afternoon is approximately the same; and during pre-noon, it is higher than during the afternoon. K_M coefficients for seedlings are approximately the same. *LCP* for seedlings in the afternoon was higher than that during the pre-noon.

On the other hand, the seedlings under consideration also have distinctive characteristics. So, at noon, photosynthesis in seedlings of artificial origin was more stochastic, while in seedlings of natural origin, there is a connection between photosynthesis and PAR. Further,

the maximum values of photosynthesis, A_m, for seedlings of artificial origin, both during pre-noon and afternoon, were significantly higher than those of seedlings of natural origin. This is primarily due to different lighting conditions of seedlings: the total PAR for artificial seedlings was 46.9 ± 2.4 mol·m^{-2} (in the first and second half of the day it was 23.5 ± 1.3 mol·m^{-2}), while for seedlings natural origin - 24.2 ± 1.3 mol·m^{-2} (in the first half of the day it was 5.8 ± 0.3 mol·m^{-2}, in the second - 18.4 ± 1.0 mol·m^{-2}) (Table 1).

Accordingly, the total CO_2 gas exchange for artificial seedlings was 0.304 ± 0.016 mol·m^{-2} (in the first and second half of the day it was the same and amounted to 0.153 ± 0.008 mol m^{-2}), whereas, for seedlings of natural origin, the total CO_2 exchange was 0.241 ± 0.013 mol·m^{-2} (in the first half of the day it was 0.103 ± 0.006, in the second – 0.138 ± 0.007 mol·m^{-2}) (Table 1).

The saturation of photosynthesis for these seedlings (Fig. 3 and Fig. 4b) occurs when PAR equals about 1500 µmol·m^{-2}·s^{-1}.

It should be noted here that the saturation values of photosynthesis obtained by us, both for artificial seedlings and for seedlings of natural origin, are fundamentally different from those presented in (Ball et al. 1997) that was amounting to about 400 µmol·m^{-2}·s^{-1}.

Thus, seedlings of artificial origin had higher productivity, and this was determined, first of all, by the amount of PAR supplied to the plants. Higher metabolic processes occurring in the leaves of seedlings of artificial origin are also indicated by higher values of *LCP* and A_d (Table 2).

Naturally, the considered physiological parameters affected the morphological characteristics of the seedlings. Thus, the average number of leaves on a seedling of artificial origin is N = 35 (SD = 16), while on a seedling of natural origin - N = 10 (SD = 5). However, such a significant difference in the number of leaves on seedlings was to some extent compensated by the height – seedlings of natural origin were 1.5 times higher.

Effect of temperature and CO2 concentration on photosynthesis

Analysis (2) showed that the optimal air temperature for photosynthesis of *R. apiculata* is T_{opt} = 35 ± 2 °C. It can be noted here that our similar studies on an adult tree *R. apiculata* of natural origin gave the same result (Đô Phong Lủu et al. 2021). According to (Ball et al. 1997), this figure is approximately 38 °C. However, the authors noted a large scatter of data and, unfortunately, do not indicate the amount of error in the determined value. In another work (Okimoto et al. 2013), two values of this temperature are given: 33 °C and 26 °C. Because the authors used similar equipment to carry out their studies, taking into account the error, we can say that the first temperature coincides with T_{opt}. Thus, the deviation of the air temperature from T_{opt}, both to a lower and to a higher side, causes a decrease in photosynthesis in *R. apiculata*. This circumstance is confirmed, for example, by studies (Sage and Kubien 2007; Kristine et al. 2022), which studied the temperature responses of various tropical plants, including those with C4 photosynthesis.

The average air temperature during measurements at noon was 37.2 °C (SD = 1.0 °C). However, such temperatures could cause a decrease in photosynthesis by only 0.1%. On the other hand, we did not measure the temperature of the leaves, which, as a result of exposure to direct solar radiation (Fig. 1a and Fig. 2), could be quite high. High leaf temperatures inhibit photosynthesis. In addition, plants could experience a water shortage. For example, our studies related to the moisture content of leaves in relation to their absolutely dry weight on an adult *R. apiculata* tree showed that from 08:50 to 15:20 the leaves were losing 34% of moisture.

It is possible that in different leaves of seedlings, water deficiency manifested itself in different ways with corresponding changes in photosynthesis. At least, this hypothesis can explain the stochastic distribution of the values of photosynthesis in artificial seedlings at noon.

In contrast to this, in seedlings of natural origin, the presence of a connection between photosynthesis and PAR was noted at noon. This is due to the fact that these seedlings in midday time were shadowed by the trees and shrubs growing behind them (Fig. 1b and Fig. 3). As a result, the leaves of these seedlings were exposed to significantly less overheating and so experienced less water deficit.

Based on what has been said, we can make the following assumption. In the studied seedlings, the water consumed during midday time was not completely restored afterwards. This can explain the significantly lower photosynthetic parameters observed in seedlings during the afternoon (Table 2) than during the pre-noon. This assumption is confirmed by the conclusions made in the work (Kumar et al. 2017).

The dependence of the intensity of photosynthesis in *R. apiculata* on the CO_2 concentration in the air is described by equation (3). It follows from this equation that in the range of CO_2 concentrations under consideration, with its increase, photosynthesis naturally increases. Obviously, this circumstance has a positive effect on plant growth. An increase in the growth of *R. apiculata* seedlings at increased CO_2 concentration in the air is noted by (Eong et al. 1997; Kumar et al. 2017).

The analysis of function (3) for extrema shows that the increase in photosynthesis occurs up to the CO_2 concentration in the air, reaching ~1000 µmol·mol^{-1}. Interpolation of the obtained results allows us to make the assumption that at a CO_2 concentration of ~1000 µmol·mol^{-1}, *R. apiculata* photosynthesis reaches maximum values and does ot increase with further increases in CO_2 concentration. This circumstance, first of all, is determined by the maximum capabilities of the photosynthetic apparatus of the leaf of the studied plant.

The presented dependences of photosynthesis on temperature and CO_2 concentration find their confirmation also in a number of works related to the study of the effect of elevated temperature and CO_2 concentration, simulating global warming, on photosynthesis of C4 plants (Alberto et al. 1996; Ghannoum et al. 2000; Read and Morgan 1996; Morgan et al. 1994).

In our case, for example, if we consider the most optimistic forecasts associated with an increase in the concentration of CO_2 in the air in the next decade from 412 ppm to 460 ppm (and this concentration is already observed over cities), then the intensity of photosynthesis in the studied seedlings will increase by about 6%. This trend will be one of the tools for stabilizing the climate on Earth.

CONCLUSIONS

PAR is an obvious determining factor influencing the photosynthesis of *R. apiculatta* seedlings under study. This determines the higher productivity of seedlings of artificial origin growing in open areas compared to seedlings of natural origin. In addition, as a result of the study, we found that the indicators characterizing the photosynthetic

features of seedlings in the pre-noon, noon and afternoon hours are fundamentally different. The best photosynthetic parameters were observed in seedlings in the pre-noon time. The main reason for this was the violation of the water balance of the leaves – the water consumed in the midday time, stored in the leaves during the night, was not fully restored later.

The optimum air temperature for photosynthesis in *R. apiculatta* seedlings is (35 ± 2) °C. With an increase in the concentration of CO_2 in the air, the intensity of *R. apiculatta* photosynthesis naturally increases. The increases of photosynthesis continue up to the concentration of CO_2 ~1000 μmol·mol^{-1} and then does not increase. We associate this circumstance with the maximum possibilities of the photosynthetic apparatus of the leaf of the studied plant.

Our developed mathematical models according to the Michaelis–Munten equation (1), Table 2, describe the dependence of photosynthesis on the PAR of the studied seedlings, as well as mathematical models describing the dependence of the intensity of photosynthesis on air temperature (2) and CO_2 concentration in the air (3), in the future, they will make it possible to move on to a general model describing the dependence of photosynthesis on three main environmental factors: PAR, temperature, and CO_2 concentration. And another important point of our research is the prospect of recalculating photosynthesis at the leaf level to the plantation level, which will ultimately allow us to quantify the CO_2 balance of the plantation.

REFERENCES

Alberto A.M.P., Ziska L.H., Cervancia C.R., Manalo P.A. (1996). The influence of increasing carbon dioxide and temperature on competitive interactions between a C3 crop, rice (Oryza sativa) and a C4 weed (Echinochloa glabrescens). Australian Journal of Plant Physiology, 23, 795-802.

Alongi D.M. (2002). Present state and future of the world's mangrove forests. Environ. Conserv, 29, 331-349.

Ball M.C., Cochrane M.J., Rawson H.M. (1997). Growth and water use of the mangroves Rhizophora apiculata and R. stylosa in response to salinity and humidity under ambient and elevated concentrations of atmospheric CO2. Plant, Cell and Environment, 20, 1158-1166.

Christensen B. (1978). Biomass and primary production of Rhizophora apiculate Bl. in a mangrove in southern Thailand. Aquatic Botany, 4, 43-52, DOI: 10.1016/0304-3770(78)90005-0.

Clough B.F., Ong J.E., Gong W.K. (1997). Estimating leaf area index and photosynthetic production in canopies of the mangrove Rhizophora apiculate. Mar Ecol Prog Ser, 159, 285-292.

Deshcherevskaya O.A., Avilov V.K., Dinh Ba Duy, Tran Cong Huan, Kurbatova J.A. (2013). Modern climate of Cat Tien national park (Southern Vietnam): climatological data for ecological studies. Geophysical processes and the biosphere, 12(2), 5-33 (in Russian with English summary).

Đô Phong Lủu, Zhirenko N.G., Nguyèn Thái Sôn, Nguyèn Trung Đủc, Huỳnh Đủc Hoàn, Nguyèn Văn ThỊnh. (2021). Photosynthetic characteristics of Rhizophora apiculate Blume in Can Gio mangrove forest, Ho Chi Minh City. Táp chí Khoa hôc và Công nghè nhièt đôi, 22(05), 3-15 (in Vietnamese with English summary).

Donato D.C., Kauffman J.B., Murdiyarso D., Kurnianto S., Stidham M., Kanninen M. (2011). Mangroves among the most carbon-rich forests in the tropics. Nature Geoscience, 4, 293–297.

Ehleringer J., Björkman O. (1977). Quantum Yields for CO2 Uptake in C3 and C4 Plants: Dependence on Temperature, CO2, and O2 Concentration. Plant Physiology, 59(1), 86-90, DOI: 10.1104/pp.59.1.86.

Eong O.J., Khoon G.W., Clough B.F. (1995). Structure and productivity of a 20-year-old stand of Rhizophora apiculata Bl. mangrove forest. Journal of Biogeographv, 22, 417-424.

Ghannoum O., Caemmerer S.V., Ziska L.H., Conroy J.P. (2000). The growth response of C4 plants to rising atmospheric CO2 partial pressure: a reassessment. Plant, Cell and Environment, 23(9), 931-942, DOI: 10.1046/j.1365-3040.2000.00609.x.

Hieke S., Menzel C.M., Ludders P. (2002). Effects of Light Availability on Leaf Gas Exchange and Expansion in Lychee (Litchi chinensis). Tree Physiol, 22, 1249-1256.

Hogarth P.J. (2007). The Biology of Mangroves and Seagrasses. New York. Published in the United States by Oxford University Press Inc.

Hogarth P.J. (2008). The Biology of Mangroves and Seagrasses. New York. Oxford: Oxford University Press.

Kaipiainen E.L. (2009). Parameters of Photosynthesis Light Curve in Salix dasyclados and Their Changes during the Growth Season. Russian Journal of Plant Physiology, 56, 445-453, DOI: 10.1134/S1021443709040025.

Kristine Y.C., Johan U., Martin G.D.K. (2022). Temperature responses of photosynthesis and respiration in evergreen trees from boreal to tropical latitudes. New Phytologist, 234, 353–374, DOI: 10.1111/nph.17951

Kumar T., Murthy T.V.R., Chellamani P., Krishnan V., Thangaradjou T., Mani M.R. (2017). Modelling photosynthetic rates of Indian red mangroves (Rhizophora mucronata Poir.) to climatic factors. Tropical Ecology, 58(4), 717-729.

Luong Thi Hoan. (2014). Forest resources and forestry in Vietnam. J. Viet. Env., 6(2), 171-177, DOI: 10.13141/jve.vol6.no2.pp171-177.

Michaelis L., Menten M.L. (1913). Die kinetik der invertinwirkung. Biochem. z., 49(352), 333-369.

Morgan J.A., Hunt H.W., Monz C.A., Le Cain D.R. (1994). Consequences of growth at two carbon dioxide concentrations and two temperatures for leaf gas exchange in Pascopyrum smithii (C3) and Bouteloua gracilis (C4). Plant, Cell and Environment, 17, 1023-1033.

Nguyen H.T. (2000). Valuation of the mangrove ecosystem in Can Gio biosphere reserve, Vietnam. Hanoi. The Vietnam MAB National Committee.

Okimoto Y., Nose A., Oshima K., Tateda Y., Ishi T. (2013). A case study for an estimation of carbon fixation capacity in the mangrove plantation of Rhizophora apiculata trees in Trat, Thailand. Forest Ecology and Management, 310, 1016-1026.

Ong J.-E., Khoon G.W., Clough B.F. (1995). Structure and productivity of a 20-year-old stand of Rhizophora apiculata Bl. mangrove forest. Journal of Biogeography, 22, 417-424.

Read J.J., Morgan J.A. (1996). Growth and partitioning in Pascopyrum smithii (C3) and Bouteloua gracilis (C4) as influenced by carbon dioxide and temperature. Annals of Botany, 77, 487-496, DOI: 10.1006/anbo.1996.0059.

Sage R.F., Kubien D.S. (2007). The temperature response of C3 and C4 photosynthesis. Plant, Cell and Environment, 30(9), 1086-1106, DOI: 10.1111/j.1365-3040.2007.01682.x.

Saintilan N., Khan N.S., Ashe E., Kelleway J.J., Rogers K., Woodroffe C.D., and Horton B.P. (2020). Thresholds of mangrove survival under rapid sea level rise. Science, 68(6495), 1118-1121, DOI: 10.1126/science.aba2656.

Simard M., Fatpyinbo L., Smetanka C., Rivera-Monroy VH, Castaneda-Moya E., Thomas N., and Van der Stocken T. (2019). Mangrove canopy height globally related to precipitation, temperature and cyclone frequency. Nature Geoscience, 12, 40-45, DOI: 10.1038/s41561-018-0279-1.

Slack C.R., Hatch M.D. (1967). Comparative studies on the activity of carboxylases and other enzymes in relation to the new pathway of photosynthetic carbon dioxide fixation in tropical grasses. Biochem. J., 103(3), 660-665, DOI: 10.1042/bj1030660.

The world's mangroves 1980–2005. (2007). FAO Forestry Paper 153, Rome. [online] Available at: www.fao.org/forestry/site/mangrove/statistics.

Thongjoo C., Choosak S., Chaichana R. (2018). Soil fertility improvement from commercial monospecific mangrove forests (Rhizophora apiculata) at Yeesarn Village, Samut Songkram Province, Thailand. Tropical Ecology, 59(1), 91-97.

Valiela I., Bowen J.L., York J.K. (2001). Mangrove forests: one of the world's threatened major tropical environments. BioScience, 51(10), 807-815, DOI: 10.1641/0006-3568(2001)051[0807:MFOOTW]2.0.CO;2.

Wenfang D., Xiong J., Zheng H., Ni S., Ye Y., Wang C. (2020). Effect of Rhizophora apiculata plantation for improving water quality, growth, and health of mud crab. Appl Microbiol Biotechnol, 104, 6813-6824, DOI: 10.1007/s00253-020-10716-7.

RESEARCH PAPER

LARGE-SCALE HYDROMORPHOLOGICAL CHARACTERISTICS OF THE PROGLACIAL RIVER KATUN (OB HEADWATERS)

Friedrich Seidl[1*], Markus Reisenbüchler[1], Peter Rutschmann[1], Liubov V. Yanygina[2], M. Schletterer[3]
[1]Chair of Hydraulic and Water Resources Engineering, Technical University Munich, Arcisstr. 21, 80333, Munich, Germany
[2]Institute for Water and Environmental Problems SB RAS, Ulitsa Molodezhnaya 1, 656038, Barnaul, Russia
[3]Institute of Hydrobiology and Aquatic Ecosystem Management, University of Natural Resources and Life Sciences, Gregor-Mendel-Straße 33, 1180, Vienna, Austria
***Corresponding author:** friedrich.seidl@tum.de
Received: February 27th, 2022 / Accepted: May 4th, 2023 / Published: July 1st, 2023
https://DOI-10.24057/2071-9388-2022-022

ABSTRACT. During the industrialization in Europe, rivers were straightened and designed to fit human activities, thus nowadays only a few natural river systems remain as reference conditions as well as guiding principles for river restoration projects. Therefore, the natural state of some river types is often described using historic records and maps. This study aims to analyze the key characteristics of a pristine proglacial river Katun in the Altai mountains and contribute to the knowledge about reference conditions. For this purpose, hydromorphological characteristics like slope, sinuosity and river width of the river Katun were analysed and summarized using different GIS techniques. Additionally, pebble counts were carried out to assess the changing sediment composition along the longitudinal continuum. Combined with River Habitat Surveys and a one-dimensional flow simulation using HEC-RAS it was possible to give a holistic overview of the dynamic fluvial system Katun in its upper, middle and lower reaches. The results confirmed the relationship between the river and its surrounding topography as they clearly show the lateral development of the Katun. As shown for the individual parameters (e.g., slope, width, depth, flow velocity, shear stress), they influence each other and are strongly dependent and characteristic for each river section. In the context of revitalisation of straightened and / or channelized river courses, it is important to focus on the processes of this interaction and provide suitable space for lateral expansion. The study can be seen as a recommendation on how to analyse hydromorphological characteristics of fluvial systems as well as to establish guiding principles in river restoration using remote sensing.

KEYWORDS: hydromorphology, ecohydraulics, proglacial river, Katun, Altai Mountains, Russia

CITATION: Seidl F., Reisenbüchler M., Rutschmann P., Yanygina L. V., Schletterer M. (2023). Large-Scale Hydromorphological Characteristics Of The Proglacial River Katun (Ob Headwaters). Geography, Environment, Sustainability, 2(16), 110-120
https://DOI-10.24057/2071-9388-2022-022

ACKNOWLEDGEMENTS: We acknowledge the „Verein Freunde des Lehrstuhls für Wasserbau und Wasserwirtschaft der Technischen Universität München e.V.", which provided financial support to the excursion in 2019.

Conflict of interests: The authors reported no potential conflict of interest.

INTRODUCTION

The European Directive 2000/60/EC established a framework for community action in the field of water policy in the European Union. It is based on the consideration that water is not a common commercial commodity, but rather an inherited asset that must be protected, defended and preserved[1]. This Water Framework Directive (WFD) aims to harmonise the water policies of all European Member States in order to achieve the best possible protection and the greatest possible restoration of the ecological quality of running waters[1]. Essentially, this balancing act between a Europe-wide standard of protection and the consideration of local particularities is to be achieved through a uniform procedure within the framework of the assessment and classification of water bodies.

The typification and standardisation required in the individual steps subsequently demanded a new, holistic approach to river characterisation and its aquatic habitats[2] and, in particular, included hydromorphology in the assessment of European watercourses (Newson and Large 2006). With the implementation of the WFD not only definitions and study objectives changed, but also a variety of new methods for the analysis and assessment of watercourses with regard to the new aspects were developed (Belletti et al. 2015). However, no common

[1]European Parliament (2000). Directive 2000/60/EC of the European Parliament and of the Council of 23 October 2000 establishing a framework for Community action in the field of water policy. OJ L 327, 22.12.2000, p. 1–73.
[2]European Standard BS EN 14614:2004 (2005). Water Quality [Accessed 08. Oct. 2019].

procedure for hydromorphological surveys of streams and rivers was developed.

The CEN[3] standard from 2002 provides an overview of the most widely accepted characteristics in the context of hydromorphological surveys. In order to determine hydromorphological reference conditions for European rivers, it is often necessary to look beyond the borders of Europe, where the industrialisation resulted in numerous heavily modified river systems and only a few rivers remained in pristine condition (Zerbe 2019).

Accordingly, this work aims to explore the possibility to derive typical hydromorphological aspects of pristine rivers by GIS-based methods in combination with one-dimensional flow simulation, using the Russian proglacial river Katun as a case study. As many rivers in Europe are affected by hydromorphological changes due to land use and flood protection, the data set from Katun can be used as guiding principal for restoration projects at similar rivers in the Alps.

STUDY AREA

The Katun River is considered to be a river system in near-natural condition, due to the low density of settlements and low industry. Thus, this river can develop and shape its course to its full extent of the dynamic processes (Mandych 2006). The biggest spatial limitations are natural characteristics, e.g., narrow gorges and terraces. Therefore, the Katun catchment forms a unique reference catchment to study large-scale hydromorphological characteristics of proglacial rivers and can make a huge contribution towards establishing guiding principles when restoring these proglacial rivers in the alpine region.

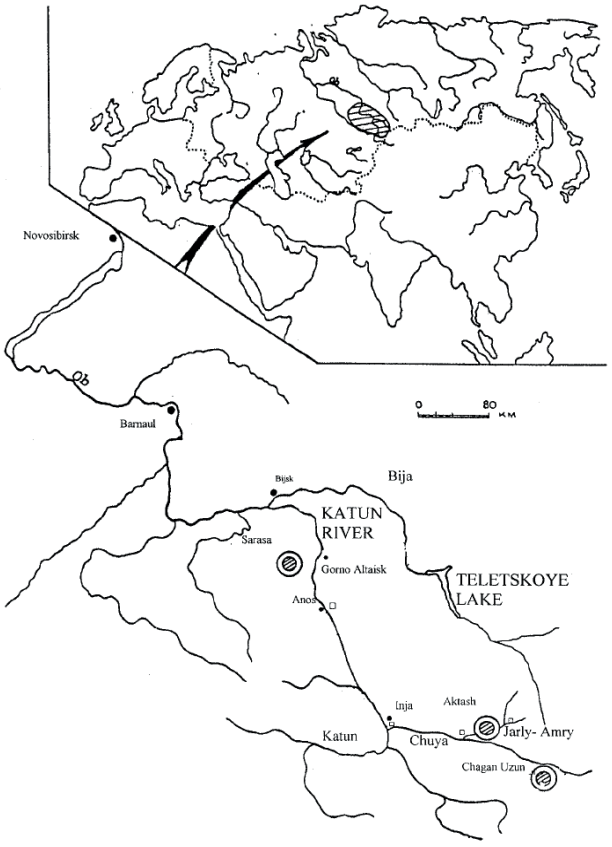

Fig. 1. Location of the Katun river in the Russian Altai Mountains (from: Baeyens et al. 2003)

The Katun River originates from the Gebler Glacier on the Belucha mountain at an elevation of 2640 m a.s.l.[4] in the Russian Altai (Haywood 2010). Along its course towards the north it covers a catchment area of about 60,900 km^2 until it reaches the village of Odintsovka at an altitude of about 200 m above sea level[4]. Downstream of the city of Biysk, after a length of 688 km it joins the river Biya (Mandych 2006; Schletterer et al. 2021a). From the junction of the two rivers the Ob is formed, which flows into the Kara Sea in the north of Siberia. On its way to the Arctic Ocean, the Ob covers a flow distance of 3650 km, making it one of the largest river systems in the world with a catchment area of 2,972,497 km^2 and a MQ near the mouth at Salekhard of 12,600 m^3/s (Shiklomanov et al. 2006). As the longest headwater river, the Katun has an important influence on the Ob River. The mean flow (MQ) of the Katun comprises about 600 m^3/s at the gauge Srostky at river km 616. The Katun is divided into upper, middle and lower reaches based on its tributaries and characteristics. The orographically left tributary Koksa near the town of Ust-Koksa at river kilometer 210 represents the border between the Upper and Middle Katun. The middle course extends to river kilometer 410, where the Sumulta River joins the Katun on the orographic right. The lower course extends from Sumulta River to the confluence with the Biya where both rivers from the Ob near the town of Biysk (Sapozhnikov 1949 Schmalfuß et al. 2022). The flow regime of the Katun can be described according to FOEN (2013) as glacio-nival. Records show an annual fluctuation in discharge typical for this flow regime, with an annual peak discharge as a result of snow and glacier melt. Based on the 1952 glacier area (749 km^2), the Katun River basin has a degree of glaciation of approximately 1% (in the upper course 1.3 %, in the middle course 2.5 % and in the lower course 0 %) (Revyakin 1978). In 1952, the glacier area of the Upper Katun was 173.3 km^2, the Middle Katun (Argut and Chuya basins) – 575.9 km^2 (Khromova et al. 2021). By 2019, the glacier area decreased by about 30% (523 km^2)[5]. Less than 20 % of the runoff is contributed by precipitation and almost 30 % comes from groundwater. The remaining 50% is made up from meltwater of snowfields or seasonal snowfall as well as meltwater from glaciers (Mandych 2006).

MATERIALS AND METHODS

Along the Katun three gauging stations are located, with freely accessible data measuring only the discharge and precipitation starting in 1938 up to the year 2000 (Fig 2). Representative months for low (February), medium (April/September) and high discharges (June) were selected from discharge curves of three different discharge stations at the Katun (Fig. 2).

The hydromorphological analyses of Katun river were carried out with GIS-based data material. The satellite data from Table 1 used in this work were obtained from the freely accessible online portals EarthData of NASA[6] and EarthExplorer of the U.S. Geological Survey[7]. To generate an equal starting point for further selecting the best

[3]CEN (2002). A guidance standard for assessing hydromorphological features of rivers. CEN TC 230/WG2/TG 5 N32, 21 pp.
[4]Esri (2013). "Topographic" [base map]. Scale Not specified. "World Topographic Map." Available at https://services.arcgisonline.com/ArcGIS/rest/services/World_Topo_Map/MapServer [Accessed 31. Oct. 2019]
[5]https://www.glacrus.ru/ледниковые-районы/алтай
[6]https://earthdata.nasa.gov/
[7]https://earthexplorer.usgs.gov/

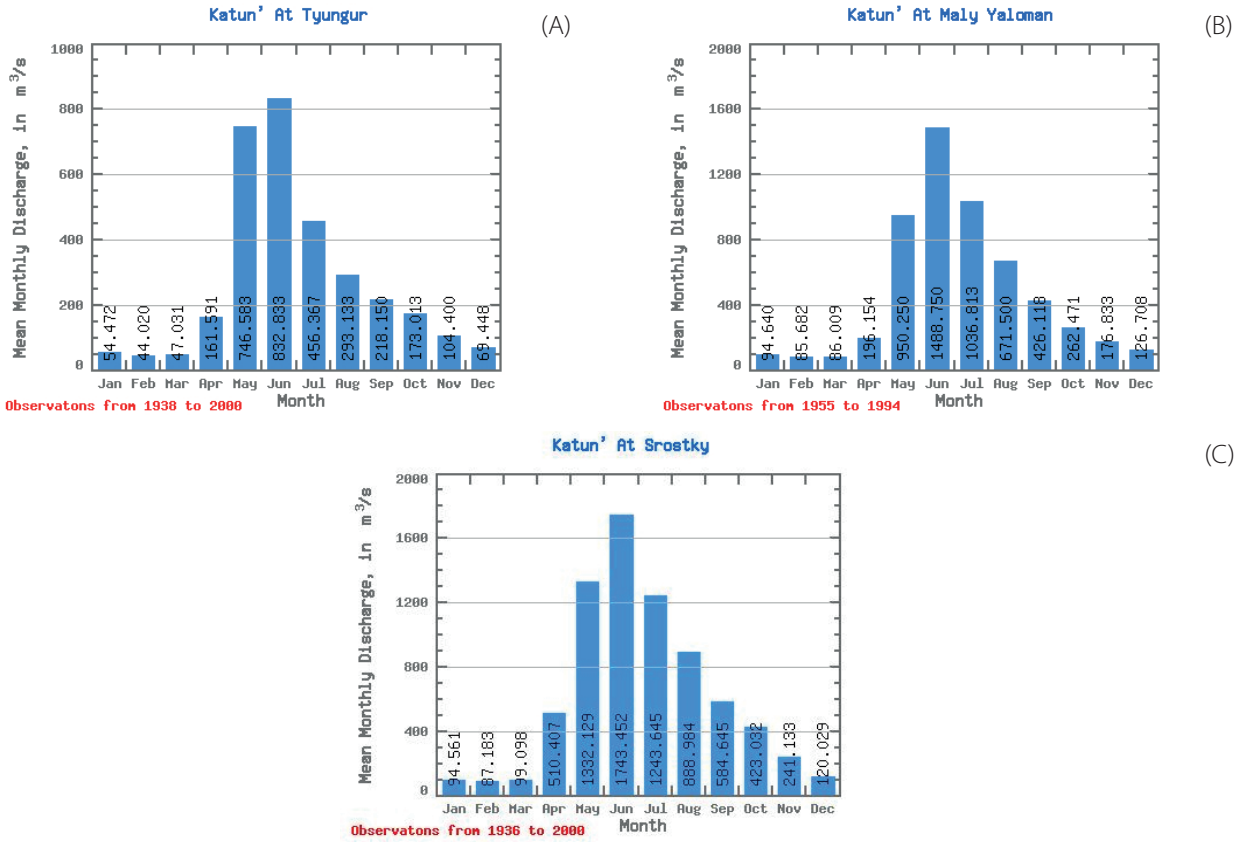

Fig. 2. Averaged monthly discharge of the Katun River in the period 1936 to 2000 at three different stations (from: Lammers et al. 2016)

fit DEM for the performed analysis, the river networks with corresponding flow order were calculated on every available DEM. Afterwards the channel of the River Katun with its most important tributary Chuya were isolated. Since fluvial ecosystems exhibit a distinct hierarchical order in nature (Allan and Castillo 2007) the derived channel was categorized based on stream order (Strahler 1957) to create distinct reference points for the evaluation of the following research. Continuing from there the data was used to extract the sinuosity, width variability and slope of the Katun as follows.

Sinuosity

In order to investigate the sinuosity, the river has to be divided into individual sections, for which the sinuosity was be determined. Therefore, to recommend an appropriate size for the sections on a river length of about 688 km, this work resorted in the first step to a simplified definition of sinuosity (Haggett und Chorley 1969), which was applied to three different section lengths (1 km, 5 km and 10 km):

$$Sinuosity = \frac{length\ of\ river\ axis}{Linear\ distance\ between\ section\ starting\ and\ end\ point} \quad (1)$$

Based on these results the second step was to identify distinctive points along the Katun for which more detailed analyses according to Mueller`s sinuosity index (Mueller 1968) were carried out (Fig. 3). The detailed calculations focused on the Hydraulic, Topographic and Standard Sinuosity Index (HSI, TSI and SSI), as well as again different river section sizes (5, 25 and 50 km) for which the three indices were considered. In addition, when selecting the

$$Channel\ Index\ CI = CL/AL \quad (2)$$

$$Valley\ Index\ VI = VL/AL \quad (3)$$

$$HSI = (CI - VI)/(CI - 1) \quad (4)$$

$$CL = Channel\ Length$$

$$TSI = (VI - 1)/(CI - 1) \quad (5)$$

$$VL = Valley\ Length$$

$$SSI = CL/VL \quad (6)$$

$$AL = Air\ Length$$

Table 1. Available Digital Elevation Models for the Study Area

DEM	Source	Temporal Cover	Resolution
GTOPO30	(USGS 1996)	1993 – 1996	30 Arc Second = 1km
GMTED2010	(USGS 2011)	Nov 2010	7.5 Arc Second = 225m
SRTM VoidFill	(USGS 2012)	Feb 2000	3 Arc Second = 90m
SRTM Global	(USGS 2014)	Feb 2000	1 Arc Second = 30m
ASTER v3.0	(NASA et al. 2001)	2000 – 2013	1 Arc Second = 30m

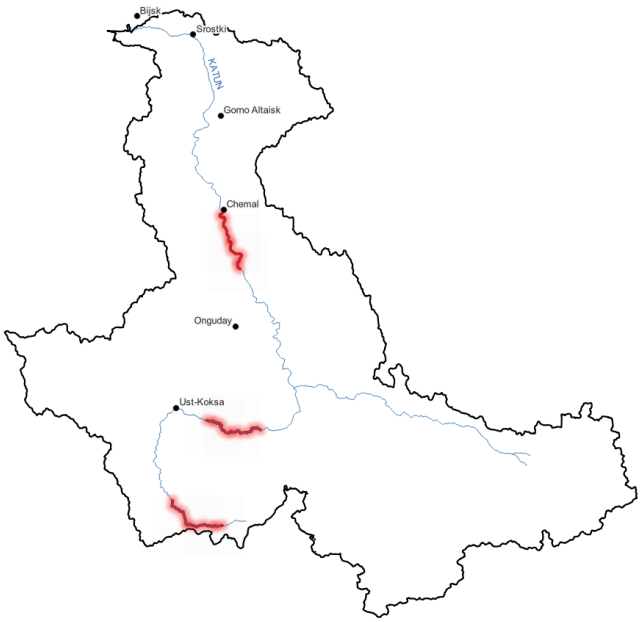

Fig. 3. Locations at the Katun selected for detailed sinuosity calculations

sections, care was taken to avoid settlements on the banks of the Katun, since bank obstructions must be assumed there (Khan et al. 2018).

River Width

The relationship between river width and discharge along the course of a river is one of the most constant relationships among hydraulic variables in natural rivers (Leopold and Miller 1956) and must be considered when analysing the river width using GIS-based data. Herein, the open-access database "Global River Widths from Landsat - GRWL" (Allen and Pavelsky 2018) was used to illustrate the overall tendencies of the river width based on the average discharge along the Katun from its source to its confluence with the Ob River. To analyse interannual variations due to fluctuations in discharge, the river-width was additionally detected from freely available Level 2 Landsat 8 data[8] using the Normalized Difference Water Index (NDWI) and the program ArcGIS[9,10]. The NDWI was calculated as follows (Du et al. 2016):

$$NDWI = (Green - NIR) / (Green + NIR) \quad (7)$$

The Landsat Imagery was gathered for the initially defined months with characteristic discharges based on Fig. 2. Due to the snow cover during winter months in the Altai Mountains, no usable Landsat data for low discharge months could be gathered. Based on the dimensions of the Katun, four hydromorphological characteristic sections with a length between 20 and 30 km were selected (Fig. 3.). One section each for the upper and middle reaches and due to the different characteristics of the upper and lower sections of the lower reach, two sections were selected for the latter. For the Chuya tributary, a short section just before the confluence with the Katun was considered additionally.

Slope

The determination of the river bottom slope was based on the digital terrain models used and the river axes calculated from them. However, it is not possible for satellites to measure the actual river bottom since the radiation is reflected at the water surface - the values of the DEM therefore correspond to the height of the water surface. While other researchers have already acknowledged this problem and looked into possible solutions (Dai et al. 2018; Purinton and Bookhagen 2017), for simplification, the slope of the water surface was equated with the bottom slope in this work under the assumption of laminar flow. In order to represent the elevation profile of the Katun in longitudinal section, individual points were generated at intervals of one kilometer along the river axes at which the raster values based on the DTMs GTOPO30, SRTM Global and GMTED2010 were extracted. The decisive factor for the choice of this distance was the resolution of the DTM GTOPO30 of 1 km. Even though a higher data density could be chosen for SRTM Global with a resolution of 30 m, this was not done in favour of comparability. At these points, the raster values of the respective terrain model were extracted. The bed slope was then derived from the elevation differences of the individual points.

Stream structure survey and Pebble Count

Additionally, a hydromorphological survey based on the River Habitat Survey (Environment Agency 2003) adapted to the circumstances was conducted by the author along the Katun River during an excursion in September of 2019 (Schletterer et al. 2021b). Surveys were carried out in the middle and lower reaches, including bedload characterisation with *Wolman-Counts* (Wolman 1954; Nikora et al. 1998; Galia et al. 2017) along the banks (Fig. 4). Limitations of this method, besides the lack of detection of fine sediments, are difficulties of measurement at large water depths and the difficult comparability with sieve curves, since the counting methodology provides a cumulative curve based on the total number and not the weight of the sample. Due to the dimensions of the Katun, measurements along the river bottom in a cross section had to be omitted in this work and the lines were measured near the banks on representative gravel bars. At least three lines were measured at each location. To ensure a sufficient amount of data, a sample size of about 150 stones per line was used in this work. The measured stones were divided into twelve different grain fraction classes ranging from grain sizes smaller than 8 mm up to over 256 mm (Table 2).

One-dimensional Model using HEC RAS

The collected data of the above-mentioned analysis was combined into a one-dimensional steady-state flow simulation using HEC RAS 5.0.7 and HEC GeoRAS 10.5 with the aim of connecting parameters observed via GIS-based methods and the rivers hydraulic processes. The values of the three available discharge stations served as authoritative input parameters for the extension of the one-dimensional flow model of the Katun. No discharge values were available for the Upper Katun thus the Tyungur (upstream) and

[8]EROS (2014). Collection-1 Landsat OLI Level-2 Surface Reflectance (SR) Science Product. Ed. by Earth Resources Observation And Science (EROS) Center.
[9]Dilts, T. E. (2015). Polygon to Centerline for ArcGIS: University of Nevada Reno. Available at: https://www.arcgis.com/home/item.html?id=bc642731870740aabf48134f90aa6165 [Accessed 31. Oct. 2019].
[10]Singh, J. (2017). Calculate Road/Stream widths. Available at: https://www.arcgis.com/home/item.html?id=ede4729410e846638520f99901542518 [Accessed 31. Oct. 2019].

Table 2. Grain fraction classes used in pebble count

Grain fraction class	1	2	3	4	5	6	7	8	9	10	11	12
Diameter [mm]	<8	8-11.3	11.3-16	16-22.6	22.6-32	32-45	45-64	64-90.5	90.5-128	128-181	181-256	>256

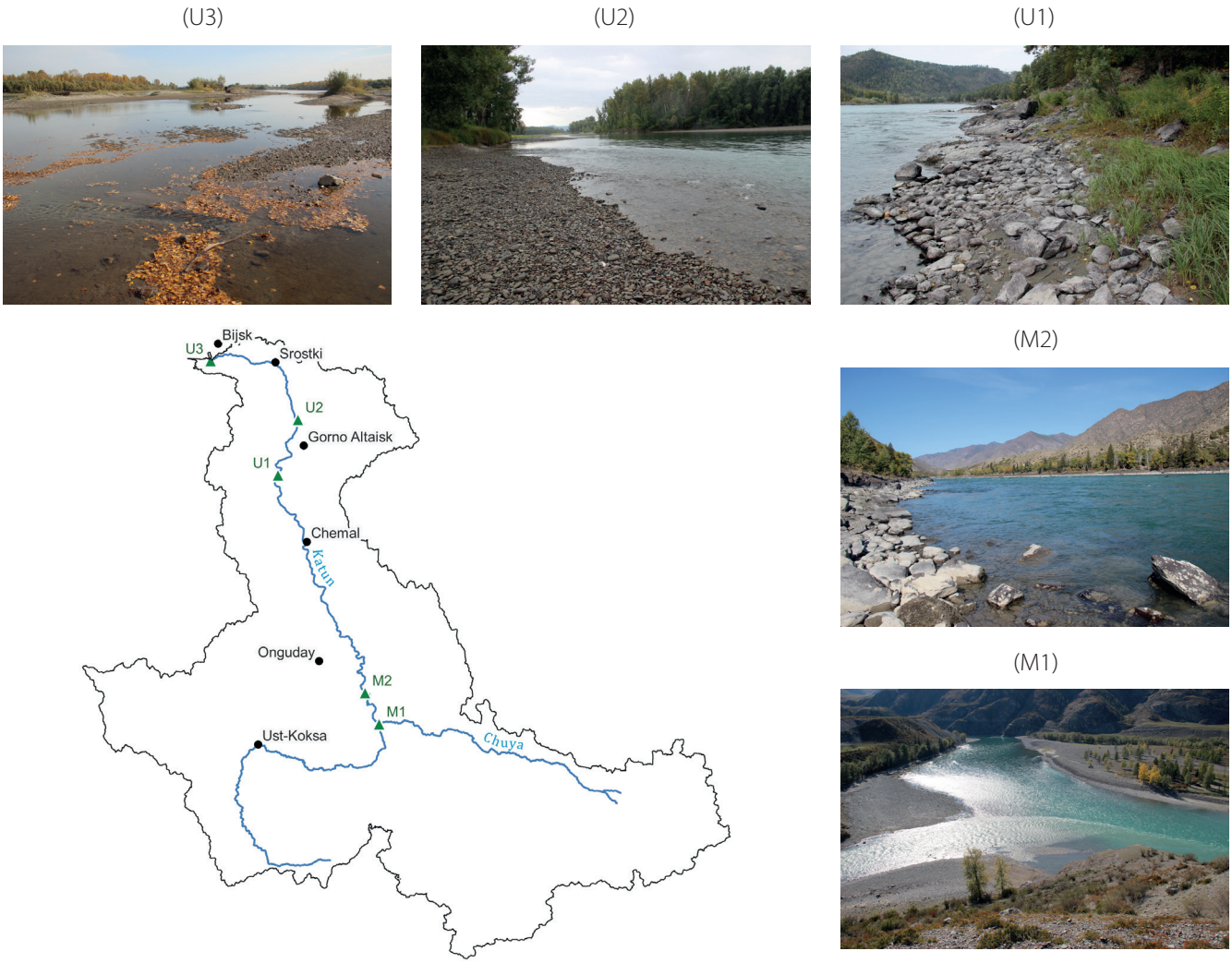

Fig. 4. Locations of stream structure surveys and pebble counts along the Katun

Srostky (downstream) stations were chosen as the start and end points of the model. This resulted in a total length of nearly 370 km, covering large portions of the Lower and Middle Katun as seen in Fig. 5. As clearly seen in the discharge, the lowest flows occur in winter and the highest ones are related to snow and glacier melt (May – July). Based on the collected discharge data from (Lammers et al. 2016), the fluctuations and long-term trends during these months were examined. Due to missing data for the Maly Yaloman station in the middle of the river section and taking into account that an adjustment of the average values under the aspect of the observed strong annual fluctuations was being considered error-prone, for the later simulations average discharge values as seen in Fig. 2 were taken (Table 3).

The remaining parameters of the model were derived from the geoinformation-based calculations already performed (geometries, slopes, river axis, etc.). Since no grain distribution of the actual riverbed could be gathered and the Manning values from the pebble count differed from the literature, the values of the recommendations from literature (Chow 1959; Brunner 2016; Arcement and Schneider 1989) were used in this work for the one-dimensional flow model as shown in Table 4. The ice thickness during the winter months with its associated roughness were determined from literature (Vuglinsky and Valatin 2018). According to Shiklomanov and Lammers (2014) and the available Landsat 8 imagery from the month of April 2019, the end of river glaciation was determined between March and April.

The Strickler Coefficient was derived using the correlation between grain size and bed roughness by inverting the calculated Manning value.

$$n = 0.034 * d^{1/6} \quad (8)$$

RESULTS AND DISCUSSION

The Katun in its upper reaches can be defined as a fourth to fifth order river. With the mouth of the Koksa, the Katun changes to sixth order. This also marks the border between the upper and middle reach in the literature. The inflow of the Chuya increases the stream order to seven. Even though the Chuya is one of the longest tributaries of the Katun (Mandych 2006), the conjunction of both rivers does not lead to a significant change in the river regime and therefore, the lower reach begins where the Sumulta River joins the Katun. Until its confluence with the Biya River, the Katun remains a seventh-order river.

The longitudinal zonation is characteristic for fluvial systems, which is associated with characteristic hydromorphology and bedload processes (Schumm 1977; Allan and Castillo 2007). Our satellite-based investigations

Table 3. Average discharge in the months of February, April, June and September

Station (river km)	February [m³/s]	April [m³/s]	June [m³/s]	September [m³/s]
Tyungur (229)	44	161	832	218
Maly Yaloman (301)	85	196	1488	426
Srostky (616)	87	510	1743	584

Table 4. Manning`s roughness values used in the one-dimensional modelling

River section	Left bank	Main channel	Right bank
Lower Katun	In winter: 0.070 In summer: 0.100	0.035	In winter: 0.070 In summer: 0.100
Medium Katun	0.05	0.04	0.05

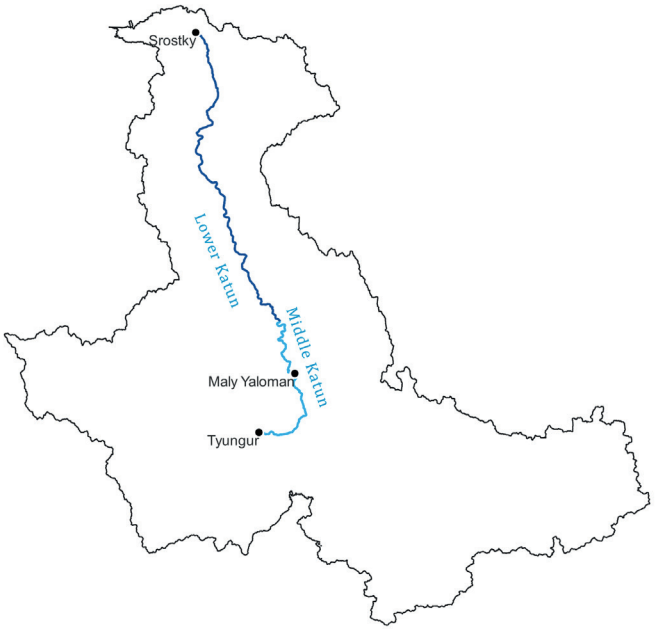

Fig. 5. River section used for one-dimensional flow simulation in HEC RAS

of the Katun River, support the published longitudinal zonation (upper, middle, lower reaches). The elevation profile shows in the linear approximation a slope ranging from 0.29 % to 0.59 % in the upper course. With increasing flow distance it drops to 0.18 % in the middle course and finally to 0.12 % in the lower course (Fig. 6). The results showed that a development of the bed slope and a possible bed deepening in the comparison of the considered years could not be represented justifiably due to the different resolution of the DEMs. Especially in the gorges of the Upper and Middle Katun, the elevation values of the DEMs with resolution ranges of 1 km and 225 m, respectively, often did not represent the water surface, but predominantly that of the adjacent slopes. Therefore, only the results of the observation of the SRTM Global with a resolution of 30 m were deemed accurate.

The different river sections are also clearly visible in the one-dimensional modelling of three different discharges using HEC-RAS. Both the shear stresses and the flow energy in the Middle Katun are a multiple of those in the Lower Katun. This is true both in winter, when the lowest discharge prevails and the river is frozen, with a shear stress of 20 N/m² to 9 N/m² and energy of 41 N/ms to 14 N/ms, and in early summer during the annual flood, with 100 N/m² to 14 N/m² and 404 N/ms to 178 N/ms (Fig. 7).

This energy gradient along the Katun River can be reassured in both the pebble count (Fig. 8) and the visual assessments of the stream structure survey conducted along the river banks. The giant bars and large boulders (Iturrizaga 2011) that shape the riverbed in the middle reaches (M1-M2) and upper lower reaches disappear once the river reaches the flat plains (U1-U3). Here it begins to meander and the predominant grain size is below 32 mm.

In addition, the widening and slowing down of the river can be seen in the simulated water depths but also in the flow velocities (Fig. 9.). The discharge data from the Katun River (Fig. 2) shows that, the volume of the flow increases with increasing flow length due to a larger catchment area caused by numerous tributaries. Within the HEC RAS simulation, the occurring velocities in the lower reaches (max. 2.36 m/s) are noticeably lower than in the middle reaches (max. 2.74 m/s). Considering the slope of the riverbed, this is an understandable relationship. If we now take the average water depths of 3.74 m in the lower reaches to 4.88 m in the middle reaches from Fig. 9 into account, the flow profile in the considered section of the lower reaches must increase, in order to accommodate the increased discharge of approximately 250 m³/s with decreasing velocities and depths. Consequently, as the flow depth decreases, an expansion in width takes place. The maximum river widths in the middle reaches range between 300 m and 400 m, up to 3,500 m in the lower reaches (Fig. 10). In contrast, in the upper section of the lower reaches, river widths of around 250 m were measured. In this area the Katun runs constricted between mountain slopes and is therefore unable to expand. To cope with the increasing discharge and the reduced width, the flow velocities increase to 1.5 m/s and 4 m/s and maximum flow depths of 2 m to 4.5 m during high discharges. As the river leaves the constricted valley and becomes wider, these values drop to 0.5 m/s to 2.5 m/s and 1 m to 2 m, respectively. The consistency of the results is maintained when annual variations are considered.

The Katun River has characteristic flow fluctuations, i.e., the strongly varying flows, over the year (Fig. 2). The river carries 20 times as much discharge in summer as in winter. The reason for this is heavy snowfall in winter, which, together with the thawing of the river at the end of the winter months, leads to increasing discharges in the following months. Since runoff data for these months are available and with the help of a study of the river ice thickness in the Altai Mountains the required parameters could be estimated, it was possible to simulate the hydraulic quantities also for February. Especially the shear stresses and the flow energy show a slowing down of the river. However, with increasing discharges, these values also increase again and in June/July, the highest erosive activity is to be expected due to the shear stresses. Due

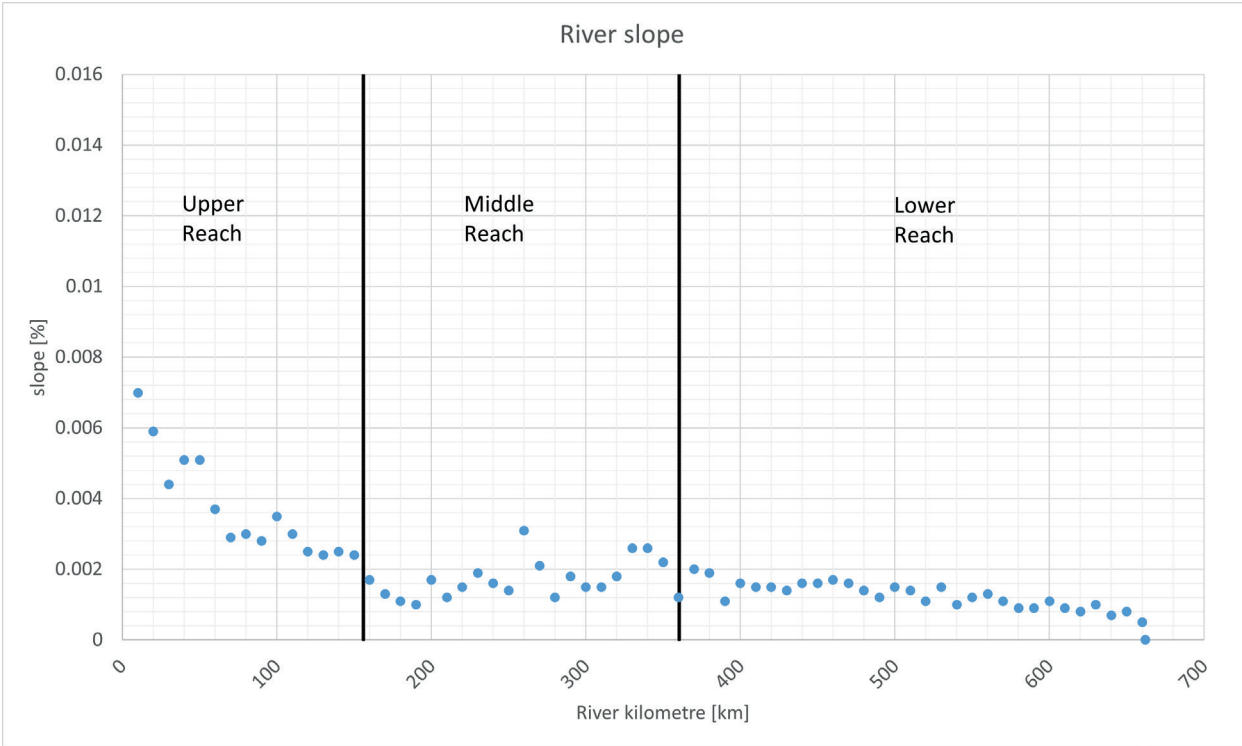

Fig. 6. River slope over 10 km flow segments based on SRTM GLOBAL

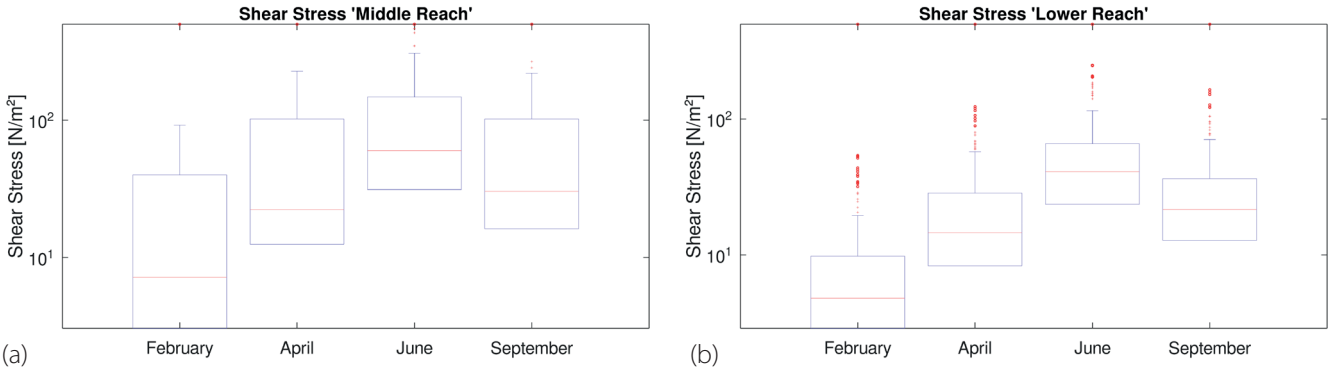

Fig. 7. Annual shear stress variability based on one-dimensional flow simulation in HEC-Ras – a) middle reach b) lower reach

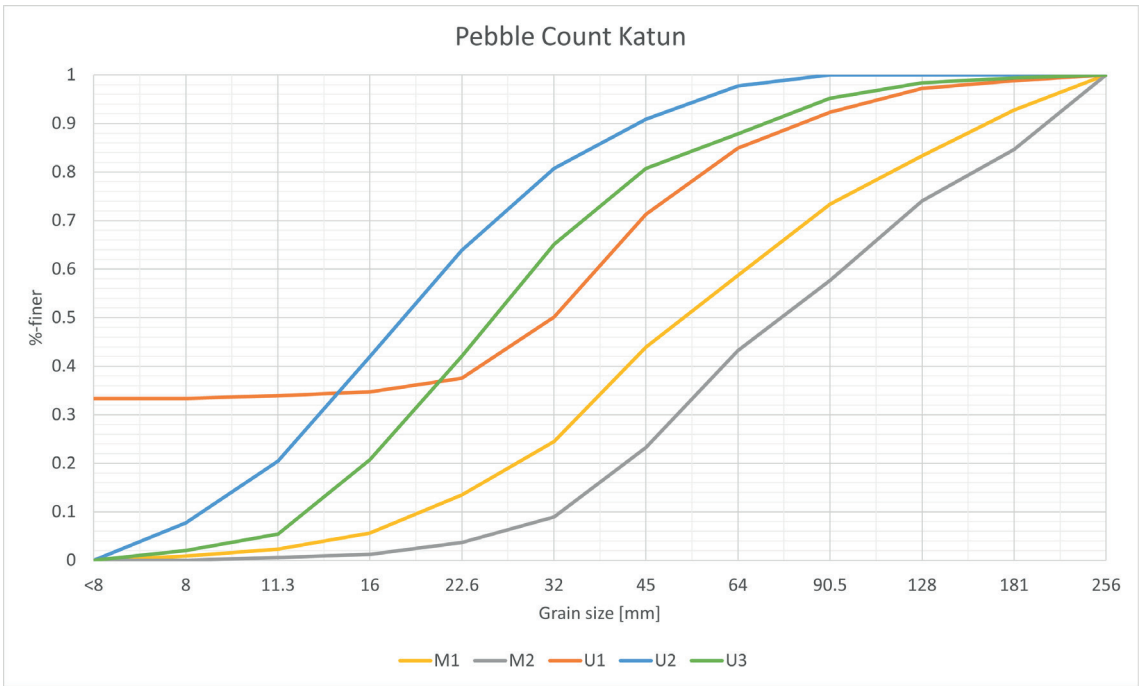

Fig. 8. Sum curve of the pebble count analysis

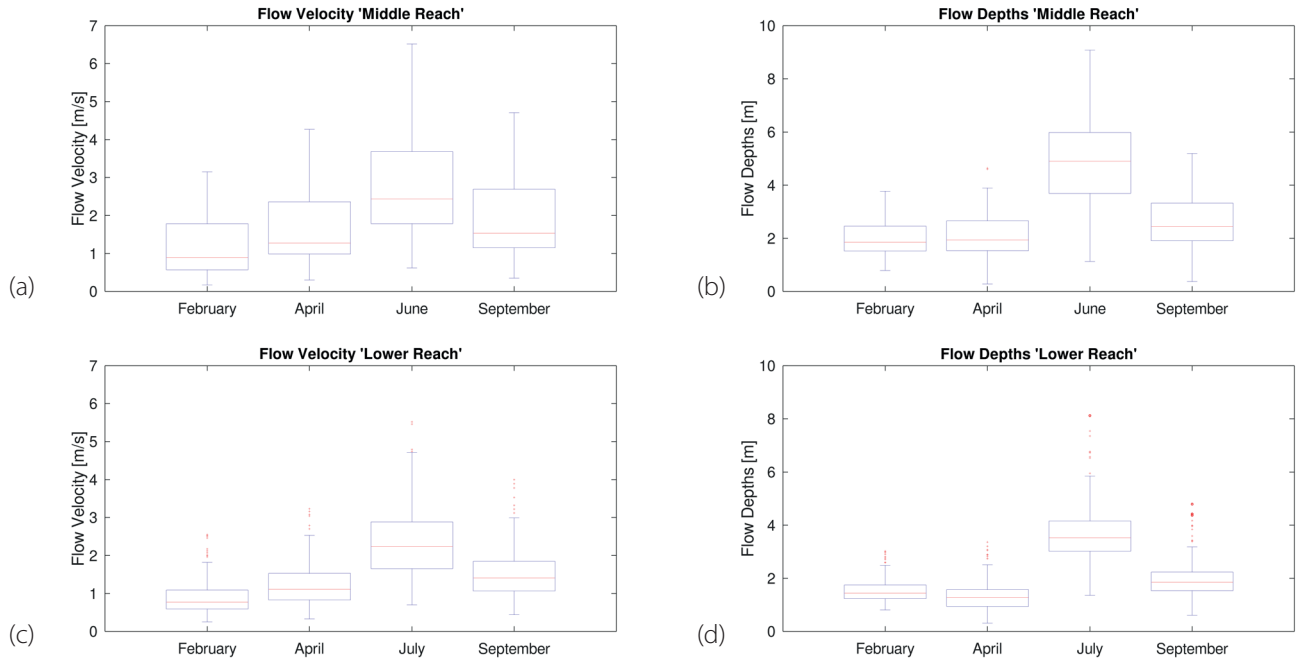

Fig. 9. Annual variability of flow velocities and corresponding flow are based on one-dimensional flow simulation in HEC-Ras – a) flow velocities middle reach b) flow depths middle reach c) flow velocities lower reach d) flow depths lower reach

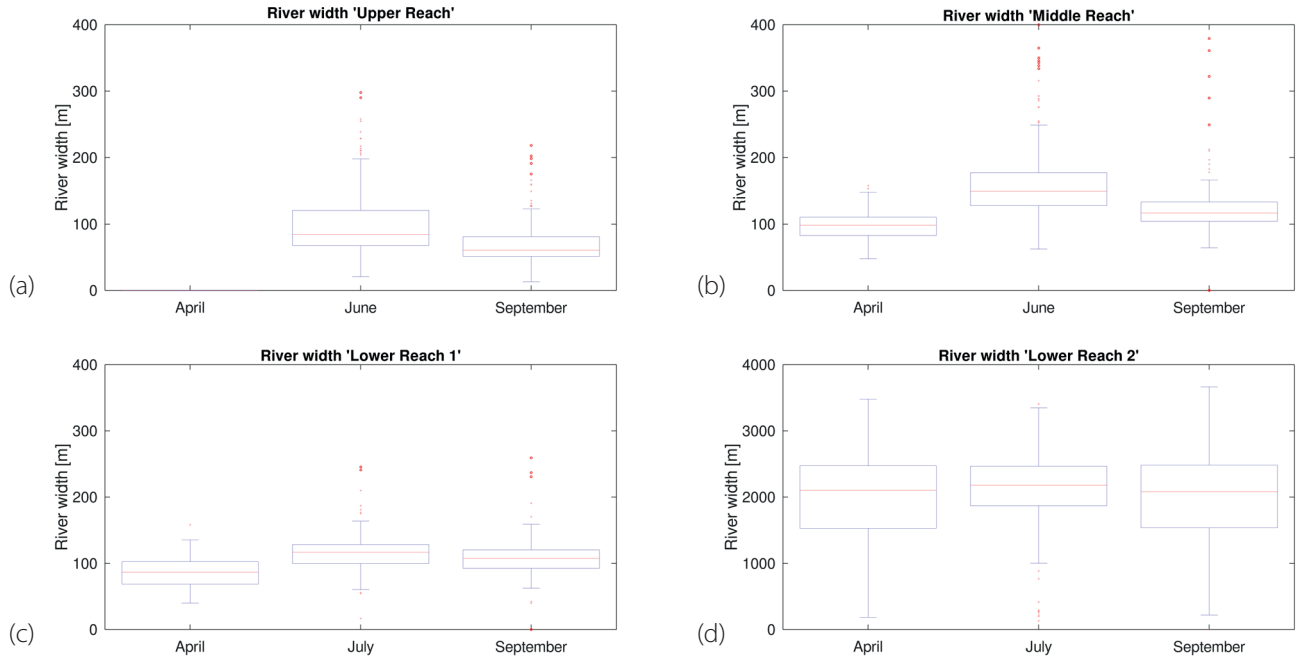

Fig. 10. Annual river width variability in the upper, middle and lower reaches of the Katun– a) River width upper reach b) River width middle reach c) River width lower reach 1 d) River width lower reach 2

to the GIS-based approach and missing data regarding riparian vegetation no statement can be made about the quality of the exchange with the floodplain areas, since more detailed models than the one used in this paper are needed for this (Maharjan and Shakya 2016).

When analysing the sinuosity of the river Katun using the simplified formula for three different section lengths along the entire Katun, the results suggest the use of 1 km for section length. For this length the calculations provide the lowest standard deviation and thus the most consistent results (Table 5).

The high difference between the two DEMs under consideration is probably due to the different resolution. Because of the resolution, the maximum values for the two years should also be viewed with caution. Both the 1.5 and 1.7 represent outliers and are at locations where the river axis does not clearly coincide with satellite data from those years. Nevertheless, such high values indicate stretches of the Katun River that can be described as strongly meandering and occur more frequently, especially in the middle and lower reaches. Based on the following, more detailed calculations of the SSI in each of the selected section the entire Katun can be described as straight to slightly sinusoidal based on Table 6. According to the different hydromorphology in the lower reaches, a determination of SSI should have been carried out for two different locations. Due to difficulties with the determination of a main river axis sole based on GIS data this was not performed.

Table 5. Results of the simplified sinuosity calculations

SRTM GLOBAL	1 km	5 km	10 km		GMTED2010	1 km	5 km	10 km
Mean	1.10	1.23	1.29		Mean	1.06	1.17	1.06
Std	0.09	0.15	0.20		Std	0.08	0.13	0
Max	1.76	1.69	2.09		Max	1.57	1.91	1.06

Table 6. Muellers sinuosity index for channel lengths of 5, 25 and 50 km in the upper, middle and lower reaches of the Katun

SSI	CL = 50 km	CL = 25 km	CL = 5 km
Upper Reach	1.02	1.03	1.09
Middle Reach	1.05	1.04	1.14
Lower Reach	0.99	1.0	0.97

Table 7. Hydromorphological characterisation of the Katun River

	Upper reach	Middle reach	Lower reach
River kilometer [km]	1 - 210	211 - 410	411 - 688
Flow order number	5	6 - 7	7
Sinuosity SSI [-]	1.03	1.04	1.00
River width [m]	65 - 110	97 - 165	86 - 108 1,975 – 2,025
Bottom slope [%]	0.41	0.19	0.14
D50 on the banks [mm]	-	52 - 77	18 - 32
Manning value n (banks) [s/m1/3]	-	0.066 – 0.07	0.055 – 0.061
Strickler value kSt (bank) [m/s1/3]	-	14.3 – 15.2	16.4 – 18.1
Gauge (Catchment in km^2)	Tyungur (13,415) *	Maly Yaloman (36,608)	Srostky (58,113)
Discharge MQ (min - max) [m^3/s]	266 (44 - 832)	466 (85 - 1.488)	614 (87 - 1.743)
Specific discharge MQ (min - max) [L/s/km^2]	19.83 (3.28 – 62.02)	12.73 (2.32 – 40.65)	10.57 (1.49 – 29.99)
Flow velocity v [m/s]	-	1.16 – 2.74	0.92 – 2.36
Maximum flow depth [m]	-	1.97 – 4.88	1.54 – 3.63
Shear stresses [N/m^2]	-	20.63 – 100.48	9.44 – 55.64
Flow energy [N/ms]	-	41.66 – 404.30	14.04 – 178.68
Dominant vegetation type of the riparian strips		Grasses / Shrubs	Saplings and trees
Vegetation structure of the riparian strips	-	simple	complex
* = Geographical location of the Tyungur gauge in the middle reaches. However, since it is located upstream of the confluence with the Argut and the Chuya, it is cited as a reference for the discharge of the upper reach.			

CONCLUSIONS

Our case study from Katun River underlines the importance of longitudinal (connectivity), lateral (floodplains), vertical (sediments) and temporal (annual variability of flow) aspects, which are the 4-dimensions of a lotic ecosystem (Ward 1989). Based on our investigations of large-scale hydromorphological characteristics along the Katun, guiding principles for glacier rivers were developed (Table 7). As shown for the individual parameters (e.g. slope, width, etc.), they influence each other and are strongly dependent as well as characteristic for each river section. In the context of revitalisation of straightened and / or channelized river courses, it is important to focus on the processes of this interaction and provide suitable space for lateral expansion. The aim of revitalisation measures should be to enable the river to support its natural dynamics and after an initial situation is created the river should form the newly gained riverscape itself.

In most rivers, which were altered by human activities, the longitudinal continuity is limited, both for fish and sediments. Straightened rivers deepen over time, which causes the adjacent riparian strips and floodplains to dry out, as the river no longer spills out during floods. The surveys along Katun river showed a diverse and structured riparian vegetation, which forms an important Habitat and migration corridor (Peredo Arce et al. 2021). Therefore, another essential aspect is recommended re-establish habitats where the development of typical riparian vegetation is enabled. This can be either achieved (i) by lowering the floodplains to enable periodical flooding of the riparian vegetation or (ii) by widening the river which decreases the shear stress, leading to a rising river bed and better connected floodplains due to newly created sedimentation.

REFERENCES

Allan J., Castillo M. (2007). Stream ecology. Structure and function of running waters. 2nd ed, reprinted. Dordrecht: Springer.

Allen G., Pavelsky T. (2018). Global extent of rivers and streams. In: Science (New York, N.Y.), 361 (6402), 585-588, DOI: 10.1126/science.aat0636.

Arcement G., Schneider V. (1989) Guide for Selecting Manning's Roughness Coefficients for Natural Channels and Flood Plains. U.S. Geological Survey Water-supply Paper: U.S. Government Printing Office.

Baeyens W., Dehandschutter B., Leermakers M., Bobrov V., Hus R., Baeyens-Volant D. (2003). Natural Mercury Levels in Geologically Enriched and Geologically Active Areas. Case Study of Katun River and Lake Teletskoye, Altai (Siberia). In: Water, Air, and Soil Pollution, 142 (1/4), 375-393, DOI: 10.1023/A:1022099410739.

Belletti B., Rinaldi M., Buijse A., Gurnell A., Mosselman E. (2015). A review of assessment methods for river hydromorphology. In: Environ Earth Sci, 73 (5), 2079–2100, DOI: 10.1007/s12665-014-3558-1.

Brunner G. (2016). HEC-RAS River Analysis System. Hydraulic Reference Manual Version 5.0. Davis, CA: US Army Corps of Engineers, Hydrologic Engineering Center, [online] Available at: https://www.hec.usace.army.mil/software/hec-ras/documentation/HEC-RAS%205.0%20Reference%20Manual.pdf [Accessed 14 Mar. 2020].

Revyakin V. (1978). Catalog of glaciers of the USSR. Altai and West Siberia. 1978. v.15, issue 1. Gidrometeoizdat (in Russian).

Chow V. (1959). Open-Channel Hydraulics. New York: McGraw-Hill Book Company.

Díaz-Redondo M., Egger G., Marchamalo M., Damm C., Oliveira R., Schmitt L. (2018). Targeting lateral connectivity and morphodynamics in a large river-floodplain system: The upper Rhine River. In: River Res Applic, 34 (7), 734-744, DOI: 10.1002/rra.3287.

Dai C., Durand M., Howat I.M., Altenau E.H., Pavelsky T.M. 2018. Estimating River Surface Eleva-tion From ArcticDEM. Geophysical Research Letters, 45, 3107–3114, DOI: 10.1002/2018GL077379.

Du Y., Zhang Y., Ling F., Wang Q., Li W., Li X. (2016). Water Bodies' Mapping from Sentinel-2 Imagery with Modified Normalized Difference Water Index at 10-m Spatial Resolution Produced by Sharpening the SWIR Band. In: Remote Sensing, 8 (4), 354, DOI: 10.3390/rs8040354.

Environment Agency (2003). River habitat survey in Britain and Ireland. Field survey guidance manual. Bristol: Environment Agency.

FOEN (2013). Fliessgewässertypisierung der Schweiz. A basis for watercourse assessment and development. Annex 5. ed. by Federal Office for the Environment FOEN. Bern, [online] Available at: https://www.bafu.admin.ch/bafu/de/home/themen/wasser/publikationen-studien/publikationen-wasser/fliessgewaessertypisierung-der-schweiz.html [Accessed 09 Apr 2020].

Galia T., Škarpich V., Gajdošová K., Krpec P. (2017). Variability Of Wolman Pebble Samples in Gravel/Cobble Bed Streams. In: ASP FC, 1, 237-246, DOI: 10.15576/ASP.FC/2017.16.1.237.

Haggett P., Chorley R. (1969). Network analysis in geography. London: Edward Arnold.

Haywood A. (2010). Siberia. A cultural history (Landscapes of the Imagination). Oxford, New York: Oxford University Press.

Huet M. (1949). Aperçu des relations entre la pente et les populations piscicoles des eaux courantes. In: Swiss Journal of Hydrology, 11, 332-351, DOI: 10.1007/BF02503356.

Iturrizaga, L. (2011). Glacier Lake Outburst Floods. In: Singh, V.P., Singh, P., Haritashya, U.K. (eds) Encyclopedia of Snow, Ice and Glaciers. Encyclopedia of Earth Sciences Series. Springer, Dordrecht, 381-399, DOI: 10.1007/978-90-481-2642-2_196.

Khan A., Rao L., Yunus A., Govil H. (2018). Characterization of channel planform features and sinuosity indices in parts of Yamuna River flood plain using remote sensing and GIS techniques. In: Arab J Geosci, 11 (17), 263, DOI: 10.1007/s12517-018-3876-9.

Khromova T., Nosenko G., Glazovsky A., Muraviev A., Nikitin S., Lavrentiev I. (2021). New Inventory of the Russian glaciers based on satellite data (2016–2019). In: Ice and Snow, 61 (3), 341–358 (in Russian), DOI: 10.31857/S2076673421030093.

Kirpotin, S., Nemceva, G. (2015) Environmental, economic and social risks of nuclear power engineering (the case of the southern part of the Ob-river basin). In: International Journal of Environmental Studies, 72 (3), 580-591, DOI: 10.1080/00207233.2015.1027589.

Lammers, R., Shiklomanov, A., Vörösmarty C., Fekete B., Peterson B. (2016). R-ArcticNet, A Regional Hydrographic Data Network for the Pan-Arctic Region. supplement to: Lammers, Richard B, Shiklomanov, Alexander I, Vörösmarty, Charles J, Fekete, Balázs M, Peterson, Bruce J (2001). Assessment of contemporary Arctic river runoff based on observational discharge records. Journal of Geophysical Research: Atmospheres, [online] Available at: http://www.r-arcticnet.sr.unh.edu/v4.0/index.html [Accessed 27 Mar. 2020].

Leopold L., Miller J. (1956). Ephemeral streams - Hydraulic factors and their relation to the drainage net. With the cooperation of U.S. Government Printing Office. Washington, DC. (Professional Paper, 282A), [online] Available at: http://pubs.er.usgs.gov/publication/pp282A [Accessed 17 Feb. 2020].

Maharjan L., Shakya N. (2016). Comparative Study of One Dimensional and Two Dimensional Steady Surface Flow Analysis. Journal of Advanced College of Engineering and Management, 2, 15-30, DOI: 10.3126/jacem.v2i0.16095.

Mandych A. (2006). Conditions and Trends in Natural Systems of the Altai-Sayan Ecoregion. In: Hartmut Vogtmann and Nikolai Dobretsov (eds.). Environmental Security and Sustainable Land Use - with special reference to Central Asia, vol. 5, Dordrecht: Kluwer Academic Publishers (NATO Security through Science Series), 231-275.

Mueller J. (1968). An Introduction to the Hydraulic and Topographic Sinuosity Indexes. Annals of the Association of American Geographers, 58 (2), 371-385. DOI:10.1111/j.1467-8306.1968.tb00650.x.

Newson M., Large A. (2006). 'Natural' rivers, 'hydromorphological quality' and river restoration: a challenging new agenda for applied fluvial geo-morphology. In: Earth Surf. Process. Landforms, 31 (13), 1606–1624, DOI: 10.1002/esp.1430.

Nikora V., Goring D., Biggs B. (1998). On gravel-bed roughness characterization. In: Water Resources Research, 34 (3), 517-527, DOI: 10.1029/97WR02886.

Peredo Arce A., Hörren T., Schletterer M., Kail J. (2021). How far can EPTs fly? A comparison of empirical flying distances of riverine invertebrates and existing dispersal metrics. Ecological Indicators, 125, 107-465, DOI: 10.1016/j.ecolind.2021.107465.

Purinton B, Bookhagen B. (2017). Validation of digital elevation models (DEMs) and comparison of geomorphic metrics on the southern Central Andean Plateau. Earth Surface Dynamics, 5, 211–237, DOI: 10.5194/esurf-5-211-2017.

Sapozhnikov V. (1949). On the Russian and Mongolian Altai, 198 (in Russian).

Schletterer M., Shevchenko A., Yanygina L., Manakov Y., Reisenbüchler M., Rutschmann P. (2021a). Eindrücke vom Oberlauf des Obs in Russland. WASSERWIRTSCHAFT, 111, 77-85, DOI: 10.1007/s35147-021-0903-7.

Schletterer M., Reisenbüchler M., Berg L., Zunic F., Rutschmann P. (2021b). Reisebericht zur Wasserbauexkursion 2019 der TU München nach Sibirien. WASSERWIRTSCHAFT, 111, 96-101, DOI: 10.1007/s35147-021-0902-8.

Schmalfuß L., Hauer C., Yanygina L. V., Schletterer M. (2022). Landscape Reading for Alpine Rivers: A Case Study from the river Biya. Geography, Environment, Sustainability, 4(15), 196-213, DOI: 10.24057/2071-9388-2022-046

Schumm S. (1977). The fluvial system. New York: Wiley (A Wiley-Interscience publication).

Shiklomanov A., Lammers R. (2014). River ice responses to a warming Arctic - recent evidence from Russian rivers. In: Environ. Res. Lett., 9 (3), 35008, DOI: 10.1088/1748-9326/9/3/035008.

Shiklomanov A., Yakovleva T., Lammers R., Karasev I., Vörösmarty C., Linder E. (2006). Cold region river discharge uncertainty – estimates from large Russian rivers. Journal of Hydrology, 326 (1–4), 231-256. DOI: 10.1016/j.jhydrol.2005.10.037.

Strahler A. (1957). Quantitative analysis of watershed geomorphology. In: American Geophysical Union Transaction, 38 (6), 913-920.

Vuglinsky V., Valatin D. (2018). Changes in Ice Cover Duration and Maximum Ice Thickness for Rivers and Lakes in the Asian Part of Russia. In: NR 09 (03), 73-87, DOI: 10.4236/nr.2018.93006.

Ward J. (1989). The four-dimensional nature of lotic ecosystems. J N Am Benthol Soc, 8, 2–8, DOI: 10.2307/1467397

Wolman G. (1954). A Method of Sampling River-Bed Material. In: Transactions, American Geophysical Union, 35 (6), 951-956.

Zerbe S. (2019). Renaturierung von Ökosystemen im Spannungsfeld von Mensch und Umwelt. An interdisciplinary textbook. 1st ed. 2019, DOI: 10.1007/978-3-662-58650-1.

Zhang D., Yang Y., Lan B. (2018). Climate variability in the northern and southern Altai Mountains during the past 50 years. In: Scientific reports, 8 (1), 32-38, DOI: 10.1038/s41598-018-21637-x.

RESEARCH PAPER

QUANTIFYING LAND USE CHANGE DYNAMICS IN AGROTOURISM DESTINATIONS: A CASE STUDY FROM VENDA NOVA DO IMIGRANTE, BRAZIL

Juan David Méndez-Quintero[1*], Charles Oliveira Fonseca Mail[1], Marcelo Antonio Nero[1], Carlos Fernando Ferreira Lobo[1], Sónia Maria Carvalho Ribeiro[1]

[1]Institute of Geosciences of the Federal University of Minas Gerais, Av. Pres. Antônio Carlos 6627, 31270-901, Belo Horizonte, Brazil.

***Corresponding author:** juan94mendez@gmail.com

Received: July 20th, 2022 / Accepted: May 4th, 2023 / Published: July 1st, 2023

https://DOI-10.24057/2071-9388-2022-115

ABSTRACT. Agrotourism is one of the main economic activities in the municipality of Venda Nova do Imigrante, located in the state of Espírito Santo, Brazil. The objective of this research was to analyse the landscape changes generated by this economic activity. The methodology's development through a stratified random selection, the thematic quality of the maps from the MAPBIOMAS platform was assessed. A confusion matrix was produced, and the kappa coefficient was calculated. Landscape metrics, Volunteered Geographic Information (VGI) from Instagram and Flickr Social Networks, satellite images and free Brazilian databases were used, along with the use of open source GIS software to analyse changes use and cover of land in the municipality generated over a period of 30 years and its relationship with agrotourism. In the results, it was obtained that the thematic quality of maps from the MAPBIOMAS platform was acceptable, the analysis of VGI in social networks was identified agrotourism farms located mainly in the south-east area of Venda Nova do Imigrante, the analysis of changes in land use and cover showed that the city had an increase in urban area around the Federal Highway BR-262 that cuts through the city and rural areas, as well as in the agrotourism farms evaluated, there was an increase in agricultural areas and planted forests.

KEYWORDS: rural tourism, space-temporal analysis, landscape metrics, volunteered geographic information, kappa coefficient, thematic quality maps

CITATION: Juan David Méndez-Quintero, Charles Oliveira Fonseca Mail, Marcelo Antonio Nero, Carlos Fernando Ferreira Lobo, Sónia Maria Carvalho Ribeiro (2023). Quantifying Land Use Change Dynamics In Agrotourism Destinations: A Case Study From Venda Nova Do Imigrante, Brazil. Geography, Environment, Sustainability, 2(16), 121-131
https://DOI-10.24057/2071-9388-2022-115

ACKNOWLEDGEMENTS: The first author thanks the Coordenação de Aperfeiçoamento de Pessoal de Nível Superior–CAPES for the exclusive dedication scholarship for master's studies. The authors thank Edgar Enrique Méndez Lozano for the revision of the English language.

Conflict of interests: The authors reported no potential conflict of interest.

INTRODUCTION

The agrotourism is an economic activity aimed to integrate tourists into agricultural communities, its main attraction is the agricultural landscape and the cultural customs of the locals (McGehee 2007; Phillip et al. 2010; Olivieri 2014). This type of tourism began in the 1960s, but gained popularity in the 80's and early 90's. In Brazil, agrotourism began to be explored at the end of the 1980s (Parra et al. 2006; Khairabadi et al. 2020), in the state of Espírito Santo, this activity began shortly after, in 1990. Due to its great impact in 1994, the Regional Development Center for Agrotourism was created in the municipality of Venda Nova do Imigrante. It was responsible for organizing agrotourism throughout the State of Espírito Santo. Currently, agrotourism is one of the main economic activities developed in the city, and its organization and touristic offer is recognized in the rest of the country, making it worthy of the title of National Agrotourism Capital (Pereira and Ribeiro 2011; Zandonadi 2013).

Agrotourism, in symmetry with other tourism segments in rural areas, promotes the conservation of natural formations necessary for the ecosystem balance together with traditional land use activities (Dublin et al. 2013; Towoliu et al. 2018), however, tourist activities can also have negative impacts on the environment (Almeida et al. 2022). In agrotourism the composition of the landscape (which are the present land uses) and the configuration of the landscape (how these land uses are distributed in space) are important characteristics because they are associated with positive and pleasant tourism experiences (Serenelli et al. 2017; Brandano et al. 2018). It is worth noting that the attractiveness of the tourism landscape in rural areas is the result of the consonance of attractions, structures, and services that allow the arrival, experiences, and permanence of the tourist (Towoliu et al. 2018).

Landscapes are dynamic and change over time, whether natural or cultural. To study these changes, one of the most used tools is landscape metrics, as they

allow us to quantify spatial structures and functions. Its initial application was in ecological studies, but due to its efficiency in evaluating land cover, especially in urban landscapes, it gained notoriety in different areas, becoming recognized in different areas of knowledge as well (Herold et al. 2005; Victorov 2012).

Landscape metrics can be used to monitor the development of tourist activity, as stated (Stankov et al. 2016) who used this type of measurement to quantify the variation in land use generated by the development of tourist activity in the municipality of Čajetina, Serbia. In the study developed by (Dimobe et al. 2017) landscape metrics were used to measure land use and land cover changes over 29 years in the tourist areas of the Nazinga Game Ranch Reserve in Burkina Faso. Another research on the tourist landscape was carried out on the island of Cos, Greece, where through the use of Geographic Information Systems (GIS) and landscape metrics, it was sought to quantitatively describe the spatial structure of the tourist landscape and to analyse the evolution of the terrain land use and occupation generated by the increase of this economic activity in the region (Gkoltsiou et al. 2013). Another similar and recent reference theme it has presented in (Wang et al. 2023) where the authors have applied remote sensing and GIS in Zhangjiajie, a famous mountain tourist city in China.

Due to the advances in connectivity that the internet has brought and the equipment of electronic devices with Global Positioning Systems (GPS), social networks have become a great source of georeferenced data (Hernández Magaña and Güiza Valverde 2016). This phenomenon brings up a term called Volunteered Geographic Information (VGI), which is defined as the information generated by human sensors, users of a platform, who voluntarily capture temporal space information that helps to understand the socioeconomic conditions and landscape of a given place (Goodchild 2007; Ramiro et al. 2016; Méndez-Quintero et al. 2022). This type of information is used in the landscape analysis of tourist sites. (Tieskens et al. 2018) proposes a methodology that uses photos from the social networks Flickr and Panoramio to estimate the correlation between the attributes of the landscape and the landscape preferences of tourists. Another research that addresses this issue is the one developed by (Payntar et al. 2021), who used artificial intelligence algorithms together with geotagged photographs obtained from the internet to identify travel patterns of an archaeological circuit in Cuzco, Peru, and in this way quantified the experiences that tourists had and the attractiveness of the landscape.

According to (Klimanova et al 2017), in the densely populated states of southern and south-eastern Brazil, the main changes in land use and land cover are related to agricultural development. The Brazilian municipality of Venda Nova do Imigante, which is well-known for its agricultural economy and its agrotourism model and is a national model, provided the soil for analysis in the current study. Given the importance of agrotourism development in Venda Nova do Imigrante, this research aims to analyse the changes in the city's landscape and its relationship with agrotourism activity. This research aims to answer the following question: what is the participation of agrotourism farms in the composition and dynamics change of land use and land cover in Venda Nova do Imigrante-ES, Brazil?

To obtain the answer to the investigation, the objectives that defined the scientific rigor for the space analysis were established, as follows:

- Validate the accuracy of the thematic maps for the years 1988 and 2018, obtained from Brazilian databases.
- List landscape metrics that make it possible to understand the change of land use between selected years.
- Access the change in land use and land cover in the municipality and selected agrotourism farms.

MATERIALS AND METHODS

Although the analysis was carried out for a Brazilian municipality, the approach proposed in this article, including a methodology that can be replicated in several case studies (Fig. 1), the applicability and potential use of landscape metrics associated with remote sensing for the analysis of agrotourism, can be relevant for the development of the activity in countries with fragile/dependent and/or developing economies.

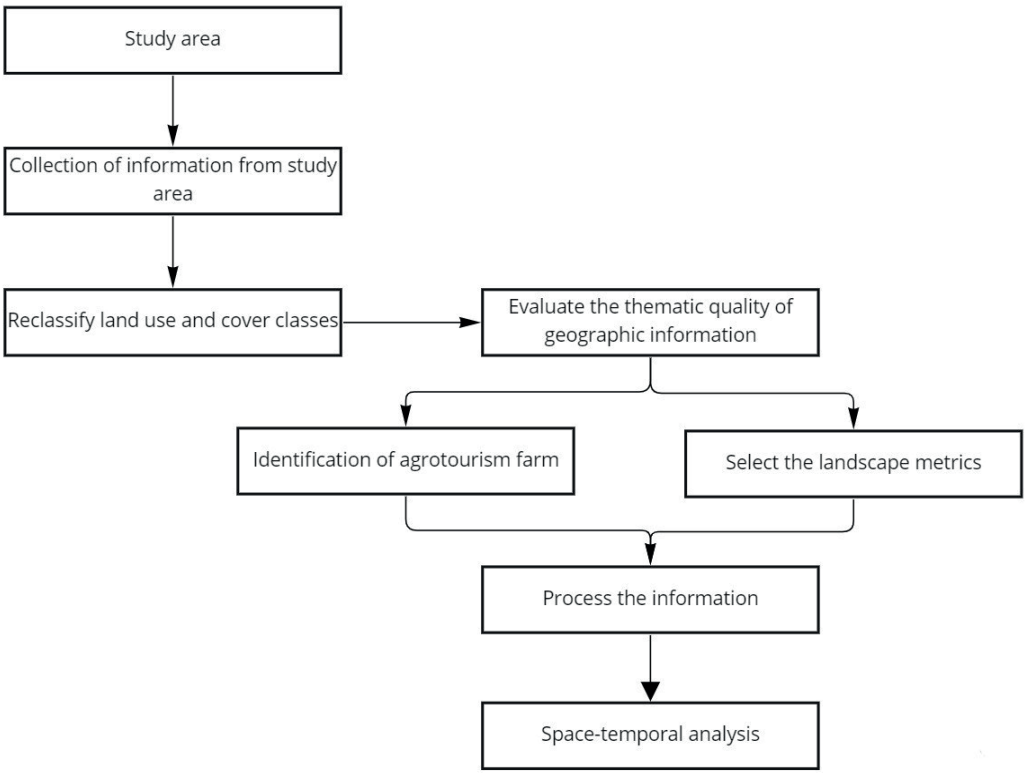

Fig. 1. Methodology flowchart

The first step was to collect thematic maps of land use and land cover and this information was reclassified according to the research objectives. Subsequently, the thematic quality of the maps was evaluated and the agrotourism farms were identified with the help of volunteer geographic information from social networks. The metrics for quantitative description of landscape were selected according to the consulted bibliography. Finally, the geographic information was processed and the space temporal analysis was carried.

Study Area

The municipality of Venda Nova do Imigrante is located in the mountainous region of the Brazilian state of Espírito Santo (Fig. 2), 106 km from Vitória the state capital. It has a land area of 188.9 km^2. Initially, it was populated by Portuguese coffee growers, but in 1892 it received a large wave of Italian immigrants, mainly from the Veneto region. The municipality area was emancipated from the municipality of Conceição do Castelo on May 10, 1988, by Decree-Law No. 4,069 / 88, obtaining its status as a municipality and current name (PVNI, 2021.)

The municipality has a strong Italian ethnic identity and the local economy is based on agriculture, especially coffee growing, fruit and vegetables on a small and medium scale as well. In recent decades, agrotourism has gained prominence as one of the main income sources. (Nogueira 2006; Zandonadi 2013).

The landscapes, in their physical dimension, were conditioned by the association of geological and geomorphological events that provided peculiar characteristics, such as the rugged relief. The lithological framework is mainly composed of metamorphic (gneiss) and magmatic (granite) rocks and thrust fault structures, typical of the Serra da Mantiqueira, due to neotectonics. The lithological framework underwent new reactivations due to the separation of the Afro-Brazilian plate (Saadim 1991; Sgarbi and Dardenne 1996; Marques Neto 2017). Weathering and denudational agents were responsible for sculpting the convex mountains, jagged valleys, and a vast river network that conditions the heterogeneity of the landscape. Also, the action of weathering in the formation of structured soils, suitable for agricultural activities, is highlighted. The original biome of Espírito Santo is the Atlantic Forest, which is characterized by semideciduous and rainforest forests (IBGE, 2004). The existence of high-altitude fields on the mountain summits is significant in addition to these phytological characteristics.

Standardization of Information and Assessment of the Quality of Geographic Information

The first step to fulfil the purposes of the research was to use thematic maps that would allow the perception of changes in land use and land cover classes. In this context, thematic maps were selected from the collection 5 available in the MAPBIOMAS Project, corresponding to the years 1988 and 2018 (Mapbiomas 2021). The raster files of the selected maps were reclassified generating 6 final classes, using the Dinamica Ego 5 software (CSR/UFMG, 2021), namely: native forest, planted forest, agriculture area, urban area, water bodies, and others.

To access the quality geographic information available on the Mapbiomas platform, a stratified random sampling with the information of the year 2018 was chosen because this year there is a larger size of agricultural and urban coverage, which allowed for standardization in the number

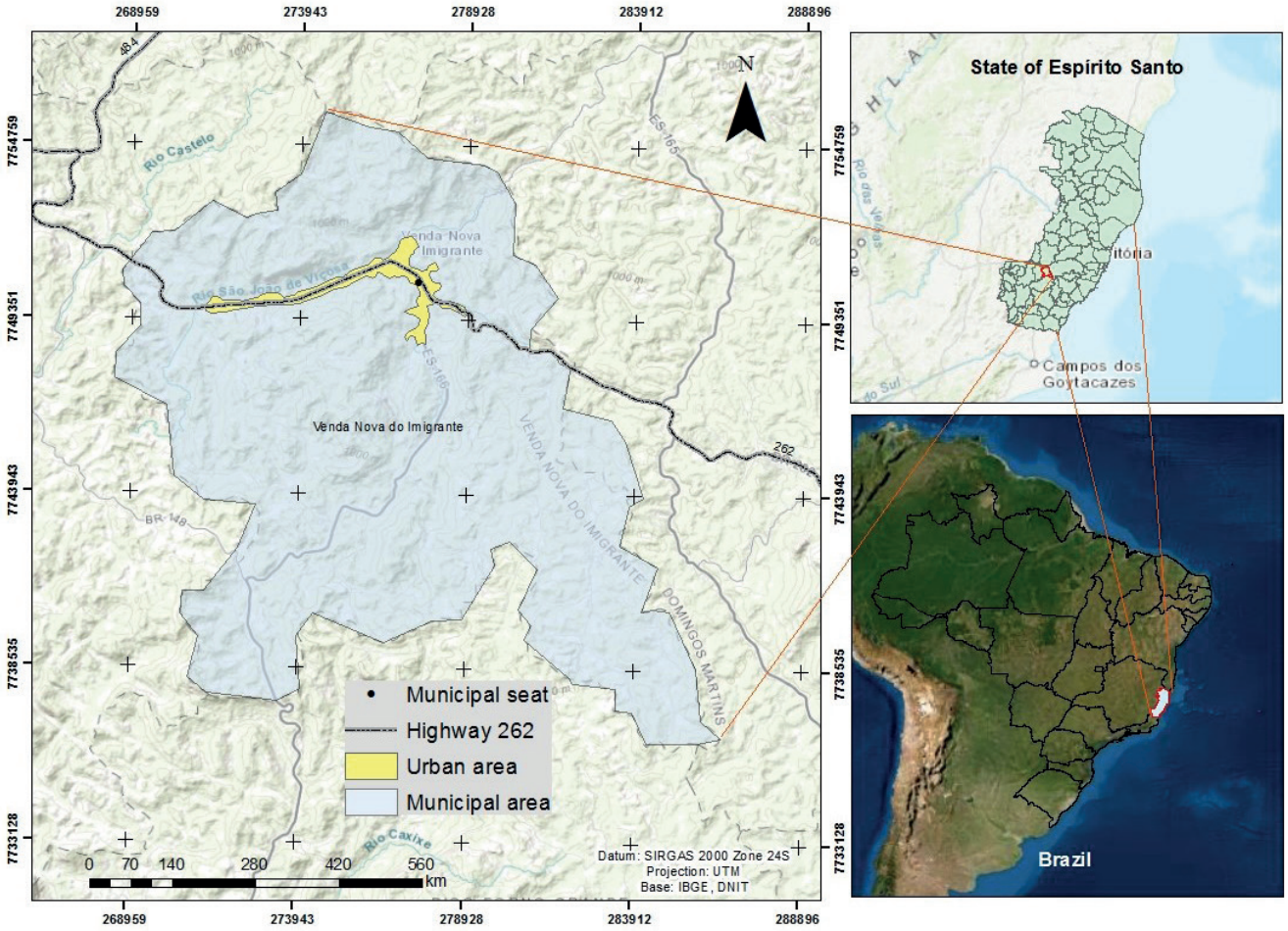

Fig. 2. Location municipality Venda Nova do Imigrante

of samples for the two years studied. Stratified random sampling allows to obtain a representation of each class of land use and occupation in proportion to the territory (FAO 2016), according to (Equation 1).

$$n = \left(Z_{\alpha/2}\right)^2 * p * q / e^2 \quad (1)$$

Equation 1 presents the calculation of the number of samples (n) defined by the multiplication of the square of the desired degree of confidence (critical value = Z(α/2)) by the expected probability of a hit (p) and by the resulting conscious result of 1 minus a probability (1-p). This value will still be divided by the squared error (e).

The geographic information of the Mapbiomas platform, for the year 1988 was compared with a Landsat 5 satellite image with a resolution of 30 meters, obtained from the database of the Earth Explorer (USGS 2021). Regarding the MAPBIOMAS information corresponding to the year 2018, a comparison was made with the CBERS 4 satellite image, with a resolution of 10 meters, obtained from the platform of the National Institute for Space Research (INPE 2021). Additionally, for a better match between the land cover obtained in MAPBIOMAS and reality, images from the Google Earth satellite and the Esri satellite were also analyzed for two time periods. The evaluation of the thematic quality of information from the MAPBIOMAS platform for mapping was carried out in the QGIS 3.18.1 software (QGIS. org, 2021), with the help of the AcATaMA plugin (Llano 2022), in order to obtain a confusion matrix for each year.

From the evaluation of the samples by the classes, the confusion matrices or error matrices for the years in question were produced, 1988 and 2018. The confusion matrix is the tool that allows us to weigh the accuracy between the sensing and the thematic map (Ariza-López et al. 2019; Alba-Fernández et al. 2020, Alba-Fernández 2021). Through the confusion matrix, different indices can be estimated, including the global accuracy and the kappa index (coefficient) used in this study (Foody 2004).

Global accuracy is a calculation that considers the summation of the number of correct answers in the classes divided by the number of samples. The value obtained allows a first comparative analysis between the mapped content, although, when considering only the diagonal of the confusion matrix, this index does not capture chance between the classes (Brites et al. 1996). Global accuracy is expressed by Equation 2.

$$G = \sum_{i=1}^{c} x_{ii} / n \quad (2)$$

Where:

$\sum_{i=1}^{c} x_{ii}$ corresponds to the summation of the diagonal of the confusion matrix and n = the total number of samples

The kappa index established by (Cohen 1960), has a wide applicability in space statistical studies, although some authors suggest variances for greater numerical veracity. Kappa gives an example of how flawless a class is. It brings innovation about the global index, as the kappa considers both the results of the main diagonal and the other values contained in columns and rows (Brites et al. 1996). Among the algebraic deductions, the kappa index with stratified random sampling was considered for the research, represented by (Equation 3).

$$K = n \sum_{i=1}^{c} X_{ii} - n \sum_{i=1}^{c} X_i + X_{+i} / n^2 - \sum_{i=1}^{c} X_i + X_{+i} \quad (3)$$

Where:

$\sum_{i=1}^{c} X_{ii}$ Matrix diagonal summary.

$\sum_{i=1}^{c} X_i + X_{+i}$ Sum of the product of the sums of the row (xi+) by the column (x+i).

n^2 Number of samples squared.

The kappa index values range from 0 to 1, with values close to zero showing that the class or category has a high level of error about remote sensing. On the other hand, values close to one have a higher degree of accuracy. It is important to emphasize the interpretation and the possibilities of analysis of the Kappa index applied by the various authors, the concepts and classification scales presented by (Fleiss et al. 1969), (Landis and Koch 1977), (Monserud and Leemans 1992) is demonstrated by (Foody 2020) (Fig. 3).

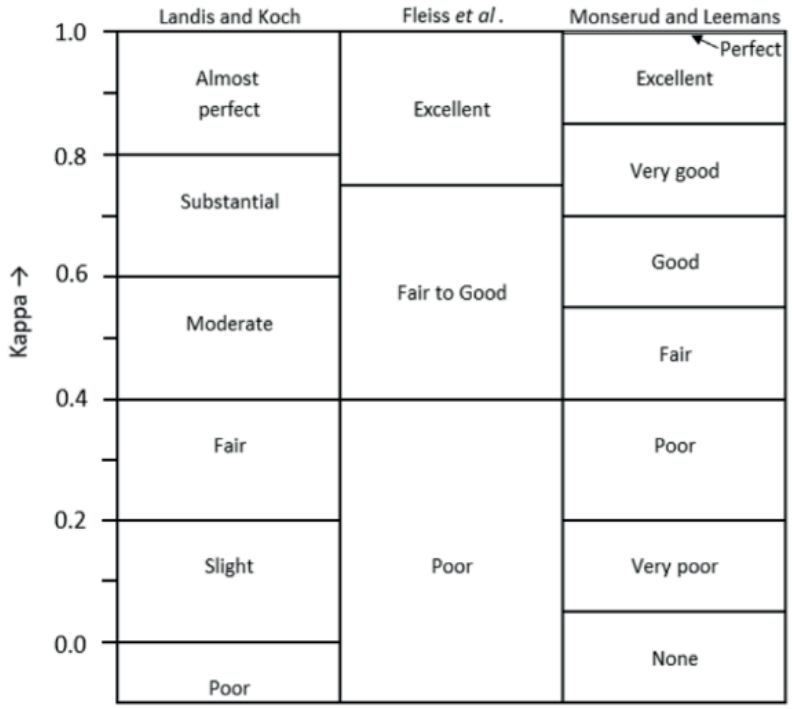

Fig. 3. Kappa index classification (Foody 2020)

Identification of agrotourism farms.

To identify the agrotourism farms in the municipality of Venda Nova do Imigrante-ES, Brazil, the geotagged photographs published between February 1, 2017 and February 1, 2021 with the location of the municipality and posted on the networks social Instagram and Flickr were consulted. The criteria for selecting the photographs were those that show agrotourism farms where tourist activities related to traditional agriculture on a family scale were prioritized. Once the farms had been identified, their location and coordinates were verified on Google Maps, and the boundary area of the properties was defined with the help of the Rural Environmental Registry (CAR) made available by the municipal management in shapefile format (PVNI, 2021).

Landscape metrics

To identify landscape changes over the 30 years analyzed, landscape metrics were selected based on the consulted bibliography (Table 1). Subsequently, the MAPBIOMAS images corresponding to the years 1988 and 2018 were analysed in the Fragstats 4.2 software (McGarigal et al. 2015).

Table 1. Landscape metrics implemented in the project (based on McGarigal and Marks 1994; Dimobe et al. 2017; Urrutia et al. 2020)

METRIC	ABBREVIATION	DESCRIPTION	ANALYSIS LEVEL	INTERPRETATION OF RESULTS
Class Area	CA	It quantifies how much a given land-use class occupies in the landscape. Values close to 0 demonstrate that the class occupies a small area concerning the total area.	Patcher	CA > 0, without limit.
Percent of Landscape	PLAND	Corresponds to the percentage of the class in the landscape.	Patcher	0 < PLAND ≤ 100
Number of Patches	NP	Number of fragments or patchers in a class.	Patcher	NP ≥ 1, without limit.
Mean area	AREA_MN	Corresponds to the average area in hectares of each class within the landscape.	Patcher	AREA_MN > 0, without limit.
Standard deviation area	AREA_SD	Informs the standard deviation from the mean area. It can thus be verified whether class sizes were maintained over time or whether significant outliers were produced.	Patcher	AREA_SD> 0, without limit.
Average distance from neighbors	ENN_MN	It exposes the average distance between the nearest neighbors (fragments), it is a metric of structural connectivity.	Patcher	ENN_MN> 0, without limit.
Standard deviation of neighbors mean	ENN_SD	Informs the variation of values, concerning the average of the distances between the closest neighbors.	Patcher	ENN_SD> 0, without limit.
Mean Shape Index	SHAPE_MN	Quantifies the shape of fragments and allows you to assess how much a class is exposed to the edge effect. Values closer to 1 mean that the shapes are more similar to the circle or square (isodiametric). On the contrary, values close to 0 demonstrate complex shapes and are more susceptible to external interference.	Patcher	MSI ≥ 1, without limit. MSI = 1 when the patch is circular (vector) or square (raster).
Patch Richness	PR	Class diversity index in the landscape. It is based on the hypothesis that the greater the number of classes in a landscape, the greater the possibility of having different species, which in turn informs the composition of classes in the landscape.	Class	PR ≥ 1, without limit
Patch Richness Density	PRD	Quantifies the density of the number of classes. While the PR informs variation in the number of classes in the landscape, the PRD measures the intensity of these classes, in turn, the size of the patches in each class will influence. The calculation is made considering the classes present in an area of 100 ha. Ranges from 1, when there is only one class per area, to infinity.	Class	PRD > 0, without limit
Shannon's Diversity Index	SHID	The Shannon Index expresses values related to landscape diversity. It increases proportionally with the richness of the blob classes in the landscape, when the landscape has only one class, they will have a value of 0. On the other hand, in landscapes with varied land use, the index will increase until reaching the maximum value of 1.	Class	SHDI = 0 when the landscape contains only 1 patch

The selected landscape metrics allow characterizing the agricultural matrix in terms of area, density, border, shape, isolation, proximity, intercalation and diversity, they are also used to analyze the development of tourist activities and the influence they have on the landscape (Dimobe et al. 2017; Urrutia et al. 2020).

RESULTS AND DISCUSSION

Reclassification of use and cover land

The thematic maps of land use and land cover obtained from the MAPBIOMAS platform were reclassified into 6 classes: native forest, planted forest, agricultural area, urban area, water bodies, and others. Fig. 4 shows the configuration of land use and land cover that the municipality had in 1988 and 2018.

Determining the number of samples for thematic quality assessment

To determine the quality of geographic information in thematic maps, the "Native Forest area" class and the "Planted Forest area" class were unified due to the difficulty of differentiating them separately in satellite images. In obtaining the number of samples, the parameter of the areas of the land use classes of the year 2018 was used. Statistically, we chose to obtain a probability of correctness of 95%. In turn, the Z(α/2) has a value of 1.96; p=0.95; q=0.05 and the error=0.025, as it is a two-tailed test. The number of samples required was 292 achieved through Equation 1 with the values expressed here. Subsequently, this number was stratified into the classes of the thematic land cover and use map (Table 2).

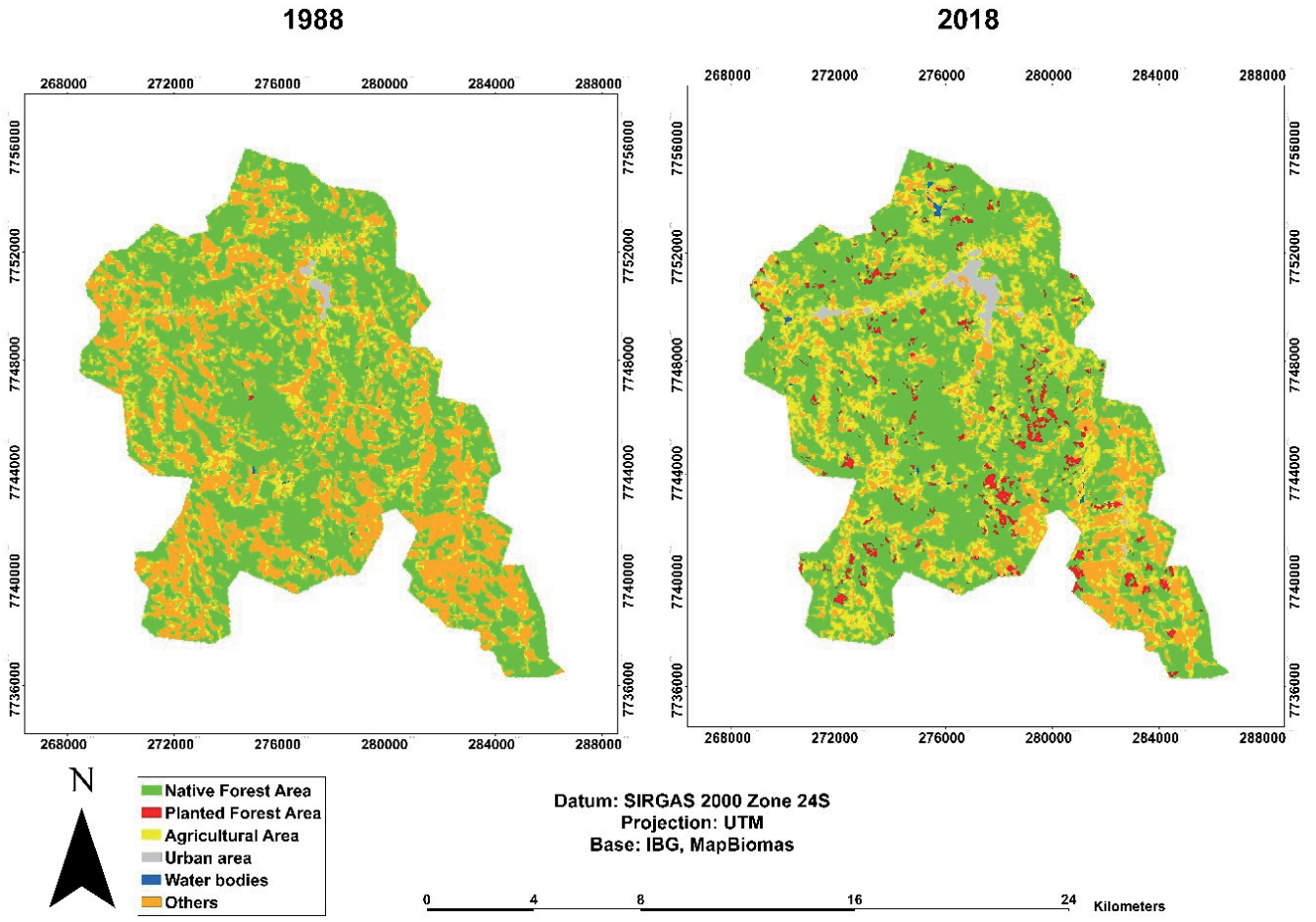

Fig. 4. Land use and land occupation Venda Nova do Imigrante in 1988 and 2018

Table 2. Proportion of samples by classes

Name of the classes	Classes area (ha)	proportion of the class	Number of samples
Native and Planted Forest	11391.12	0.603	166
Agricultural area	4451.22	0.236	69
Urban area	304.65	0.016	10
Water bodies	36.45	0.002	5
Others	2702.07	0.143	42
Total	18885.51	1	292

The forest class obtained 176 samples, while the urban class and water bodies accounted for 5 and 0 respectively. Thus, for adequate representation of the classes, 10 forest samples were reduced and distributed equally between the urban and water bodies classes.

Confusion matrix, global accuracy, and kappa index

The confusion matrix for the year 1988 (Table 3) and year 2018 (Table 4) were generated from the comparison of images obtained from the Landsat 5 and CBERS 4 satellites respectively with the thematic maps of the MAPBIOMAS platform through the AcATaMA plugin, available in QGIS.

The global accuracy value obtained with the help of the AcATaMA plugin was 0.82 and the kappa index value 0.67, these values are acceptable in thematic quality, according to the scales of the different authors (Table 4).

For the year 2018, the global precision value was 0.85 and the kappa index was 0.75, which allows reliability in the thematic map.

Selection and identification of agrotourism farms

A total of 15,420 photographs of the municipality of Venda Nova do Imigrante were analyzed on the Instagram social network corresponding to the period of time determined in the methodology, of which 23 complied with the specification of the research, in relation to the social network Flicker, it was analyzed 509 photographs and only 6 met the selection parameter. From the photographs that met the parameters, a total of 6 farms were identified and their coordinates were consulted on google maps (Table 5).

In relation to the selected photographs, it was observed that in the social network Instagram the photos published mainly reflected tourists and the activities they carried out, allowing to analyze the relationship between the tourist and the place, while in the social network Flickr, the photographs were focused on landscapes, allowing to analyze the attractions of tourist sites and agricultural places. Although the social network Instagram had a greater number of photographs, most of these photographs were of commercial products and selfies, on the other hand, the social network Flicker in most of its photographs were of rural and municipality landscapes and a small portion corresponded to cultural events. The identified agrotourism farms were situated in the municipal area's south-eastern region (Figure 5).

Description of the landscape of Venda Nova do Imigrante

With the help of the FRAGSTATS 4.2 software, the selected landscape metrics for the municipality area corresponding to the years 1988 and 2018 were analyzed (Table 6).

Table 3. Confusion Matrix for the Year 1988

Thematic raster classes	Native and Planted Forest	Agricultural area	Urban area	Water bodies	Others	**Total**
Native and Planted Forest	147	3	0	1	15	166
Agricultural area	16	42	0	1	10	69
Urban area	0	0	10	0	0	10
Water bodies	3	0	0	2	0	5
Others	7	6	0	1	34	42
Total	173	45	10	5	59	292

Table 4. Confusion Matrix for the Year 2018

Thematic raster classes	Native and Planted Forest	Agricultural area	Urban area	Water bodies	Others	**Total**
Native and Planted Forest	146	15	0	0	5	166
Agricultural area	9	51	0	0	9	69
Urban area	0	2	8	0	0	10
Water bodies	0	0	0	5	0	5
Others	0	5	0	0	37	42
Total	155	73	8	5	51	292

Table 5. Agrotourism farms selected for the study and geographic coordinates in decimal degree

FARMS	LATITUDE	LONGITUDE
Agroturismo Familia Brioschi	-20,377697	-41,132806
Família Busato Agroturismo	-20,371011	-41,128060
Pousada Bela Aurora	-20,417500	-41,130765
Carnielli	-20,365476	-41,125312
Vinhos Tonole	-20,362892	-41,118941
Fazenda Saúde	-20,370351	-41,112043

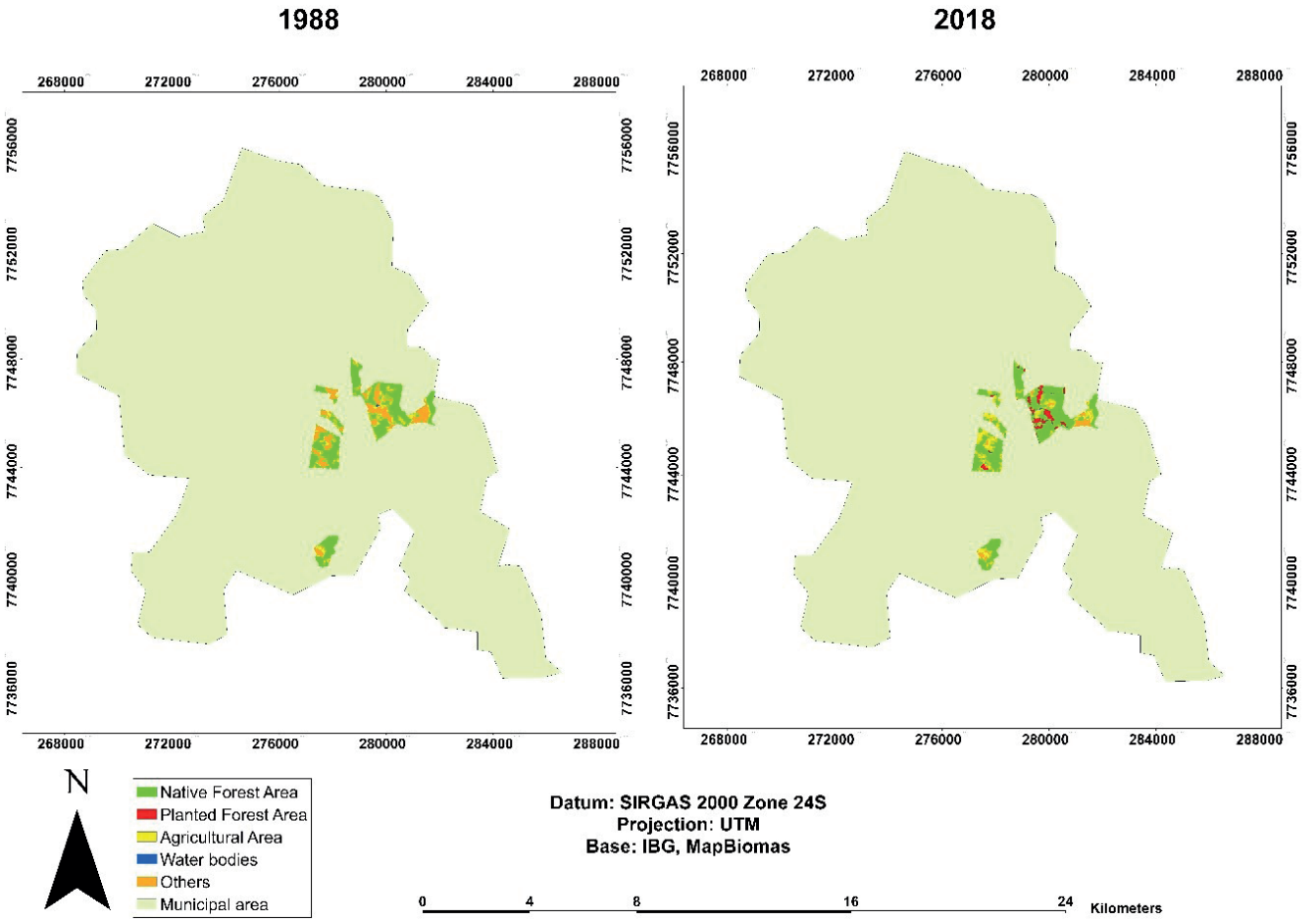

Fig. 5. Location of the agrotourism farms selected for the study

Table 6. Results of the landscape metrics of Venda Nova do Imigrante in 1988 and 2018

LANDSCAPE METRICS	USE AND COVERAGE LAND											
	Native Forest Area		Planted Forest Area		Agricultural Area		Urban area		Water bodies		Others	
	1988	2018	1998	2018	1988	2018	1988	2018	1988	2018	1988	2018
CA (ha)	9986.85	10682.28	5.94	708.84	2470.32	4451.22	81.18	304.65	4.95	36.45	6336.27	2702.07
PLAND (%)	52.88	56.56	0.03	3.75	13.08	23.57	0.43	1.61	0.03	0.193	33.55	14.31
NP	289	264	5	277	1531	895	5	19	4	17	381	510
AREA_MN (ha)	34.56	40.46	1.19	2.56	1.61	4.97	16.24	16.03	1.24	2.14	16.63	5.30
AREA_SD (ha)	272.50	400.11	0.94	3.74	3.39	19.03	19.75	44.03	0.89	3.16	87.39	18.17
SHAPE_MN	1.76	1.66	1.31	1.54	1.59	1.84	1.82	1.57	1.20	1.45	1.57	1.50
ENN_MN (m)	87.24	79.84	1612.22	203.92	88.98	80.38	193.03	231.38	1360.09	1234.48	120.29	132.25
ENN_SD (m)	45.65	31.99	1370.30	228.36	50.32	38.60	74.69	244.09	1723.40	1317.46	78.14	99.89

	1988	2018
PR	6	6
PRD	0.03	0.03
SHDI	1	1.14

It can be observed that in 30 years the municipality had an increase in the size of the native forest, planted forest, agriculture area, urban area and water bodies classes, and a reduction in the area of the other class. The number of patches (NP) in the forest and agriculture classes decreased but had increase in the average area value (AREA_MN), which suggests that there was a greater connectivity in these classes. But the standard deviation (AREA_SD) in these same classes also increased, inferring the presence of areas of different sizes.

Shape is an important metric to identify the edge effect on natural formations. The higher its value, the greater the interference (negative effect) of neighboring classes on the ecosystem. When comparing this metric (SHAPE_MN) between years, it was found that there was a reduction in pressure on the formation of natural forests. On the other hand, in local agriculture, largely associated with agroforestry, the increase in the average shape should be considered positive, as the plantations are interspersed with natural formations and thus demonstrate the permanence of the practice of sustainable cultivation over the years.

The planted forest showed an increase of approximately 703 ha between years, accounting for 3.75% of the vegetation cover in 2018. The growth in the number of fragments demonstrates that these plantations were spread throughout the territory, with the average area of the surrounding class of 2.6 ha.

The urban patch, in 1988, the year of its political and territorial emancipation, occupied 81 ha (0.43%) with the presence of 5 fragments with an average area of 16 ha. In 2018 the urban area came to represent 304.65 ha (1.6%) with an increase in the number of fragments to 19, maintaining its average area of 16 ha. These values are explained by the expansion of the urban center along 262 Highway and the formation of small villages.

The water bodies in the first year accounted for 4 fragments with a total area of 4.95 ha, 0.03% of the territory. In the second year, there were 17 fragments with an area of 36.45 ha (0.19%). The increase in water bodies is related to artificial damming for sport fishing and leisure.

At the landscape level, when comparing the Patch Richness (PR) between 1988 and 2018, it was found that there was an increase only in the planted forest class, which did not cause a significant change in the PR. Another metric that corroborates the configuration of classes between the years evaluated was the Patch Richness Density (PRD), which quantifies the number of classes per 100 hectares that also remained constant.

In the landscape category, it was found that the municipality in both years had a good indicator of the Shannon Diversity Index (SHDI), and in 1988 the SHDI = 0.99, and in the year 2018 SHDI = 1.14. In a way, it can be said that the Shannon in both remained close to the value of 1. It should be noted that the SHDI is calculated using the weighted geometric mean of the landscape classes. In turn, its alteration may occur due to variation in Patch Richness (PR) or Class Percentage (PLAND). As explained above, the PR remained constant over the years and responsible for the small variation was the PLAND with the increase in the classes of forest (from 52.88% to 56.56%) and agriculture (from 13.08% to 23.57%) in detriment to the reduction of the other class (from 33.55% to 14.31%) which includes: exposed soil, mining, and other unidentified coverage.

Analysis of landscape metrics on selected farms

With the help of the FRAGSTATS 4.2 software, the landscape metrics selected for the area of the chosen farms, corresponding to the years 1988 and 2018, were also analyzed (Table 7).

Interesting information on soil cover was provided by the analyzed farms. In 1988, the forests had 28 fragments that corresponded to 58% of their coverage, with an average area of 12.3 ha. Agriculture had 77 fragments responsible for 12% of occupation with an average area of

Table 7. Results of landscape metrics of agrotourism farms in Venda Nova do Imigrante in 1988 and 2018

LANDSCAPE METRICS	USE AND COVERAGE LAND									
	Native Forest Area		Planted Forest Area		Agricultural Area		Water bodies		Others	
	1988	2018	1998	2018	1988	2018	1988	2018	1988	2018
CA (ha)	344.07	388.17	0	49.50	72	112.77	0.63	1.17	175.59	40.68
PLAND (%)	58.09	65.54	0	8.36	12,16	19.04	0.11	0.20	29.65	6.87
NP	28	19	0	22	77	52	1	1	36	19
AREA_MN (ha)	12.29	20.43	0	2.25	0,94	2.17	0.63	1.17	4.88	2.14
AREA_SD (ha)	21.63	46.20	0	3.13	0,87	4.32	0.00	0	8.04	3.47
SHAPE_MN	1.69	2.01	0	1.41	1.47	1.54	1.17	1.63	1.35	1.40
ENN_MN (m)	112.94	226.42	0	222.38	100.52	111.90	N/A	N/A	142.50	302.99
ENN_SD (m)	77.14	566.40	0	226.42	99.06	126.98	N/A	N/A	143.85	207.49

	1988	2018
PR	4	5
PRD	0.68	0.84
SHDI	0.94	1

0.94 ha. The class "other" covered farms, with 36 fragments that together accounted for 29% with an average area of 4.88 ha.

Compared to the values for the years 2018, it can be seen that part of the class "other" has been replaced by both native and planted forests and by agriculture. The class "other" reduced to 19 fragments and occupied 6.87% and its average area became 2 ha; native forest increased to 64.53% with 19 fragments. Agriculture also increased to 19% with 52 fragments and its average area increased to 2.17 ha. It is also observed that the planted forest class became present in 2018. They now represent 8.36% of the total of selected farms, with the number of 22 fragments with an average area of 2.25 ha.

Regarding the landscape category, the PR, PRD and SHDI metrics showed an increase between the years. The expansion of the forest and agriculture classes and the emergence of the planted forest class took place over the other class, which represented on farms, mainly exposed soil. Its reduction became a gain in diversity due to the recovery of degraded areas for forest restoration and crop planting.

CONCLUSIONS

The systematization and analysis of the data allowed for the quantification of the content and structure of the landscape as well as its temporal history. It was found that the municipality of Venda Nova do Imigrante had a significant growth in agricultural and urban areas together with a reduction in the class other constituted mainly by exposed land. The recovery of soil through reforestation and agricultural production is one of the points where agrotourism farms play a part in the dynamics of change in land use and cover.

The methodology presented in this study allowed to satisfactorily identify and analyze changes in land use in agrotourism places and at the same time allowed to evaluate the quality of the maps used. In relation to the sources of information and the software used, they are free, which allows lower costs in this type of spatial analysis.

It was concluded that the Mapbiomas platform is adequate for land use and cover land change studies, however, the thematic quality of the oldest maps is difficult to validate due to the limited supply of high space resolution images at the time.

The social networks Instagram and Flickr showed a large volume of VGI of the municipality; however, the volume was low for the analysis of agrotourism places. This shows a low efficiency in capturing information on this type of tourism.

REFERENCES

Alba-Fernández M.V., Ariza-López F.J., Rodríguez-Avi J. and García-Balboa J.L. (2020). Statistical methods for thematic-accuracy quality control based on an accurate reference sample. Remote Sensing, 12(5), 1–16, DOI: 10.3390/rs1205081.

Alba-Fernández M.V. (2021). Aplicación de los test de equivalencia al control tipo temático de magnitudes asociadas a un Modelo Digital de Elevaciones. Revista Cartográfica, 103, 165–181, DOI: 10.35424/rcarto.i103.993.

Almeida E.S., Sartori, R.A., and Zaú A.S. (2022). Trail Impacts In A Tropical Rainforest National Park. Geography, Environment, Sustainability, 15(2), 5–12, DOI: 10.24057/2071-9388-2021-036.

Ariza-López F.J., Rodríguez-Avi J., Alba-Fernández M.V. and García-Balboa J.L. (2019). Thematic accuracy quality control by means of a set of multinomials. Applied Sciences (Switzerland), 9(20), 1–14, DOI: 10.3390/app9204240.

Brandano M.G., Osti L. and Pulina M. (2018). An integrated demand and supply conceptual framework: Investigating agritourism services. International Journal of Tourism Research, 20(6), 713–725, DOI: 10.1002/jtr.2218.

Brites R.S., Soares V.P. and Ribeiro C.A.A.S. (1996). Verificação da exatidão em classificações de uma imagem orbital mediante a utilização de três índices. Revista Árvore, 20(3), 415–424.

Cohen J. (1960). A Coefficient of Agreement for Nominal Scales. Educational and Psychological Measurement, 20(1), 37–46, DOI: 10.1177/001316446002000104.

CSR/UFMG. (2021). Dinamica EGO , No. 5, [online] Available at: https://csr.ufmg.br/dinamica.

Dimobe K., Goetze D., Ouédraogo A., Forkuor G., Wala K., Porembski S. and Thiombiano A. (2017). Spatio-Temporal Dynamics in Land Use and Habitat Fragmentation within a Protected Area Dedicated to Tourism in a Sudanian Savanna of West Africa. Journal of Landscape Ecology(Czech Republic), 10(1), 75–95, DOI: 10.1515/jlecol-2017-0011.

Dublin D., Bancheva A. and Freitag A. (2013). Local Initiatives for Sustainable Development in Rural Hokkaido: a Case Study of Samani. In: Geography, Environment, Sustainability, 6(2), 72–79, DOI: 10.24057/2071-9388-2013-6-2-72-79.

FAO. (2016). Map accuracy assessment and area estimation : a practical guide. In: FAO , Issue 46, 69, [online] Available at:. http://www.fao.org/3/a-i5601e.pdf.

Fleiss J.L., Cohen J. and Everitt B.S. (1969). Large sample standard errors of kappa and weighted kappa. Psychological Bulletin, 72(5), 323–327, DOI: 10.1037/h0028106.

Foody G.M. (2004). Thematic map comparison: Evaluating the statistical significance of differences in classification accuracy. Photogrammetric Engineering and Remote Sensing, 70(5), 627–633, DOI: 10.14358/PERS.70.5.627.

Foody G.M. (2020). Explaining the unsuitability of the kappa coefficient in the assessment and comparison of the accuracy of thematic maps obtained by image classification. Remote Sensing of Environment, 239 (August 2019), 111630, DOI: 10.1016/j.rse.2019.111630.

Gkoltsiou A., Terkenli T.S. and Koukoulas S. (2013). Landscape indicators for the evaluation of tourist landscape structure. International Journal of Sustainable Development and World Ecology, 20(5), 461–475, DOI: 10.1080/13504509.2013.827594.

Goodchild M.F. (2007). Citizens as sensors : the world of volunteered geography. GeoJournal, 69, 211–221, DOI: 10.1007/s10708-007-9111-y.

Hernández Magaña A.I. and Güiza Valverde F.N. (2016). Información Geográfica Voluntaria (IGV), estado del arte en Latinoamérica. Revista Cartográfica, 93, 35–55, DOI: 10.35424/rcarto.i93.426.

Herold M., Couclelis H. and Clarke K.C. (2005). The role of spatial metrics in the analysis and modeling of urban land use change. Computers, Environment and Urban Systems, 29(4), 369–399, DOI: 10.1016/j.compenvurbsys.2003.12.001.

IBGE. Instituto Brasileiro de Geografia e Estatística. (2004). Mapa de vegetacao do Brasil , 3rd ed.

INPE. (2021). Catálogo de imagens, [online] Available at: http://www.dgi.inpe.br/CDSR/.

Khairabadi O., Sajadzadeh H. and Mohammadianmansoor S. (2020). Assessment and evaluation of tourism activities with emphasis on agritourism: The case of simin region in Hamedan City. Land Use Policy, 99, 1–12, DOI: 10.1016/j.landusepol.2020.105045.

Klimanova O., Naumov A., Greenfieldt Y., Prado R.B., and Tretyachenko D. (2017). Recent regional trends of land use and land cover transformations in Brazil. Geography, Environment, Sustainability, 10(4), 98–116, DOI: 10.24057/2071-9388-2021-036.

Landis J.R. and Koch G.G. (1977). The Measurement of Observer Agreement for Categorical Data. Biometrics, 33(1), 159–174.

Llano X.C. (2022). AcATaMa, [online] Available at: https://plugins.qgis.org/plugins/AcATaMa/.

Mapbiomas. (2021). Coleção 6 (1985-2020), [online] Available at: https://mapbiomas.org/.

Marques Neto R. (2017). O horst da mantiqueira meridional: proposta de compartimentação morfoestrutural para sua porção mineira. Revista Brasileira de Geomorfologia, 18(3), 561–577, DOI: 10.20502/rbg.v18i3.1118.

Mcgarigal K., Cushman S.A., Ene E. (2015). FRAGSTATS (4.2.1), [online] Available at: https://www.umass.edu/landeco/research/fragstats/downloads/fragstats_downloads.html#FRAGSTATS.

McGarigal K. and Marks B.J. (1994). FRAGSTATS: spatial pattern analysis program for quantifying landscape structure. In: USDA Forest Service General Technical Report PNW, Vol. 2, Issue 503, 128 [online]. Available at: https://www.umass.edu/landeco/pubs/mcgarigal.marks.1995.pdf.

McGehee N.G. (2007). An agritourism systems model: A Weberian perspective. Journal of Sustainable Tourism, 15(2), 111–124, DOI: 10.2167/jost634.0.

Méndez-Quintero J.D., Morais B.R., Nero M.A., Elmiro M.A.T. and Ribeiro S.M.C. (2022). Sistemas de informação geográfica e sensores remotos no planejamento do turismo rural. uma revisão de metodologias. Caminhos de Geografia, 23(86), 95–103, DOI: 10.14393/RCG238658196.

Monserud R.A. and Leemans R. (1992). Comparing global vegetation maps with the Kappa statistic. Ecological Modelling, 62(4), 275–293, DOI: 10.1016/0304-3800(92)90003-W.

Nogueira V.S. (2006). Identidade étnica italiana e agroturismo em Venda Nova do Imigrante, Espírito Santo. Tematicas, Campinas, 14(27), 117–137, DOI: 10.20396/tematicas.v14i27/28.13635.

Olivieri F.M. (2014). Rural Tourism and Local Development: Typical Productions of Lazio. Almatourism-Journal of Tourism Culture and Territorial Development, 8(3), 36–59, DOI: 10.6092/issn.2036-5195/4620.

Parra C. de S., Silva C.P. and Chehade M.B. (2006). Agroturismo como fonte de renda para pequeno agricultores. REvista Científica Eletrônica De Turismo, 5, 1–7.

Payntar N.D., Hsiao W.L., Covey R.A. and Grauman K. (2021). Learning patterns of tourist movement and photography from geotagged photos at archaeological heritage sites in Cuzco, Peru. Tourism Management, 82(May 2020), 104-165, DOI: 10.1016/j.tourman.2020.104165.

Pereira L.L. and Ribeiro A. das C. (2011). A aglomeração produtiva de agroturismo em Venda Nova do Imigrante : estrutura e impactos na geração de riqueza local. RACE - Revista de Administração, Contabilidade e Economia, 10(1)(1977), 75–90, [online] Available at: https://portalperiodicos.unoesc.edu.br/race/article/view/797.

Phillip S., Hunter C. and Blackstock K. (2010). A typology for defining agritourism. Tourism Management, 31(6), 754–758, DOI: 10.1016/j.tourman.2009.08.001.

PVNI. (2021). Prefeitura Municipal de Venda Nova do Imigrante, [online] Available at: http://vendanova.es.gov.br/site/index.php [Accessed 8 Jul. 2022].

QGIS.org. (2021). QGIS, 3.18.1, [online] Available at: https://qgis.org/en/site/forusers/download.html

Ramiro A.G., Gonçalves G.R. and Gómez J.M.N. (2016). Uso De Los Sig Para Determinar El Potencial Del Turismo Rural. Congreso Internacional de Turismo Rural y Desarrollo Sostenible, 10, 857–870.

Saadi A. (1991). Ensaio sobre a morfotectônica de Minas Gerais: tensões intraplaca, descontinuidades crustais e morfogênese. Universidade Federal de Minas Gerais.

Serenelli C., Savelli S., Idone M.T. and Pettine L. (2017). Learning from the Route: a Pilot Project on Landscape Reading along the Itinerary of Via Lauretana Senese. Almatourism-Journal of Tourism Culture and Territorial Development, 8(6), 42–64, DOI: 10.6092/issn.2036-5195/6661.

Sgarbi G.N.C. and Dardenne M.A. (1996). Evolução Climática Do Gondwana Na Região Centro-Sul Do Brasil E Seus Registros Geológicos Continentais Durante O Mesozóico, Enfatizando O Arco Do Paranaíba, a Borda Nne Da Bacia Do Paraná E a Porção Meridional Da Bacia Sanfrasciscana, No Oeste Do Estado D. Geonomos, 4(1), 21–49, DOI: 10.18285/geonomos.v4i1.193.

Stankov U., Klauco M., Dragicevic V., Vujicic M.D. and Solarevic M. (2016). Assessing land-use changes in tourism area on the example of Cajetina municipality (Serbia). Geographica Pannonica, 20(2), 105–113, DOI: 10.5937/GeoPan1602105S.

Tieskens K.F., Zanten B.T. Van, Schulp C.J.E. and Verburg P.H. (2018). Landscape and Urban Planning Aesthetic appreciation of the cultural landscape through social media : An analysis of revealed preference in the Dutch river landscape. Landscape and Urban Planning, 177(May), 128–137, DOI: 10.1016/j.landurbplan.2018.05.002.

Towoliu B., Permana D.E., Gahung M.D. and Lumettu A. (2018). Ecotourism Village Feasibility Assessment Analysis : The Case. Almatourism-Journal of Tourism Culture and Territorial Development, 9(17), 137–152. DOI: 10.6092/issn.2036-?-5195/7593.

Urrutia A.L., González-Gónzalez C., Van Cauwelaert E.M., Rosell J.A., García Barrios L. and Benítez M. (2020). Landscape heterogeneity of peasant-managed agricultural matrices. Agriculture, Ecosystems and Environment, 292, 1–10, DOI: 10.1016/j.agee.2019.106797.

USGS. (2021). EarthExplorer [online]. Available at: https://earthexplorer.usgs.gov/.

Victorov A. (2012). Landscape Metrics From the Point of View of Mathematical Landscape Morphology. In: Geography, Environment, Sustainability, 5(1), 30–40, DOI: 10.24057/2071-9388-2012-5-1-30-40.

Wang T., He J., and Ning Z. (2023). Observations on the development of townships around mega-tourist attraction caused by land use change — the case of Zhangjiajie, China. Journal of Asian Architecture and Building Engineering, DOI: 10.1080/13467581.2023.2167494.

Zandonadi B.M. (2013). Agroturismo e as transformações Sócio-espaciais em Venda Nova do Imigrante , Es. Universidade Federal do Espírito Santo..

RESEARCH PAPER

PROTECTION OF INTACT FOREST LANDSCAPES IN RUSSIA: ROLE OF GOVERNMENT, MARKET-DRIVEN AND BUYERS' RESTRICTIVE APPROACHES

Andrey Ptichnikov[1*], Alexander Dunn[2]
[1]Institute of Geography, Russian Academy of sciences, Russia, Moscow, Staromonetny 29.
[2]Sustainability communication consultant. United Kingdom, London, 4 Grenville Avenue
***Corresponding author:** aptichnikov@igras.ru
Received: July 13th, 2022 / Accepted: May 4th, 2023 / Published: July 1st, 2023
https://DOI-10.24057/2071-9388-2022-110

ABSTRACT. Leading environmental organizations recognize intact forest landscapes as priority areas for conserving forests. A quarter of global intact forest landscapes (IFL), are found in Russia, and since 2000, the country has lost over 7,5% (or 21 million ha) of its IFLs due to logging, forest fires and road construction. With the projected logging rates Russia's IFLs will completely disappear in 150 years, and IFLs that are "rich" in timber will do so in 50 years. Protection of IFLs is the serious challenge, not only due to associated biodiversity loss, but also due to outstanding carbon sequestration and climate change mitigation role of IFLs.

The objective of this research is to define the key drivers and factors and to examine how government and market-driven approaches contribute to the preservation of intact forest landscapes in Russia. A further objective is to assess the merits of consumers restriction measures, such as phase-out of IFL product purchases, as proposed by some environmentalists.

According to our research, voluntary forest certification (market-driven approach) was the main tool for IFL protection in Russia until recently. A market-driven FSC voluntary certification scheme includes moratoria agreements to preserve almost 3 million ha of IFLs. Additionally, between 2010 and 2020 more than 770 thousand ha of IFLs were established in two national parks and three nature reserves in North-West Russia with the primary goal to protect IFLs, mainly in former FSC "no logging" zones. Market-driven approach is currently the main tool used to protect IFLs in Russia.

KEYWORDS: hydromorphology, ecohydraulics, proglacial river, Katun, Altai Mountains, Russia

CITATION: Ptichnikov A., Dunn A. (2023). Protection Of Intact Forest Landscapes In Russia: Role Of Government, Market-Driven And Buyers' Restrictive Approaches. Geography, Environment, Sustainability, 2(16), 132-141
https://DOI-10.24057/2071-9388-2022-110

ACKNOWLEDGEMENTS: Mikhail Karpachevsky and Alexander Titkov from Forest Stewardship Council (FSC) Russia provided excellent research support and insightful feedback on an early draught of this study, which the authors gratefully acknowledge. The research was implemented in the frame of FSC project "White paper on intact forest landscapes in Russia and the Greenpeace great northern forest protection campaign" and the Institute of Geography Russian academy of sciences theme "Assessment of physical geographical, hydrological and biotical changes of environment and its consequences for establishing basics of sustainable nature management AAAA-A19-119021990093-8 (FMGE-2019-0007).

Conflict of interests: The authors reported no potential conflict of interest.

INTRODUCTION

IFL (Intact forest landscape) mapping team[1] and (Potapov et al. 2017) defines intact forest landscape (IFL) as an unbroken expanse of natural ecosystems within the zone of current forest extent, showing no signs of significant human activity and large enough that all native biodiversity, including viable populations of wide-ranging species, could be maintained. Although all IFL are within the forest zone, some may contain extensive naturally tree-less areas, including grasslands, wetlands, lakes, alpine areas. A territory that contains both forest and non-forest ecosystems that are only slightly impacted by human economic activity, with an area of at least 500 km^2 (50,000 ha) and a minimum width of 10 km (measured as the diameter of a circle that is entirely inscribed within the boundaries of the territory) is technically referred to as an IFL (Potapov et al. 2017). The findings of IFL mapping and monitoring between 2000 and 2020, study of IFL degradation reasons and comparison of protection method efficiency have all been published by the IFL Mapping team.

At the moment, scientists, NGOs, and decision-makers are all interested the preservation of intact forest landscapes. Researchers are focusing on threats to IFLs and their loss (Betts et al. 2017; Donald et al. 2019; Grantham et al. 2021; Heino et al. 2015; Williams et al. 2020), protection and conservation of IFLs on government and indigenous people lands, in forest concessions (Chazdon 2018; Fa et al. 2020; Karpachevsky 2022; Ptichnikov and Karpachevsky 2020; et al.). The significant number of policy and research papers cover the international and national IFLs frameworks, monitoring and values of IFLs (CBD 2021,

[1]Intactforestlandscape.org

Hansen et al. 2020; Hansen et al. 2021; IPBES 2019; Watson et al. 2018).

With 815 million ha of forested area, Russia represents more than 22% of the world's forests (FAO 2020). Nearly all forests belong to the Federal Government and their commercial use is implemented through leasing (concessions) to private forest companies. According to the Forest Code, regional forestry authorities and federal forestry agencies organize and oversee forest management. Around 223 million ha are currently (the end of 2021) under commercial lease, from that around 180 million ha under forest management lease (the rest – under hunting and agricultural lease of forests) (Filipchuk et al. 2022).

The area of intact forest landscapes (IFL's) in Russia is estimated currently between 225 and 250 million ha, according to FSC Russia assessments 2021[2]. According to (Dobrynin et al. 2021) the total area of intact forest landscapes within FSC (Forest stewardship council)-certified concessions in Russia was 5.8 million ha in 2021. The area of IFL outside FSC certified logging concessions is likely more than 10 million ha, based on results of own estimation[3]. Some IFL are in leasing for non-logging purposes, for example hunting management, and no major logging threats exists for such concessions (The National strategy 2021). The total area of leased IFL under threat of logging is likely more than 16 million ha, or around 7% of the total IFL area. 93% of IFL are outside of logging concessions and are not affected by commercial logging (Fig. 1).

Russia's national of forest sector growth strategy until 2030 calls for an increase in harvesting volume of 70 million m^3, comparing to 2021 (The National strategy 2021). The majority of this harvesting increase may happen in the new concessions outside currently leased forests, mostly in the areas of pioneer logging, including intact forests. Although it is impossible to foresee the exact scale of this development, risks to IFL are more likely to grow than lessen in the years to come.

Although Russian Federation is a signatory to the Convention of Biodiversity (CBD), taking part in all CBD-related activities, and being a member of IUCN, the Russian current legislation, in our opinion, does not recognize the unique significance of IFL's. IFL's are widely offered by the Government for commercial use through leasing. If the places are not protected areas, leaseholders – harvesting companies – have complete legal authority to log the intact forest landscapes. Protection of IFL's is important to protect forest biodiversity, to reduce carbon emissions from deforestation and forest degradation and to stimulate sustainable forestry management practice use.

By our opinion the policy of Russian government toward recognition of intact forest landscapes was to some extent controversial. The government has mentioned these into the National Forest Policy as forests of high conservation value (Basics of state policy 2013). The Ministry of Natural Resources of Russia includes a new special category of forests – known as the "national heritage" forests – in the new forest inventory instruction (Forest inventory 2020). The initial intention was to use this category to protect IFLs in some of the most pressing areas and hot spots. However, the intended purpose to protect some parts of intact forest landscapes has changed as a result of

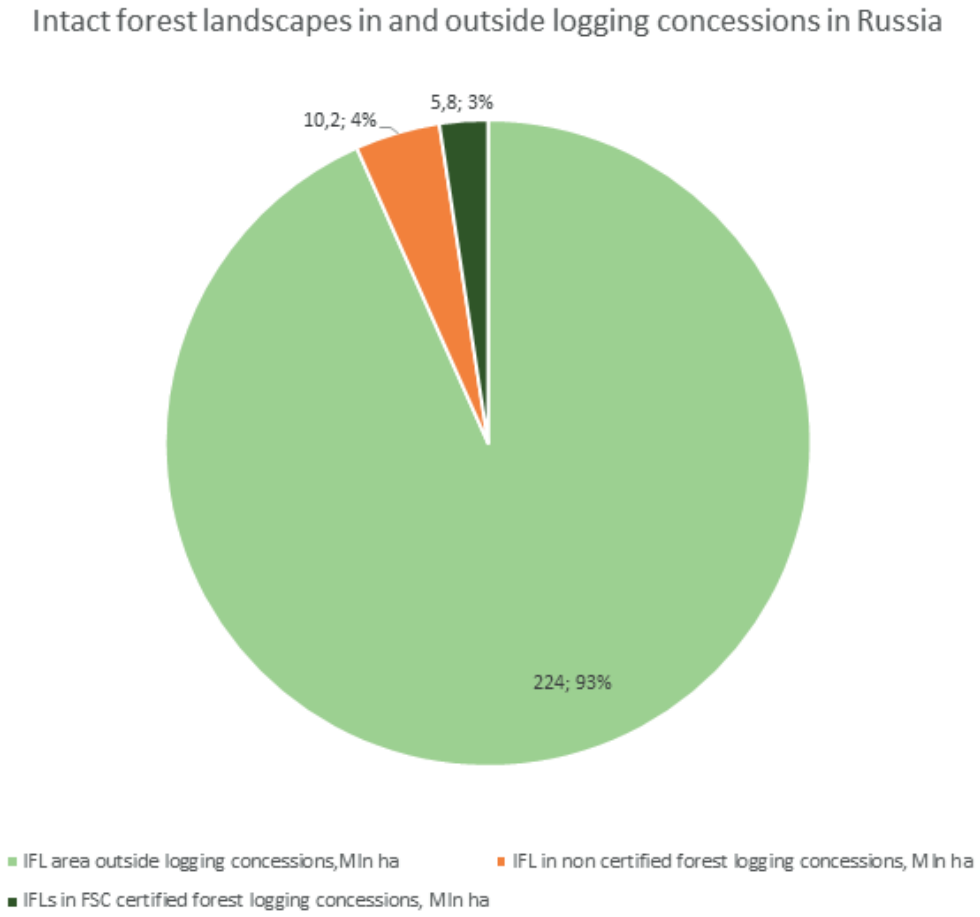

Fig. 1. Intact forest landscapes in and outside logging concessions in Russia, in million ha and percent of the area (authors own assessment, based on Dobrynin et al. 2021, and FSC Russia 2021 data)

[2]Stricter rules protect biodiversity and intact forest landscapes in Russia. Source: https://fsc.org/en/newsfeed/stricter-rules-protect-biodiversity-and-intact-forest-landscapes-in-russia

[3]The share of FSC certified and non-certified forest lease in IFL ranges from 19% in Khabarovsk region to 65% in Irkoutsk region, according FSC Russia private communication.

modifications to the 2020 instruction. The changes make intact forest landscapes smaller, fragmented homes for extinct and endemic species rather than large intact landscapes.

The FSC National Forest Stewardship Standard is currently the only normative document that fully recognizes intact forest landscapes and provides the need for their management and preservation (FSC National standard v2-1). Despite the partial leave of FSC certification in Russia, forest management standard and certification are still operational in the beginning of 2023. In the same time the FSC FM certified forest area is decreasing in 2022-2023 due to impossibility to sell FSC forest products from Russia with FSC claim[4].

FSC certification is considered as powerful tool to institutionalize IFL concept, ensure protection of core IFLs due to its standards requirements. FSC is the international forest certification scheme, driven by markets. An extensive literature on FSC as a private, market-driven governance institution, NGO (non-governmental organisations) roles in promotion FSC and FSC impacts is available (Cashore et al. 2004; Cashore et al. 2006; Tysiachniouk 2006; Marx and Cuypers 2010; Giessen et al. 2016).

The 2008 adoption of the first iteration of the Russian national FSC standard – amended in 2012 and 2015 – described the preservation of the core areas of intact forests landscapes in consideration of the socioeconomic circumstances of the area (FSC National standard V 6.01). Adoption of the Motion 65 at FSC General assembly 2015 was the turning point in the protection of IFLs, as this Motion required protection of vast majority of IFLs within certified forests (FSC ADV 20-007-018). This motion was driven by environmental organizations, including some radical ones, but also by more constructive WWF[5], WRI and other FSC environmental chamber members (Dobrynin et al. 2021). New FSC Russia national standard in 2020 was based on international generic indicators – IGIs. The standard requires 80%, 50% and 30% of IFL within concession to be conserved, depending on the protection and management measures taken by the certified company. According to the standard certificate holders (CH's) are requires to protect 80% of intact forest landscapes (IFLs) if they only zone IFLs and designate a core conservation area, 50% of IFLs if they also ensure the preservation of biological diversity and mimic natural forest dynamics in their forest management, or 30% of IFLs if they also initiate and/or carry out measures to reduce climate change (FSC National standard V2-1).

In addition to the active interaction with FSC certification scheme, in 2017 Greenpeace International[6] launched the report "Eye on taiga: How industry claimed sustainable forestry is destroying great northern forest" (Greenpeace 2017) and following campaign[7]. Greenpeace advised consumers through its campaign "to phase out from buying IFL based products, whether FSC certified or not". Campaign was also aimed to accelerate establishment of Dvinsko-Pinejsky zakaznik to protect around 300-450 thousand ha of remaining IFLs in Archangelsk region. Greenpeace report and campaign were accompanied by a number of publications in Russian Forest forum[8], claiming that FSC certification is not efficient to ensure protection of IFLs, that restrictive measures, such as total "phase out from buying IFL based products" is the right approach to protect IFLs in boreal forests, and primarily in Archangelsk. The debate over the best strategy to safeguard IFLs was started by a Greenpeace report and campaign. Campaign has clearly accelerated establishment of the Dvinsko-Pinejsky zakaznik[9], but discussion on efficiency of phasing out from buying IFL based products in presence of FSC certified forests is still on-going among environmentalists and forest product buyers and consumers[10,11].

This article provides the overview of government-driven, market-driven and restrictive approaches to protect IFLs, assesses and compares its outcomes against protection of IFL's from logging and provides recommendations for further actions to enhance protection of intact forest landscapes in Russia.

MATERIALS AND METHODS

The discourse on Russian forests that we have established and analyzed in this research is non-state actor-driven and prioritizes preserving intact forest landscapes over the vulnerable forests with significant conservation significance. The following list of key elements of the discourse under analysis is offered in connection to its conceptualization, institutionalization and materialization:

Table 1. The key components of authors analysis for IFL in Russia (based on authors assessment and Dobrynin et al. 2021)

Discourse	Conceptualization	Institutionalization	Materialization	Key drivers	Key actors
Protection of intact forest landscapes	Last large unfragmented primary forest landscapes, shelters of biodiversity and carbon sinks. The priority category of primary forest to be conserved	FSC Forest management standard	Voluntary logging moratoria (later on some of moratoria may be transformed in protected areas (PA's)	Markets, EU legislation to some extent	Companies with green procurement policies, national public procurement
		NGO/ scientists vision on IFL values	Protected areas	National obligations to CBD	Scientists, some NGO's
		Consumer campaigns	Exclusion of suppliers with IFLs in leasing from forest products procurement, despite the fact of FSC certification	Corporate risk management under NGO pressure	Radical NGOs

[4]FSC Russia and FSC International end their partnership. Available at: https://fsc.org/en/newsfeed/fsc-russia-and-fsc-international-end-their-partnership [Accessed 13 Jul. 2022].
[5]Nominated as "foreign agent" by Ministry of Justice of Russia in May 2023
[6]Nominated as unwanted organization in Russia in May 2023
[7]Eye on Taiga. Available at: https://www.greenpeace.org/international/publication/7355/eye-on-the-taiga/
[8]www.forestforum.ru (now this web-site is not operational) [Accessed 21 Feb. 2022].
[9]State environment expertize endorsed the project of Dvinsko-Pinejsky zakaznik. Gosudarstvennaya expertiza odobrila proekt Dvinsko-Pinejskogo zakanika. Available at: https://new.wwf.ru/resources/news/arkhiv/gosudarstvennaya-ekologicheskaya-ekspertiza-odobrila-proekt-dvinsko-pinezhskogo-zakaznika/
[10]IKEA logging old-growth forest for low-price furniture in Russia. Available at: https://news.mongabay.com/2012/05/ikea-logging-old-growth-forest-for-low-price-furniture-in-russia/#:~:text=A%20new%20campaign%20is%20targeting,of%20old%20and%20biodiverse%20forests
[11]Certification schemes such as FSC are greenwashing forest destruction. Available at: https://www.greenpeace.org/international/press-release/46802/certification-schemes-such-as-fsc-are-greenwashing-forest-destruction/

The methodology used by authors included four main steps:

1. Collection of information for each individual case of protection of IFLs during 2001-2021 in form of protected areas, voluntary logging moratoria or other approaches (e.g., public commitment et al). The number of IFL protection instances that were reviewed increased from 3 to 5 in the first five years to 40-45 in the final five years of the investigation. Information was collected using FSC certificates global data base (info.fsc.org), hcvf.ru web-site section of logging moratoria agreements, authors observations, analysis of literature cross-checked through interviews with key actors, mainly NGO's.

2. Assessment of key drivers and actors in the defense of IFLs and their categorization as market-driven, NGO/scientist-driven, and consumer campaign-driven for each case identified. Assessment was provided on the basis of hcvf.ru web-site section, analysis of literature, including several issues of Sustainable Forest Management Journal, published by WWF Russia.

3. Comparison of results for the end of 2021 following a quantitative study of each strategy's results. This analysis was based on the data, collected during step 1 and 2.

4. Providing recommendations to key actors, based on effectiveness of each approach to protect IFLs.

The lead author did participant observations in 2004–2018 while participating in NGO activities in Russia, and again in 2018–2022 while working on his research project. They constitute the source of the autoethnography materials. Autoethnography implies a critical look at various social beliefs and management practices based on personal experience, self-observation and reflexive exploration, which are used in various research fields (Anderson 2006; Mosse 2005; Winkel 2012). In addition to policy documents, government laws, and certification requirements, opinions, debates in internet forums, press announcements, and other materials were useful to the research. The analysis of technical and policy documents was supported by scrutiny of relevant academic and grey literature in Russian and English.

A logic of interpretative analysis to understand the meanings Russian forest policy players attribute to forest discourses (Yanow 2007). The logic of interpretative analysis implies that meanings of policy and governance issues are context specific. The meanings are created by the many players and scholars in their capacity as meaning-makers, in addition to being taken from documents and events that are pertinent to policy. Interpretative analysis was carried by the researchers.

RESULTS

Market-driven approaches to protect IFLs

Russia has over 61 million ha of FSC-certified forests by the middle of 2021 (Dobrynin et al. 2021). According to FSC Russia[12], 3 million ha of intact forest landscapes are conserved under moratoria agreements as of January 2021 (1.2 million ha under permanent moratoria agreements, 1.8 million ha under temporary moratoria agreements). The total area of FSC-certified IFLs in Russia was 5.8 million ha, around 52% of these landscapes are conserved as no-logging moratoria zones[13]. Principle 9 of the Russia FSC national standard (FSC National standard V2-1) include moratoria agreements between certificate holders (CH's) and stakeholders, who are represented mainly by ecological organizations. The web-site www.hcvf.ru, which was created by WWF Russia, serves as the foundation for the map of FSC-certified forests with intact forest landscapes (Fig. 2).

As required by FSC NFSS, FSC's approach for protecting IFLs including putting aside certain IFL regions through moratoria agreements between certificate holders and stakeholders. Each logging moratorium is ended for the whole five-year term of each FCS certificate; commitments may be long-term (until the end of the forest lease) or

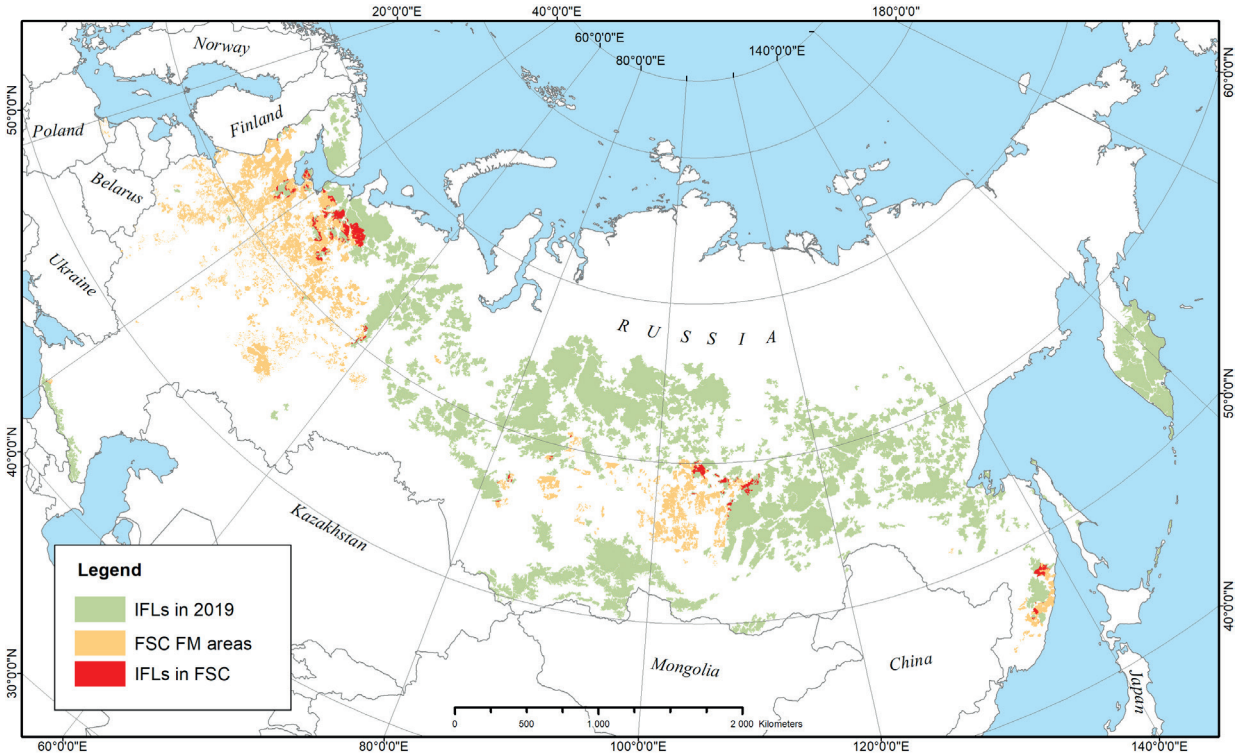

Fig. 2. SC certified forests with intact forest landscapes in Russia, 2021 (source: www.hcvf.ru, provided by WWF Russia)

[12]http://maps.fsc.ru/ [Accessed 12 Jan. 2021].
[13]https://fscrus.nextgis.com/resource/0 [Accessed 12 Jan. 2021].

short term (for the length of the certification agreement) (Dobrynin et al. 2021). Short term agreement can be extended up to unlimited number of cycles of certification. There are numerous examples of CHs continuing to safeguard IFLs over two or more cycles of FSC certification, and if they are interested in FSC certification, they may continue to do so for longer.

The moratoria agreements were concluded between CHs and key stakeholders, such as environmental NGO's (WWF, Transparent World, Silver Taiga et al). The list of moratoria is available on www.hcvf.ru/ru/moratorium. Since the beginning of the FSC and ASI (Accreditation service international) Credibility Project in Russia in 2013, the rate of the moratoria agreements that have been reached has increased by three times[14]. Prior to its 7th General Assembly, FSC Russia made a survey among the members on quality aspects of certification. Around 70% of respondents stated that since 2013, high conservation value forests (HCVF) have improved in terms of quality, transparency, and the protection of biodiversity on logging sites.[15].

Evolution of protected areas approach for IFLs conservation in Russia

Some environmental organizations propose protected areas alone—without FSC certification—will serve as the primary tool for IFL protection[16]. They highlight the fact that FSC certification does, in theory, authorize some logging of IFLs; depending on the scope of the moratoria agreement, anything between 20 and 70 percent of IFL area may be logged under FSC certification. In that case, protecting IFL through the lobbying and advocacy efforts of scientists and non-governmental organizations (NGO) protected areas (PA's) appears to be a more attractive option. In reality this traditional approach now has some clear limitations in Russia.

Due to strong investment and harvesting activity in commercial forests and high demand for forest leasing for logging activities, the potential of establishing official PAs in IFLs in commercial forestry zones has considerably declined over the past 10 to 15 years, notably in European part of Russia (Ptichnikov 2019). Only one PA was established in Russia's European region in the past 20 years, in 2007, as a consequence of persistent lobbying by scientific and environmental organizations. It is the 70,000 ha Kalevala National Park in Karelia, where IFLs are safeguarded. A national park called "Onejskoye Pomorie" was established in 2013 in the Archangelsk region mainly due to long-term lobbying from scientists and NGO's, but also with a support from local FSC certified leaseholder. Due to its dedication to FSC standards and certification, this company, which leased forest on the Onega peninsula, agreed to omit part of those forests with high conservation values from its lease (Tysiachniuk 2006).

According to the Forest Code, even though certified forests are under a logging ban or a standard forest management plan that includes logging, leaseholders are still required to pay forest fees (Forest Code 2006). Because of this, leaseholders often want to keep moratoria zones out of the leasing area.

Moratoria zones are established mostly in IFL core zones. If these moratoria zones are not available for leasing, FSC certified leaseholders will no longer be able to purchase wood from them because doing so would be against the FSC controlled wood standard (avoid contentious wood from high conservation value forests that are not available for leasing) (FSC STD 40-005 V3-1). If a former moratoria zone is later acquired under new lease by a non-certified company, the new leaseholder will encounter difficulties in selling such timber to neighboring FSC-certified enterprises. As a result, new harvesting projects in core IFL zones frequently fail in their first stages if they are even initiated. For regional governments, creating protected areas in former moratoria zones is actually the greatest option because such woods cannot actually be commercially logged. PA's in former moratoria areas can be a source of investments into tourism and recreation, hunting and fishing. Such activities are normally compatible with PA status, especially in case of regional zakazniks (corresponds to IUCN IV category).

Mondi Group and Komi republic environmentalists are not only agreed to exclude around 150 thousand ha of the most valuable IFL's from logging in moratoria zones, but also initiated the establishment of Koygorodsky National Park in the south of Komi, enlarging "moratoria" IFL to approximately 50 thousand ha. Large Karpogorsky zakaznik (natural reserve) was established in the Komi Republic in 2022 in the area that Mondi had previously leased but abandoned in 2015 after Komi environmentalists learned that Karpogorsky core IFL area had the highest conservation value[17].

Uftugo-Ilishsky zakaznik in Archangelsk was established with support of Ilim group in 2015 to protect IFL core zone in Verkhnetoemsky IFL massive. The highest value of this massive was defined by the Archangelsk branch of WWF Russia in 2009. Ilim group, which protected this area from logging and later from lease in collaboration with environmentalists and the local government, partially leased this territory[18].

Around 677 thousand ha of core IFLs were excluded from lease for logging purposes and converted into PA's by initiative of responsible FSC certified companies in the frame of their commitments to sustainability and FSC values in North-West Russia in the last decade (Table 1). In the regions of Komi and Archangelsk, further PAs are in the works.

Our research indicates that market-driven approaches, represented by FSC certification, play a major role in the protection of intact forest landscapes, primarily in European part of Russia. Because IFLs in Siberia and the Russian Far East only cover a small area and are therefore excluded from leasing, the situation there is rather different. That can be explained by the impact of nearby China market, which may consume any type of timber from non-certified forests.

[14]Again, about the improvement of quality of certification in Russia. I snova o povyshenii kachestva certifikatsii v Rossii. Press-release of the FSC Russia, 21 of June 2016. Available at: https://ru.fsc.org/ru-ru/news/id/470 [Accessed 21 Feb. 2022].
[15]Ptichnikov A. Report of executive body of FSC Russia for 2013-2016. Otchet ispolnitelnogo organa FSC Rossii za 2013-2016. Presentation at the 7th conference of FSC Russia, 13 of April 2016. Slide 8. Available at: https://ru.fsc.org/ru-ru/o_nas/fsc_in_russia/conferences/vii/-123 [Accessed 12 Feb. 2022].
[16]Private communications with Swiss and Russian active environmentalists
[17]Silver taiga web-site: www.silvertaiga.ru [Accessed 12 Jul. 2022].
[18]Uftugo-Ilishsky zakaznik has celebrated its 5 years anniversary. Available at: http://www.dvinainform.ru/economy/2020/11/24/63241.html

Table 2. Protected areas established in core IFL areas and set-aside from leasing by FSC-certified companies

Protected area established in former moratoria, adjacent or affected areas, since 2015	Administrative regions	Former lease of companies	Total area, thousand ha
Koygorodsky national park	Kirov, Komi	Mondi (in Komi)	56,7
Dvinsko-Pinejsky zakaznik	Archangelsk	Titan and 6 other companies	300
Uftugo-Ilishsky zakaznik	Archangelsk	Ilim	70
Karpogorsky zakaznik	Komi	Mondi	250
Total			677

The main discourse in Russia regarding the preservation of intact forest landscapes has changed from the traditional approach, based on lobbying and advocacy work of scientists and NGOs, typical for the end of the 1980s, and the beginning of the 1990s, and the 2000s, to the new discourse, based on preservation within moratoria zones inside FSC certified leases and/or following establishment of PAs in the former logging moratoria zones, excluded from lease and their surrounding areas. This kind of conversation was common at the end of the 2000s and in the 2010s up until 2021 (Fig. 3).

Efficiency of buyer's restriction measures to protect IFLs in boreal forests

In its report Greenpeace International[19] (Greenpeace 2017) raises concerns regarding FSC certification in the area as well as the problem of the destruction of intact forest landscapes (IFLs) in Russia. The FSC certification's ability to guarantee conservation and the prudent use of high conservation value forests in Russia is called into doubt in the abovementioned report, which details the status of intact forest landscape loss in Russia. Among others, the report addresses the following issues: "Russia has the highest rate of IFL loss of all Great Northern Forest countries that still have IFLs, amounting to some 1.36 million hectares per year. The sheer scale of the crisis in Russia can be judged from the fact that this rate of IFL loss is more than the average annual rate of deforestation in the Brazilian Amazon rainforest…". "While FSC may have mechanisms in place to limit IFL destruction within the supply chains of FSC-certified companies, there is still considerable uncertainty about how and when these standards will be implemented on the ground, as well as how much IFL will actually be protected as a result of these standards".

Numerous NGOs, stakeholders and forestry companies have different perspectives on the current protections for IFLs provided by FSC, as well as the reasons behind their total devastation. While radical NGO's suggest that the FSC is not doing enough, other organizations agree that the National Forest Stewardship Standards (NFSS)'s stringent

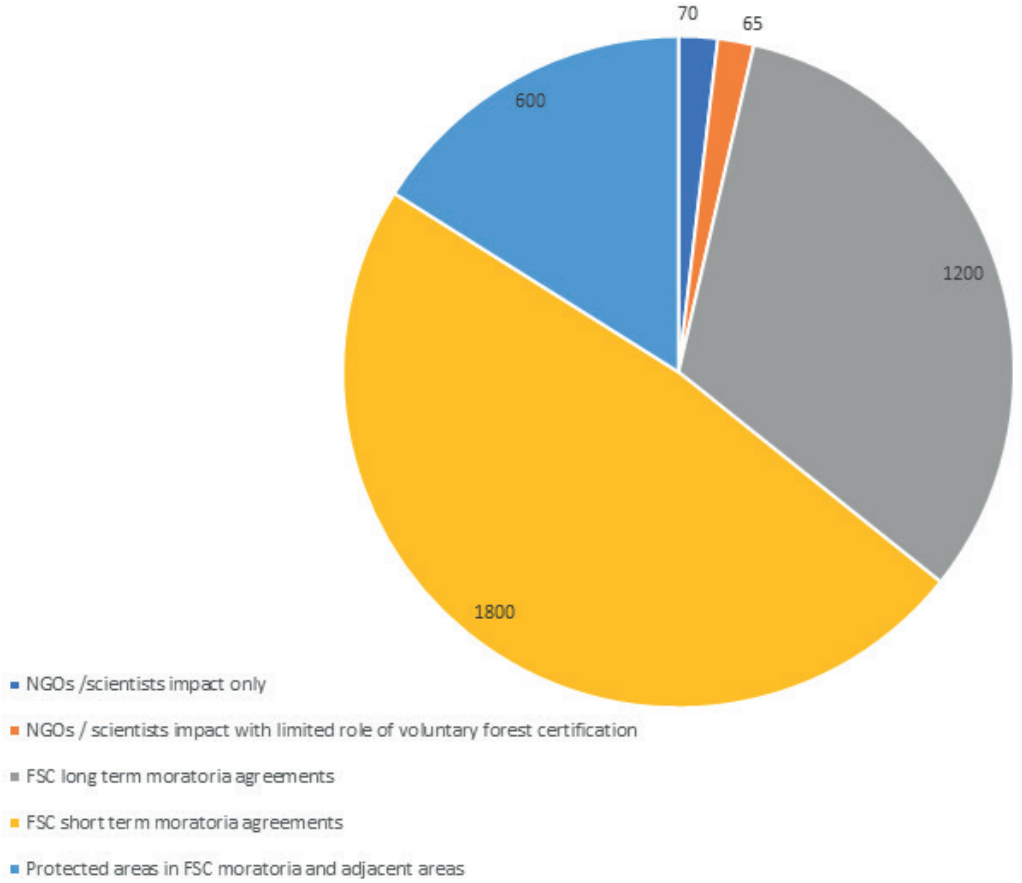

Fig. 3. Main reasons for IFLs protection in Russia (based on calculated area of protected IFL in thsd ha. As per end of 2021)

[19] Nominated unwanted organization in Russia in May 2023

requirements make the FSC certification standards the only programme that provides some IFL protection in forestry operations (Tysiachniouk and McDermott 2016; Ulubina 2014; Ulybina and Fenell 2013).

In particular, FSC Russia's NFSS requires that management of IFLs be established after consultation with stakeholders and FSC Certificate Holders (CH). These include ENGOs such as WWF, Transparent Worldand others (Dobrynin et al. 2021). IFL protection through FSC entails very active engagement and negotiation with all concerned stakeholders to define specific areas of protection through far-reaching consensus, including agreements among these bodies on the protection of the most valuable (or core) parts of IFLs and the management of IFL areas where the social and economic interests of the local population need to be considered equally. The result of the negotiation process is normally a moratorium agreement. The list of moratorium agreements is available on www.hcvf.ru web-site.

The reaction to the Great Northern Boreal campaign by Greenpeace from key Russian leaseholders that are responsible for the voluntary protection majority of IFLs in Russia was studied through the interview in 2017. We interviewed ten large FSC-certified companies from the European geographical region of Russia, Siberia and Russian Far East, which set aside 65% of all IFLs in Russia. These businesses were all made aware of the Greenpeace campaign. Three of the four FSC-certified companies said that they are considering switching to other certification programmes because of the dangers associated with the current campaign. Four FSC certified companies reported a scenario of significant reputational risk for them. Another FSC certified company notified significant reputational risk (it is a double FSC/PEFC certified company), and five others did not provide an assessment of the campaign risks.

Nine CHs with 600,000 ha of IFL would switch to other certification programmes like PEFC if all IFLs were to be excluded from management. PEFC does not need the protection of IFLs. Only one FSC CH will stay in FSC under any conditions. That means that a vast majority of IFLs will be under risk of logging if all IFLs are being excluded fully from management due to campaign requirement.

In practice phasing out campaign resulted in acceleration of establishment of Dvinsko-Pinejsky zakaznik (2019), which protected 300 thousand ha of intact forest landscape. The campaign tagline urging people to cease purchasing FSC-certified goods from concessions run by IFLs is divisive for IFLs. The campaign's practical implementation could hasten the demise of IFL if businesses switch to certification programmes that don't treat IFLs with the same care that FSC does, like PEFC Russia (PEFC Russia Standard).

Key results of assessment

Our research found that the main tool for IFL protection in Russia is the voluntary forest certification (market-driven approach). Around 3 million ha of IFLs were protected under moratoria agreements within market-driven FSC voluntary certification scheme. In addition, two national parks and three nature reserves with a total area of more than 770 thousand ha of IFLs were established in North-West Russia in 2010s–2020s with the primary aim to protect IFLs, mainly in former FSC moratorium "no logging" zones. Market-driven process is currently the main instrument to protect IFLs, responsible for almost 96% of IFL protection after 2001.

In the same way as it was at end of the 1990s and the beginning of the 2000s, the government-driven approach to protecting intact forest landscapes, based on the lobbying and advocacy power of NGO's and scientists, is no longer a significant tool to protect IFL's from logging. Due to the current strong demand for forest lease from logging companies, the government can no longer afford to protect more or less significant forest areas with IFLs that are within reach of logging companies.

The consumer campaign tool, which aims keep IFL fibres out of products despite despite their FSC certification, seems to be a very contentious tool and could hasten the logging of IFL as forest firms switch to less stringent certification programmes, like PEFC. The consumer-driven approach has hastened the formation of PA in the last surviving IFL in the Archangelsk region, however in practice this "worst" case scenario was not realized. From that point of view consumer campaign may be considered as extraordinary but risky tool to accelerate protection of IFL's in some IFL hot spots.

DISCUSSION

The causes of intact forest landscapes loss in Russia

Currently the globally significant areas of boreal IFLs are found in Russia and Canada, and tropical IFLs in Brazil and Congo basin. IFLs in Russia and Canada are under threat of logging due to their presence in forest concessions. While there are some IFL tracts in Sweden, Norway, China and other boreal countries, they are generally either not included in logging concessions or are protected by national law.

The situation in Canada is to some extent similar to Russia. Almost 5% of Canada's IFLs were degraded or fragmented by human activity between 2000. Nowadays 11.7% of IFLs were located within forestry concessions. In contrast to Russia, only 6% of IFL reduction was located within oil/gas facilities, pipelines, wells, and seismic lines concessions, which accounted for 60% of IFL degradation. In Canada IFL conservation is linked to the preservation of caribou habitats (Conservation Biology 2018), however in Russia, there isn't a single flagship species that might be related to IFL conservation.

According to abovementioned analysis IFL in Russia was lost at a pace of 1.36 million ha each year between 2000 and 2013, amounting to over 17.7 million ha. In order to reverse the loss of intact forest landscapes, it is important to understand the causes of IFL loss. According to the analysis by WWF (WWF Russia 2018), there are three main causes of IFL destruction in Russia:

- Logging and building of roads for timber transportation
- Forest fires
- Mining and prospecting, development of infrastructure and transportation of minerals, oil and gas.

60% of IFL losses are due to human related forest fires, 23% – due to logging and 17% – due to mining and prospecting. More than 50% of loss due to forest fires has occurred in two regions – Yakutia republic and Krasnoyarsk region. The fastest IFL loss due to logging happens in the forested areas next to the most productive and commercially harvested forested areas. Total loss of 'timber rich' IFLs, is expected to take place much quicker, that other IFLs, likely in 48-50 years (WWF Russia 2018).

The rate of IFL loss in FSC-certified concessions and the rate of IFL loss in non-certified concessions cannot currently be compared due to a lack of data. This will be a subject of a further research. In order to reverse the degradation of IFLs, priority measures should therefore be

taken to strengthen protection of IFL's from forest fires, road and pipelines construction, geological survey and mining projects.

Despite the differences between Russia and Canada, only a strong commitment from the government as the forest owner will be able to solve the IFL problem in both nations. The role of market-driven approaches of IFL protection are rather in raising awareness and drive following government decisions.

CONCLUSIONS

It is important to consider that other natural and human-induced factors, such as forest fires, mining and pipeline operations, and road construction, account for the majority of the IFL loss in Russia and are not the sole source of IFL degradation. Protection of IFL against all impact factors is a complex task. We believe that protection of IFL's through voluntary certification should also be connected to the additional economic benefits for CHs that can be derived from protecting the intact forest landscapes and which constitute a motivating factor for their enhancement.

One of the recently open possibilities is the development of nature climate solutions, aimed to decrease emissions from logging and forest fires, and to increase GHG (green house gazes) sequestration by forests due to better forest management. Forest company can be partially compensated for not logging some IFLs in their lease through obtaining and trading certified emission reductions (CER) for forest protection above baseline scenario of forest management. The example of such approach is demonstrated by pilot project, implemented by FSC CH Terneyles. The project was registered by Verra VCS (Voluntary carbon standard) international climate certification scheme and can generate up to 198 000 tonnes of CO_2 equivalent after validation[20]. At the start of 2022, 1 CER was worth around 5-6 USD. There are some other examples of such projects in Russia and worldwide (Ptichnikov et al. 2021; Krenke et al. 2021).

Success in conservation can be achieved by the combined efforts of responsible enterprises, NGOs, and governments, and it requires key stakeholders to join it in this effort. There are added areas where IFL protection can be enhanced. For example, an alternative but equally strong approach to enhancing conservation of IFLs lies in a strengthening of FSC controlled wood (CW) standards. The new version of CW standard (FSC STD 40-005 ver. 3.1 (FSC STD CW 40-005 V3-1) prohibits or significantly limits the supplies of controlled wood from IFL areas.

Strengthening Government engagement through enhancing protective measures such as the creation of protective sites under a National Heritage Category in Forest inventory instruction is another approach that we consider worth developing in Russia. Boosting ecosystem services certification alternatives, such as carbon sequestration and climate projects in IFLs is a new way forward and these can be integrated into management schemes as an overarching approach. Finally, landscape approach to IFL management[21] seems to be important complementary measure to ensure better IFL protection.

REFERENCES

Anderson L. (2006). Analytic autoethnography. Journal of Contemporary Ethnography, 35, 373–395, DOI: 10.1177/0891241605280449.

Basics of state policy on using, protection, safeguarding and regeneration of forests. Order of Government of Russian Federation from 26 of September 2013, 1724-R (in Russian).

Betts M.G., Wolf C., Ripple W.J., Phalan B., Millers K.A., Duarte A., et al. (2017). Global forest loss disproportionately erodes biodiversity in intact landscapes. Nature, 547, 441–444, DOI: 10.1038/nature23285.

Cashore B., Auld G., Newsom D. (2004). Governing Through Markets: Forest Certification and the Emergence of Non-State Authority. Yale University Press: New Haven, CT, USA, DOI: 10.12987/9780300133110.

Cashore B., Gale F., Newsom D., Scott D., Branford N., Coppock J. (2006). Confronting Sustainability: Forest Certification in Developing and Transitioning Countries, Report Num., Yale F&ES Publication Series: New Haven, CT, USA.

CBD (2021). First Draft of the Post-2020 Global Biodiversity Framework, [online] CBD/WG2020/3/3. Available at: https://www.cbd.int/doc/c/abb5/591f/ 2e46096d3f0330b08ce87a45/wg2020-03-03-en.pdf [Accessed 10 Feb. 2023].

Chazdon R.L. (2018). Protecting intact forests requires holistic approaches. Nature Ecology and Evolution, [online] 2(6), 2, p. 915. Available at: https://www.nature.com/articles/s41559-018-0546-y [Accessed 10 Feb. 2023].

Conservation Biology Institute. (2018). Canada's Intact Forest Landscapes. In: Data Basin, [online] Available at: https://databasin.org/articles/c6c75b7c47fe4965a5ba55670fd28983/> [Assessed 10 Feb. 2023].

Dobrynin D., Jarlebring N.Y., Mustalahti I. et al. (2021). The forest environmental frontier in Russia: Between sustainable forest management discourses and 'wood mining' practice. Ambio A Journal of the Human Environment, 50(12), 2138–2152, DOI: 10.1007/s13280-021-01643-6.

Donald P., Arendarczyk B., Spooner F. and Buchanan G. (2019). Loss of forest intactness elevates global extinction risk in birds. Animal Conservation, 22(4), 341–347, DOI: 10.1111/acv.12469.

Fa J.E., Watson J.E., Leiper I., Potapov P., Evans T.D., Burgess N.D., et al. (2020). Importance of Indigenous Peoples' lands for the conservation of Intact Forest Landscapes. Frontiers in Ecology and the Environment, 18(3), 135–140. DOI: 10.1002/fee. 2148.

FAO. (2020). Global Forest Resources Assessment 2020: Main report. Rome. The Russian Federation Forest Sector Outlook Study to 2030, DOI: 10.4060/ca9825en.

Filipchuk A.N., Malysheva N.V., Zolina T.A., Fedorov S.V., Berdov A.M., Kositsyn V.N., Yugov A.N., Kinigopulo P.S. (2022). Analytical review of the quantitative and qualitative characteristics of forests in the Russian Federation: results of the first cycle of the state forest inventory, Forestry information, 1, 5–34 (in Russian), DOI: 10.24419/ LHI.2304-3083.2022.1.01.

Forest inventory instruction (with changes from 12 of May 2020). (2023), [online] Available at: https://docs.cntd.ru/document/542621790 [Assessed 12 Jan. 2023]

FSC International. (2023), [online] Our Vision and Mission. Available at: https://ic.fsc.org:443/en/about-fsc/vision-mission. [Assessed 12 Jan. 2023].

[20]Protection of high conservation value forests by Terneyles group. Available at: https://registry.verra.org/app/projectDetail/VCS/1544

[21]Finding the Balance: A Landscape Approach to IFLs. Available at: https://ga2017.fsc.org/finding-the-balance-a-landscape-approach-to-ifls/

FSC International (2023), [online] The 10 Principles. Available at: https://ic.fsc.org:443/en/certification/principles-and-criteria/the-10-principles. [Assessed 12 of January 2023].

FSC ADVICE 20-007-018. (2023). Advice note for the interpretation of the default clause of Motion 65, [online] Available at: https://ic.fsc.org/en/what-is-fsc-certification/consultations/current-processes/advice-note-on-the-development-of-indicators-for-the-protection-of-intact-forest-landscapes-and-indigenous-cultural-landscapes-in-brazil-canada-the-congo-basin-and-russia [Assessed 12 Jan. 2023].

FSC National Stewardship standard for Russian Federation, [online] Version 6.01. Available at: https://ru.fsc.org/preview.russian-national-fsc-standard.a-911.pdf [Assessed 21 Feb. 2022. At the moment site is closed].

Giessen L., Burns S., Sahide M.A.K., Wibowo A. (2016). From governance to government: The strengthened role of state bureaucracies in forest and agricultural certification. Policy and Society 35(1), 71–89, DOI: 10.1016/j.polsoc.2016.02.001.

Grantham H., Tibaldeschi P., Izquierdo P., Jones K., Mo K., Rainey H., et al. (2021). The emerging threat of extractives sector to intact forest landscapes. Frontiers in Forests and Global Change, DOI: 10.3389/ffgc.2021.692338.

Greenpeace International[22] (2017). Eye on taiga: How industry claimed sustainable forestry is destroying great northern forest", [online] 6 of March 2017. Available at: https://www.greenpeace.org/international/publication/7355/eye-on-the-taiga/ [Assessed 12 Jan. 2023].

Hansen A.J., Burns P., Ervin J., Goetz S.J., Hansen M., Venter O., et al. (2020). A policy-driven framework for conserving the best of Earth's remaining moist tropical forests. Nature Ecology and Evolution, 4(10), 1377–1384, DOI: 10.1038/s41559-020-1274-7.

Hansen A.J., Noble B.P., Veneros J., East A., Goetz S.J., Supples C., et al. (2021). Toward monitoring forest ecosystem integrity within the post-2020 Global Biodiversity Framework. Conservation Letters, DOI: 10.1111/conl.12822.

Heino M., Kummu M., Makkonen M., Mulligan M., Verburg P.H., Jalava M., Räsänen T.A. (2015). Forest loss in protected areas and intact forest landscapes: A global analysis. PLoS ONE, 10(10), DOI: 10.1371/journal.pone.0138918.

Hcvf.ru, (2023). High conservation value forests in Russia web-site, [online] Available at: https//www. hcvf.ru. [Assessed 12 Jan. 2023].

Intergovernmental Panel for Biodiversity and Ecosystem Services (IPBES). (2019). Global Assessment Report on Biodiversity and Ecosystem Services, IPBES Secretariat: Bonn, Germany, [online] Available at: https://www.ipbes.net/global-assessment-report-biodiversity ecosystem-services [Accessed 2 Nov. 2022).

Karpachevsky M. State of intact forest landscapes in Russia and the role of FSC certification in its protection. (2022). Sustainable forest management, 70 (in Russian), DOI: 10.47364/2308-541X_2022_70_3_36.

Krenke A.N., Ptichnikov A.V., Shvarts E.A., Petrov I.K. (2021). Assessments of the Forest Carbon Balance in the National Climate Policies of Russia and Canada. Doklady Earth Sciences, 501(2), 1091–1095, DOI: 10.1134/S1028334X21120060.

Mackey B., Kormos C.F., Keith H., Moomaw W.R., Houghton R.A., Mittermeier R.A., et al. (2020). Understanding the importance of primary tropical forest protection as a mitigation strategy. Mitigation and Adaptation Strategies for Global Change, 25(34), 763–787, DOI: 10.1007/s11027-019-09 891-4.

Marx A., Cuypers D. (2010). Forest certification as a global environmental governance tool: What is the macro-effectiveness of the Forest Stewardship Council?. Regulation and Governance, 4, 408–434, DOI: 10.1111/j.1748-5991.2010.01088.x.

Mosse D. (2005). Cultivating development: An ethnography of aid policy and practice. London: Pluto Press.

Potapov P., Hansen M., Laestadius L., Turubanova S., Yaroshenko A., Thies C., Smith W., Zhuravleva I., Komarova A., Minnemeyer S., Esipova E. (2017). The last frontiers of wilderness: Tracking loss of intact forest landscapes from 2000 to 2013. Science Advances, DOI: 10.1126/sciadv.1600821.

PEFC Russia Standard of forest management and use. (2015). Standart lesoupravleniya I lesopolzovania, [online] Available at: http://www.pefc.ru/doc/PEFC-RUSSIA-ST-01-2015_16%2002%202016_RUS_16022016.pdf [Assessed 21 Feb. 2022].

Ptichnikov A., Karpachevskiy M. (2020). Impact assessment research of Motion 65 implementation for boreal forests of the Russian Federation. Motion 34/2017 report. FSC Russia.

Ptichnikov A.V., Shvarts E.A., Kuznetsova D.A. (2021). The Greenhouse Gas Absorption Potential of Russian Forests and Possibilities for Carbon Footprint Reduction for Exported Domestic Products. Doklady Earth Sciences, 499(2), 683-685, DOI: 10.1134/S1028334X21080122.

Sabatini F.M., Keeton W.S., Lindner M., Svoboda M., Verkerk P.J., Bauhus J., et al. (2020). Protection gaps and restoration opportunities for primary forests in Europe. Diversity and Distributions, 26(12), 1646–1662, DOI: 10.1111/ddi.13158.

The FSC National Forest Stewardship Standard of Russian Federation. (2022), [online] National Standard (NS). Available at: https://fsc.org/en/document-centre/documents/resource/183 [Assessed 12 Jul. 2022].

The National Strategy for the Development of the Forest Sector of Russian Federation until 2030. (2021) (in Russian). Government decree №312-p from 11.02.2021.

Tysiachniouk M. (2006). Forest Certification in Russia. Confronting Sustainability: Forest Certification in Developing and Transitioning Countries. Yale School of Forestry and Environmental Studies: New Haven, CT, USA, 261–297.

Watson J.E., Evans T., Venter O., Williams B., Tulloch A., Stewart C., et al. (2018). The exceptional value of intact forest ecosystems. Nature, Ecology and Evolution, 2, 599–610, DOI: 10.1038/s41559-018-0490-x.

Williams B.A., Venter O., Allan J.R., Atkinson S.C., Rehbein J.A., Ward M., et al. (2020). Change in terrestrial human footprint drives continued loss of intact ecosystems. One Earth, 3, 371–382, DOI: 10.1016/j.oneear.2020. 08.009.

Winkel G. (2012). Foucault in the forests – A review of the use of 'Foucauldian' concepts in forest policy analysis. Forest Policy and Economics, 16, 81–92. DOI: 10.1016/j.forpol.2010.11.009.

Yanow D. (2007). Interpretation in policy analysis: On methods and practice. Critical Policy Analysis, 1, 110–122, DOI: 10.1080/19460171.2007.9518511.

Ptichnikov A. (2019). Market based forest conservation opportunities. Izvestiya Rossiiskoi Akademii Nauk. Seriya Geograficheskaya, vol. 2019, №6, 97-106 (in Russian), DOI: 10.31857/S2587-55662019697-106.

Forest Code of Russian Federation. (Lesnoy codex Rossiskoy federatsii) (in Russian).

FSC-STD-40-005 (2017). Requirements for sourcing FSC controlled wood. V3-1 EN, [online] Available at: https://fsc.org/en/document-centre/documents/resource/373 [Assessed 12 Jul. 2022].

Intact forest landscapes in Russia: current condition and losses over the last 13 years (2018). WWF Russia, [online] Available at: https://wwf.ru/en/resources/publications/booklets/intact-forest-landscapes-in-russia-current-condition-and-losses-over-the-last-13-years/ [Assessed 12 Jul. 2022].

[22]Nominated as unwanted organization in Russia in May 2023

Tysiachniouk M. and McDermott C.L. (2016). Certification with Russian characteristics: Implications for social and environmental equity. Forest Policy and Economics, 62, 43–53, DOI: 10.1016/j.forpol.2015.07.002.

Ulybina O. (2014). Interaction, cooperation and governance in the Russian forest sector. Journal of Rural Studies, 34, 246–253, DOI: 10.1016/j.jrurstud.2014.02.005.

Ulybina O. and Fennell S. (2013). Forest certification in Russia: Challenges of institutional development. Ecological Economics, 95, 178–187, DOI: 10.1016/j.ecolecon.2013.09.004.

RESEARCH PAPER

PROBLEMS OF SUSTAINABLE MANAGEMENT OF WATER RESOURCES OF LAKE SEVAN AND ITS BASIN

Trahel G. Vardanyan[1*]
[1]Yerevan State University, Yerevan, Alex Manoogian 1, 0025, Yerevan, Armenia
***Corresponding author:** tvardanian@ysu.am
Received: January 23rd, 2021 / Accepted: May 4th, 2023 / Published: July 1st, 2023
https://DOI-10.24057/2071-9388-2023-007

ABSTRACT. Numerous rivers, lakes and other water features have suffered significant alterations as a result of human economic activity. As a result, hydrometric, hydrological, biological, ecological conditions, as well as morphometric elements of these objects were violated.

In this regard, Lake Sevan and its basin might be used as a well-known example. There has never been any instance in the history of limnology where a lake's level was artificially lowered by 18 meters over 3 to 4 decades (1930–1970), and by another 2 meters at the end of the 20th century (1990–2000). Additionally, the lake's water volume dropped from 58 billion m^3 to 32 billion m^3.

The Sevan problem first surfaced in the late 19th and early 20th centuries and is still a problem today. However, it has many meanings/soundings at different times. Based on this, we usually divided the entire study period into several stages.
It should be noted that the ecosystem has suffered irreparable losses as a result of the use of the Lake Sevan resources, inadequate water resource management, and both positive and negative effects of these factors.

We disagree with the assertions of many experts that problems can only be prevented or solved by raising the lake level. Therefore, extensive actions must be taken in the Sevan basin management area, regardless of the lake's level.

KEYWORDS: Lake Sevan, level fluctuations, hydrological regime, water balance, water resources management, anthropogenic transformation

CITATION: Vardanyan T. G. (2023). Problems Of Sustainable Management Of Water Resources Of Lake Sevan And Its Basin. Geography, Environment, Sustainability, 2(16), 142-151
https://DOI-10.24057/2071-9388-2023-007

ACKNOWLEDGEMENTS: The research project № 21T-1E192, sponsored by the Science Committee of RA, provided funding for the work.

Conflict of interests: The authors reported no potential conflict of interest.

INTRODUCTION

A great deal of rivers, lakes, and other water features have changed significantly as a result of man's economic activity. As a result, hydrometric, hydrological, biological, ecological conditions, as well as morphometric elements of these objects were violated.

There has never been another case where a lake level was artificially lowered by 18 meters for 3–4 decades (1930–1970), and by another 2 meters at the end of the 20th century (1990–2000). The volume of water in the lake also decreased from 58 billion m^3 to 32 billion m^3, making Lake Sevan and its basin a classic example in this regard in the field of limnology. The quantitative change of the lake water has also brought about a qualitative change. Well before the artificial change in lake level (in 1893), the total mineralization reached 714 mg/l. After 1980 the mineralization sharply decreased, reaching lows of 660.2 mg/l and 647.8 mg/l at the moment. The massive outflow of salty water, which removed the salts that had been accumulating in the lake for ages, is significantly related to the decrease in the total general mineralization of the lake water. Only the sulfate ion (SO_4) increased about 1.8 times from the examined ionic composition, which had an impact on the flavour of the water and might encourage bacterial growth. And Water transparency decreased from 14.3 meters to 4.5 meters (Vardanian et al. 2021).

It should be mentioned that the lake's hydrological regime changed as a result of the lake's level dropping and the economic growth of the basin. The latter caused the disruption of the hydrochemical and hydrobiological regimes of the lake. The quality of water deteriorated and water turbidity increased. Both the inner water substances circulation and the biological substance circulation were altered.

The Sevan problem, which first surfaced in the late 19th and early 20th centuries, is still a problem today. However, it has many meanings/soundings at different times. Based on this, we divided the entire study period into several stages (Fig. 2).

In the last fifty years, thousands of scientific articles and theses have been published, and hundreds of theses have been successfully defended in Armenia and many other countries. Government decisions and programs have been adopted regarding saving the lake (the latest one is The "2022-2027 Management Plan of the Sevan Basin Management Area"[1] is the most recent government decision and program involving

[1]https://www.irtek.am/views/act.aspx?aid=119092

lake preservation. Numerous foreign funding initiatives have also been executed.

Despite all of this, I believe the Sevan problem will continue to be a concern for a very long time.

RESEARCH AREA, MATERIAL AND METHODS

Research area

The transformation of lake ecosystems, one of hydro ecology's most significant research fields, is represented by Lake Sevan as a dramatic example. Sevan is one of the high-mountainous freshwater lakes in the world and the largest lake in Caucasus. Sevan is thought to be a large freshwater reservoir that supplies not just Armenia but also other nations in the area (Fig. 1).

Lake Sevan is regarded as a miracle of nature, an ecologically and economically significant water body, and a national treasure for Armenia. At 1900 meters above sea level, it is one of the highest lakes in the world and is located in the dry subtropical climate area. But because it is a freshwater lake situated in the arid subtropical climate area, it is very uncommon. Other lakes in the same area, such as Van and Urmia (in the Armenian Highland), the Dead Sea, Tuz (Middle East), Lobnor (Central Asia), Issik-Kul (Central Asia), are all salty and their water is unfit for irrigation and drinking (Vardanian 2012). The salinity of Lake Sevan water is only 600-700 mg/l (Parparova 1979, Vardanian 2009).

Thus, it is a major source of water for Armenia, and potentially for other countries in the region.

Since antiquity, people have been aware of Lake Sevan; knowledge about it may be found in the works of Greek chroniclers and geographers. On the map that Ptolemy drew, Lake Lychnites, according to the French traveler Saint-Martain, is actually Lake Sevan (Gabrielian 1980). There are several theories explaining the creation of the lake, with the tectonic-retaining idea being the most logical (Sargsian 1962). According to this theory, the lake was formed in a tectonic depression as a result of dams created by lava flows from the Geghama mountains. Lake Sevan is divided by the Noratus and Artanish promontories into two major basins, Big and Small Sevan. In the upper Pleistocene volcanic outflows finally blocked the valley of the Hrazdan River, between 150-200 thousand years ago (Paffenholtz 1950).

The numerous streams that run into the lake are fed by mountain ranges that are more than three thousand meters high, which surround the lake. Along the main axis of the lake, to the north-east, are the folded block mountains of the Areguni, Sevan, and East Sevan, while the Geghama and Vardenis volcanic mountains encircle the area to the south-west (Fig. 1). The Hrazdan River currently provides the natural outflow, and the river's waters are used downstream for irrigation and hydropower generation.

The Lake Sevan basin is characterized by a continental mountain-steppe landscape. The coastal zone of the Lake Sevan is characterized by a temperate climate with warm long summers and relatively cold winters. The climate changes slightly in higher elevations, with summers becoming cooler and winters becoming colder. The basin's high elevation and the air's relative dryness are what cause the region to get more than 2500 hours of sunshine annually (in Martuni, about 2800 hours). The warmest month is August, when the average monthly temperature ranges from 8.8°C (Yeratmber) to 17.6°C (Shorzha). The coldest month is January with an average monthly temperature of -4.6°C (Shorzha) to -12.3°C (Yeratmber). The average annual temperature ranges from -2.3°C (Yeratmber) to 6.4°C (Shorzha). A stable snow cover develops in the winter. The precipitation in the basin ranges from 386 (Tsovak) to 857 (Yeratumber) mm. During the year, the maximum amount of precipitation is observed in spring, mainly in May, and the minimum - in winter (Climate Bulletin of the Republic of Armenia 2011).

Water from inflowing rivers, surface precipitation, and groundwater influx supply Lake Sevan with water. Water is

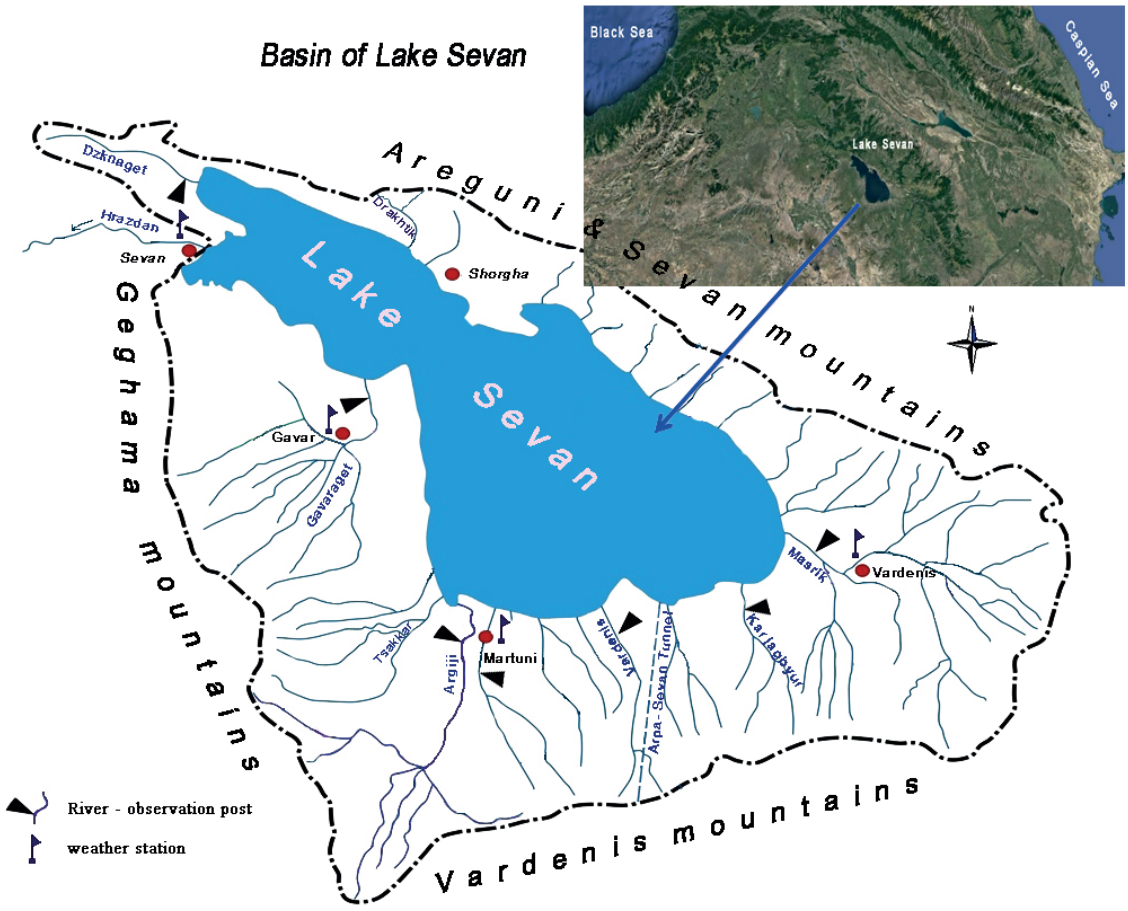

Fig. 1. The river network of Lake Sevan

removed from the lake by evaporation, infiltration, and flow out through the Hrazdan river.

The primary source of water is rivers. There are 28 rivers and streams are longer than 10 km (Table 1). The river network is rather dense in the south and south-western parts of the basin, which has the largest rivers, the Argiji, Gavaraget, Masrik, and Vardenis (Fig. 1).

The scientific study of Lake Sevan started at the end of the 19th century. The first relatively comprehensive survey was undertaken by (Markov 1911). In 1928 Davidov established the Hydro- Meteorological Bureau of Sevan, installed hydrological and meteorological stations, and commenced routine observations. Eventually the lake's water balance (Davidov 1938), and salinity balance (Lyatti 1932) were estimated. Since then, a variety of alterations in these balances have occurred as a result of human activity added to natural occurrences, most noticeably seen in variations in lake levels.

MATERIAL AND METHODS

The Armstatehydromet official observations (Climate Bulletin of the Republic of Armenia 2011; Fourth National Communication on Climate Change 2020), the Hydrometeorology and Monitoring Center state non-commercial organization, data from various departments (Institute of Hydro ecology and Fisheries; Yerevan State University; et al.), and currently available scientific sources were used to implement the article (Bagdasaryan 1990).

The fundamental concepts and techniques of spatial-temporal analysis (general geographic, physical-geographic, hydrometeorological, socio-economic, hydro ecological), as well as the synthesis of pertinent data and generalizations, were utilized to analyze the initial data (Mann 1945; Rusinov 1970; Shelutko 2007; Gagarina 2012; Chichasov 2013).

We used field expeditionary observations, processing techniques of specialised databases, geographic information systems, empirical-statistical and genetic theoretical models, methods of mathematical statistical analysis, and other methods and techniques used in practise in the study of hydrometeorological and hydrochemical information (Aliokhin 1970; Rozhdestvensky et al. 1974; Kendall 1975; Shelutko 1984; Trofimov et al. 2001).

RESULTS AND DISCUSSION

The transformation of hydrometric and hydrological regime and existing problems

As previously said, we divided the duration of the Lake Sevan problem study traditionally into a number of stages (Fig. 2), which we will talk about in detail below:

- Problem presenting stage (beginning of the 20th century)
- Implementation stage of the main problem (1930 – 1950s)
- Emergence stage of a new problem (1960 – 1970s)
- New problem prevention stage (1980 – 2000s)
- Current stage issues

Table 1. Some hydrometric and hydrological characteristics of relatively large rivers of the basin of Lake Sevan (Vardanian et al. 2021)

River-observation post	River length, km	Size of watershed basin, km^2	Mean height of watershed, m	Mean annual discharge, m^3/sec	Runoff , l/sec km^2
Argiji-V. Getashen	51	384	2470	5.55	14.5
Gavaraget-Noraduz	41	467	2430	3.51	7.5
Masrik-Torf	45	685	2310	3.42	4.9
Vardenis-Vardenik	24	116	2680	1.64	14.1
Karchaghbjur-Karchaghbjur	26	117	2650	1.15	9.8
Martuni-Geghovit	20	85	2760	1.41	16.6
Dzknaget-Tsovagjugh	21	85	2220	1.06	12.5

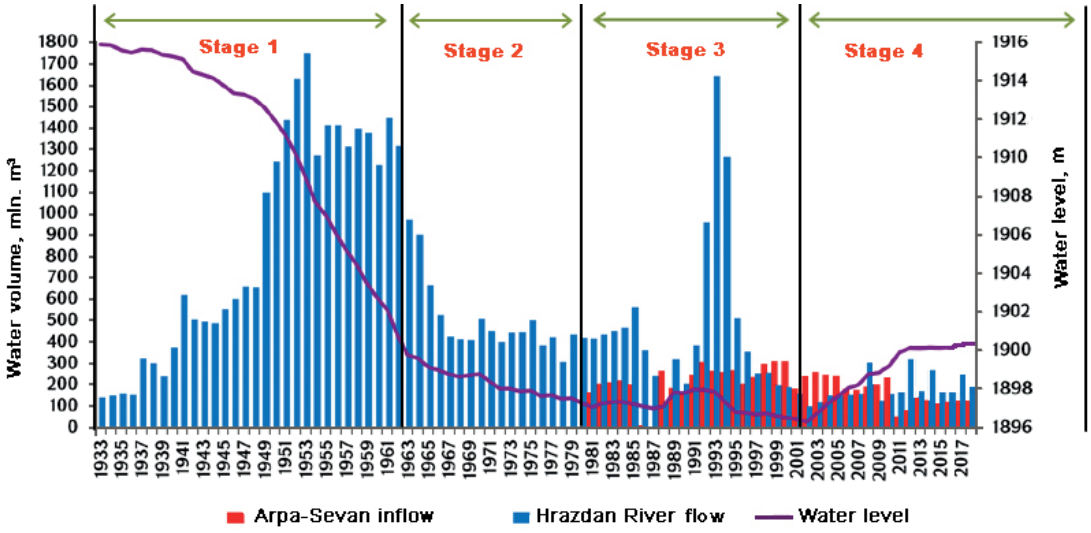

Stage 1. Implementation stage of the main problem (1930 - 1950s) Stage 2. Emergence stage of a new problem (1960 - 1970s)	Stage 3. New problem prevention stage (1980 - 2000s) Stage 4. Current stage issues

Fig. 2. The graph of perennial fluctuation of Lake Sevan level: annual total water outflow volume and Arpa-Sevan inflow (According to Hydrometeorology and Monitoring Center of RA)

Problem presenting stage (beginning of the 20th century)

The concept of using Lake Sevan water in a practical way appeared at the beginning of the 20th century. Because of Armenia's dry subtropical climate, potential evaporation considerably exceeds the amount of precipitation. A limited resource for agriculture is water. There are hundreds of thousands of hectares of fertile land in the Ararat valley, which is south of and 1000 m lower than Lake Sevan. But their annual precipitation is close to 250-300 mm, and potential evaporation is above 1000 mm. In the meantime, the lake's evaporation caused millions of cubic meters of water to evaporate.

A water resources management project for the lake was designed to ensure the efficient use of Sevan's water and fish resources, and it calls for the annual discharge of 1025 million cubic meters of water from the lake's centuries-old water reserves through the Hrazdan River: 375 million cubic meters for irrigation and 650 million cubic meters for energy (Musaelian 1993; Gabrielian 1980).

The Hrazdan River's bed was first suggested to be deeper, and the discharge was intended to be artificially increased. This would reduce the lake level by 55 m and increase the outflow of the Hrazdan river by 14-15 times, draining Big Sevan but using the water to irrigate 120 thousand ha immediately downstream and in the Ararat valley. Additionally, it would permit the development of a series of hydroelectric facilities on the Hrazdan River (Vardanian et al. 2007).

Before 1930, Lake Sevan's surface was 1916 meters above sea level in its natural state. The surface of the drainage area of the lake before its artificial drop (1930s) was 3475 km^2, that is larger than the surface of the lake by 2.5 times (1416 km^2), and the volume of lake water was 58.5 billion m^3 (Table 2).

In its natural state, the water balance of Sevan was stable (Table 3). The largest component of the balance was evaporation, 1210 million m^3 per year, and the outflow through the Hrazdan River was only 50 million m^3.

The Hrazdan River's bed was first suggested to be deeper, and the discharge was intended to be artificially increased. This would drain Big Sevan but use the water to irrigate 120 thousand ha directly downstream and in the Ararat valley, lowering the lake level by 55 m and raising the Hrazdan river's outflow by 14–15 times. Additionally, it would enable the development of a series of hydroelectric facilities on the Hrazdan river. But, the First World War came into play (Vardanian et al. 2007).

In our opinion, this decision was correct and realistic for the given period. It was based on the socio-economic situation of the country. Armenia was an agrarian country, it did not have any fuel and energy resources. In other words, the country partially addressed a number of crucial economic difficulties with the help of this approach of water resource management.

Implementation stage of the main problem (1930 - 1950s)

The concept wasn't given another thought until the Soviet times. In 1931, after partial changes, the project was approved by the government and construction started. After building Kanaker and Yerevan hydropower stations, the construction of Sevan-Hrazdan hydropower cascade (Fig. 3) was interrupted by the Second World War. Work re-started in the early 1950s, and further power stations were built.

The water balance of the lake underwent the greatest change at this stage (Fig. 2, Table 3). The outflow of water through the Hrazdan River in 1950-1953 reached its historical maximum volume of 1.7-1.8 billion m^3 (Fig. 2).

Table 2. Some hydrometric and hydrological indicators of Lake Sevan

Indices	Unit of Measurement	In natural state (Davidov, 1938)	At the lowest level (2001)*	Present-day Condition*
Drop of lake level	m	0.0	19,43	15,48
Height above sea level	m	1915.89	1896.46	1900.41
Watershed surface	km^2	3475	3649	3613
Lake surface	km^2	1416	1242	1278
Maximum depth	m	98.7	79.3	83.2
Water volume	km^3	58.5	32.8	38.3
* According to Hydrometeorology and Monitoring Center of RA				

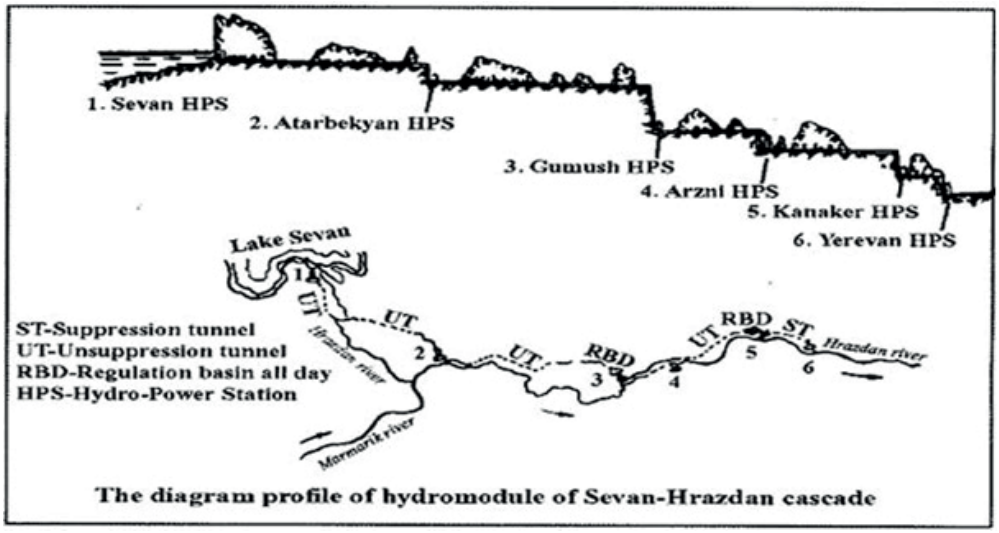

Fig. 3. The Plan of Sevan-Hrazdan Hydropower Cascade (Vardanian et al. 2007)

In this respect, Sevan is the only lake, which is considered to be a large natural laboratory, where one can observe all those processes, connected with the decrease of erosion basis of flowing into the lake rivers, and which cannot be studied under laboratory conditions. Among these processes, the hydrological, thermal, hydro-chemical, carbon regime of the lake, as well as biological conditions, which have served as a rich material for scientific researches, are rather important.

The activation of channel processes that flow into lake rivers was brought on by a decrease in erosion basis. It caused the river valleys' balanced profiles, which were created over thousands of years, to be violated. The active down-cutting erosion destroyed the foundations of bridges and caused their collapse.

Down-cutting erosion is characteristic of all the rivers which flow into Lake Sevan. But at the mouth of the Argiji, the main inflowing river, where the river has deepened its riverbed by 10-15 m, the erosion is quite visibly exhibited (Fig. 4).

Some of the irrigation, electricity, and industrial issues were already partially resolved at this point. However, the government realized that it is necessary to make some changes in the water resources management plan of Lake Sevan. Examine the topic of additional level reduction in particular.

Emergence stage of a new problem (1960 - 1970s)

At this point, it was evident that the physical, chemical, and biological characteristics of Lake Sevan and its surroundings had been significantly impacted by the lake's level fall. The water balance of the lake continued to remain negative. The difference between water inflow and outflow was -845 mln. m^3, and the level dropped to 17-18 m (Fig. 2, Table 3).

The changes that have created better circumstances for algae development and the early warning indicators of eutrophication are the most visible. The first signs of the lake's eutrophication were recorded in 1964, when green and blue algae blossomed in the lake. The ecosystem as a whole has deteriorated as a result of changes in lake conditions, as have changes in a number of lake-related processes (including bio-degradation, sedimentation and diffusion). Despite the waters still having oligotrophic lake conditions, the quantity of bacteria per liter was more than twice what it had been prior to the lake's level reduction in the 1960s. However, starting in the 1980s, the number of

Table 3. The water balance of Lake Sevan in different years (million m^3)

Balance Component	In natural state, Davidov V. K. (1927-1934)	Hydro-meteorological Department of RA		(2002-2009)*	Hydrometeorology and Monitoring Center of RA (2018)
		(1951-1970)	(1981-2000)		
Inflow					
Precipitation	550	498	507	593	497
River flow	720	749	777	735	725
Arpa-Sevan flow	-	-	236	219	142
Subsurface flow	50	78	80	94	94
Total	**1320**	**1325**	**1600**	**1641**	**1458**
Outflow					
Evaporation	1210	1053	1102	1045	1 203
Hrazdan River flow	50	1093	513	157	201
Subsurface flow	60	24	10	14	14
Total	**1320**	**2170**	**1625**	**1216**	**1418**
Inflow-Outflow	**0**	**-845**	**-25**	**+425**	**+40**

*Ecology of lake Sevan during the period of water level rise the results of Russian-Armenian biological expedition for hydroecological survey of lake Sevan (Armenia).

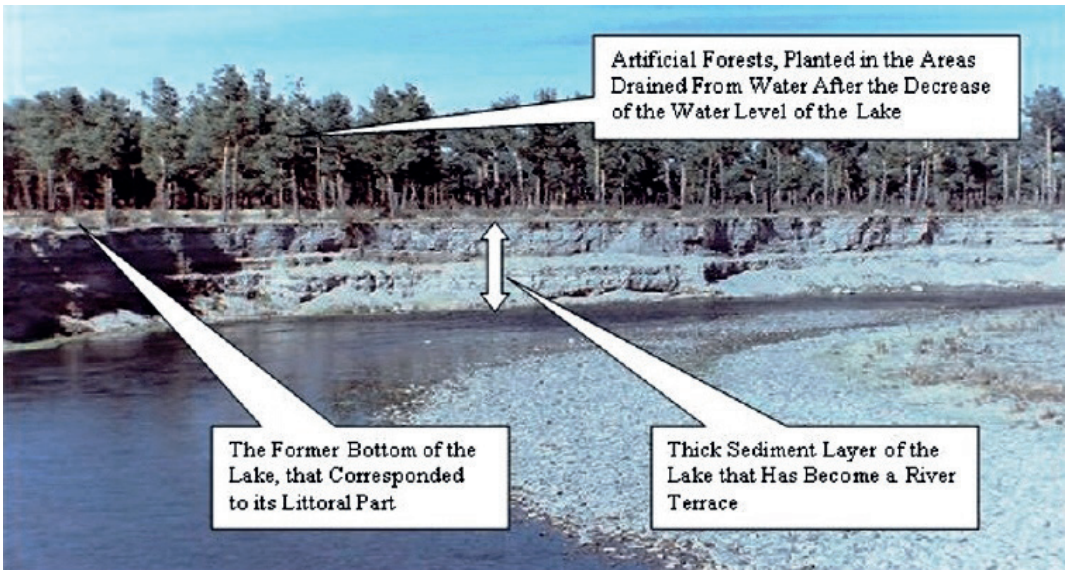

Fig. 4. The riverbed of the Argiji river, which [riverbed] has deepened as a result of the drop of Lake Sevan level

bacteria quadrupled once more, creating a concentration that currently reflects the elements of a mesotrophic lake. The drainage of the lake also had important effects for the fauna. The primary trout breeding habitats were eliminated as parts of the lake's rocky bottom dried out. In addition, around 10 thousand ha of wetland and semi-wetland areas also dried out. These areas were previously used by up to 160 species of migratory birds, and only 50 of these species are currently recorded. The populations of mammal and reptile species in the area have also declined significantly, and there is evidence of changes in species composition (The Biodiversity of Armenia 1999).

As the deterioration of the lake environment became more apparent and better understood, restoration and increased lake levels became a consideration in any project involving the lake.

Concern for the preservation and restoration of Lake Sevan and its environment first became apparent in the 1960s. Water from nearby river basins has to be supplied to the lake in order to achieve restoration. In 1961 it was proposed to construct the Arpa-Sevan water-carrying tunnel. The planned tunnel was 48 km long, passed under the Vardenis mountain range (Fig. 1) and was supposed to carry 250 million m^3 of water annually from the Arpa river in Sevan (Fig. 5).

New problem prevention stage (1980-2000s)

After the construction of Arpa-Sevan tunnel in 1982-1990, a positive water balance was established in the lake and the level started to rise gradually (Fig. 2). As a result, biological and chemical changes and associated physical processes encouraged biological productivity and the lake rehabilitation became sustainable.

Despite the stabilization of the level and the average annual volume of water drained by the Arpa-Sevan tunnel (236 million m^3), the lake balance still remained negative (-25 million m^3) (Table 3).

Meanwhile, design and construction started on a new water transfer project. This would obtain a supply of water from the Vorotan river basin, adjacent to the Arpa River. Annually 150-170 million m^3 would come through a 20 km tunnel into Kechut reservoir, built on the Arpa River. The water would then travel through the Arpa-Sevan tunnel and into Lake Sevan from there. At the same time, the outflow from the lake would not exceed 100-120 million m^3. These conditions would enable the lake to stabilize as well as gradually raise its levels. Construction started in 1990.

However, the sustainability was interrupted by the economic and energy crisis in Armenia (Disintegration of the USSR, Karabakh war, economic blockade), and since 1992, large water releases from the Lake restarted (1.6-1.7 billion m^3). Construction of the Vorotan-Arpa tunnel was also stopped.

Thus, the lake's secondary destabilization began, resulting in a further drop in level, which led to the buildup of organic materials in the lake, a trend towards eutrophication, and the reemergence of the serious issues. During this time, the level of the lake continued to decrease and in 2001 reached its historical minimum mark (1896.46 m) and the volume was only 32.8 km^3, instead of the previous 58.5 km^3 (Table 2).

Current stage issues

The biggest problem of the current stage is the effective management of the Sevan basin management area.

An increase in lake levels over the current value is required if Lake Sevan is to be restored as a viable freshwater lake. During the past 20-30 years, the status and processes within Lake Sevan has been investigated by a number of scientific- research institutes, scientific expedition groups, and scientists from Armenia, the former USSR, and foreign countries. They agree that a rise in lake level is needed in order to slow down or stop the eutrophication processes in the lake and reverse the deterioration of the lake environment. Most suggest that the lake level must be increased by at least 6 meters.

In order to raise the water level of the lake, to restore and preserve the ecosystem, a number of large-scale measures were taken. In particular, in 2001, the Law of the Republic of Armenia on measures for restoration, conservation, reproduction and use of the Lake Sevan ecosystem was adopted[2].

According to this law, in the field of raising water level of Lake Sevan, it was planned to put into operation the Vorotan-Arpa hydro junction, which construction was

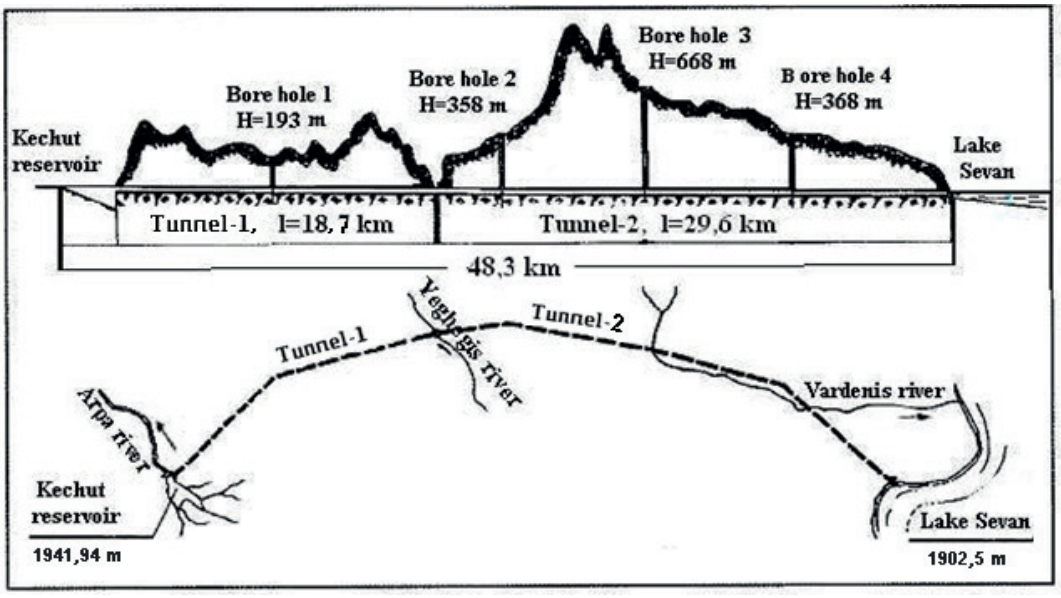

Fig. 5. The Plan of Arpa-Sevan Tunnel (Vardanian et al. 2007)

[2]https://www.arlis.am/DocumentView.aspx?docid=137373

stopped in the 1990s, and to ensure the stable operation of the Arpa-Sevan water pipeline.

As a result, an annual increase in the level of Lake Sevan was expected about 21.6 cm. According to these calculations, during the 30 years planned by the complex program, the volume of Sevan water would increase by around 8.8 billion m^3, which is equivalent to a 6.5 m increase in the lake level. According to the ecological balance, Lake Sevan will have an additional water supply following the required 6 m rise in lake level, which will be seen as a highly significant and strategically significant natural resource for energy and other economic branches.

The Vorotan-Arpa water tunnel was put into operation in 2004 according to the law, which was intended to transfer a part of the water of the Vorotan River to Sevan. Unfortunately, this aqueduct hasn't functioned in any way since the day it was launched for reasons that are unclear.

In 2008, the President of the Republic of Armenia issued a proclamation establishing the Sevan Lake Issues Commission for the supervision of the specified works, monitoring observations, and submission of new proposals[3].

This commission contributed significantly to later lake level stabilization. As a result, the level of Sevan rose by more than 3 m (Fig. 2).

However, due to ineffective management of the water basin, inaccurate estimates, and favorable meteorological conditions in those years, a double increase in lake level instead of the anticipated annual increase of 21.6 cm took place. The lake level increased by nearly 2.5 metres in just 6 years (2002–2007).

As a result, a new issue emerged, namely, the coastal green zone (tree-shrub vegetation) and recent constructions is under water (Fig. 6). Significant water levels rose quickly and unexpectedly, leaving no time to clean the shoreline of vegetation, putting the lake at risk of eutrophication once more.

Based on this situation, in the years that followed, the lake's quick increase was slowed, mostly by increasing outflows through the Hrazdan River, making it possible to clear the buildings and coastal green zone. In addition, climatic conditions became more unfavorable (precipitation decreased, droughts increased). Even now, this process is still in motion. As a result, the lake became frequently covered with blue-green algae (Vardanian et al. 2021).

Changes in the shoreline of Lake Sevan in 1973-2015 were analyzed more thoroughly in the paper (Hovsepyan et al. 2019), using the spectral index NDWI (Normalized Difference Water Index).

The bloom event in 2018 reached unprecedented levels, and therefore, stirred intense media attention (Gevorgyan et al. 2020). The lake continued to bloom in 2019-2022 too (Fig. 7).

Our studies have shown that only raising the lake level is not enough. In order to effectively manage the water resources of the lake and develop the Ecosystem, it is necessary to ensure a stable level of the lake during the year. Drastic fluctuations during the year, such as the level of Lake Sevan, should not be subjected. Utilizing historical data from the Armenian Monitoring Center's measurements for the most recent year (2022), we can observe that the lake level varied by 42 cm in just four months (Fig. 8), or roughly 511 million m3 of water volume. That is, as much water as the approximate combined flow

Fig. 6. The coastal green zone is under water (https://blog.168.am/blog/251490.html; https://www.ecolur.org/hy/news/sevan/2039/)

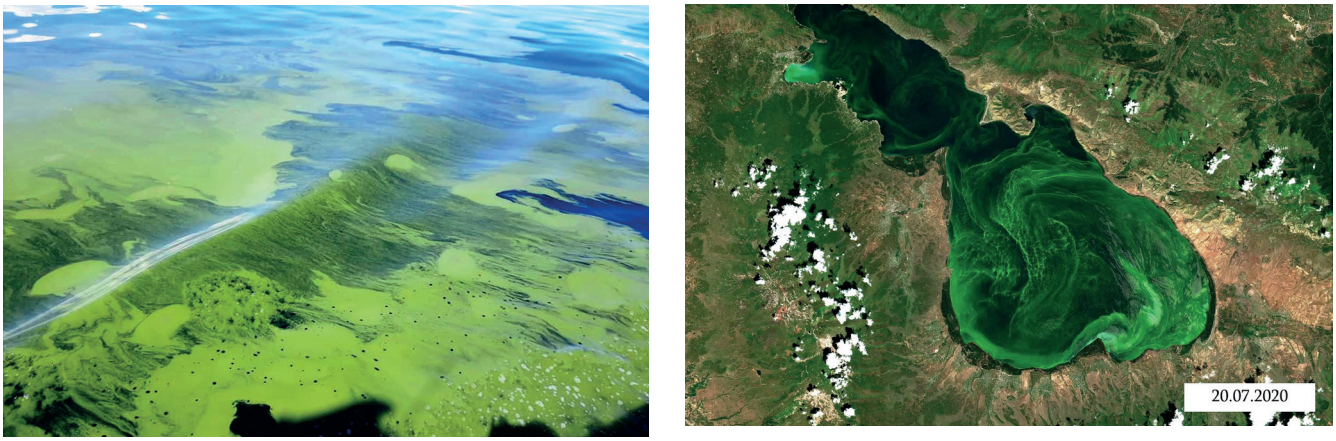

Fig. 7. Satellite images of Lake Sevan blooming in 2020 (https://hetq.am/en/article/146637)

[3]https://www.arlis.am/DocumentView.aspx?DocID=48718

of all rivers entering the lake during a year with low water levels.

It is hard to predict the future developments of these processes. However, the issue of lake Sevan is not entirely settled, the ecosystem of the lake is damaged, undergoing the process of eutrophication. The flora and fauna of the water and coast underwent serious and irreversible changes.

The last document adopted by the government regarding Lake Sevan was the adoption of the decision on the "2022-2027 Management Plan of the Sevan Basin Management Area"[4].

The document's primary goal is to strike a balance between the interdependent relationships among water users, including agriculture, fisheries, industry, energy and the environment, in order to assist the bodies in charge of managing water resources, administrative bodies, and the general public in making decisions regarding the wise and effective use of water resources. Hopefully this program will help to improve the ecosystem.

The main ways of solving current problems

The following methods of ecosystem regulation are provided as a result of our investigation into and analysis of the history and present issues of the Sevan Basin Management Area.

1. It is known that the management of natural resources in the direct influence zone of the Sevan catchment basin is carried out by various state administration bodies, governorates and communities. From the analysis of the management system, it follows that there is no single governing body in the region, as a result of which the ecological condition of Lake Sevan and its catchment continues to deteriorate. Therefore, in order to address the issue, new legislation must be passed, existing water law must be improved, institutional capacity must be increased, and a water monitoring system must be put in place.

2. In the management of current problems, it is extremely important to clarify the quantitative indicators of the water balance components of the Sevan Lake basin. Specifically, the amounts of available dynamic water resources' inflow and outflow. However, our monitoring observations and studies show that the indicators of these components do not have sufficient reliability. The cause is that there aren't enough evaporators, the calculation methods for groundwater flow entry and exit aren't specified, and hydro-meteorological measurement and testing equipment is frequently out of date.

3. There is a highly stressed water-economic balance in the Sevan basin management area. Water intake in the basin is carried out for drinking-domestic, irrigation, water desalination, industry, hydropower and fish farming purposes, in accordance with water use permits. However, there are many unauthorized water users. In other words, a specific amount of water is not taken into consideration or seen as a loss. As a result, the supply and demand of water require significant attention. Monitoring of the water use licenses issued by the competent department is required in order to ascertain the true demand for water. At the same time, improvement of water supply and irrigation networks is needed to reduce water losses. It is time for the state to define the priorities of the water use sectors in the basin and to implement the SCADA (Supervisory Control and Data Acquisition) system for the main water users, which will enable more efficient collection and processing of actual water use data.

4. Qualitative and quantitative pressures on the Sevan Basin Management Area have increased in the last decade. Anthropogenic load has increased. As a result, household waste and domestic sewage from the villages and industries in the basin can flow freely via the rivers or into the lake. There are only three mechanical wastewater treatment plants in the entire basin of Lake Sevan (Gavar, Martuni and Vardenis). Water does not undergo biological and chemical treatment.

5. For sustainable management of the ecosystem, it is necessary to clear the forests and bushes in the flooded areas, to build new wastewater treatment plants, to re-equip the old ones, to build a sewage system and a sanitary landfill. In addition, we propose to build modern phytoremediation plants in small communities in the basin (up to 2-3 thousand inhabitants), which are widely used all over the world.

6. The climate change scenarios show a negative impact on the conditions for life in the Lake, and the pessimistic (the worst) scenario suggests a decrease in the total river

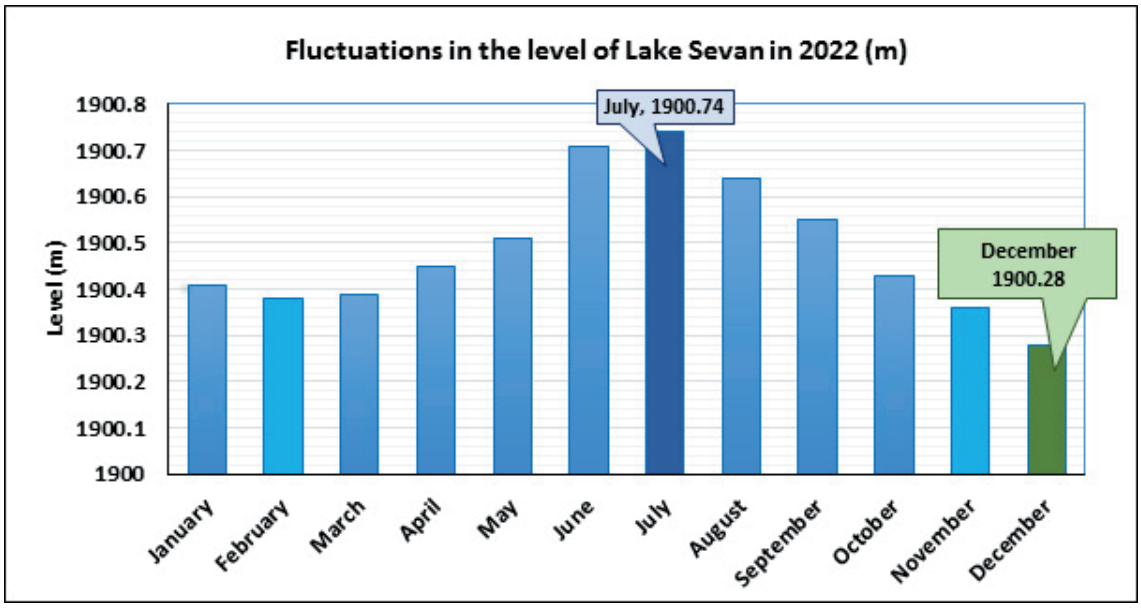

Fig. 8. Fluctuations in the level of Lake Sevan in 2022 (According to Hydrometeorology and Monitoring Center of RA)

[4]https://www.irtek.am/views/act.aspx?aid=119092

inflow into the Lake Sevan by about 34% (265 million m^3) and increase of Lake surface evaporation rate by 36.5% (292.6 million m^3) by 2100 as compared to the baseline conditions (1961-1990). The Lake level will decrease by about 16 cm in a year.

Considering this circumstance, we propose to diversify agriculture and industry in the effective and sustainable management of water resources. Create water-saving strategies, introducing drip irrigation in particular and diverse water billing schemes.

CONCLUSION

The ecosystem has suffered irreparable losses as a result of centuries-old fluctuations in the level of Lake Sevan and in general in the water, thermal, water-chemical, and water-biological regimes that created diverse issues at different eras and had both positive and bad features.

Although the RA Ministry of Environment has taken and is taking a variety of steps to stabilise the biological condition of the Lake, it is difficult to anticipate how these processes will develop in the future. However, the issue of lake Sevan is not entirely settled, the ecosystem of the lake is damaged, undergoing the process of eutrophication. The flora and fauna of the water and coast underwent serious and irreversible changes.

We believe that only raising the lake level cannot prevent or solve existing problems, as many experts claim. Given the fact that the lake level rise is limited (only 2 meters can be raised, because the entrance of the Arpa-Sevan tunnel to Lake Sevan is located at 1902.5 m. (Fig. 5) in height, and the lake level was 1900.28 m. (Fig. 8) in December 2022), the solution to the problem is unrealistic. In our opinion, raising the level can only provide a temporary solution to the ecosystem, contributing to the self-cleaning of the lake water. If the remaining issues are not resolved, the lake will soon encounter the same issue once more. Therefore, in the Sevan basin management area, which was covered in detail above, complicated actions must be implemented regardless of the lake's level.

Finally, a mathematical model for sustainable management of water resources should be developed and implemented for the entire basin.

REFERENCES

Aliokhin O.A. (1970). Fundamentals of hydrochemistry: monograph – Leningrad. Hydrometeorological publishing house, 446 (in Russian).

Bagdasaryan B. (1990). Atlas of the natural conditions of the natural resources of the Republic of Armenia, Hydrology. Yerevan, Publishing House of the Institute of Geological Exploration of the Academy of Sciences, 112 (in Russian).

Chichasov G.N. (2013). Numerical methods for processing and analysis of hydrometeorological information. LLC, BORGES, 235 (in Russian).

Climate Bulletin of the Republic of Armenia. (2011). Arm state hydromet, Yerevan, 150.

Davidov V.K. (1938). The Water balance of Lake Sevan: Materials on the research of Lake Sevan and its basin. Hydrometeorological publishing house, Part VI, Leningrad, 82 (in Russian).

Ecology of Lake Sevan during the period of water level rise the results of Russian-Armenian biological expedition for hydro geological survey of Lake Sevan (2010). (Armenia) (2005-2009). Publishing house, Science DNTs, Russia, 348.

Fourth National Communication on Climate Change. (2020). Yerevan. UNDP Armenia. 213.

Gabrielian H.K. (1980). The Pearl Sevan, Yerevan, 135 (in Armenian).

Gagarina O.V. (2012). Assessment and regulation of the quality of natural waters: criteria, methods, existing problems: Study guide. Udmurt University, Izhevsk Publishing house, Russia, 199.

Gevorgyan G., Rinke K., Schultze M., Mamyan A., Kuzmin A. et al. (2020). First report about toxic cyanobacterial bloom occurrence in Lake Sevan, Armenia. Internat Rev Hydrobiol 105(5-6), 131-142, DOI: 10.1002/iroh.202002060.

Hovsepyan A., Tepanosyan G., Muradyan V., Asmaryan S., Medvedev A., Koshkarev A. (2019). Lake Sevan Shoreline Change Assessment Using Multi-Temporal Landsat Images. Geography, environment, sustainability, 12(4), 212-229, DOI: 10.24057/2071-9388-2019-46.

Kendall M.G. (1975). Rank Correlation Methods: 4th edition, Griffin, London, UK, 202.

Lyatti S.Ya. (1932). The hydro chemical study of Lake Sevan: Materials on the research of Lake Sevan and its Basin, 4(2), 36 (in Russian).

Mann H.B. (1945). Nonparametric tests against trend. Econometrica, 13, 245-259.

Markov E.S. (1911). Lake Gokcha. Geographical description of the lake. Part 1: Physical Geography, St. Petersburg, 193, [online] Available at: http://resolver.gpntb.ru/purl?docushare/dsweb/Get/Resource4926/Markov__E.S.__Ozero__Gokcha_ch.1.pdf

Musaelian S.M. (1993). The Ecology and Economy of Lake Sevan and its Basin. Yerevan, 164 (in Russian).

Paffenholtz K.N. (1950). About the Origin of Lakes Sevan, Van and Urmia. Proceedings of Academy of Sciences of Armenian SSR, Geological Series, 1, 125-138.

Parparova R.M. (1979). Hydrochemical regime of Lake Sevan according to data from 1976. Proceedings of the Sevan hydrobiological station, 17, 38-50, [online] Available at: http://sevan.asj-oa.am/137/ (in Russian).

Rozhdestvensky A.V., Chebotarev A.I. (1974). Statistical methods in hydrology, 424 (in Russian).

Rusinov M.I. (1970). Statistical Methods in Hydrology. L., Gidrometeoizdat, 272 (in Russian).

Sargsian S.G. (1962). Petrographo-Mineralogical Research of Lake Sevan Basin. publishing house. AN Arm. SSR, Yerevan, 154 (in Russian).

Shelutko V.A. (1984). Statistical models and research methods for long- term runoff fluctuations, 159 (in Russian).

Shelutko V.A. (2007). Methods of processing and analysis of hydrological information: study-guide allowance. St. Petersburg State University, 191 (in Russian).

The Biodiversity of Armenia (1999). The first report. RA ministry of nature protection, Armenia, 11-15.

Trofimov A.M., Igonin E.I. (2001). Conceptual patterns of modeling in geography. Development of basic ideas and techniques of mathematization and formalization in geography. Kazan, 340 (in Russian).

Vardanian T. (2012). On Some Issues of the Anthropogenic Transformation of Water Ecosystems (Case Study of Lake Sevan). In: Fernando, H., Klaić, Z., McCulley, J. (eds) National Security and Human Health Implications of Climate Change. NATO Science for Peace and Security Series C: Environmental Security. Springer, Dordrecht, DOI: 10.1007/978-94-007-2430-3_29.

Vardanian T. (2009). The Hydro-Chemical Changes of Lake Sevan Water After the Artificial Lowering of the Water Level. In: Bahadir, A.M., Duca, G. (eds) The Role of Ecological Chemistry in Pollution Research and Sustainable Development. NATO Science for Peace and Security Series C: Environmental Security. Springer, Dordrecht, DOI: 10.1007/978-90-481-2903-4_8.

Vardanyan T., Robinson P. (2007). Lake Sevan: The loss and restoration of the "pearl of Armenia". Managing Water Resources in a Changing Physical and Social Environment. In: Peter J Robinson, Tony Jones, and Ming-ko Woo, Home of Geography: Societa Geografica Italiana, Rome, 67-77, [online] Available at: https://www.homeofgeography.org/uk/Publication/vol7.html.

Vardanyan T.G., Frolova N.L., Galstyan H.S. (2021). The Characteristics of Extreme Maximum Runoff of The Rivers of Armenia in The Context of Global Climate Change. Geography, environment, sustainability, 14(1), 196-208, DOI: 10.24057/2071-9388-2020-122.

Vardanyan T., Danielyan Y., Muradyan Z. (2021). Anthropogenic Transformation of Lake Ecosystems and Existent Problems (Case Study of Lake Sevan). Adv in Hydro and Meteorol, 1(1), [online] Available at: https://irispublishers.com/ahm/pdf/AHM.MS.ID.000504.pdf.

ges.rgo.ru/jour/

ISSN 2542-1565 (Online)